Molecular characterization of carnitine palmitoyltransferase 1C

Esther Gratacòs i Batlle

UNIVERSITAT DE BARCELONA

Facultat de Farmàcia

Departament de Bioquímica i Biologia Molecular

MOLECULAR CHARACTERIZATION OF CARNITINE PALMITOYLTRANSFERASE 1C

Esther Gratacòs i Batlle

2010

UNIVERSITAT DE BARCELONA

Facultat de Farmàcia

Departament de Biologia Cel·lular i Anatomia Patològica

Programa de doctorat de Neurociències

Bienni 2002-2004

MOLECULAR CHARACTERIZATION OF CARNITINE PALMITOYLTRANSFERASE 1C

Memòria presentada per Esther Gratacòs i Batlle per optar al títol de doctor per la Universitat de Barcelona.

Dra. Núria Casals Farré
Directora de tesi
Universitat Internacional de Catalunya

Dr. Josep Clotet Erra
Co-director de tesi
Universitat Internacional de Catalunya

Esther Gratacòs Batlle
Doctoranda

Dr. Fausto García Hegardt
Tutor de tesi
Universitat de Barcelona

Portada:
Cèl·lules SH-SY5Y transfectades transitòriament amb el plàsmid pCPT1C-EGFP (imatge presa a les 72h post-transfecció).
Disseny de Ricard Gratacòs Batlle

A tota la meva família.

L'EXERCICI DE LES OMBRES

Relaxa't.

Contempla totes les ombres que projecten

els objectes o les persones que tinguis al voltant.

Procura esbrinar quina part de l'objecte o de la persona es reflecteix.

Continua contemplant, però, al mateix temps,

enfoca el problema que vulguis resoldre i

busca-hi totes les solucions equivocades possibles.

Finalment, continua contemplant i pensa en les

solucions encertades que hagin sobrat.

Elimina-les una a una, fins que només

hi quedi la solució exacta per al problema.

Diari d'un mag. Paulo Coelho

AGRAÏMENTS

Al final del llarg camí de la tesi, només em vénen que ganes de donar les gràcies als quatre vents. Hi ha tantes persones que directa o indirectament han fet possible aquest treball... que tinc la necessitat de dedicar-vos a tots un record en aquest escrit.

A la Montse Forns, que em va despertar les ganes de saber com funciona el nostre organisme.

A molts professors tant de Medicina com de Bioquímica, que han incrementat les ganes de saber i que m'han transmès la seva vocació.

A tots els companys de Bioquímica, que van crear un ambient fèrtil per a acabar tots dedicant-nos a la ciència. Sobretot vosaltres Ivan, Rosa, Lluís i Ester, que amb les trobades que fem de tant en tant, posem tot en dubte i reconstruïm la "humanitat".

A la Dra. Carmen Gomar que em va portar fins el Dr. Gual, on vaig poder participar de la feina realitzada en el seu laboratori de Neuroelectrofisiologia, en aquells moments a càrrec del Dr. Morales que va confiar en mi en primer lloc. *Gracias Miguel, porque ahora, con la distancia del tiempo, veo que aprendí mucho de tu experiencia*. Allà, he de tenir un record especial per l'Azu (que vas ser la meva primera "mestra de trucs" de laboratori), i pel David i la Núria que em vau ensenyar que, per fer una tesi, cal un bon coixí d'amics que et sustenti, i vosaltres vau ser el meu primer coixí.

A vosaltres, Pep i Núria, que vau ser la meva porta a la ciència i a l'educació. Gràcies pel vostre exemple, per transmetre la vostra vocació en cada cosa que feu. Per buscar sempre solucions als problemes que sorgeixen. Per estar disponibles en tot moment i sobretot, gràcies per confiar en mi des del primer dia. Gràcies per ensenyar-me gairebé tot el que sé! Segur que sense vosaltres, jo no estaria per presentar la tesi...

Al Dr. Fausto García Hegardt, per qui sento gran admiració, *por su ejemplo, su sabiduría y su capacidad de transmitir el verdadero sentido de la ciencia, al servicio de la sociedad. Gracias por las aportaciones realizadas durante los seminarios y vía email. Gracias también por solucionar aspectos "más burocráticos".*

A tota la colla de Farmàcia, a la Guille i la Dolors per la seva proximitat i visió de la ciència, a la Laura per tots els teus consells (científics i extra-científics), per la teva disponibilitat per ajudar a tothom i per la teva capacitat de donar ànims i motivació. De la primera etapa gràcies també al David (per ensenyar-me tot el referent als assaigs d'activitat), al Toni, a l'Assia, a la Irene (per tot el tema dels assaigs de desglicosilació). De l'etapa "més" actual, a la Paula, el Chandru, la Yolanda i al Pep (Pep, gràcies per fer-te càrrec del tema més "oficial" quan va fer falta).

Al Paulino, *gracias Paulino por tu ayuda con el modelo estructural, y las correcciones del texto. Pero sobretodo por todos los emails intercambiados. Han sido una dosis de motivación y energía muy valuosa durante el proceso de escritura de la tesis.*

I a tots els "coixins" de la UIC:

A tu Patricia, gràcies per compartir tots els alts i baixos durant aquests anys, per ensenyar-me el teu ordre, la teva capacitat de treballar i la teva perseverància. Gràcies per tots els "cerbellets" i mostres de controls pels westerns. Ens queden pendents moltes pluges d'idees que espero que poguem anar fent.

A tu Tània, per la teva alegria, per ser tant carinyosa i per les converses "científiques" compartides. Gràcies per cuidar-me! I pels anticossos!

A tots els del lab: Sara-Aspirina, gràcies per ser sempre una dosi d'alegria; Aloa, gràcies per cuidar-me; Àlex, gràcies per compartir opinions sobre tantes coses que ens envolten; Maher, gràcies per oferir-te sempre a ajudar-me en el que calgués; Mònica, Carles, Marc, Diana, Deborah,... i a tots, merci també per totes les estones compartides en seminaris, dinars, sopars o amb cafès després de dinar. Gràcies per animar aquestes estones!

A vosaltres "yeast girls", Sandra i Natàlia (i des del darrer any, també la Sara) per totes les plaques, medis, tampons i solucions que m'heu deixat, per posar-me, o treure, els llevats quan passàveu per allà en diumenge. I pels grans moments!

A la Mercè i el Dani García que m'han donat un cop de mà molt útil en diferents moments.

A la MªJosé per ser-hi en els primers temps quan pel laboratori estava jo sola i apareixies tu portant històries de "l'exterior"!

A vosaltres Dani Martí, Jordi Caballé i Pedro Corzo, entre tants d'altres alumnes, que m'heu fet adonar que això d'ensenyar realment val la pena.

A tu Maria, que des de la distància, sempre m'envies dosis d'energia.

I evidentment tota aquesta feina no l'hauria pogut fer si no tingués la família esplèndida que tinc. Vull tenir un record molt especial pels meus avis i àvies, als que hi són i als que ja no, que sempre m'han fet sentir estimada, amb el seu amor incondicional, i que segur que des d'on sigueu, estareu contents de veure que m'encanta el que faig. Pare, Mare, gràcies per recolzar-me sempre en les meves decisions i ajudar-me en tot allò que ha calgut. Mai podré arribar a fer res que expressi tota la gratitud que sento per tot el que heu fet i que continueu fent per mi. Xavi i Ricard, ja sabeu que podeu comptar amb mi tal i com jo compto amb vosaltres. Gràcies Ricard pel disseny de la portada i pels consells estètics per la tesi.

I per acabar, gràcies a tu Cristian perquè a sobre que t'has d'emportar la pitjor part, ho fas de bon humor i sempre em fas veure la cara positiva de les coses. Gràcies per suportar totes les nits que jo he hagut de treballar. Per solucionar tots els temes de casa sense posar mai mala cara. Per tots els teus consells i per l'ajuda informàtica. Gràcies per ser un pare tant genial per la Laia, i per ser-hi sempre que jo ho necessito. I a tu Laia, gràcies, perquè sentir que venies a la vida per compartir-la amb nosaltres, em va fer prendre la decisió de continuar en el món de la ciència. Sense la dosi d'energia que vaig tenir durant l'embaràs i durant els primers anys de la teva vida, no hauria arribat mai fins aquí.

Des d'aquí, us envio a tots, el petó més dolç!

INDEX

INDEX

ABBREVIATIONS

aa	amino acid
ACC	acetyl-CoA carboxylase
ACS	acyl-CoA synthetase
AD	activation domain
ADE2	phosphoribosyl-aminoimidazole carboxylase
AgRP	agouti-related protein
AMP	adenosine monophosphate
AMPK	AMP-activated protein kinase
ARC	arcuate nuclei
ATP	adenosine triphosphate
BD	binding domain
bp	base pair
BSA	bovine serum albumin
CACT	carnitine-acylcarnitine translocase
CART	cocaine-amphetamine-regulated transcript
CAT or CrAT	carnitine acetyltransferase
cDNA	complementary DNA
Ci	Curie
CNS	central nervous system
CoA	coenzyme A
COT or CrOT	carnitine octanoyltransferase
CP	lateral ventricular choroid plexus
CPT1	carnitine palmitoyltransferase 1
CPT2	carnitine palmitoyltransferase 2
CRD	cysteine-rich domain
Cx	cerebral cortex
DEPC	diethylpyrocarbonate
DG	dentate gyrus
DIV	days in vitro
DMEM	Dulbecco's modified Eagle Medium
DMSO	dimethyl sulfoxide
DNA	deoxyribonucleic acid
DNase	deoxyribonuclease
dNTPs	2'-deoxynucleosides 5'-triphosphate
DO	dropout
DTE	dithioeritritol
DTT	dithiothreitol
E16	embryonic day 16
E. coli	*Escherichia coli*
ECL	electrochemical luminescence
EDTA	ethylenediamine-tetraacetic acid
EGFP	enhanced green fluorescent protein
ER	endoplasmic reticulum
ERAD	endoplasmic reticulum associated degradation
EST	expressed sequence tag
FAS	Fatty Acid Synthase
FAS	fatty acid synthase
FBS	Fetal Bovine Serum
FFA	free fatty acids
Fwd	Forward
g	grams
GFAP	Glial Fibrillary Acidic Protein
GSH	glutathione, reduced form
GST	glutathione S-transferase
h	hours
Hb	habenulae
HC	hippocampus
HET	heterozygote
HFD	high fat diet
HIS3	imidazoleglycerol-phosphate dehydratase
Hs	*Homo sapiens*
icv	intracerebroventricular injection
Ig	immunoglobulin
IMM	inner mitochondrial membrane
ip	intraperitoneal
IPTG	isopropyl-β-D-thiogalactoside
kbp	kilobase pair
kcal	kilocalories
K_D	dissociation constant
kDa	kiloDalton
kJ	kiloJoule
K_m	Michaelis constant
KO	knock-out
LacZ	β-galactosidase
LB	Luria-Bertani broth
LC-CoA	long chain fatty acyl-CoA
LCFA	long chain fatty acids
LEU2	beta-isopropylmalate dehydrogenase
LiAc	lithium acetate
LSD	dorso-lateral septal
mA	milliamperes
MAM	mitochondrial associated membranes
MCD	malonyl-CoA decarboxylase
mCi	millicurie
MCS	multiple cloning site
MEL1	α-galactosidase
min	minute
ml	milliliter
mM	millimolar
Mm	*Mus musculus*
mRNA	messenger RNA
mTOR	mammalian target of rapamycin

NCBI	National Center for Biotechnology Information
NeuN	neuronal Nuclei
NFD	normal fat diet
nmol	nanomol
NPY	neuropeptide Y
OD	optical density
OMM	outer mitochondrial membrane
PAGE	polyacrylamide gel electrophoresis
PAT	palmitoyl-acyl transferase
PBS	phosphate buffered saline
PCR	Polymerase Chain Reaction
PEG	polyethylene glycol
PNGase F	peptide-N-glycosidase F
POMC	proopiomelanocortin
PUFA	polyunsaturated fatty acid
PVN	paraventricular nucleus
ref.	reference
Rev	Reverse
Rn	*Rattus norvegicus*
RNA	ribonucleic acid
RNase B	ribonuclease B
ROS	reactive oxygen species
rpm	revolutions per minute
RT	reverse transcription
s	seconds
SC	standard chow
SCh	suprachiasmatic
SD	synthetic defined
SDS	sodium dodecyl sulphate
ST1326	(r)-n-tetradecylcarbamoyl-aminocarnitine
SV	synaptic vesicle
TAE	Tris(hydroxymethyl) aminomethane acetate salt
TAG	triacylglycerol
TBS-T	tris buffered saline-Tween-20
TDGA	tetradecylglycidic acid
TE	Tris-EDTA
TM	transmembrane domain
TRP1	phosphoribosylanthranilate isomerase
U	Units
UAS	upstream activating sequences
UCP2	uncoupling protein 2
UPR	unfolded protein response
URA3	orotidine 5-phosphate decarboxylase
V	Volts
VLDL	very low density lipoproteins
VMH	ventromedial hypothalamus
vs.	versus
w/ v	weight/volume
WB	Western blot
WT	wild type
Y2H	yeast two hybrid
µg	microgram
µl	microliter
µM	micromolar
3-D	three-dimensional

INTRODUCTION

1. CARNITINE ACYLTRANSFERASES

Mitochondrial β-oxidation is the main pathway for degrading fatty acids and obtaining energy for the cell. The main step in this pathway is the transport of long chain fatty acyl groups into the mitochondrial matrix. The transport of fatty acids is performed by a group of enzymes with acyltransferase activity (carnitine acyltransferase family) and a transporter in the inner mitochondrial membrane (McGarry et al., 1989). Different enzymes belong to the carnitine acyltransferase family, each of them having specificity for a determinate length of the fatty acyl group used as a substrate:

- Carnitine acetyltransferase (CrAT or CAT) uses acetyl-CoA as a substrate (Bieber, 1988).
- Carnitine octanoyltransferase (CrOT or COT) facilitates transport of fatty acids (C8-C10) from peroxisomes to mitochondria (Ferdinandusse et al., 1999).
- Carnitine palmitoyltransferases (CPTs) 1 and 2 facilitate transport of long chain fatty acids (C16-C20) to the mitochondrial matrix where they will be β-oxidated (McGarry et al., 1989).

1.1 Carnitine palmitoyltransferase system

The carnitine palmitoyltransferase system (CPT) permits entry of long chain fatty acyl-CoA (LC-CoA) into the mitochondria for β-oxidation by consecutive transesterifications (see Figure 1) involving different activities (Kerner and Hoppel, 2000). The first component of this system is carnitine palmitoyltransferase 1 (CPT1), an integral transmembrane protein of the mitochondrial outer membrane that catalyzes the transfer of acyl moieties from CoA to carnitine. The acylcarnitine product can then traverse the inner membrane by means of a carnitine-acylcarnitine translocase (CACT). CPT2, on the matrix side of the inner membrane, reverses CPT1 reaction, retransferring the acyl group to CoA-SH. The acyl-CoA then undergoes β-oxidation and ultimately yields acetyl-CoA (Zammit, 2008; Rufer et al., 2009).

The reaction catalyzed by CPT1 is the key regulatory site controlling the flux through β-oxidation, by virtue of its inhibition by malonyl-CoA, an intermediate in fatty acid biosynthesis (McGarry and Foster, 1980). This reaction is not only central to the control of fatty acid oxidation, but it also determines the availability of long chain acyl-CoA for other processes, notably the synthesis of complex lipids.

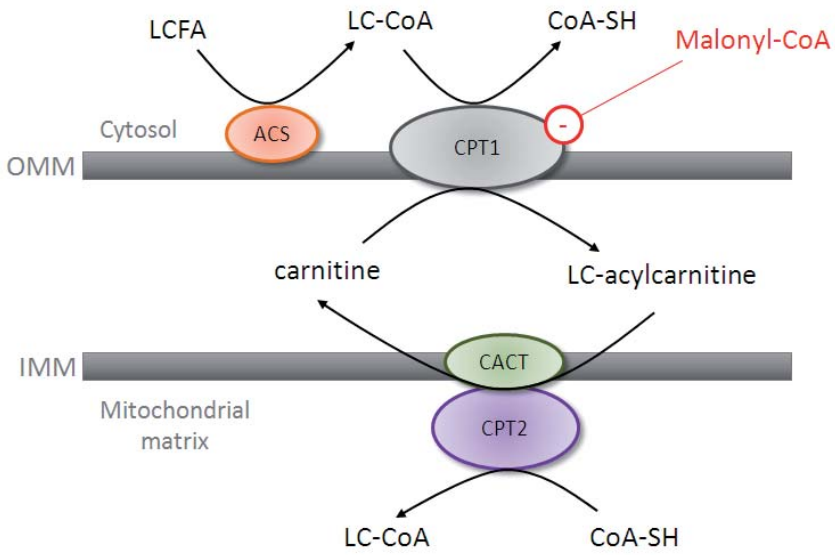

Figure 1. **LCFA translocation into the mitochondria by the carnitine palmitoyltransferase system.** LCFA (long chain fatty acids) are activated to LC-CoA by the action of the acyl-CoA synthetase (ACS). Transport of LC-CoA from the cytosol to the mitochondrial matrix involves the conversion of LC-CoA to acylcarnitines by CPT1, translocation across the mitochondrial inner membrane by the carnitine acylcarnitine translocase (CACT) and reconversion to LC-CoA by CPT2. The physiological inhibition of CPT1 enzymes by malonyl-CoA is also repsresented (in red). OMM: outer mitochondrial membrane; IMM: inner mitochondrial membrane.

The CPT1 enzyme exists in at least three isoforms in mammals:

- CPT1A has also been referred to as the liver isoform or L-isoform (L-CPT1). It is the most ubiquitously expressed isoform and it is found not only in liver mitochondria, but also in mitochondria of the pancreas, kidney, lung, spleen, intestine, brain and ovary (Esser et al., 1993; Britton et al. 1995; McGarry and Brown, 1997).
- CPT1B is also known as the muscle isoform (M-CPT1). It was first identified in skeletal and cardiac muscle mitochondria, but also occurs in adipose tissue and the testis (Yamazaki et al., 1995; Esser et al., 1996).
- CPT1C has been recently reported and is a brain-specific protein that shows high sequence homology with the other isoforms but its function remains unknown (Price et al., 2002).

In this study, all three genes and isoforms will be referred to using capital letters. A, B and C will be used to specify each isoform.

1.2 CPT1A and CPT1B

CPT1A and CPT1B have been extensively studied since they were cloned for the first time. The identity in amino acid residues is high (62%), but both isozymes present significantly different kinetic and regulatory properties: CPT1A displays higher affinity for its substrate carnitine and lower affinity for the physiological inhibitor malonyl-CoA than the muscle isoform (Esser et al., 1996; McGarry and Brown, 1997; Zammit, 2008) (see Table 1). This differential sensitivity to

the reversible inhibitor of the enzyme is probably involved in the finer regulation of fatty acid oxidation in heart and skeletal muscle, in comparison to liver.

	CPT1A	CPT1B
Amino acids	773	772
Mass	88 kDa	88 kDa
Malonyl-CoA IC_{50}	2.5 µM	0.03 µM
Carnitine K_m	30 µM	500 µM
Human chromosome locus	11q13	22q13.3
Tissue expression:		
Liver	++++	–
Skeletal muscle	(+)	++++
Heart	+	+++
Kidney	++++	(+)
Lung	++++	(+)
Spleen	++++	–
Intestine	++++	–
Pancreas (islets and	++++	–
Brown adipose tissue	(+)	++++
White adipocytes	+	+++
Ovary	++++	
Testis	(+)	++++
Human fibroblasts	++++	–
Brain	+	
Cerebellum	–	+++
Human deficiency described:	Yes	No

Table 1. Overview of mitochondrial CPT1 enzymes. Relative levels of CPT1 isoform expression for each organ are based on northern blot analysis (and in some cases [^{3}H]etomoxir-CoA labelling), but do not indicate precise ratios.(+), trace expression compared with the alternative isoform; -, undetected. Tissue expression data refer to the rat, except in the case of fibroblasts and brain. (Table modified from McGarry and Brown, 1997).

CPT1A and CPT1B are both localized in the outer mitochondrial membrane with two transmembrane domains (TM1 and TM2) and the N- and C- termini facing the cytosolic side (Fraser et al., 1997). It has also been demonstrated that residues within the N-terminal domain of CPT1 (comprised among amino acid positions 1-150), including both transmembrane domains and a downstream region, contain key information for directing the enzyme to its target localization (Cohen et al., 1998; Cohen et al., 2001).

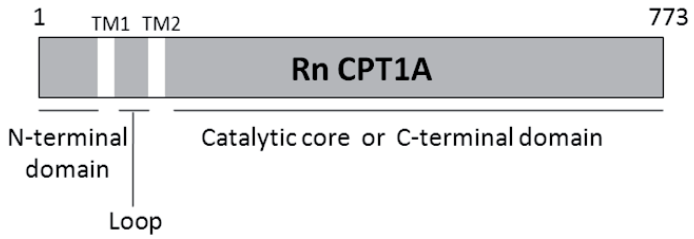

Figure 2. Schematic representation of the structural domains of rat CPT1A sequence. TM1 (residues 48-75) and TM2 (residues 103-122) represent domains traversing the outer mitochondrial membrane. N- and C-terminal domains are facing the cytosol and the loop region is oriented towards the intermembranous space.

In addition, the amino acid residues that are critical for catalytic activity or malonyl-CoA sensitivity have been identified for both enzymes, and three-dimensional structures have been predicted (Figure 3) based on the carnitine acetyl transferase (CAT), carnitine octanoyl transferase (COT) and carnitine palmitoyltransferase 2 crystals (CPT2) (López-Viñas et al, 2007). The most important residue in CPT1A for the catalysis is His^{473} because when mutated, catalytic activity is abolished (Morillas et al., 2001). It has also been shown that mutations in Glu^{26} and Lys^{561} decrease malonyl-CoA sensitivity, confirming that interactions between the N- and C-terminal domains are critical for malonyl-CoA binding and sensitivity (López-Viñas et al., 2007).

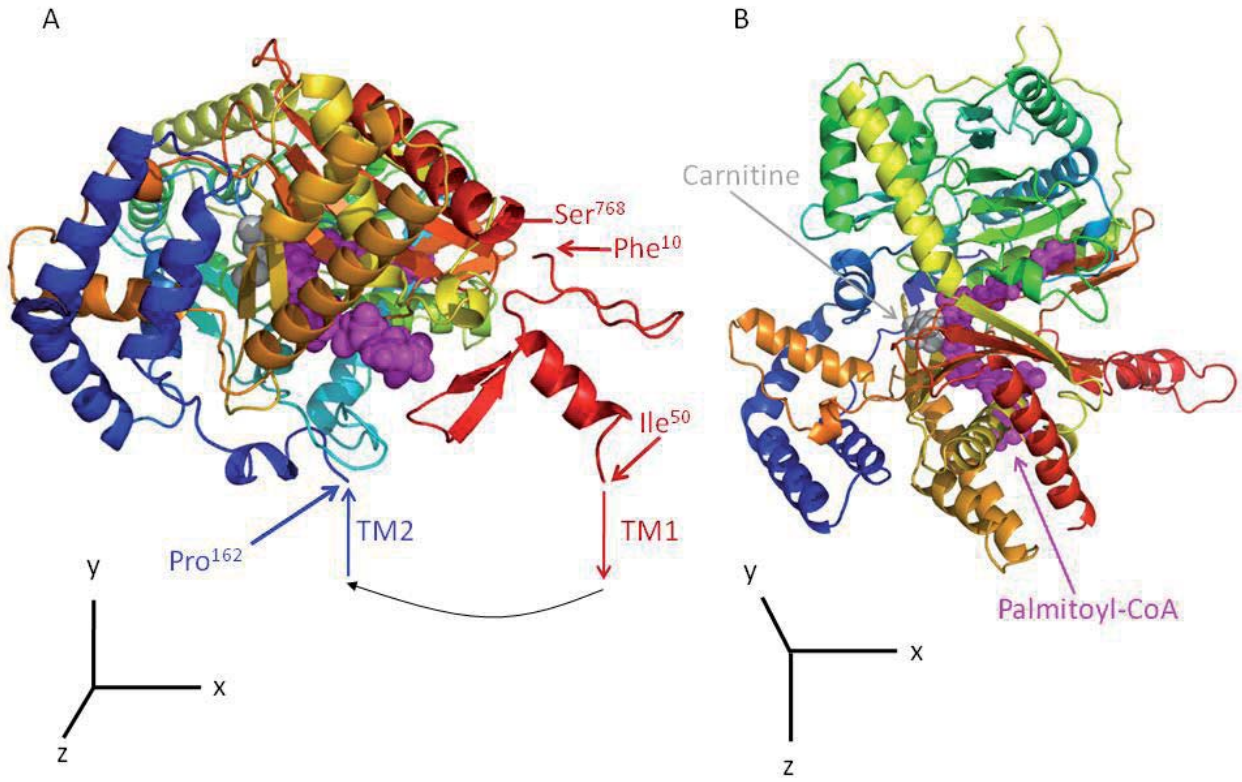

Figure 3. Structural model of rat CPT1A. A proposed model for CPT1A is shown in the ribbon plot representation. The putative sites for carnitine (gray) and palmitoyl-CoA (magenta) are indicated. **(A)** A frontal view of the model in which residues flanking the modeled region have been highlighted [regions modeled: from Phenilalanine 10 to Isoleucine 50 (in blue) and from Proline 162 to Serine 768]. In this model the hypothetic position of transmembrane domains 1 and 2 (TM1, TM2), and the loop region between them, have been represented by red, blue and black arrows respectively. **(B)** A top view of the model.

1.3 Physiological regulation of CPT1A and CPT1B in liver and muscle

CPT1 is tightly regulated by its physiological inhibitor malonyl-CoA, and thus CPT1 is the most physiologically important regulatory step in mitochondrial fatty acid oxidation (McGarry and Foster, 1980). This process allows the cell to signal the relative availability of lipid and carbohydrate fuels in liver, heart, skeletal muscle, and pancreatic β-cells (Zammit, 1999).

In the liver, malonyl-CoA acts as a key metabolite which ensures that fatty acid oxidation and *de novo* fatty acid synthesis do not occur simultaneously. In case of carbohydrate feeding (high insulin) hepatic lipogenesis is active, the concentration of malonyl-CoA rises, CPT1 is suppressed and newly formed LC-CoA are directed into esterification products (triacylglycerides, TAG) forming very-low density lipoproteins (VLDL). VLDLs are then transported to adipose tissue for storage (McGarry and Brown, 1997). Conversely, in ketotic states (low insulin) carbon flow through glycoslysis diminishes, malonyl-CoA levels fall and fatty acid synthesis comes to a halt. In this context, CPT1 is highly activated and incoming free

fatty acids (FFA) readily undergo β-oxidation with accelerated production of ketone bodies (McGarry and Foster, 1980; McGarry et al., 1989).

In the case of non lipogenic tissues such as heart and skeletal muscle, malonyl-CoA acts mainly as a signaling intermediate. Malonyl-CoA concentration fluctuates with feeding and fasting, as in liver (McGarry et al., 1983). Thus, the flux of synthesis and turnover of malonyl-CoA mediates the fatty acid oxidative potential of muscle (Wolfgang and Lane, 2006). During fasting, malonyl-CoA levels decrease and CPT1 activity increases the entry of fatty acids into the mitochondria producing a high oxidative rate in muscle. On the other hand, CPT1 inhibition mediated by increases in malonyl-CoA levels produced during feeding decreases the β-oxidation rate. Notably, muscle expresses a mitochondrial bound acetyl-CoA carboxylase (ACC2) that produces malonyl-CoA, but contains little or no fatty acid synthase (FAS). Therefore, malonyl-CoA levels must be cleared through enzymatic activities other than FAS. It has been shown that muscle expresses malonyl-CoA decarboxylase (MCD) in abundance (McGarry and Foster, 1980), thus MCD decreases malonyl-CoA levels in this tissue. The flux of synthesis and turnover of malonyl-CoA mediates the fatty acid oxidation potential of muscle (Wolfgang and Lane, 2006).

2. A NEW BRAIN-EXPRESSED ISOFORM: CPT1C

Performing *in silico* database searches based on human CPT1A cDNA nucleotide or protein sequence, a new gene was identified. This new gene was designated CPT1C due to its high similarity to the other isoforms of CPT1 (Price et al., 2002). The new isozyme contains an extended tail (of approximately 30 aa) at the C-terminal end in contrast to the other isoforms (Figure 4).

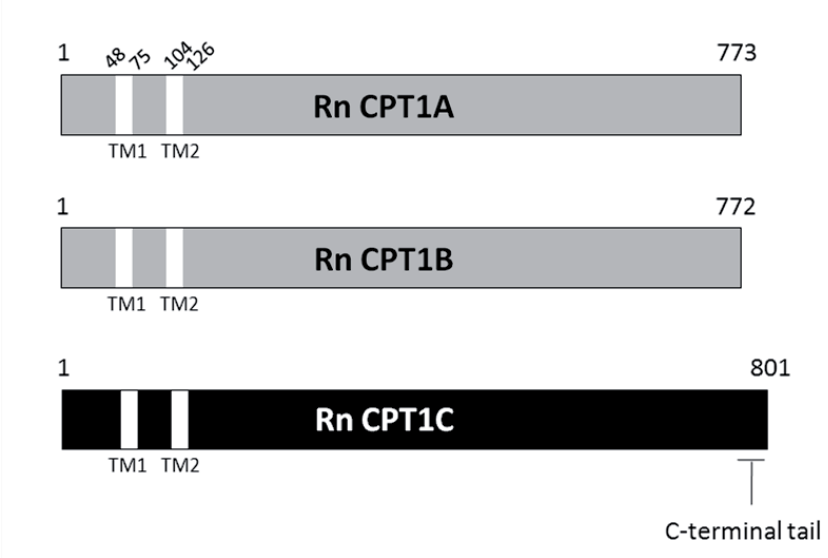

Figure 4. Schematic representation of rat (Rn) CPT1A, CPT1B and CPT1C showing the extended C-terminal tail of CPT1C. Transmembrane domains (TM1 and TM2) and the amino acid positions from the begining to the end are also shown.

The analysis of amino acid sequence similarity and identity percentage among different isoforms revealed that CPT1C is more similar to CPT1A than to CPT1B (see Table 2)

	CPT1A vs. CPT1C	CPT1B vs. CPT1C	CPT1A vs. CPT1B
% Identity	52.4	50.6	62.3
% Similarity	69.6	66.3	77.7

Table 2. Comparison of amino acid sequence among three isoforms of CPT1. Amino acid sequence identity and similarity comparison between different CPT1 isoforms was performed *in silico*. CPT1C has higher degree of similarity with CPT1A than with CPT1B. (From Wolfgang et al., 2006).

The study of the phylogram from the three isozymes indicates that three CPT1 genes diverged approximately at the same time, and presumably, two independent duplication events occurred, close together in evolutionary time (Price et al., 2002).

When looking for CPT1C EST sequences from other species, no orthologous sequences could be found in species other than mammals, while the other isoforms are expressed in organisms like birds, fishes, reptiles, amphibians or insects. This suggests that CPT1C has a specific function in more evolved brains (Price et al., 2002; Sierra et al., 2008).

Expression studies indicate that CPT1C is localized exclusively in the central nervous system, with homogeneous distribution in all areas (hippocampus, cortex, hypothalamus, and others) (Figure 5). The pattern resembles that of FAS, acetyl-CoA carboxylase 1 (ACC1) (enzymes related to biosynthesis) rather than CPT1A or ACC2 (enzymes related to β-oxidation) (Price et al., 2002; Sorensen et al., 2002; Dai et al., 2007).

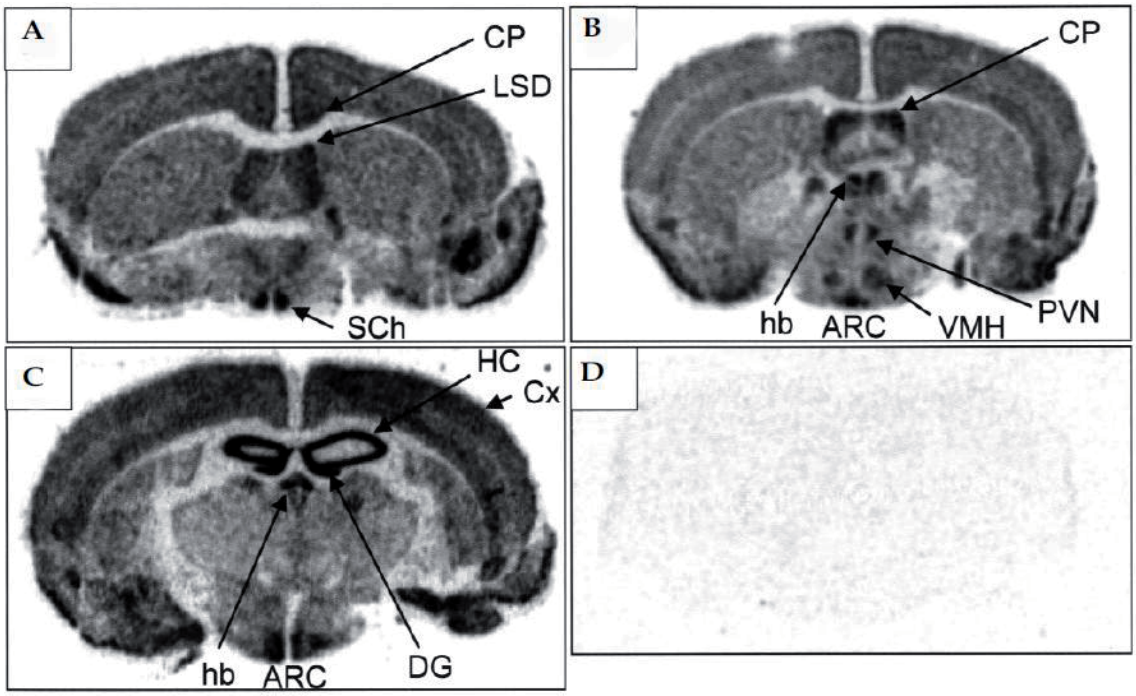

Figura 5. Detection of CPT1C mRNA transcripts in mouse brain by *in situ* hybridization. (A–C) Sections moving towards the posterior of the brain, probed with ^{35}S-labeled antisense probe. (A) A section containing dorso-lateral septal (LSD) and suprachiasmatic (SCh) nuclei. (B) An oblique section containing lateral ventricular choroid plexus (CP), paraventricular (PVN) and arcuate nuclei (ARC), and ventromedial hypothalamus (VMH). (C) An oblique section through the hippocampus (HC), habenulae (hb), and ARC. (D) Hybridization of a sense probe. The figures show scanned autoradiographs. DG, dentate gyrus; Cx, cerebral cortex. (From Price et al., 2002).

To identify the cell types expressing CPT1C in the brain, co-localization studies with a neuronal marker (Neuronal Nuclei, NeuN), or an astrocyte marker (Glial Fibrillary Acidic Protein, GFAP) were performed by our group. Figure 6 shows co-labeling of CPT1C with NeuN confirming that CPT1C is expressed mainly in neurons. No co-localization was detected between CPT1C and GFAP indicating that CPT1C is not present in brain astrocytes (Sierra et al., 2008).

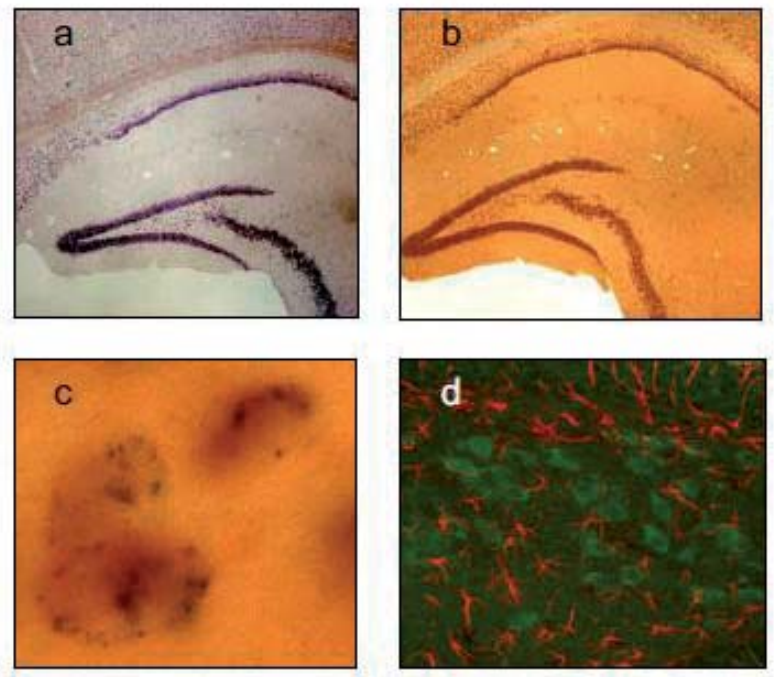

Figure 6. **Co-localization studies of CPT1C mRNA with NeuN and GFAP proteins in brain sections.** Brain sections were processed using *in situ* hybridization with CPT1C antisense Riboprobe (a) or immunocytochemistry with NeuN primary antibodies and biotinylated secondary antibodies (b) or both methods (c). (d) Mouse adult brain sections were processed by double immunocytochemistry with CPT1C antibodies (green stain) and GFAP (red stain). (From Sierra et al., 2008)

2.1 CPT1C enzyme activity

Analysis of the amino acid sequence of these proteins reveals that all residues important for carnitine acyltransferase activity are conserved in CPT1C, as well as the malonyl-CoA binding site.

Despite this, when performing CPT1 radiometric activity assays, no catalytic activity was found even when assaying a large range of acyl-CoA, which are good substrates for CPT1A and CPT1B (Price et al., 2002; Wolfgang et al., 2006). Perhaps, the extended C-terminal tail of CPT1C is disturbing the catalytic activity of the enzyme.

The ability of CPT1C to bind malonyl-CoA has been demonstrated, and it has been suggested that CPT1C regulates malonyl-CoA availability in the brain (Price et al., 2002; Wolfgang et al., 2006).

2.2 Subcellular localization

CPT1C has a high sequence similarity to CPT1A and CPT1B. Therefore, it has been proposed that CPT1C would have the same intracellular localization, which is the outer mitochondrial membrane (Price et al., 2002). The first 147 N-terminal residues of rat CPT1A, encompassing its two transmembrane (TM) segments, specify both mitochondrial targeting and anchorage at the outer mitochondrial membrane (OMM). Residues 123-147, located immediately downstream of TM2, function as a noncleavable, mitochondrial matrix targeting signal. The

hydrophobic transmembrane segments act as stop-transfer sequences that anchor the translocating CPT1 into the OMM (Prip-Buus et al., 1998; Cohen et al., 2001).

Comparison of the first 150 residues of rat CPT1A and CPT1C protein sequences shows 40% identity and 60% similarity within this region. These percentages are lower than those observed for the whole protein sequence indicating that this region is quite divergent and it might contain specific residues for targeting the protein to other locations (see Figure 7).

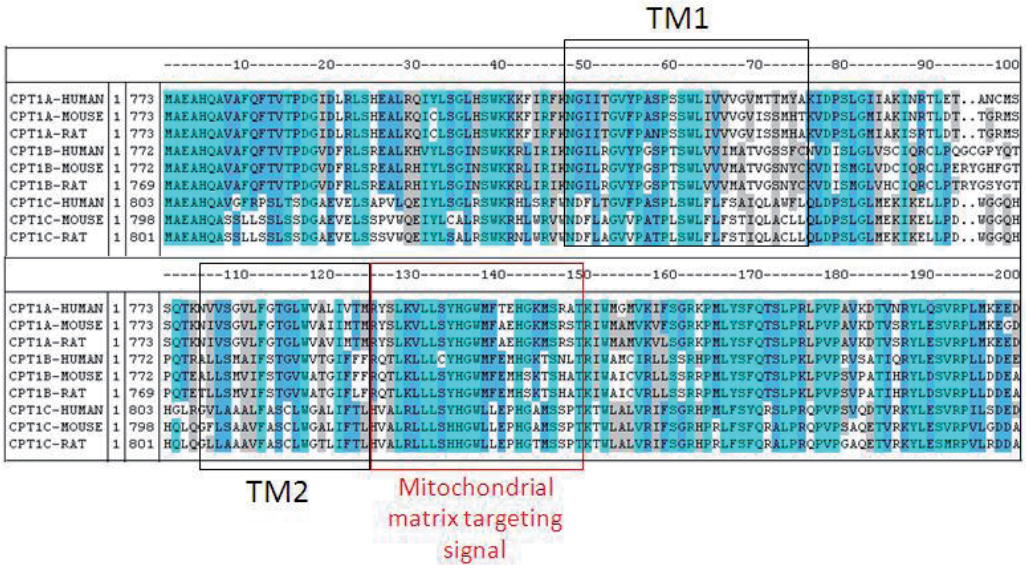

Figure 7. Alignment of the 200 first residues of human, rat and mouse sequences of CPT1A, B and C. Squared in red are the residues corresponding to the mitochondrial matrix targeting signal described by Cohen et al., 2001, which contains some changes in CPT1C. Squared in black are transmembrane domains 1 and 2. Colouring of similar residues is performed according to average BLOSUM62 score: identical residues, corresponding to high values in BLOSUM62 score, are coloured in cyan, semi-conserved residues, with a score of 1.5, are coloured in midblue and residues showing lower scores, below 0.5, are coloured in lightgray.

3. CPT1C IN VIVO

In order to elucidate the role of this isozyme in energy homeostasis, two groups have published their studies on mice with targeted deletion of CPT1C gene (Wolfgang et al., 2006; Gao et al., 2009).

In the first knockout (KO) mice model developed by Lane and colleagues (Wolfgang et al., 2006), KO mice showed no apparent developmental abnormalities or alterations in any organ size, and did not show differences in body temperature when compared with their wild type littermates. When fed a standard laboratory chow (SC), KO mice showed a reduction in whole body weight (of approximately 15%) and a decrease in food intake (by ≈25%) (Figure 8).

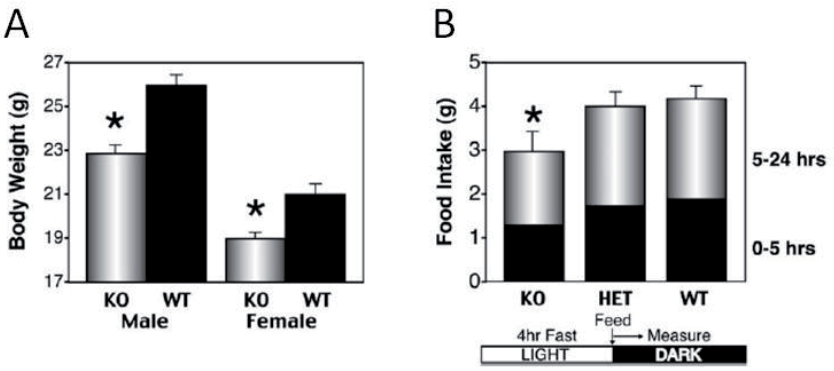

Figure 8. CPT1C KO mice are hypophagic and have a lower body weight than WT mice. (*A*) Body weight was significantly lower in CPT1C KO males (*, $P < 0.0001$; $n = 10$ per group) and females (*, $p < 0.005$; $n = 10$ per group). (B) CPT1C KO mice exhibit lower food intake than WT or heterozygous littermates (*, $p < 0.05$; $n = 6$ per group) after a short (4-h) fast just before the dark cycle (modified from Wolfgang et al., 2006).

When fed a high fat diet (HFD), CPT1C KO mice were more susceptible to obesity (increased weight gain despite reduced food intake) (see Figure 9), became mildly insulin-resistant and showed lower peripheral energy expenditure (Wolfgang and Lane, 2006).

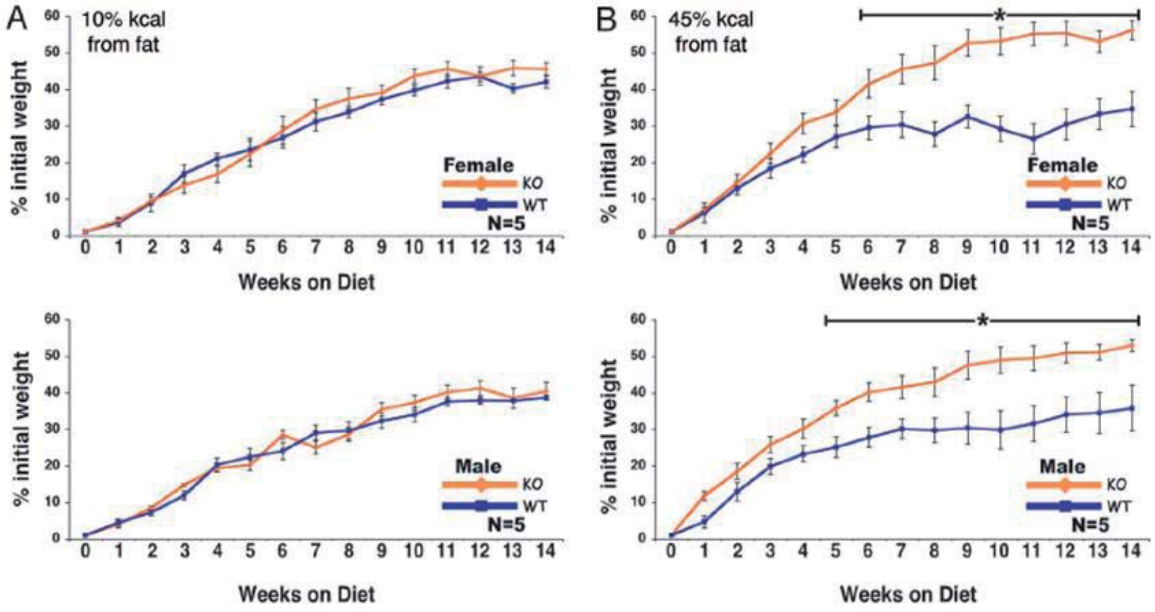

Figure 9. CPT1C KO mice are more susceptible to the effect of a high-fat diet. Male and female WT and CPT1C KO mice ($n = 5$ per group) were fed a control diet (10% of total kcal from fat; 1 kcal = 4.18 kJ) (*A*) or a high-fat diet (45% of total kcal from fat) (*B*) for 14 weeks. Animals were weighed weekly at 14h 00 min. Initial body weights (average grams) were as follows: male WT, 25.9 g; male KO, 22.9 g; female WT, 20.9 g; and female KO, 19.0 g (*, $P < 0.05$).(From Wolfgang et al., 2006).

The CPT1C KO mice model developed by Wu and colleagues (Gao et al., 2009) displayed a similar basic phenotype to that of the previous model. In addition, they found that the liver and muscle expression of genes promoting fatty acid oxidation (such as CPT1A) was markedly decreased in CPT1C KO mice on a high fat diet compared to WT mice. In line with these results, CPT1 activity and palmitate oxidation was also lower in KO mice on HFD (Figure 10).

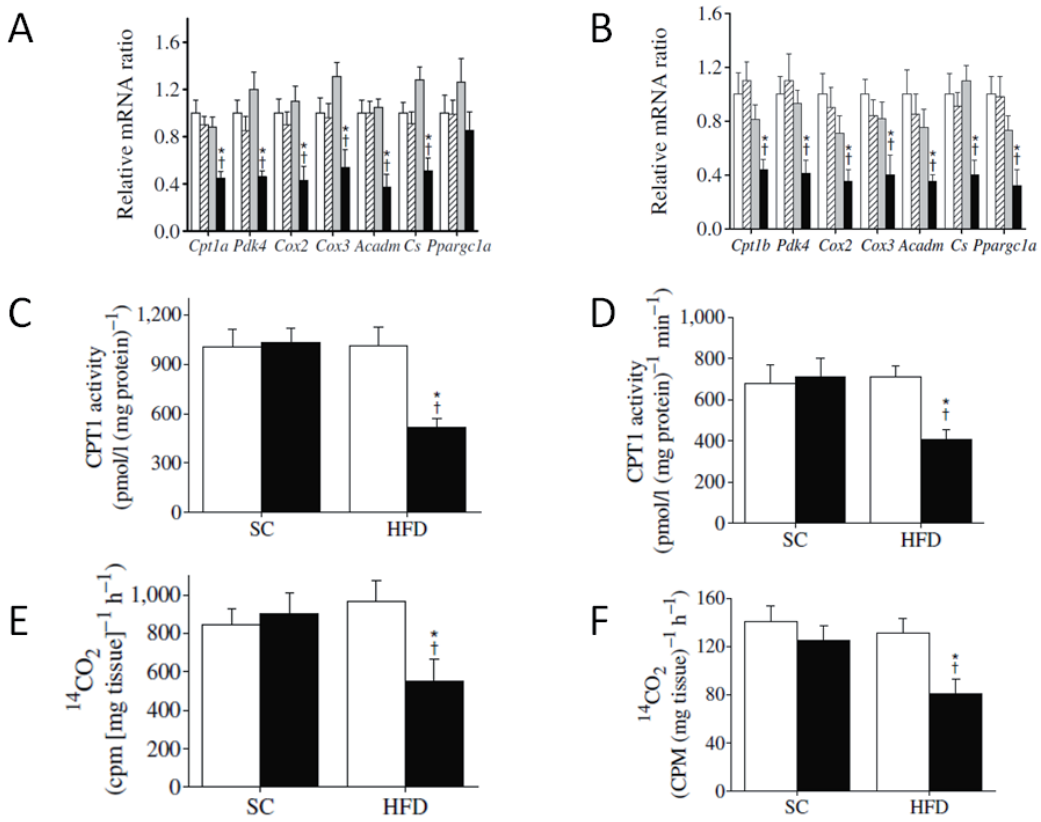

Figure 10. Expression of some oxidative genes, analysed by real-time PCR, CPT1 activity and fatty acid oxidation in liver (A, C, E) and skeletal muscle (B, D, F) (n=5-6). (A) Liver and (B) soleus muscle expression of some oxidative genes. White bars, standard chow (SC) WT; hatched bars, SC KO; gray bars, HFD WT; black bars, HFD KO. Values are means ± standard error of the mean. *p < 0.05 compared with WT mice on HFD; †p < 0.05 compared with KO mice on SC. (C) Liver and (D) muscle CPT1 activity and liver (E) and (F) muscle fatty acid oxidation. White bars, WT; black bars, KO. (Modified from Gao et al., 2009).

Additionally, overexpression of CPT1C in the hypothalamus is sufficient to protect KO mice from body weight gain when fed a high fat diet (Figure 11) (Dai et al., 2007).

Taken together these results suggest that CPT1C is protective against the effect of fat feeding on body weight and that CPT1C is necessary for the regulation of energy homeostasis.

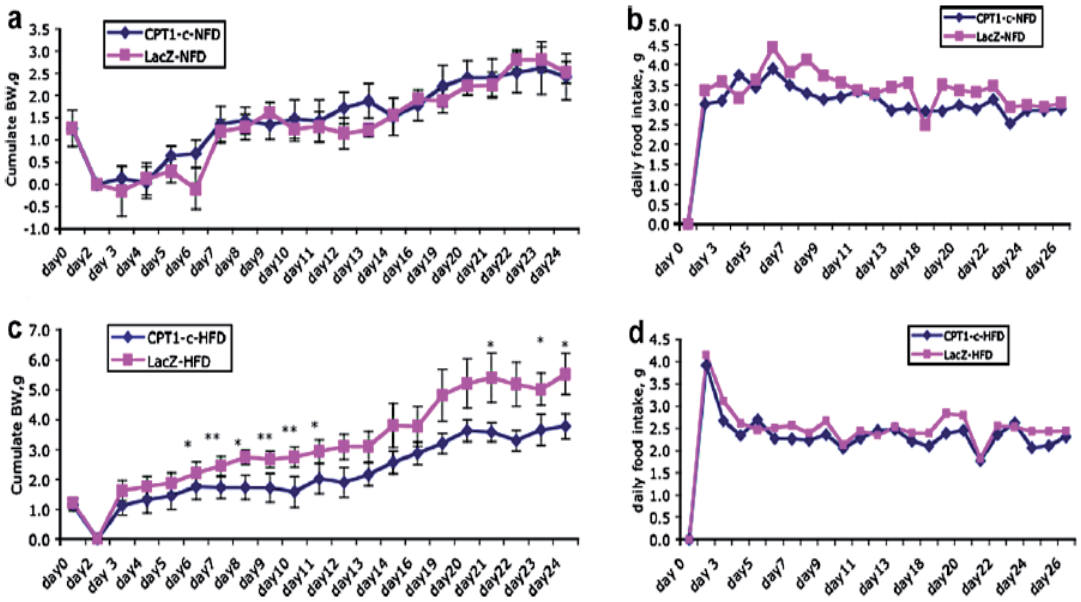

Figure 11. Effect of bilateral stereotactic injection of adenoviral CPT1C or LacZ (control) vectors into the ventral hypothalami on body weight and food intake of mice (three mice/treatment) fed a normal (NFD) or a high-fat (HFD) diet. Cumulative body weight gain and food intake were measured daily for two weeks beginning at day 1 after stereotactic injection. Asterisks refer to the level of statistical significance ($^{*}p \leq 0.05$ or $^{**}p \leq 0.001$) (From Dai et al., 2007).

4. REGULATION OF FOOD INTAKE AND ENERGY HOMEOSTASIS

Hypothalamic nuclei are responsible for integrating multiple signals (informing about energy status from different peripheral tissues through neuronal and hormonal signals, like insulin, leptin, ghrelin or adipokines) and for responding to changes in energy status by altering the expression of specific neuropeptides (NPY, AgRP, POMC, CART) to adjust food intake to whole-body energy demands (López et al., 2008). Restriction of food intake leads to increased firing of a specific subpopulation of neurons, and induces the expression of the hypothalamic orexigenic neuropeptides: neuropeptide Y (NPY) and agouti-related protein (AgRP) mRNAs, and decreases expression of the hypothalamic anorexigenic neuropeptides: proopiomelanocortin (POMC) and cocaine-amphetamine-regulated transcript (CART). In combination, these changes provoke increased food intake and reduced energy expenditure. When fasted animals are re-fed, the inverse response occurs (Hu et al., 2003).

Neurons involved in monitoring the amount of available fuel in the body and thus modulating energy intake and expenditure, must have the ability to sense these conditions through various signals. Different hypothesis have been proposed about the nature of these signals. Recent developments support the “lipostatic hypothesis”. This hypothesis states that signals proportional to the amount of body fat modulate the amount of food eaten at each meal to maintain whole-body energy balance, via both humoral action and nutrient signaling. The humoral signals proposed to date include leptin and ghrelin, endocannabinoids, insulin, among others. Nutrients signaling energy status can be glucose, circulating free fatty acids or amino acids (branched-chain amino acids) (Horvath et al., 2008). There are evidences supporting each of them:

1. There are glucose-specific sensing mechanisms involving ATP, one being the AMPK pathway (described below) and an ATP independent mechanism mediated by glucokinase (Dunn-Meynell et al., 2002; Ainscow et al., 2002).
2. It has been reported that intracerebroventricular (icv) injection of oleate inhibits food intake (Obici et al., 2002; Lam et al., 2005). Other fatty acids (like palmitate) did not have any effect on feeding behaviour.
   The physiological source of brain fatty acids is not known. It is possible that fatty acids are derived from the blood through the "leaky" blood-brain barrier in the region of the arcuate nucleus of the hypothalamus (a region responsible for monitoring energy status). Alternatively, hypothalamic fatty acids may be of endogenous origin derived from either phospholipid turnover or *de novo* biosynthesis (Wolfgang and Lane, 2006). It has been shown that hypothalamic neurons possess the metabolic machinery for fatty acid synthesis (Kim et al., 2002; Gao and Lane, 2003).
3. Administration of low doses of leucine in the third ventricle reduced food intake significantly in rats (Morrison et al., 2007). The reduction of food intake is due to the activation of the mammalian target of rapamycin (mTOR) pathway (Cota et al., 2006).

Neurons have developed mechanisms to monitor energy availability in the extracellular space. One of these mechanisms includes an increase in AMPK activity when AMP/ATP ratio increases (i.e. during fasting). It is widely accepted that changes in the phosphorylation state of AMPK, an AMP-activated protein kinase, affects the phosphorylation state and activity of ACC, thus affecting feeding behaviour (Kahn et al., 2005). AMPK activation requires phosphorylation of Thr^{172} of the catalytic α subunit by LKB1 kinase (Carling, 2004; Kahn et al., 2005)

It has been shown that activation of AMPK in the hypothalamus, using adenoviruses expressing constitutively active AMPK, is sufficient to increase food intake and body weight whereas repression of hypothalamic AMPK activity, induces anorexia (Minokoshi et al., 2004). Additionally, alterations in AMPK activity are associated with the corresponding changes in orexigenic and anorexigenic neuropeptide expression (Kim et al., 2004).

Both ACC isoforms (ACC1, cytosolic and ACC2, anchored to the outer mitochondrial membrane) are found in hypothalamic neurons and are known to be phosphorylated and thereby inhibited by AMPK. Therefore, activation of AMPK reduces the flux of substrates in the fatty acid biosynthetic pathway and reduces malonyl-CoA levels, which in turn will induce CPT1 activity activating the entry of fatty acids into the mitochondria for β-oxidation (López et al., 2007).

Humoral signals, like leptin and ghrelin, act through similar targets (the hypothalamic AMPK/malonyl-CoA/CPT1 axis) but have opposite effects (Figure 12) (Minokoshi et al., 2004; Gao et al., 2007; Wolfgang et al., 2007; López et al., 2008). Centrally administered leptin inhibits hypothalamic AMPK activity, which in turn switches on fatty acid synthesis pathway and decreases oxidation, leading to suppression of food intake (Minokoshi et al., 2004). Central administration of ghrelin decreases hypothalamic *de novo* fatty acid synthesis and increases fatty acid oxidation through selective activation of AMPK and CPT1, respectively. Pharmacologic or genetic inhibition of AMPK or CPT1 blunted ghrelin feeding-promoting effects (López et al., 2008). The effects of ghrelin on hypothalamic mitochondrial respiration and on food intake have been shown to be mediated by UCP2. Fatty acid β-oxidation promotes

generation of reactive oxygen species (ROS), which together with fatty acids, promote UCP2 transcription and activity. UCP2 activity neutralizes ROS, enabling continuous CPT1-promoted fatty acid β-oxidation (Horvath et al., 2008).

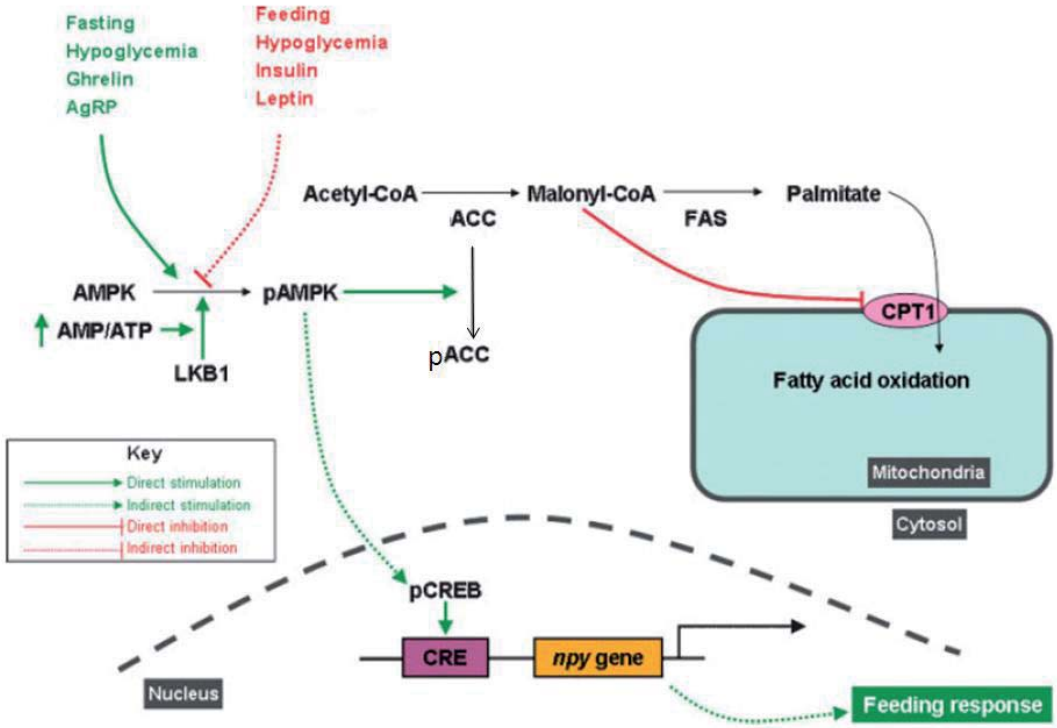

Figure 12. Mechanisms of AMPK regulation in the brain. In the hypothalamus, positive energy balance signals inhibit AMPK phosphorylation, whereas negative energy balance signals stimulate AMPK phosphorylation and activation. These signals are integrated and progress through alterations in the LKB1 pathway. A series of metabolic events (such as modulation of fatty acid synthesis) and gene transcription events (such as npy gene) is initiated, eventually leading to an inhibition or stimulation of the feeding response. (Modified from López et al., 2007)

In fact, affecting hypothalamic CPT1 activity also modifies feeding behaviour. Evidence shows that pharmacologic inhibition of CPT1 in the CNS of rodents, results in reduction of food intake and loss of body weight (Obici et al., 2003). In the mentioned work, Rossetti and colleagues decreased the activity of CPT1A by administering to rats a ribozyme-containing plasmid designed specifically to decrease the expression of this enzyme, or by icv infusion of pharmacological inhibitors of its activity (TDGA or ST1326). They found that either genetic or biochemical inhibition of CPT1 activity was sufficient to substantially decrease food intake and endogenous glucose production in peripheral tissues. These results indicate that changes in the rate of lipid oxidation in selective hypothalamic neurons signaled nutrient availability to the hypothalamus, which in turn modulates feeding behaviour, and the endogenous input of nutrients into the circulation (Obici et al., 2003).

It cannot be discarded that the effects on feeding behaviour are mediated by malonyl-CoA instead of being CPT1 activity itself or the acyl-CoA levels.

In fact, increasing evidence has implicated malonyl-CoA as a possible mediator in the hypothalamic pathway that indicates energy status and mediates the feeding behaviour of rodents:

FAS inhibition

The main evidence stems from the observation that potent pharmacologic inhibitors of FAS (C75 and cerulenin) suppress food intake causing substantial weight loss (primarily fat) in obese as well as lean mice (Loftus et al., 2000). The reduction of food intake is rapid (< 2 h) and dose-dependent and occurs either by inrtaperitoneal (ip) or icv administration of the inhibitors, being the icv delivery of C75 effective at much lower levels, consistent with a CNS site of action (Loftus et al., 2000; Hu et al., 2003). In addition, icv injection of C75 rapidly increases the concentration of malonyl-CoA in the hypothalamus (Hu et al., 2003). Concomitant with the rise in malonyl-CoA, neurons in the arcuate nucleus are activated (Gao and Lane, 2003) followed by down-regulation of key orexigenic and up-regulation of anorexigenic peptides in the hypothalamus (Loftus et al., 2000; Hu et al., 2003; Aja et al., 2006). However, prior injection of an ACC inhibitor, which blocks malonyl-CoA formation, blunts the C75-induced rise in hypothalamic malonyl-CoA concentration and prevents the suppression of food intake (Hu et al., 2003). These results suggest that levels of malonyl-CoA play a key role by acting both as a substrate of FAS and as an inhibitor of CPT1.

Genetic manipulation of MCD

Other studies have shown that delivery of viral MCD expression vector into the ventral medial hypothalamus of mice by bilateral stereotactic injection increases food intake and body weight gain and reverses the C75-mediated suppression of food intake (Hu et al., 2005). Similar effects were obtained when injecting a viral MCD vector in the medial basal hypothalamus of rats. These findings indicate that nutritional modulation of the hypothalamic abundance of malonyl-CoA is required to restrain food intake, and that a primary impairment in this central nutrient-sensing pathway is sufficient to disrupt energy homeostasis and induce obesity (He et al., 2006).

Physiological levels of malonyl-CoA in the hypothalamus

It has also been observed that nutritional and physiological perturbations also markedly alter hypothalamic malonyl-CoA concentration and food intake. In the fasted state (that produces hunger) hypothalamic malonyl-CoA concentration is low (0.1-0.2 µM), whereas re-feeding after fasting (that produces satiation) causes malonyl-CoA levels to rise to 1-1.4 µM (Hu et al., 2003).

In this context, it has been proposed that CPT1C may be a regulated target of malonyl-CoA in hypothalamic neurons that regulate food intake and peripheral energy expenditure. Given the fact that CPT1C binds malonyl-CoA with a K_D of ≈0.3 µM (Price et al., 2002) that lies within the dynamic range of hypothalamic malonyl-CoA concentration in fasted and refed states (≈0.1-1.4 µM), it is possible that CPT1C is a downstream target of malonyl-CoA. What is not known is the enzymatic role of CPT1C or how it is linked to a downstream regulatory target that controls food intake and/or energy expenditure (reviewed in Wolfgang and Lane, 2006; Lane et al, 2008).

The present study further examines the physiological role of CPT1C by fully characterizing the enzyme at the molecular level (analysis of the enzymatic activity, the subcellular localization, its membrane topology and its interacting proteins).

OBJECTIVES

OBJECTIVES

General objective:

To determine the physiological function of CPT1C.

Specific objectives:

1. *In silico* identification of potential residues disturbing CPT1C enzymatic activity through the construction of a 3-D structural model of CPT1C by homology modeling.

2. To determine the kinetic parameters of CPT1C in the yeast expression system.

3. To study the subcellular localization of CPT1C.

4. To determine the topology of this membrane spanning protein.

5. To identify interacting partners of CPT1C.

EXPERIMENTAL PROCEDURES

1. MOLECULAR BIOLOGY

1.1 Plasmid vectors

The following plasmid vectors were used for cloning strategies:

a) pYES 2

The pYES 2 plasmid vector (Invitrogene, ref. V825-20) is a high-copy vector of 5.9 kbp used for protein expression in yeast under the galactose promoter GAL1. It contains the ampicillin-resistance gene for selection in *E.coli*. It also contains a yeast gene, URA3, allowing yeast that carry this plasmid to grow on a synthetic medium lacking Ura.

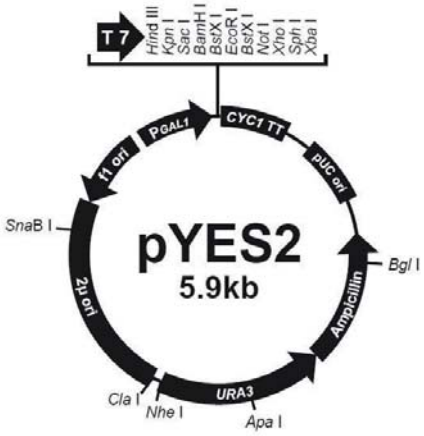

Figure 13: Map of pYES2 plasmid vector for protein expression in yeast.

b) pEG (KG)

The vector pEG(KG) is a plasmid vector of approx. 10 kbp and was used for expression of GST fusion proteins in yeast under the galactose promoter GAL1 (Mitchell et al., 1993). It contains the ampicillin resistance gene for selection in *E.coli* and the yeast gene, LEU2, for nutritional selection. The expressed fusion protein contains the GST moiety at the N-terminus of the protein cloned into the multiple cloning site (MCS).

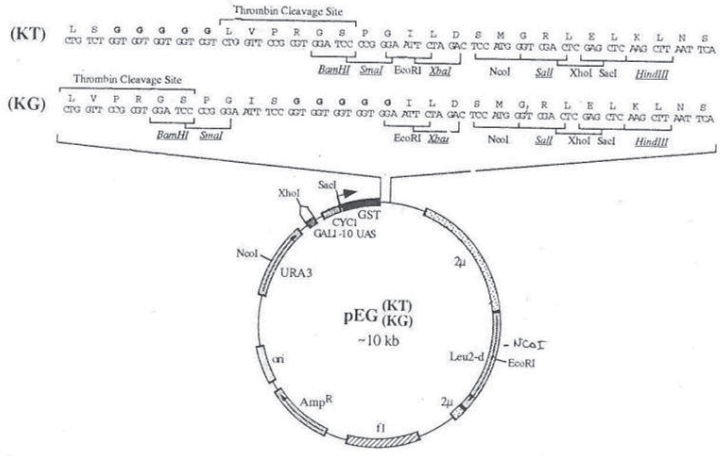

Figure 14. Map of pEG(KG) plasmid vector for GST fusion protein in yeast. The protein cloned into the MCS is C-terminally fused to the GST protein.

c) pGBT9

The pGBT9 plasmid vector (Clontech, ref. U07646) is a vector of 5.5 kbp that generates a hybrid protein that contains the sequences for the GAL4 DNA-binding domain (GAL4 DNA-BD) at the N-terminus of the protein cloned into de MCS. The fusion protein is expressed in yeast host cells and it is targeted to the yeast nucleus by nuclear localization sequences encoded by the GAL4 DNA-BD, making it suitable for a yeast two-hybrid assay. It carries the ampicillin resistance gene for selection in *E.coli* and the TRP1 nutritional marker that allow yeast auxotrophs carring pGBT9 to grow on limiting synthetic medium lacking Trp.

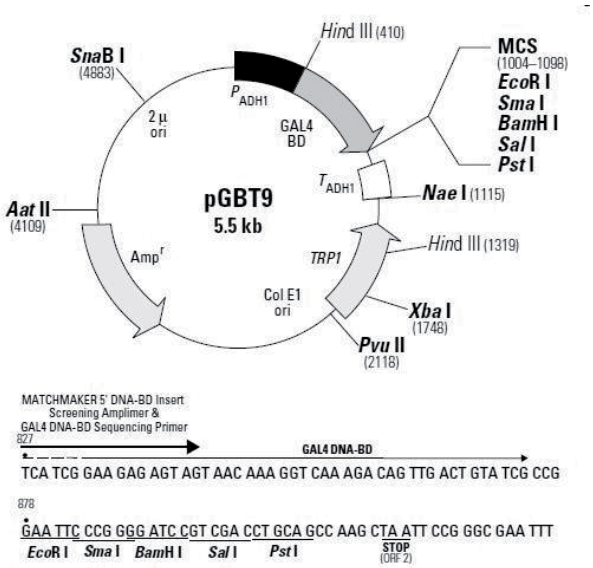

Figure 15. Map of pGBT9 plasmid vector for expressing a fusion protein containing the GAL4 DNA-binding domain (GAL4 DNA-BD) at the N-terminus of the protein cloned into de MCS, to perform a two-hybrid assay.

d) pBluescript II SK (+/-) phagemid

The pBluescript II SK (+) (Stratagene. ref. 212205) is a 2.9 kbp phagemid derived from pUC19. The SK designation indicates the polylinker is oriented such that lacZ transcription precedes from Sac I to Kpn I. It contains the ampicillin resistance gene.

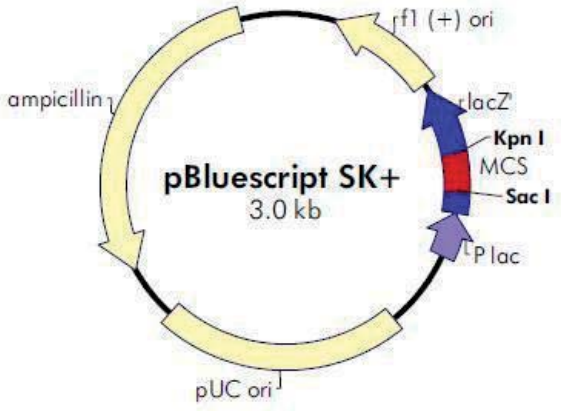

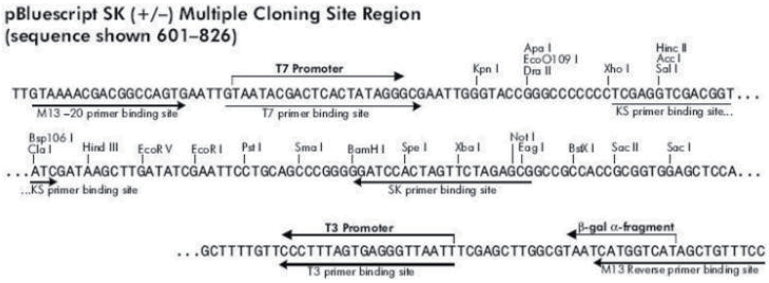

Figure 16. Map for pBluescript plasmid vector and its MCS used for subcloning purposes. This plasmid can be also used for site directed mutagenesis.

e) pGEX-6P-1

The pGEX-6P-1 plasmid vector (Amersham Biosciences, ref. 27-4597-01) is a GST gene fusion vector of approx. 4.9 kbp that allows bacterial expression and purification of desired target proteins in high yields with high levels of enrichment. The expressed protein encodes the GST moiety at the N-terminus end of the protein cloned into the MCS. It also encodes the recognition sequence for site-specific cleavage by PreScission Protease between the GST domain and the MCS, in order to remove the GST tagging if desired. It contains ampicillin resistance gene for plasmid selection.

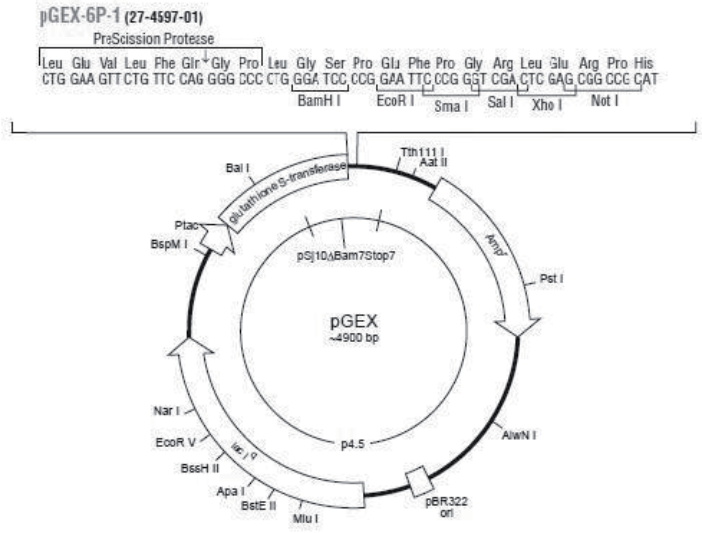

Figure 17. Map for pGEX-6P-1 plasmid vector for expressing a GST fusion protein in *E. coli*. The fusion protein encodes the GST moiety at the N-terminus of the protein cloned into the MCS.

f) pEGFP-N3

The pEGFP-N3 plasmid vector (BD Biosciences, ref. 6080-1) is a plasmid vector of approx. 4.7 kbp designed to allow expression of proteins fused to the N-terminus end of the enhanced green fluorescent protein (EGFP). The recombinant EGFP vector can be transfected into mammalian cells using standard transfection methods. The vector contains the ampicillin resistance gene and the pUC19 origin of replication for propagation in *E.coli*.

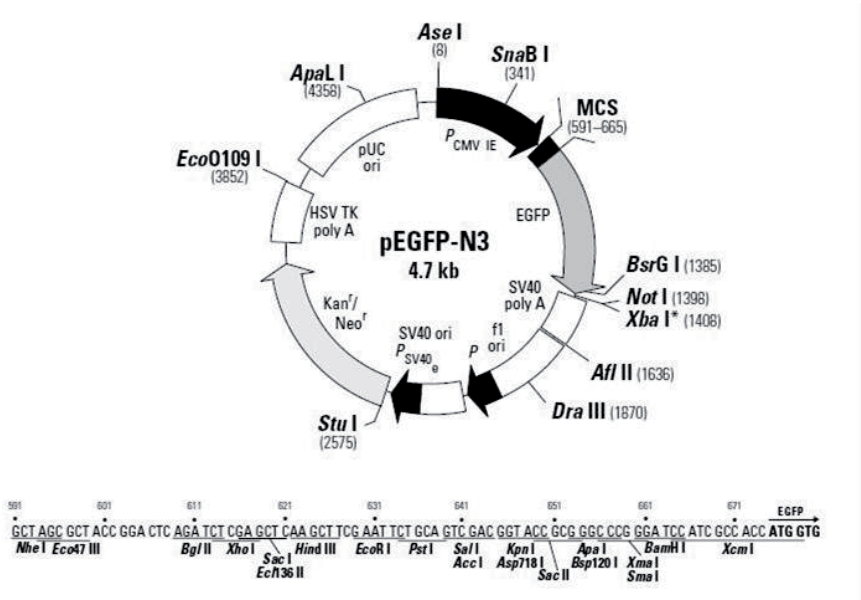

Figure 18. Map for pEGFP-N3 plasmid vector which encodes the EGFP variant C-terminally tagged to the protein cloned into the MCS. It is suitable for expression in mammalian cells in culture.

g) pIRES2-EGFP

The pIRES2-EGFP plasmid vector (BD Biosciences, ref. 6029-1) is a vector of approx. 5.3 kbp designed to translate the protein cloned into the multiple cloning site and the enhanced green fluorescent protein (EGFP) from a single bicistronic mRNA. The vector contains the SV40 origin of replication for expression in mammalian cells. It also contains the Kanamycine/Neomycin resistance gene for bacterial or mammalian cells selection and a suitable origin of replication for bacterial propagation.

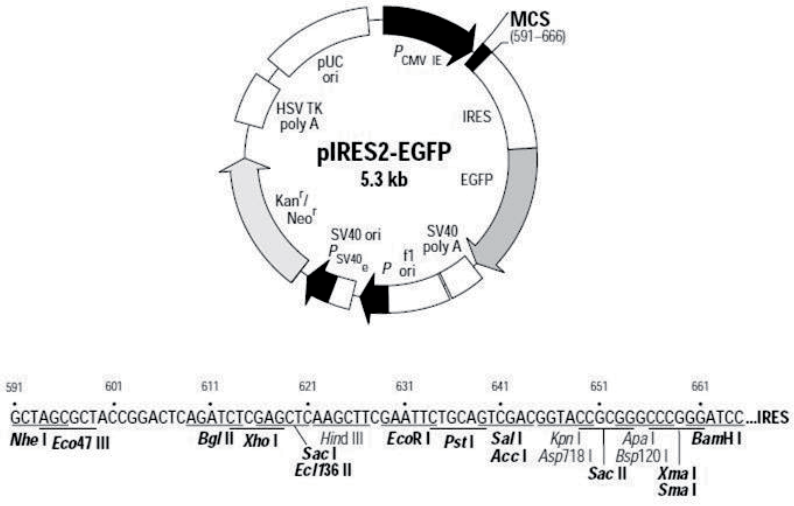

Figure 19. Map of pIRES2-EGFP for expression in cultured mammalian cells of EGFP and the protein cloned into the MCS in two different reading frames.

1.2 Plasmid DNA preparation and subcloning strategies

Plasmid DNAs were obtained from bacterial cultures containing the plasmid of interest, growing them in LB medium with the appropriate antibiotic and the later purification of the plasmid DNA from the cell lysate.

Minipreparations of plasmid DNA were obtained using the *Minipreps DNA Purification System* (Promega, A1330) where the yield of high-copy-number plasmids obtained is about 3-5 µg DNA per millilitre of the original bacterial culture. When higher amounts of plasmid DNA were needed, the *QUIAGEN Plasmid Maxi kit* (QUIAGEN, ref. 12163) was used. In this case up to 500 µg DNA could be obtained.

For subcloning strategies: enzymatic restriction, DNA dephosphorylation and ligation were performed following standard methods.

1.3 PCR DNA amplification

The polymerase chain reaction, PCR, was used to amplify DNA fragments to be cloned.

For the PCR reaction mix and PCR conditions standard methods were used with slight modifications for different amplifications (see specific annealing temperatures in Table 3).

1.4 DNA sequencing

For DNA sequencing the *ABI PRISM® BidDye Terminator v3.1 Cycle Sequencing Ready reaction Kit* was used following the manufacturer's instructions.

Samples were analyzed in an *ABI PRISM 3700 DNA Analyzer* (Applied Biosystems) at the Scientific-Technique Services of the "Universitat de Barcelona".

1.5 DNA resolution and purification

1.5.1 DNA resolution in agarose gels

The agarose gels were prepared with low-melting-temperature agarose dissolved in 1x TAE electrophoresis buffer containing 0.5 µg/ml ethidium bromide (Genaxis, ref. GX12420). Samples are loaded in 1x loading buffer and electrophoresis is run with 1x TAE electrophoresis buffer at 75- 100 V.

1x TAE electrophoresis buffer: 40 mM Tris-acetate pH 8.3, 1 mM EDTA

10x sample loading buffer: 0.42% bromophenol blue, 0.42% xylene cyanol FF, 50% glycerol in bidistilled water.

1.5.2 DNA purification

To extract and purify a DNA fragment from the agarose gel the *QIAquick Gel Extraction kit* (QUIAGEN, ref. 28706) was used. Briefly, the agarose gel fragment containing the desired DNA is dissolved in a chaotropic agent and the DNA is selectively adsorbed into a silica resin which has been optimized to enhance recovery of 40 bp to 50 kbp DNA fragments. Impurities such as RNA, proteins, salts and other components of the sample are removed during washing steps. The pure DNA is eluted in water and is suitable for other manipulations.

1.6 DNA and RNA spectrophotometric quantification

RNA and DNA were quantified in a spectrophotometer measuring the absorbance at 260 and 280 nm in 1 ml quartz cuvettes.

1.7 Plasmid constructs

Different plasmid constructs were generated for specific objectives. The obtained plasmid constructs and a brief description of the strategy followed for each were (for primer sequence and other specific information see Table 3):

1. **pGEX- C-term CPT1C**: C-terminal 115 amino acids of rat CPT1C (2056-2406 bp) with engineered BamHI ends (using primers: F4RnCPT1C and R3RnCPT1C) were PCR amplified and subsequently cloned into BamHI site of pGEX-6P-1.

2. **pCPT1A-EGFP**: from base pair 1 to 2319 of rat CPT1A cDNA sequence (excluding the stop codon to allow fusion with EGFP) was amplified using primers F3RnCPT1A and R3RnCPT1A, that introduced HindIII and EcoRI sites at each end, respectively. Primer reverse sequence also introduced base pairs needed to maintain the reading frame that allowed correct fusion with EGFP.

3. **pCPT1C-EGFP:** from base pair 1 to 2403 of rat CPT1C cDNA sequence (also excluding stop codon) was amplified using primers F1bisRnCPT1C and R5RnCPTca that introduced BamHI sites at each end. Primer reverse sequence also introduced base pairs to maintain the reading frame with EGFP.

4. **pCPT1·AC-EGFP**: 465 bp of 5' end of rat CPT1A sequence (which encodes the two trans-membrane domains and the mitochondrial import signal described by the Prip-Buus group) was amplified with primers F3RnCPT1A and R6RnCPT1A, incorporating HindIII and HpaI sites, respectively. The amplified segment was cut with the respective enzymes and pCPT1C-EGFP plasmid was also digested with HindIII and XmnI (which generates blunt end as HpaI does). The desired fragments were excised from an agarose gel and purified for ligation.

5. **pCPT1·CA-EGFP**: 462 bp of 5' end of rat CPT1C sequence was amplified using F7RnCPT1C and R7RnCPT1C primers, that incorporated HindIII and PpuMI sites, respectively. The amplified fragment and the pCPT1A-EGFP plasmid (from a Miniprep of BL21 transformed with the plasmid because PpuMI is sensitive to dcm methylation) were cut with the respective enzymes. The desired fragments were excised from an agarose gel and purified for ligation.

6. **pYES·ACA**: A chimera containing the catalytic core of CPT1C (from aa position 171 to 664) and N- and C-terminus of CPT1A in pYES2 was constructed. CPT1C core was amplified with primers F6RnCPT1C and R4RnCPT1C introducing AatII and SalI sites, respectively. The amplified fragment and pYES-CPT1A were cut with AatII and SalI, and the desired fragments were excised and purified from agarose gel for subsequent ligation.

7. **pGBT9-HsCPT1C**: A fragment from base pair position 393 to the end of the cDNA sequence was amplified with primers F1HsCPT1C and R1HsCPT1C containing BamHI ends. This fragment was subcloned into BamHI of pGBT9.

8. **pGBT9-MmCPT1C**: A fragment from base pair position 393 to the end of the cDNA sequence was amplified with primers F1MmCPT1C and R1MmCPT1C containing SmaI and SacI ends respectively. This fragment was subcloned into the same sites of pGBT9.

9. **pIRES-Loop** was obtained using site-directed mutagenesis with primers that introduced G→C change at base pair 258 and an A→C mutation at base pair 263 wich changed two codons in positions 85 and 88 from KIK to NIT. Site mutagenesis was performed in pBluescript containing full length cDNA of CPT1C and confirmed by direct sequencing. The correct clones were further sublcloned into pIRES using BamHI sites and the direction of the insert was confirmed by enzymatic restriction with SacI.

10. **pIRES-Nterm** was created by PCR amplifying the sequence of the first 63bp from rat CPT1C cDNA with a forward primer incorporating a SacI site (also contained in the MCS of pIRES), and a 3' primer adding base pairs for incorporating the amino acids NIT (asparagine, isoleucine and threonine) at base pair 63, after a Valine in position 22, and 3' flanked by a SacI. Then pIRES-CPT1C was digested with SacI and the biggest fragment was gel purified for further ligation with the PCR fragment already digested with SacI.

The recovery of the amplified fragments was done with the *QIAquick PCR purification kit* (QUIAGEN, ref. 28104) or through excision of the desired fragment from the agarose gel and purification with the *QIAquick Gel Extraction kit* (QUIAGEN, ref. 28706).

All constructs were confirmed by enzymatic restriction and direct sequencing.

Information in Table 3:

- **Insert (subcloned fragment in bp)**: The information between brackets refers to the nucleotides from the cDNA sequence that were subcloned into the plasmid vector, nucleotide positions are indicated in base pairs. The inserts were obtained using PCR amplification using primers described in the corresponding columns.
- **Primer Fwd (restriction enzyme)**: The restriction enzyme indicated between brackets corresponds to the 5' engineered site for subcloning. The sequence is indicated in 5'→3' direction.
- **Primer Rev (restriction enzyme)**: The restriction enzyme indicated between brackets corresponds to the 3' engineered site for subcloning. The sequence is indicated in 5'→3' direction.
- **Annealing temperature**: temperature used for each set of primers in the annealing step of the PCR (expressed in °C).
- **Antibiotic resistance**: Antibiotic resistance beard by the plasmid vector and used for plasmid propagation in *E. coli* cells.

Nº	Plasmid construct	Insert (subcloned fragment in bp)	Cloning sites	Primer Fwd (Restriction enzyme)	Primer Rev (Restriction enzyme)	Annealing temperature	Antibiotic resistance
1	pGEX-Cterm CPT1C	Rn CPT1C C-terminus (2056-2406bp)	BamHI	F4 Rn CPT1C (BamHI) 5' ggatccgtgcagcagacacacctgttc 3'	R3 Rn CPT1C (BamHI) 5' ggatcctcacaagttggtggaggatttg3'	56	Ampicillin
2	pCPT1A-EGFP	Rn CPT1A without stop codon (1-2421bp)	HindIII/EcoRI	F3 Rn CPT1A (HindIII) 5' tgctaagcttatggcagaggctcaccaag 3'	R3 Rn CPT1A (EcoRI) 5' ccgaccgcggagaattctttttagaattgatggtg 3'	60	Kanamycin
3	pCPT1C-EGFP	Rn CPT1C without stop codon (1-2403bp)	BamHI	F1bis Rn CPT1C (BamHI) 5' cgcggatcctataaaatggctgaggcacaccaggc 3'	R5 Rn CPT1C (BamHI) 5' cgcggatcccaagttggtggaggatttggg 3'	60	Kanamycin
4	pCPT1·AC-EGFP	Rn CPT1A (1-480bp)	HindIII/XmnI	F3 Rn CPT1A (HindIII) 5' tgctaagcttatggcagaggctcaccaag 3'	R6 Rn CPT1A (HpaI) 5' agaggttaaccttgaccatagccatccagatctt 3'	63	Kanamycin
5	pCPT1·CA-EGFP	Rn CPT1C (1-474bp)	HindIII/PpuMI	F7 Rn CPT1C (HindIII) 5' cgcaagctttataaaatggctgaggcacac 3'	R7 Rn CPT1C (PpuMI) 5' ctgagaggaccttgaccaatgccagccaggt 3'	63	Kanamycin
6	pYES·ACA	Rn CPT1C (511-1993 bp)	AatII/SalI	F6 Rn CPT1C (AatII) 5' gacgtcctcccgcggcagccagtgcccgga 3'	R4 Rn CPT1C (SalI) 5' gtcgacgtggagaagccgggacatgatg 3'	60	Ampicillin
7	pGBT9-HsCPT1C	Hs CPT1C (393-2412bp)	BamHI	F1 Hs CPT1C (BamHI) 5' cgcggatcctgtcctaccacggctggcttc 3'	R1 Hs CPT1C (BamHI) 5' cgcggatcctcagaagtcggtggatgtc 3'	62	Ampicillin
8	pGBT9-MmCPT1C	Mm CPT1C (393-2403bp)	SmaI/SalI	F1 Mm CPT1C (SmaI) 5' tcccccggggtcccaccatggctggcttc 3'	R1 Mm CPT1C (SalI) 5' gccgacgtcgactcacaagttggtggaggatgt 3'	52	Ampicillin
9	pIRES-Loop	Site-directed mutagenesis (Glycosylation site at loop region)	Changes at bp 258 (G→C) and 263 (A→C)	F10 Rn CPT1C 5' ccctaggactgatggagaacattacagagttgctgccagactgg 3'	R9 Rn CPT1C 5' ccagtctggcagcaactctgtaatgttctccatcagtcctaggg 3'	68	Kanamycin
10	pIRES-Nterm CPT1C	Glycosylation site at Nterminus (1-63bp)	SacI	F2 pIRES (SacI) 5' gatctcgagctcaagcttcga 3'	R10 RnCPT1C (SacI) 5' cccgagctctgtaatgttcacttctgccccgtcggaactgag 3'	60	Kanamycin

Table 3. Plasmid constructs engineered for this study. Features and abbreviations described in the text.

1.8 Bradford method for protein quantification

Protein was measured according to the manufacturer's instructions (BioRad protein assay, ref. 500-001 MT), using BSA as a protein standard in the range of 2-25 µg/ml. BSA standard stock was prepared in water at 0.1 mg/ml and the absorbance of the blank, standard curve or the samples was measured at 595 nm in a spectrophotometer with plastic cuvettes in a total volume of 1 ml.

1.9 Protein separation and Western blot

SDS-PAGE electrophoresis was used to separate proteins by their molecular weight using different percentages depending on the predicted weight of the protein to be analyzed.

When Western blot was not being performed, the gel at the end of the electrophoresis was stained with Bio Safe Coomassie (BioRad, ref. 161-0786) to evaluate the protein content of the sample.

When Western blot was to be performed, the proteins in the gel were transferred to Immobilon PVDF membranes (Millipore, ref. IPVH 00010). The side of the membrane in contact with the gel was marked to identify the side where proteins were, for later antibody incubation and detection. The transference is performed at 4^{o}C for 2 h at 300 mA. Once it is finished, membrane is immersed in blocking solution for 1 h and the gel is stained with Bio Safe Coomassie to determine the degree of transferred protein.

2x Protein Loading Buffer: 130 mM Tris-HCl pH 6.8, 6% SDS, 15% β-mercaptoethanol, 20% sucrose and 0.05% bromophenol blue. It is prepared freshly at the moment of use.

5x Electrophoresis buffer : 25 mM Tris, 250 mM glycine and 0.1% SDS. It is stored at room temperature.

Transfer buffer: 12 mM Tris, 20% methanol and 96 mM glycine. It is stored at 4^{o}C.

1.9.1 Antibody incubation

Blocking the membrane:

Non-specific binding sites are blocked by immersing the membrane in blocking solution for 1 h on an orbital shaker at room temperature. After this time, membrane is rinsed and washed three times for 5 min in TBS-T on an orbital shaker.

Primary antibody incubation:

Incubations were done overnight at 4^{o}C on an orbital shaker. After this time, membranes were rinsed and washed three times for 5 min in TBS-T on an orbital shaker. The first antibody could be reused by storing it at -20^{o}C.

Primary antibodies used were:

- **Anti CPT1A**: rabbit CPT1A specific polyclonal antibody against amino acids 317-430 of the rat liver CPT1A (Prip-Buus). Diluted 1/1,000 in blocking solution.
- **Anti CPT1C**: rabbit CPT1C specific polyclonal antibody against the last 14 amino acids of the *Mus musculus* sequence of CPT1C (Sigma Genosys). Diluted 1/500 in blocking solution.
- **Anti CPT1C-Nterminus**: rabbit CPT1C specific polyclonal antibody against amino acids 11-27 of the *Mus musculus* sequence of CPT1C (Genscript). Diluted 1/100 in blocking solution.
- **Anti GST**: goat polyclonal antibody against Glutathione S-Transferase (Abcam, Ref. ab6613). Diluted 1/10,000 in blocking solution.

Secondary antibody incubation:

Incubations were performed for 1 h at room temperature on an orbital shaker. After this time, membranes were rinsed and washed three times for 5 min in TBS-T on an orbital shaker.

Secondary antibodies were detected using ECL reagent (Amersham Biosciences, ref. RPN 2106).

Secondary antibodies used were:

- **Donkey anti- rabbit IgG** (Amersham Biosciences, ref. NA 9340) was used for detecting CPT1A or CPT1C primary antibodies. A dilution of 1/5,000 in blocking solution was used.
- **Donkey anti- goat IgG** (Santa Cruz Biotechnologies, ref. SC-2020) for GST antibody detection. It was used in 1/10,000 dilution in blocking solution.

TBS-T: 0.1% Tween20 in 1X TBS (20 mM Tris, 137 mM NaCl, 3.9 mM HCl). It is stored at room temperature.

Blocking solution: 5% (w/ v) nonfat dried milk in TBS-T.

1.9.2 Reprobing membranes

Following ECL detection the membranes may be stripped of bound antibodies and reprobed several times. The membranes were stored wet and wrapped in a refrigerator (2–8°C) after each immunodetection.

The complete removal of primary and secondary antibodies from the membrane was possible following the protocol outlined below.

1. Submerge the membrane in stripping buffer (100 mM 2-Mercaptoethanol, 2% SDS, 62.5 mM Tris-HCl pH 6.7) and incubate at 50°C for 30 minutes with occasional agitation.
2. Wash the membrane for 3 × 10 minutes in TBS-T at room temperature using large volumes of wash buffer.

2. MICROBIOLOGY

2.1 Bacteria

2.1.1 Bacterial strains and growth conditions

The *Escherichia coli (E. coli)* strains used in this study are: BL21 for bacterial expression of recombinant proteins (a protease deficient strain) and DH5α for plasmid propagation.

- **BL21***: E. coli* B F^-, ompT, hsdS (r_B^-, m_B^-), gal, dcm.
- **DH5α**: F^- / endA1 glnV44 thi-1 recA1 relA1 gyrA96 deoR nupG Φ80d*lacZ*ΔM15 Δ(*lacZYA-argF*) U169, hsdR17(r_K^- m_K^+), λ–

They were grown in autoclaved LB liquid broth or LB agar plates made from Pronadisa powder (Luria Broth Cat. 1551.00 and Luria Agar Cat. 1552.00, respectively) with the antibiotic necessary for plasmid selection.

2.1.2 Preparation of competent *E. coli* cells

Competent cells are those cells which have been treated to increase their capacity to introduce a circular exogenous DNA. They are obtained by concentration through successive washes in water and 10% glycerol.

Competent cells were prepared in the laboratory following the next protocol:

1. A single colony of *E. coli* cells is inoculated into 5 ml LB medium with the appropriate antibiotic and grown o/n at 37ºC with moderate shaking.
2. The next day, 500 ml of LB plus antibiotic is inoculated with the 5 ml preinocul and grown for approx. 2 h in the shaker at 37ºC to an OD_{600} of 0.5-0.6.
3. Cells are then chilled on ice for 10 min and centrifuged at 1,600 x *g* for 15 min at 4ºC (centrifugation stopped without brake).
4. Cells should be kept at 4ºC for the subsequent steps.
5. After that, the pellet is immediately resuspended in 10 ml of sterile and ice-cold $CaCl_2$
6. Centrifuge again at 1,100 x *g* for 5 min at 4ºC.
7. Resuspend the pellet in 10 ml of sterile and ice-cold $CaCl_2$.
8. Centrifuge again at 1,100 x *g* for 5 min at 4ºC.
9. Discard the supernatant and resuspend the pellet in 2 ml $CaCl_2$.
10. 100 µl aliquots are stored at -80ºC.

$\underline{CaCl_2}$: 60 mM $CaCl_2$, 15% glycerol, 10mM PIPES pH 7. Filter the solution and store at 4ºC.

2.1.3 Bacterial transformation protocol

The transformation process consists of introducing the plasmid DNA into the competent bacterial cells for later amplification, plasmid purification or protein expression.

Plasmid DNA was introduced by the heat-shock method as follows:

1. Thaw competents *E. coli* cells (DH5α or BL21) on ice.
2. Add 1-5 µl of DNA in each transformation tube.
3. Add 50-100 µl competent cells in a 13 ml polystyrene tube (Sarstedt 55.468.001). To transform a DNA construct use 30-50 µl of competent cells. In order to transform a ligation use 100 µl of competent cells. Mix by pipetting up and down only once.
4. Incubate the tubes on ice for 30 min.
5. Heat-shock the cells for 1 min 30 s at 42°C.
6. Put tubes back on ice for 2 min.
7. Add 1 ml of LB (with no antibiotics). Incubate tubes for 1 hour at 37ºC with vigorous shaking (250rpm).
8. Spin down briefly in a microcentrifuge. Remove supernatant and resuspend the cell pellet with 100 µl of LB medium in the tube by softly pipetting.
9. Plate out the suspension on an LB agar plate containing the appropriate antibiotic and incubate the plates up-side-down overnight at 37°C.
10. Pick colonies about 12-16 hours later.

2.1.4 GST fusion protein expression in bacteria

The Glutathione S-transferase (GST) Gene Fusion System is a system for the expression, purification, and detection of fusion proteins produced in *E. coli*. The system is based on IPTG inducible, high-level expression of genes or gene fragments as fusions with *Schistosoma japonicum* GST (Smith et al., 1988). Expression in *E. coli* yields fusion proteins with the GST moiety at the amino terminus of the protein cloned into de MCS. The fusion protein accumulates within the cell's cytoplasm.

GST-Cterminal CPT1C fusion protein (last 117 amino acids of CPT1C, fused to GST) was expressed in BL21 *E. coli* as follows:

1. Inoculate one single colony of the bacterial strain expressing the construct (Cterminal end of CPT1C fused to GST cloned into pGEX-6P-1) into 30 ml aliquot of LB broth containing ampicillin (Ampicillin from Roche, Ref. 93175220) (Change volumes depending on expression scale. For

smaller culture volumes downscale volumes of all subsequent steps). Grow overnight at 37^{o}C with 200rpm shaking.
2. Inoculate 3 L of LB with antibiotic with 30 ml of the overnight culture from step 1.
3. Grow the culture at 37^{o}C with shaking to an OD_{600} of 0.35 (this should take 2-3 hours).
4. Continue to grow the culture at 18^{o}C to an OD_{600} of 0.5 (this should take 2-3hours).
5. Induce the expression of the protein by adding IPTG to a final concentration of 100 µM.
6. Incubate the culture for an additional overnight at 18^{o}C with shaking.
7. Centrifuge the bacterial culture for 15minutes at 3200 x g.
8. Discard the supernatant.
9. Freeze the pellets at -70^{o}C.

100 mM IPTG: Dissolve 500 mg of isopropyl-β-D-thiogalactoside (IPTG) in 20 ml of distilled H_2O. Filter-sterilize and store in small aliquots at -20 °C.

2.1.5 GST fusion protein purification

Expressed GST fusion proteins are purified from bacterial lysates by affinity chromatography using a batch-based method (Glutathione Sepharose 4B.). GST fusion proteins are captured by the affinity medium, and impurities are removed by washing. Fusion proteins are eluted under mild, non-denaturing conditions using reduced glutathione. The purification process preserves protein antigenicity and function. If desired, cleavage of the protein from GST can be achieved using a site-specific protease (Prescission Protease) whose recognition sequence is located immediately upstream from the multiple cloning site on the pGEX plasmids.

The purification of GST-Cterminal CPT1C fusion protein was performed as described below:

1. Thaw and resuspend the pellets from 3 L expression in 50 ml of Breaking Buffer preheated at 37^{o}C. (For smaller culture volumes downscale volumes of all subsequent steps).
2. Incubate in a water bath at 37^{o}C for 10 min.
3. Sonicate the bacterial suspension on ice, in short 5 second-bursts alternated with 5 seconds of resting on ice. Thirty cycles at an amplitude of 50% and cycle 4 in an ultrasonic processor UP50H (Hielscher, GmbH).
4. Centrifuge the bacterial lysate at 13,000 x g for 10min at 4^{o}C to remove insoluble material.
5. Transfer the supernatant to a fresh tube.
6. Add 500 µl of ATP solution and incubate in a water bath at 37^{o}C for 10min (in order to avoid co-purification of some chaperonins with GST).
7. Centrifuge at 1,300 x g for 5min at 4^{o} C to remove additional insoluble material.
8. Transfer the supernatant to a fresh tube.
9. Add 1 ml of 50% slurry of glutathione-Sepharose beads (Glutathione Sepharose 4B, Pharmacia Biotech, Ref. 17-0756-01) preequilibrated in PBS.
10. Incubate for 30 minutes at 4^{o}C, rotating the tube end over end to ensure mixing.
11. Centrifuge at 500 x g for 5 minutes at 4^{o}C to pellet the beads.
12. Carefully discard the supernatant (do not disrupt the pellet).
13. Wash the beads twice in 5 ml of ice-cold PBS by centrifuging at 500 x g for 5 minutes at 4^{o}C. Remove the supernatant.
14. Gently resuspend the beads in 5 ml of Prescission buffer.
15. Add 0.5 mL of Prescission solution.
16. Incubate overnight at 4^{o}C, rotating the tube end over end.
17. Centrifuge at 500 x g for 5 minutes at 4^{o}C.
18. The supernatant now contains the expressed protein while GST and Prescission protease remain bound to the beads.

Breaking buffer: 1x PBS pH 7.3, 10 mg/ml DNAse I, 10 mg/ml RNAse, 1 mg/ml Lysozyme

ATP solution: 0.4 M ATP (Roche), 1 M Magnesium sulphate heptahydrate (Merck), 1M Tris HCl, pH 7.0

Prescission buffer: 50mM Tris-HCl pH 7.0, 150mM NaCl, 1mM EDTA, 1mM DTT

Prescission solution: 480 µl Prescission buffer, 20 µl PreScission Protease (Pharmacia Biotech, Ref. 27-0843-01) (2 U/100 µg of bound GST-fusion protein)

2.1.6 Solubilization of inclusion bodies

High-level expression of foreign fusion proteins in *E. coli* often results in formation of inclusion bodies. Inclusion bodies comprise dense, insoluble aggregates that are failed folding intermediates (Martson, 1986; Hober et al., 1999). Formation of inclusion bodies can be advantageous in purifying an active form of an expressed fusion protein that otherwise may be unstable in the soluble fraction. However, the steps needed to solubilize and refold the fusion protein can be highly variable and may not always result in high yields of active protein.

The final protocol used to solubilize the inclusion bodies was as follows:

1. Thaw and resuspend the pellets from 50 ml of an overnight induction of the GST-fusion protein in 4 ml of Lysis solution preheated at 37^{o}C.
2. Incubate in a water bath at 37^{o}C for 10 min.
3. Sonicate the bacterial suspension on ice, in 5 seconds-bursts alternated with 5 seconds of resting on ice. Fifty cycles at an amplitude of 60% and cycle 5 in an ultrasonic processor UP50H (Hielscher, GmbH).
4. Centrifuge the bacterial lysate at 13000 xg for 10 min at 4^{o}C.
5. Freeze the supernantant in a new tube. Resuspend the pellet in 1.5 ml of Isolation Buffer. Sonicate as above.
6. Centrifuge the bacterial lysate at 13000 xg for 10 min at 4^{o}C.
7. Repeat steps 5 and 6.
8. Resuspend the pellet in 2.5 ml of Solubilization Buffer.
9. Stir for 60 min at room temperature with soft orbital agitation.
10. Centrifuge the sample at 13000 xg for 15 min at 4^{o}C.

Lysis solution pH 8: 20 mM Tris HCl pH 8, 10 mg/ml DNase, 10 mg/ml RNase, 1 mg/ml Lysozyme

Isolation Buffer: 2 M Urea, 20 mM Tris HCl pH 8.0, 0.5 M Na Cl, 2% Triton X-100

Solubilization Buffer: 20 mM Tris HCl pH 8, 6 M Guanidine hydrochloride (Sigma), 0.5 M NaCl, 1 mM Beta-mercaptoethanol (Sigma)

2.2 Yeast

The yeast strain used in most of the studies was *Saccharomyces cerevisiae* w303-1A. In the yeast two-hybrid assay *Saccharomyces cerevisiae* AH109 (Clontech, ref. 630444) was used. This yeast strain is designed for detecting protein interactions during a two-hybrid screening.

The genotypes of these strains are:

- **W303- 1A**: MATa {leu2-3,112 trp1-1 can1-100 ura3-1 ade2-1 his3-11,15}
- **AH109**: MATa, trp1-901, leu2-3, 112, ura3-52, his3-200, gal4Δ, gal80Δ, LYS2 : : $GAL1_{UAS}$-$GAL1_{TATA}$-HIS3, $GAL2_{UAS}$-$GAL2_{TATA}$-ADE2, URA3 : : $MEL1_{UAS}$-$MEL1_{TATA}$-lacZ

These strains were grown in autoclaved, complete YPD medium (1% yeast extract, 2% peptone and 2% dextrose). The strains that bear a plasmidic DNA should be grown in the minimal dropout medium for nutritional selection of the yeast cells that carry the desired plasmid vector.

Complete minimal dropout medium (SD), per liter:

- 1.3 g dropout powder (lacks a single amino acid, or more but contains the rest)
- 1.7 g Yeast Nitrogen base without amino acids or ammonium sulfate
- 5 g $(NH_4)_2SO_4$ (ammonium sulphate)
- 20 g dextrose

For solid media, agar is added at a concentration of 2%. A pellet of sodium hydroxide should be added per liter to raise de pH enough to prevent agar breakdown during autoclaving.

2.2.1 Lithium Acetate mediated yeast transformation

The method chosen for introducing foreign DNA into yeast was the lithium acetate (LiAc)-mediated method (reviewed in Guthrie & Fink, 1991).

When setting up any type of transformation experiment, be sure to include proper controls for evaluating transformation efficiencies.

The protocol for transformation of yeast cells was performed as follows (for large scale transformations, upscale all volumes described here):

1. Inoculate 5 ml of YPD or SD with several colonies, 2–3 mm in diameter.
   (Note: For host strains previously transformed with another autonomously replicating plasmid, use the appropriate SD selection medium to maintain the plasmid.**)**
2. Incubate at 30°C overnight with shaking at 250 rpm to stationary phase (OD_{600}>2.5).
3. Transfer 5 ml of overnight culture to a flask containing 50 ml of YPD. Check the OD_{600} of the diluted culture and, if necessary, add more of the overnight culture to bring the OD_{600} up to 0.2–0.3.
4. Incubate at 30°C for 3 hr with shaking (250 rpm). At this point, the OD_{600} should be 0.4–0.6.
5. Place cells in 50-ml tube and centrifuge at 800 x g for 3 min at room temperature (20–21°C).
6. Discard the supernatant and thoroughly resuspend the cell pellet in 1 ml of sterile 1x TE/ 1x LiAc. (Prepare 1x solution fresh just prior to use .To prepare 10 ml of 1x TE/ LiAc solution mix: 8 ml of sterile deionized H_2O, 1 ml of 10x TE and 10x LiAc.)
7. Centrifuge at 1,800 x g for 3 min at room temperature.
8. Decant the supernatant.
9. Resuspend the cell pellet in 300 µl of freshly prepared, sterile 1x TE/1x LiAc.
10. Add 1-5 µl (0.1 µg) of plasmid DNA and 10 µl (0.1 mg) of herring testes carrier DNA to a fresh 1.5-ml tube and mix.
11. Add 100 µl of yeast competent cells to each tube and mix well by vortexing.
12. Add 600 µl of sterile 1x PEG/LiAc solution to each tube and mix. (Also prepare fresh prior to use. To prepare 10 ml of 1x PEG/ LiAc solution mix: 8 ml of 50% PEG, 1 ml of 10x TE and 10x LiAc.)
13. Incubate at 30°C for 30 min with shaking at 100 rpm.
14. Add 70 µl of DMSO. Mix well by gentle inversion. Do not vortex.
15. Heat shock for 15 min in a 42°C water bath.
16. Chill cells on ice for 1–2 min.
17. Centrifuge cells for 1 min at 800 x g at room temperature. Remove the supernatant.
18. Resuspend cells in 100 µl of sterile YPD.
19. Plate 100 µl on each SD agar plate that will select for the desired transformants.
20. Incubate plates, up-side-down, at 30°C until colonies appear (generally, 2–4 days).

10x Lithium acetate: 1 M lithium acetate (Sigma Cat No. L-6883). Adjust to pH 7.5 with diluted acetic acid and autoclave.

10x TE buffer**:** 0.1 M Tris-HCl, 10 mM EDTA, pH 7.5. Autoclave.

50% PEG 3350: (Polyethylene glycol, avg. mol. wt. = 3,350; Sigma Cat No. P-3640) prepare with sterile deionized H_2O; if necessary, warm solution to 50°C to help the PEG go into solution.

100% DMSO: (Dimethyl sulfoxide; Sigma Cat No. D-8779)

2.2.2 Protein expression in yeast

The plasmid pEG(KT) (see section named "Plasmid vectors") is a widely used plasmid for expressing high levels of GST fusion proteins in the yeast *Saccharomyces cerevisiae*. The plasmid pYES2 is also a plasmid for protein expression in yeast. Both plasmids encode the protein cloned into the MCS under the control of the galactose promoter, GAL1.

The protocol for expressing the recombinant proteins in these vectors is as follows (for smaller or bigger expression volumes, down- or up-scale all subsequent volumes):

1. Inoculate 5 ml of SD Ura- with several colonies, 2–3 mm in diameter.
2. Incubate at 30°C overnight with shaking at 250 rpm.
3. Inoculate 20 ml of Ura-/ 2% Lactic with 5ml overnight cultures from step 2.
4. Incubate at 30°C overnight with shaking at 250 rpm.
5. Induce expression inoculating 25 ml of Ura- / 2% Lactic / 2% Galactose with 25 ml overnight cultures from step 4.
6. Incubate at 30°C for 6h with shaking at 250 rpm.
7. Centrifuge cells for 5 min at 3,200 xg at 4^{o}C. Remove the supernatant.
8. Resuspend the pellet in 1 ml B buffer.
9. Centrifuge for 5 min at 4,000 rpm in a microcentrifuge. Remove the supernatant.
10. Freeze the pellets at -70^{o}C.

B buffer: 10mM Hepes pH 7.8, 1mM EDTA, 10% Glycerol, 100 µM PMSF, 500 nM Benzamidine, 1 µg/ml Pepstatin A (Sigma, Ref. P4265), 2 µg/ml Leupeptin (Sigma).

2.2.3 Yeast mitochondria isolation

As CPT1 activity assays are performed with mitochondrion-enriched fractions from yeast extracts (obtained in the previous section), we obtained fresh mitochondria for each CPT1 activity assay.

To obtain the mitochondrion-enriched fractions, we performed the next protocol:

1. Take yeast cells pellet (from 50 ml culture) from -70^{o}C freezer.
2. Centrifuge them for 5min at 3000 xg at 4^{o}C. Remove the supernatant.
3. Resuspend in 1 ml of B buffer (described in previous protocol). Repeat steps 2 and 3 twice.
4. Resuspend the pellet in 300 µl of B buffer.
5. Add the same volume of glass beads.
6. Lyse cells in a Fast Prep (MP biomedicals) at a speed of 5 m/s during 2 cycles of 30 s each, and with a rest on ice of 30s between both cycles.
7. Elute the lysate in a collection tube by centrifuging at 700 xg for 1 min.
8. Add 100 µl af B buffer to the glass beads to recover all the lysate and centrifuge again at 700 xg for 1 min.
9. Mix both flow-throughs and centrifuge for 10 min at 700xg at 4^{o}C.
10. Collect the supernatant in a new tube.

11. Resuspend the pellet in 500 µl of B buffer and vortex for 10 s.
12. Centrifuge for 10 min at 700xg at 4^{o}C. Collect the supernatant in the same tube as in step 10.
13. Vortex both supernatants for 10 s and centrifuge for 1h at 16000 xg at 4^{o}C.
14. The supernatant is the microsomal fraction.
15. Resuspend the pellet in 50 µl of B buffer. This is the mitochondrial fraction.
16. Perform a Bradford assay to quantify both fractions.

The resulting fractions can be used either for radiometric CPT1 activity assay or for recovery of GST fusion proteins using Gluthathione Sepharose beads.

2.2.4 GST fusion protein purification

As described for GST fusion proteins expressed in *E. coli*, it is also possible to purify GST fusion proteins expressed in yeast (proteins derived from the expression in the pEG(KT) plasmid vector) by affinity chromatography using a batch-based method (Glutathione Sepharose 4B.). In this case, GST fusion proteins are purified from yeast mitochondrial or microsomal fractions obtained in the previous section.

In order to purify GST fusion proteins, the next steps were performed:

1. Take 50 µl of the microsomal or mitochondrial fraction from the yeast extracts obtained previously and add them to 200 µl of slurry of Gluthathione Sepharose beads pre-equilibrated with B Buffer.
2. Put the tubes for 6 h at 4^{o}C with end-over-end rotation.
3. Centrifuge for 5 min at 100 xg at 4^{o}C. Discard the supernatant.
4. Wash the Sepharose beads with 100 µl of B buffer and centrifuge again for 5 min at 100 xg at 4^{o}C
5. Resuspend the beads with 50 µl Protein sample buffer 2x to load the sample in SDS-PAGE.
6. Boil the samples for 5 min and store them at -70^{o}C and further analyze them by SDS-PAGE electrophoresis.

2.2.5 Plasmidic DNA recovery from yeasts

Different methods have been used to recover a plasmid vector from a yeast cell. In this study we chose the glass beads method to break the cells and subsequently transformed the obtained plasmid into *E. coli* cells for further propagation.

1. Grow 3 ml yeast culture in YPD or selective medium overnight to saturation.
2. Pour or pipet 1.5 ml of culture into microcentrifuge tubes. Spin in microfuge for 2 min at 720 xg.
3. Aspirate the supernatant. Resuspend the pellet in 100 µl of STET buffer.
4. Add the same volume of glass beads (approx. 0.2 g)
5. Lyse cells in a Fast Prep (MP biomedicals) at a speed of 5 m/s during 3 cycles of 30 s each.
6. Add 100 µl of STET buffer and vortex for 10 s.
7. Boil samples for 10 min.
8. Put samples on ice and centrifuge at microcentrifuge maximum speed for 10 min at 4^{o}C.
9. Recover 100 µl of the supernatant and put them in a new tube with 50 µl of 7.5 M ammonium acetate (filtrated) and mix.
10. Store samples at -20^{o}C for 1 h.
11. Centrifuge at microcentrifuge maximum speed for 10 min at 4^{o}C.
12. Recover 100 µl of the supernatant and put them in a new tube.
13. Add 200 µl of cold absolute ethanol and mix.

14. Centrifuge at microcentrifuge maximum speed for 5 min at 4^{o}C.
15. Discard the supernatant. Wash the pellet by adding 200 µl of cold 70% ethanol and invert 3 times.
16. Centrifuge at microcentrifuge maximum speed for 5 min at 4^{o}C.
17. Discard the supernatant and air-dry the pellet.
18. Resuspend the pellet with 10 µl of water.
19. Use 5 µl of the solution to transform *E. coli* DH5α for plasmid propagation.

STET buffer: 50mM pH8 Tris, 50mM pH8 EDTA, 5% Triton X-100, 0.08g/ml Sucrose

2.2.6 Yeast two hybrid

The yeast two-hybrid principle

For the analysis of protein interactions we performed a two-hybrid assay using the *Matchmaker Two-Hybrid System 3* (Clontech) that incorporates many features that reduce the incidence of false positive results. It is a system that can be used to screen a library for novel proteins that interact with a known bait protein, or to test two previously cloned proteins for an interaction. In addition, because the two-hybrid assay is performed *in vivo*, the proteins are more likely to be in their native conformations, which may lead to increased sensitivity and accuracy of detection.

In the present study the bait gene (cDNA CPT1C) was expressed as a fusion to the GAL4 DNA-binding domain (DNA-BD) in pGBT9 plasmid vector, while a cDNA library (Human fetal brain cDNA library (Clontech, Ref. 638804)) was expressed as a fusion to the GAL4 activation domain (AD) (Fields & Song, 1989; Chien *et al*., 1991). The expressed fusion proteins are targeted to the yeast nucleus by nuclear localization sequences encoded by the GAL4 DNA-BD or by the SV40 T-antigen cloned into the 5' end of the GAL4 AD sequence.

When the bait protein and one from the library interact, the DNA-BD and AD are brought into proximity, thus reconstituting an active Gal4 transcription factor which activates transcription of reporter genes (Figure 20).

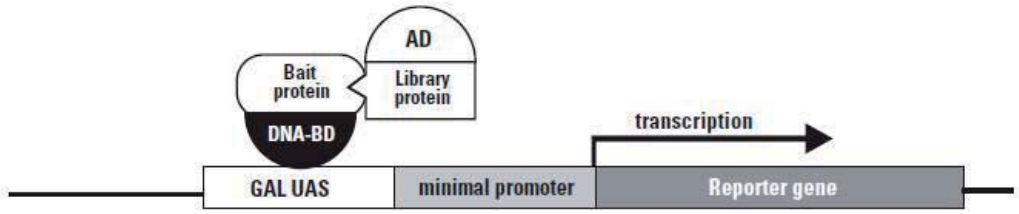

Figure 20. The two-hybrid principle. The DNA-BD is amino acids 1–147 of the yeast GAL4 protein, which binds to the GAL UAS upstream of the reporter genes. The AD is amino acids 768–881 of the GAL4 protein and functions as a transcriptional activator.

The yeast strain used was AH109, which virtually eliminates false positives by using three reporters—*ADE2*, *HIS3*, and *MEL1* (or *lacZ*)—under the control of distinct GAL4 upstream activating sequences (UASs) and TATA boxes (Figure 21). These promoters yield strong and specific responses to GAL4. As a result, two major classes of false positives are eliminated: those that interact directly with the sequences flanking the GAL4 binding site and those that interact with transcription factors bound to specific TATA boxes.

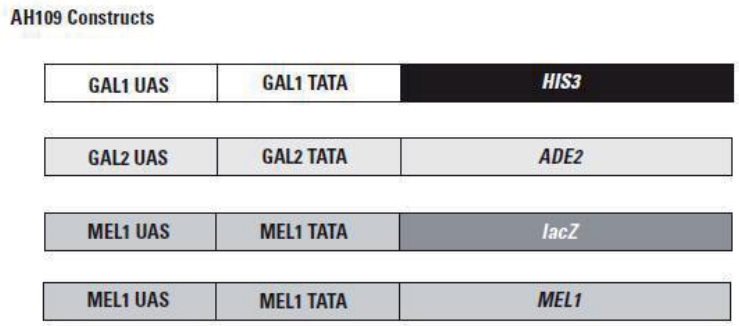

Figure 21. Reporter constructs in yeast strain AH109. Strain AH109 is a derivative of strain PJ69-2A and includes the *ADE2* and *HIS3* markers (James *et al.*, 1996). *MEL1* is an endogenous GAL4-responsive gene. The *lacZ* reporter gene was introduced into PJ69-2A to create AH109. The *HIS3, ADE2,* and *MEL1/lacZ* reporter genes are under the control of three completely heterologous GAL4-responsive UAS and promoter elements—GAL1, GAL2, and MEL1, respectively.

The reporter genes in AH109 are:

- The ***ADE2*** reporter alone provides strong nutritional selection.
- The use of **H*IS3*** reporter in addition to ADE2 nutritional selection reduces the incidence of false positives and allows controlling the stringency of selection (James *et al*., 1996).
- Either the ***MEL1*** or ***lacZ*** reporter genes can be used for blue/white screening. These genes encode α-galactosidase and β-galactosidase, respectively. *MEL1* is an endogenous gene found in several yeast strains. Because α-galactosidase is a secreted enzyme, it can be assayed directly on X-α-Gal (Cat. No. 630407) indicator plates for the blue/white screening.

Y2H Controls

In order to assess the validity of the assay, *Matchmaker Two-Hybrid System 3* provides positive and negative control vectors (information about plasmid vectors in the next table):

- Positive controls

  pCL1 encodes the full-length, wild-type GAL4 protein and provides a positive control for α-galactosidase and β-galactosidase assays.

  pGBKT7-53 and pGADT7-T encode fusions between the GAL4 DNA-BD and AD and murine p53 and SV40 large T-antigen, respectively. p53 and large T-antigen interact in a yeast two-hybrid assay (Li & Fields, 1993; Iwabuchi *et al.*, 1993).

- Negative control

  pGBKT7-Lam encodes a fusion of the DNA-BD with human lamin C and provides a control for a fortuitous interaction between an unrelated protein and either the pGADT7-T control or the AD/library plasmid. Lamin C neither forms protein complexes nor interacts with most other proteins (Bartel *et al*., 1993; Ye & Worman, 1995).

In control experiments, sequential transformation of control plasmid vectors was performed. The first plasmid to be introduced was pGADT7-T and later on pGBKT7-p53 and pGBKT7-Lam were cotransformed and plated on interaction plates (SD/-Ade/-His/-Leu/-Trp/X-α-Gal) (see Figure 10B) and on SD/-Leu/-Trp plates to determine the transformation efficiency (see Figure 10A).

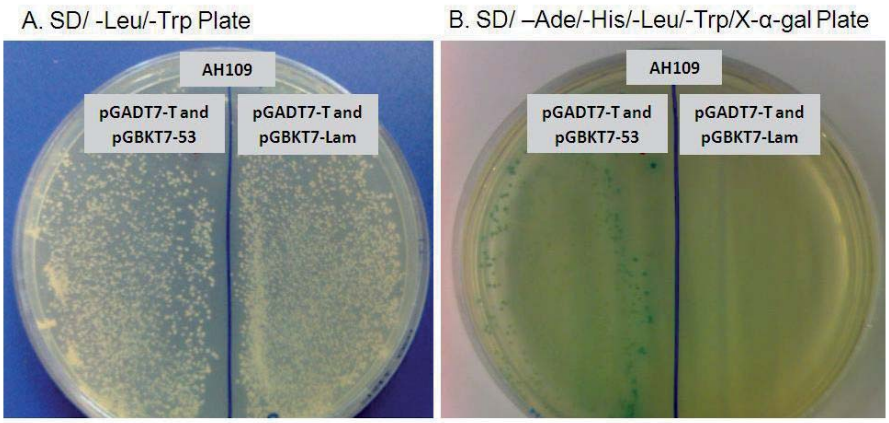

Figure 22. AH109 strain was sequentially co-transformed with control plasmids. **A**. SD/-Leu/-Trp plates to determine transformation efficiency. **B**. SD/-Ade/-His/-Leu/-Trp/X-α-gal plate (interaction plate) to verify positive interaction for pGADT7-T and pGBKT7-53 cotransformation with growth of blue colonies and negative interaction for pGADT7-T and pGBKT7-Lam for negative interaction with no colonies grown on it.

Vector information

Y2H Vectors	Fusion	Yeast selection	Bacterial selection
pCL1	GAL4	LEU2	Ampicillin
pGADT7-T	AD/T-antigen	LEU2	Ampicillin
pGBKT7-53	DNA-BD/p53	TRP1	Kanamycin
pGBKT7-Lam	DNA-BD/lamin C	TRP1	Kanamycin
pACT2	AD-library	LEU2	Ampicillin
pGBT9	DNA BD- CPT1C	TRP1	Ampicillin

Bait protein

Given that protein interactions involving membrane proteins are mostly undetectable in this system and as long as CPT1C is a membrane protein, a region of CPT1C which did not include any of both transmembrane domains was cloned into pGBT9 vector (from base pair 393 to the 3' end of the cDNA) (see section 1.7).

Library transformation

In the yeast two hybrid assay, AH109 was first transformed with the DNA-BD/bait (CPT1C) plasmid through a small-scale transformation (as described in section 2.2.1), selected transformants are then grown up and transformed with the AD fusion library (Human fetal brain) through a large-scale transformation (using 300 ml of culture to obtain 1,5 ml of competent cells).

Transformed cells were plated on SD/-Ade/-His/-Leu/-Trp agar plates. Also a 1:10 dilution was plated on a SD/-Leu/-Trp to determine the cotransformation efficiency.

The colonies grown on SD/-Ade/-His/-Leu/-Trp plates (7-10 days after transfection) were streaked on SD/-Ade/-His/-Leu/-Trp/X-α-gal plate and blue colonies were sequenced using Matchmaker 5' and 3' AD-LD Insert Screening Amplimers (see Figure 23).

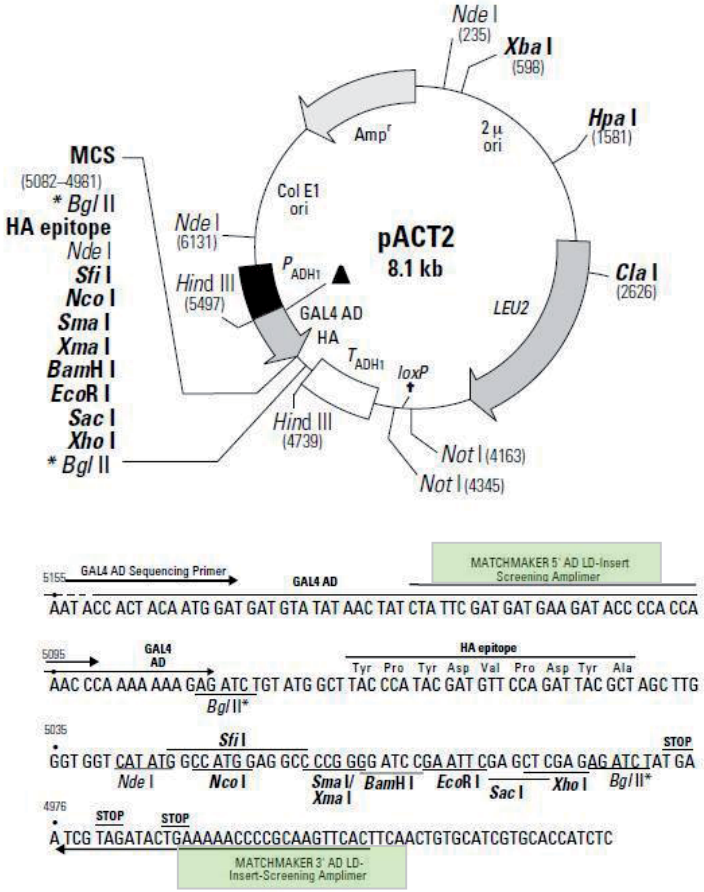

Figure 23. pACT2 generates a fusion protein of the GAL4 AD (amino acids 768–881), an HA epitope tag, and a protein encoded by a cDNA in a fusion library (cDNAs are cloned into EcoRI/XhoI sites). The primers used to sequence the inserts are emphasized in green squares.

Colony PCR analysis

AD/library inserts were amplified by PCR performing the next protocol:

1. Use a pipetman tip to transfer yeast cells into a PCR tube.
2. Heat the opened tube at maximum intensity in the microwave.
3. Close tube caps and store at -70°C for at least 15 min.
4. Prepare PCR premix.
5. Take tubes from -70°C on ice and quickly add 49 µl of the premix at each tube and put them into the Thermalcycler.
6. Heat the samples at 94°C for 5 min.
7. Put the tube on ice again and add 0.5 µl of Expand high Fidelity or Taq polymerase
8. Run 15 PCR cycles, pause the program and add the remaining 0.5 µl of the polymerase.
9. Finish PCR cycle.
10. PCR products were analyzed by agarose gel electrophoresis
11. In gel samples were excised and DNA fragments were recovered from the gel with the *QIAEX II Gel Extraction kit* (QUIAGEN, ref. 20021) for subsequent sequencing. For DNA extraction manufacturer's instructions were followed.

12. Sequencing reaction was performed on the purified DNA fragments using the same Matchmaker 5' (forward) and 3' (reverse) AD-LD Insert Screening Amplimers. (Sequencing protocol described in section "DNA sequencing").
13. BLAST and GeneBank database searches were performed to characterize the sequenced fragments.

PCR premix (1 reaction, Final volume 50 µl):

10x buffer without $MgCl_2$	5 µl
50mM $MgCl_2$	10 µl
dNTPs 10mM	5 µl
Primer Forward 50 µM	1 µl
Primer Reverse 50 µM	1 µl
Sterile bidistilled water	27 µl
Taq polymerase	1 µl

PCR program for sequencing inserts:

1)	Denaturation	94°C 1 min
2)	Annealing	58°C 1 min
3)	Extension	68°C 6 min
4)	Cycles from step 1	30
5)	Final extension	68°C 6 min

We isolated plasmidic DNA (following protocol described in section 2.2.5) of the interesting clones to retest the interaction directly.

3. CELL BIOLOGY

3.1 Cell lines and maintenance

All cell types were grown on sterile glass coverslips (12mm diameter glass coverslips #1 (Menzel-Gläser)) coated with poly-L-lysine (Sigma, ref. P4707), in 24-wells trays for subsequent analysis by fluorescence microscopy.

- Cell line **SH-SY5Y**, derived from human neuroblastoma bone metastatic tumor, was grown at 37°C with 5% CO_2 in Dulbecco's modified Eagle medium (DMEM) (PAA, ref. E15-009) containing 10% inactivated fetal bovine serum (FBS) (Gibco, ref. 16030-074), 2mM glutamine (Gibco, ref. 25030-024) and penicillin/streptomycin (100 U/ml / 100 µg/ml) (Gibco, ref. 15140-148).
- Cell line **HEK293T**, derived from human embryonic kidney, was grown at 37°C with 5% CO_2 in DMEM containing 15% FBS, 2mM glutamine and penicillin/streptomycin (100 U/ml / 100 µg/ml).
- Cell line **PC12**, derived from a pheocromocytoma of the rat adrenal medulla, was grown at 37°C with 5% CO_2 in Kaighn's modification of Ham's F12 medium (F12K) (Invitrogen, ref. 21127-022) containing 15% Horse serum (HS) (Gibco, ref. 16050-122) and 2.5% FBS, 2 mM glutamine and penicillin/streptomycin (100 U/ml / 100 µg/ml).
- **Primary cultures of cortical neurons** were prepared from E16 mice (OF1 mice from Charles River) and were obtained as described in (Gavin et al, 2008):

  E16 mouse embryos were obtained by caesarean section after anaesthetizing the mother. Brains were removed from the embryos and washed in ice-cold 0.1 M PBS containing 6.5 mg/ml glucose.

The meninges were removed and the cortical lobes were isolated. Tissue sections (500 µm thick) were obtained using a McIlwain II tissue chopper (Mickle Laboratory Eng., Gomshall, UK). Tissue pieces were trypsinized for 15min at 37^{o}C. Trypsinization was stopped by addition of horse serum (one fourth volume). After centrifugation, neurons were dissociated by triturating 40 times in 0.1 M PBS containing 0.25% DNAse with a polished Pasteur pipette. Dissociated cells were collected by centrifugation at 150 x g for 5 min and then counted. Cells were plated at 3,000 cells/mm^{2} on 1 mm coverslips coated with poly-d-lysine (Sigma, Ref. P6407). Cells were fed with 0.5 ml of culture media. The serum-free culture medium was Neurobasal Basal Media (Invitrogen, ref. 21103-049) supplemented with 2 mM glutamine, 6.5 mg/ml glucose, antibiotics and B27 supplement (Invitrogen, ref. 17504-044). Cells were used for immunofluorescence processing after 6 days *in vitro.*

3.2 Transfection protocol

Transfection is the process of introducing foreign genetic material into cultured mammalian cells using non-viral methods. Transfection usually involves opening of transient pores in the cell membrane to allow the uptake of the genetic material desired. This process can be performed using the calcium phosphate method, electroporation or by mixing a cationic lipid with the genetic material to produce liposomes, which fuse with the cell membrane and introduce their cargo inside the cells. This last method is the chosen one for our studies and transient transfections were realized with two different commercially available transfection reagents.

For transfection of cell lines Metafectene (Biontex) or Lipofectamine 2000 (Invitrogen) were both suitable and transfections were performed as recommended by the manufacturer (transforming 1 µg of DNA and using 2 µl of transfection reagent for transforming each well of a 24-well tray). The cells were incubated with the transfection reagent and the DNA for 6 h, and after this time, the medium was replaced by new complete medium.

For transfection of primary culture cells, Lipofectamine showed higher transformation efficiency and the exact protocol is described here:

LIPOFECTAMINE 2000 in mouse hippocampal primary cultures.

1. Two days before transfection, half of the medium was replaced by fresh medium without antibiotics (store the retired medium, called “conditioned medium”, at 4^{o}C).
2. The day of transfection cells were incubated with the DNA (1 µg/well) and Lipofectamine (2 µl) for 2 hours. Then, half of the medium was replaced by the conditioned medium previously stored.
3. Then cells were incubated at 37^{o}C in a CO_2 incubator until the day of fixation (usually 48h after transfection).

Plasmids used for transfection were:

- pDS Red-RE
- pEGFP N3 (empty vector)
- p CPT1C-EGFP
- pCPT1A-EGFP
- pCPT1AC-EGFP
- pCPT1CA EGFP
- pIRES2-EGFP (empty vector)
- pIRES2-CPT1A
- pIRES2-CPT1C (different constructs used for deglycosylation assays)

3.3 Mitotracker staining protocol

MitoTracker Orange CM-H_2TMRos (M-7511) (Molecular Probes) is a reduced, nonfluorescent dye that fluoresces upon oxidation. This dye also stains mitochondria in live cells and its accumulation is dependent upon membrane potential. The dye is well-retained after aldehyde fixation. Stocks were prepared following manufacturer’s instructions.

The experimental procedure was as follows:

1. To prepare the staining solution, dilute 1 mM MitoTracker stock solution to the final working concentration of 500 nM in appropriate growth medium.
2. Remove the media from cells grown on coverslips (precoated with poly-L-lysine) in 24-wells tray, and add prewarmed (37°C) staining solution containing MitoTracker.
3. Incubate 30 minutes under growth conditions.
4. After staining is complete replace the staining solution with fresh prewarmed PBS and wash twice with PBS.
5. Replace PBS with PBS containing 4% formaldehyde and incubate at room temperature for 20 minutes.
6. After fixation, rinse the cells three times in PBS and drain the coverslips on absorbent paper.
7. Mount the coverslips in 6µl of Mowiol on an ethanol cleaned slide (Mowiol is an anti-fade mounting medium) and store slides flat at 4°C protected from light.
8. Analyze by fluorescence microscopy or confocal fluorescence microscopy.

3.4 Immunofluorescence on cells

Different cell types were grown and transfected as described previously in this manuscript. At the desired moment immunostaining was performed on these cells as follows:

1. Remove the growth medium and rinse twice with PBS 1x in the same multiwell plate. It is important to never let cells dry.
2. Aspirate PBS and cover cells in the same multiwell tray with Fixation solution 1 ml.
3. Allow cells to fix for 15 min at room temperature.
4. Aspirate fixative and rinse three times in PBS.
5. Rinse twice in PBS-glycine for 5 min each.
6. Aspirate last wash solution and cover cells in Triton permabilization solution for 10 minutes at room temperature to permeabilize all cell membranes.
7. Block specimen in blocking buffer for 20 min at room temperature.
8. While blocking prepare primary antibody by diluting as indicated in the antibody table in Antobody dilution buffer (Calculate a final volume of 30µl for each coverslip). For double labeling, prepare a cocktail of the primary antibodies at their appropriate dilution in Antibody dilution buffer.
9. Aspirate blocking solution and incubate with diluted primary antibody for 1 hour at 37°C in a humid box (to prevent drying)
10. Rinse twice in PBS-glycine for 5 min each.
11. Incubate each coverslip in 30 µl of fluorochrome-conjugated secondary antibody diluted in Antibody dilution buffer for 1 h at 37^{o}C in a dark humid chamber (to prevent drying and fluorochrome fading). For double labeling, prepare a cocktail of fluorochrome conjugated secondary antibodies at their appropriate dilution in Antibody dilution buffer.
12. Rinse twice in PBS-glycine for 5 minutes each.
13. Drain the coverslips on absorbent paper
14. Mount the coverslip in 6 µl of Mowiol on an ethanol cleaned slide (Mowiol is an anti-fade mounting medium.)
15. Store slides flat at 4°C protected from light.
16. Analyze by fluorescence microscopy or confocal fluorescence microscopy.

Fixation solution: 3% formaldehyde in 100 mM phosphate buffer with 60 mM sucrose. Formaldehyde is toxic, use only in fume hood.

PBS-Glycine: 20 mM glycine in 10 mM PBS.

Triton permabilization solution: 1% Triton X-100, 10 mM PBS, 20 mM Glycine

Blocking buffer: 1% BSA in 10 mM PBS, 20mM glycine, 1% Triton X-100

Antibody dilution buffer: 10 mM PBS, 20 mM Glycine, 1% BSA, 0.2% Triton X-100 and the corresponding antibody

Antibodies:

- 1:50 **Anti Calnexin** , mouse monoclonal IgG1 (BD Biosciences, ref. 610946)
- 1:100 **Anti-Calreticulin**, mouse monoclonal IgG1 (BDBiosciences, ref. 612136)
- 1:500 **Alexa Fluor 546 Goat anti-mouse IgG** (Molecular Probes, ref. A-11030)
- 1:100 **CPT1C rabbit polyclonal** (Sigma, Genosys)
- 1:500 **Alexa Fluor 488 Goat anti-rabbit** $F(ab')_2$ (Molecular Probes, ref. A-11070)

3.5 Microsome purification

In order to obtain fractions enriched in CPT1C, we proceeded to purify microsomes from cells transiently overexpressing CPT1C.

Cells were recovered by centrifugation at 1,200 x*g* for 5 min at 4 °C, washed in 1.5 ml of PBS, and re-suspended in 2 ml of lysis buffer. Cells were disrupted by Dounce homogenization (30 pulses with loose pestle and 30 pulses with tight pestle). Homogenates were centrifuged at 2,000 x *g* for 3 min at 4 °C to remove cell debris.

This crude extract was further centrifuged at 10,000 x*g* for 30 min at 4 °C to remove the mitochondrial fraction. Supernatant was centrifuged at 100,000 x *g* for 1 h at 4 °C to sediment the microsomal fraction.

Pellets were immediately resuspended in the appropriate buffer depending on subsequent uses, and quantified by Bradford method.

Lysis buffer: 250 mM sucrose, 10 mM Tris, pH 7.4, 1 mM EDTA, supplemented with 1 mM phenylmethylsulfonyl fluoride, 0.5 mM benzamidine, 10 ng/ml leupeptin, and 100 ng/ml pepstatin

3.6 RNA isolation

Total RNA isolation from tissue was performed using Trizol Reagent (Life Technologies, Cat. No. 15596) following manufacturer's instructions. One brain was extracted from the skull of an adult mouse and was homogenized 25 times on ice, using the loose pestle of a Douncer with 3 ml of Trizol Reagent.

Total RNA was extracted for subsequently subcloning purposes.

In order to eliminate the DNA from the sample to perform cDNA synthesis, a DNaseI treatment (Invitrogen, ref. 18068-015) was previously performed. DNaseI is a deoxyribonuclease that digests single and double stranded DNA to oligodeoxy-ribonucleotides containing a 5' phosphate.

DNase I reaction mix:

- Up to 7 µl DEPC-treated water containing 2 µg from the total RNA extract
- 1 µl of 10x DNase buffer (supplied with the kit)
- 1 µl of DNaseI Amplification grade (≥10,000 U/mg)

The reaction mix was incubated for 15 min at room temperature, and then the enzyme was inactivated by the addition of 1 µl of 25 mM EDTA to the reaction mixture and the tube was heated for 10 min at 65°C. The inactivation of the enzyme is important because it could degrade newly synthesized DNA in subsequent steps. The RNA sample must be kept on ice until cDNA synthesis reaction mixture is prepared.

3.7 cDNA synthesis

Reverse Transcription (RT reaction) is a process in which single-stranded RNA is reverse transcribed into complementary DNA (cDNA) by using total cellular RNA, a reverse transcriptase enzyme (Moloney Murine Leukemia Virus Reverse Transcriptase: M-MLV RT (Invitrogen, ref. 28025-013)), a primer, dNTPs

and an RNase inhibitor. Three types of primers can be used for RT reaction: oligo (dT) primers, random (hexamer) primers and gene specific primers with each having its pros and cons.

The protocol was performed as follows:

1. Starting with 10 µl of the DNaseI reaction mixture (containing 2 µg of RNA as described in previous section), add 1 µl of 50 µM Oligo dT to the same tube.
2. Also add 1 µl of 10 mM dNTP mix.
3. Heat the sample at 65°C for 5 min to denature RNA secondary structure.
4. Chill on ice to let the primer anneal to the RNA and spin.
5. Add 4 µl of 5x First Strand buffer (250 mM Tris-HCl (pH 8.3 at room temperature), 375 mM KCl, 15 mM $MgCl_2$) supplied with the kit.
6. Into the same tube add also 2 µl 0.1M DTT and 1 µl of RNase OUT (RNase inhibitor also supplied with the kit), mix gently and incubate 2 min at 37°C before adding 1 µl of M-MLV reverse transcriptase and mix by pipetting up and down.
7. Incubate 50 min at 37°C.
8. Inactivate the reaction by heating at 70°C for 15 min.
9. For the removal of the template RNA to eliminate complementary RNA is achieved by adding 1 µl of RNaseH (New England Biolabs, ref. 0297S) and incubate for 20 min at 37°C.

A PCR with the desired primers (as described in "Table 1") can be performed on this total RNA extract for subcloning the full length cDNA of CPT1C from *Mus musculus* into the appropriate vector.

4. BIOCHEMISTRY

4.1 Deglycosylation assay

Glycosylation is one of the most common post-translational modifications of proteins in eukaryotic cells. Mammalian glycoproteins contain three major types of oligosaccharides (glycans): N-linked, O-linked and glycosylphosphatidylinositol (GPI) lipid anchors.

N-linked glycans are attached to the protein backbone via an amide bond to an asparagine residue in an Asn-Xaa-Ser/Thr motif, where X can be any amino acid, except proline. Variation in the degrees of saturation at available glycosylation sites results in heterogeneity in the mass and charge of glycoproteins.

Although sites of potential N-glycosylation can be predicted from the consensus sequence Asn-Xaa-Ser/Thr, it cannot be assumed that a site will actually be glycosylated. Therefore the sites of glycan attachment must be identified and characterized by analytical procedures.

Peptide-N-glycosidase F (PNGase F) (Sigma, ref. P7367) is one of the most widely used enzymes for the deglycosylation of glycoproteins. The enzyme releases asparagine-linked (N-linked) oligosaccharides from glycoproteins and glycopeptides. A tripeptide with the glycan-linked asparagine as the central residue is the minimum substrate for PNGase F.

Positive control

Bovine pancreatic Ribonuclease B (RNase B) (Sigma, ref. R1153) is a glycoprotein that contains only N-linked glycans. RNase B contains a single glycosylation site at Asn^{34}. The activity of PNGase F is routinely assayed using RNase B by monitoring the mobility shift of approx. 3 kDa in 15% SDS-PAGE gels after deglycosylation.

The deglycosylation assay was performed as follows:

1. Dilute 160 µg of protein from microsomal fractions (obtained as described in section "Microsome purification") of HEK293T cells transfected with different constructs of pIRES2-EGFP (constructs that bear glycosylation sites in different regions of CPT1C protein), in 20mM ammonium bicarbonate, pH 8, to a final volume of 45 µl. For positive control, use 45 µl of RNase B (1.1 mg/ml).
2. Add 5 µl of denaturation solution and vortex the samples.
3. Heat the solution to 100°C for 10 min to denature de protein (in order to facilitate the access of the deglycosilating enzyme (PNGase F) to the N-glycans attached to the protein).
4. Allow the solution to cool and spin down the sample.
5. Add 5 µl of 15% Triton X-100 and mix.
6. Add 10 µl of the prepared PNGase F enzyme solution (500U/ml) to the reaction mixture. For negative controls add sterile bidistilled water instead of the enzyme.
7. Incubate at 37°C for 3 h adding 0.5 µl protease inhibitor mix every one hour.
8. Stop the reaction by heating the samples to 100°Cfor 5 min. Cool the sample and spin it down.
9. Add 65 µl of 2x Protein sample buffer. Boil the sample for 5 min and analyze in SDS-PAGE electrophoresis using and Western blot.

Denaturation solution: 0.2% SDS, 100 mM 2-mercaptoethanol

4.2 CPT1 activity assay

CPT1 activity assays were performed with mitochondrion-enriched fractions from yeast extracts obtained as described previously in Microbiology protocols. When mitochondria are frozen, membranes can be broken, allowing CPT2 to contribute to the measured activity. To avoid CPT2 interferences freshly obtained mitochondria were used for each experiment.

CPT1 activity was determined by the radiometric method as previously described (Morillas et al., 2000) with minor modifications.

The substrates for the CPT1 activity assay are L-[*methyl*-^{3}H]-carnitine hydrochloride (Amersham Biosciences, ref. TRK762) and palmitoyl-CoA, and the reaction is done in the following direction:

$$^{3}\text{H-carnitine} + \text{palmitoyl-CoA} \longrightarrow \text{palmitoyl-}^{3}\text{H-carnitine} + \text{CoA-SH}$$

The procedure takes advantage of the fact that the product of the reaction, palmitoyl-^{3}H-carnitine, is soluble in an organic medium. Therefore, it can be separated by extraction from the radioactive substrate, ^{3}H-carnitine, that has not been reacted and which will remain in the aqueous phase.

The final concentrations of the components in the reaction are:

CPT1 reaction mix: 105 mM Tris-HCl pH 7.2, 2 mM KCN, 15 mM KCl, 4 mM $MgCl_2$, 4 mM ATP, 250 µM GSH, 50 µM Palmitoyl-CoA, 400 µM L-[*methyl*-^{3}H]carnitine (0.3 mCi), 0.1% defatted BSA.

Deacylases convert the substrate acyl-CoA in acyl plus CoA-SH, generating ATP. This process would reduce the availability of the substrate palmitoyl-CoA in the reaction. Therefore, ATP is added to the reaction mix to minimize this process, by inverting the equilibrium of the deacylase reaction and by stimulating the reaction of the acyl-CoA synthetases and thus regenerating the substrate palmitoyl-CoA. KCN is added to avoid mitochondrial oxidation. Glutathione (GSH, reduced form) is used as a reduction agent instead of dithiothreitol (DTT) or dithioeritrol (DTE) because DTT and DTE have been shown to reduce malonyl-CoA sensitivity (Saggerson and Carpenter., 1982). Defatted BSA is added to protect mitochondria from the detergent effect of fatty acids. However, BSA concentration must not be higher than 0.1% because this could give a sigmoidal effect in the enzyme *v.s.* acyl-CoA kinetic (Prip-Buus et al., 1998). Finally, KCl is added because it increases enzyme activity (Saggerson, 1982).

The procedure for the CPT1 activity assay is as follows:

1. The reaction mix is prepared in a 15 ml tube kept on ice. (GSH is prepared by dissolving it in water on the day of the experiment). Samples are done in duplicate.
2. The following amounts are per point:

CPT1 reaction mix/point

Bidistilled water	92.33 µl
4X CPT1 buffer	40 µl
1 mM palmitoyl-CoA	10 µl
80 mM ATP	10 µl
30% BSA	0.67 µl
25 mM GSH	2 µl
16 mM ^{3}H-carnitine	5 µl
Total volume	160 µl

3. Protein samples are prepared on ice in 1.5 ml tubes by diluting the protein in 4x CPT1 buffer and by adjusting the volume with bd. water up to 40 µl. The blank contains bidistilled water instead of protein.

Protein samples

Protein	15-100 µg
4x CPT1 buffer	10 µl
Bidistilled water up to	40 µl

4. One by one, 160 µl of the reaction mix is added to each protein sample. Samples are vortex-mixed and placed on a water bath at 30°C for exactly 5 min.
5. Reaction is stopped with the addition of 200 µl of 1.2 M HCl. Samples are vortex-mixed and placed on ice.
6. Extractions of the product of the reaction, palmitoyl-^{3}H-carnitine, are done by adding 600 µl of water-saturated butanol. Samples are vortex- mixed and centrifuged for 2 min at 13,000 rpm in a microcentrifuge.
7. 400 µl of the upper phase is added to another 1.5 ml tube with 200 µl of bidistilled water. Samples are vortex-mixed and centrifuged for 2 min at 13,000 rpm.
8. 250 µl of the upper phase is counted in plastic scintillation vials with 5 ml of scintillation liquid (Ecolite, ICN). ^{3}H radioactivity is counted in a RackBeta apparatus.

Specific activity of the enzyme is calculated as follows:

$$\text{S.A.}(\text{nmol}\cdot\text{mg}^{-1}\ \text{prot}\cdot\text{min}^{-1}) = \frac{\text{cpm x 600 µl}}{\text{S.R. x mg prot. x min x 250 µl}}$$

Where **cpm** are the counts per minute and **S.R.** is the ^{3}H-carnitine specific radioactivity (approx. 3000 cpm/nmol).

4X CPT1 buffer: 420 mM Tris-HCl pH 7.2, 8 mM KCN, 60 mM KCl, 16 mM $MgCl_2$. Stored at 4°C.

16 mM ^{3}H-carnitine: 6.6 mg of cold carnitine is dissolved in 982.3 µl of 95% ethanol plus 982.3 ml of bd. water and 125 µl of L-[*methyl*-^{3}H] carnitine hydrochloride (80 Ci/mmol) is added. Aliquots of 125 µl are stored at -80°C.

5. BIOINFORMATICS

Bioinformatics tools have been used to align sequences, to find homologies, to model the 3-D structure of CPT1C and to predict the topology of the protein and its glycosylation sites. To analyze information on proteins obtained in the Y2H assay, searches in different databases from the NCBI and others, have been performed.

5.1 Alignments

A multiple amino acid sequence alignment of the different isoforms of CPT1 from human, mouse and rat was performed with CLUSTALW and viewed with Belvu software (Sonnhammer and Hollich, 2005) (http://sonnhammer.sbc.su.se/Belvu.html). Sequences were obtained from UniprotKB databases (http://www.uniprot.org) with the following accession numbers:

	Protein
Human CPT1A	P50416
Mouse CPT1A	P97742
Rat CPT1A	P32198
Human CPT1B	Q92523
Mouse CPT1B	Q924X2
Rat CPT1B	Q63704
Human CPT1C	Q8TCG5
Mouse CPT1C	Q8BGD5
Rat CPT1C	Q3KR63

Table 4. Accesion numbers from UniProtKB database of the mRNA and protein sequences from the different isoforms of CPT1 from various species used in this study (in alignments and for modeling purposes).

5.2 3-D protein modeling of CPT1C N- and C-terminal domains

Structural model of the rat CPT1C protein was performed by standard comparative modeling methods and the software DeepView (Guex and Peitsch, 1997), using the 3-D CPT1A model, which in turn, is based on crystal structures of murine and human CRAT, COT and CPT2 (Jogl and Tong, 2003; Wu et al., 2003; Jogl et al., 2005; Hsiao et al., 2006). To optimize geometries, models were energy minimized using the GROMOS 43B1 force field implemented in DeepView (Guex and Peitch, 1997), using 500 steps of steepest descent minimization followed by 500 steps of conjugate-gradient minimization. Sequence identity within the modeled region between rat CPT1A and modeled rat CPT1C was 55%, with a Blast e-value of 8.8×10^{-225} The quality of the model was checked using the analysis programs (Anolea, Gromos and Verify3D) provided by the SWISS-MODEL server (http://swissmodel.expasy.org/) (Schwede et al., 2003; Arnold et al., 2006; Kiefer et al., 2009). Structures were manipulated using the Swiss-PDB viewer and were rendered using Pymol (DeLano, 2002 (*)).

(*)DeLano, W. L. (2002). The PyMOL Molecular Graphics System, 0.83 ed. *DeLano Scientific, San Carlos, CA.*

5.3 Topology predictions

To predict the membrane topology of CPT1C, two transmembrane topology prediction servers were used:

- **TMHMM version 2.0** (http://www.cbs.dtu.dk/services/TMHMM/) (Sonnhammer et al., 1998; Krogh et al., 2001; Moller et al., 2001).
- **HMMTOP version 2.0** (http://www.enzim.hu/hmmtop/) (Tusnády and Simon, 1998; Tusnády and Simon, 2001).

They both use hidden Markov model (HMM). HMM is widely used in bioinformatics; its most widespread use is in aligning sequences and generating profiles for protein families. The main characteristics displayed by these two prediction servers are:

TMHMM is a method used to predict transmembrane helices and the in/out orientation relative to the membrane. It incorporates different parameters for the prediction. One of these parameters is the abundance of positively charged residues in the part of the sequence on the cytoplasmic side of the membrane, "the positive inside rule"

HMMTOP is another HMM method independently developed, that is built on a very similar HMM architecture, but the method used for prediction is different. The version used here also incorporates preliminary experimental information into the topology prediction thus increasing the prediction accuracy of the method.

5.4 Prediction of endogenous glycosylation sites

We used NetNGlyc 1.0 server (http://www.cbs.dtu.dk/services/NetNGlyc) to find potential N-glycosylation sites in CPT1C. The NetNglyc server predicts N-Glycosylation sites in human proteins using artificial neural networks that examine the sequence context of Asn-Xaa-Ser/Thr sequons. The method incorporates a prediction of the presence and location of signal peptide/non-signal peptide cleavage sites in amino acid sequences from different organisms based on a combination of several artificial neural networks and hidden Markov models. A warning is displayed if a signal peptide is not detected. In transmembrane proteins, only extracellular domains may be N-glycosylated. This is currently not checked by the NetNGlyc server, therefore cytoplasmic and transmembrane sequence regions may be predicted to be glycosylated - this should, of course, be ignored.

5.5 Databases used for obtaining information on proteins

The main database used was the "Entrez gene" resource from the NCBI (http://www.ncbi.nlm.nih.gov/gene) (Maglott et al., 2006)

Some of the components of the Gene record describe key characteristics of the gene, its function, and its products. It contains a summary that provides a quick synopsis of what is known about the gene, the function of its encoded protein or RNA products, disease associations, spatial and temporal distribution, and so on. It also includes links to additional information in other databases which have also been consulted, as well as links to bibliography on PubMed.

6. ANTIBODIES PRODUCTION

To perform the molecular characterization of CPT1C it was very important to have tools for its detection at the protein level. At that moment there were not commercially available antibodies to CPT1C, therefore we raised antibodies against two different epitopes of the protein: one located at the C-terminal end of the protein and another one located at the N-terminal region of the protein. These two regions contained divergent sequences among both isoforms and potentially allowed specific detection of the protein.

6.1 Antibody to C-terminal CPT1C: Anti-CPT1C

In order to raise an antibody against CPT1C, a strategy similar to that used by Price *et al*., 2002 was followed. They selected the last C-terminal 135 amino acids of mouse CPT1C sequence (a region predicted to be highly antigenic and showing little similarity to CPT1A or CPT1B).

In this study, the last 115 amino acids of rat CPT1C were cloned into pGEX-6P-1 expression vector. This plasmid vector allowed bacterial expression of the described peptide N-terminally tagged with GST (Figure 24). The recombinant protein expressed was named GST-Cterm CPT1C.

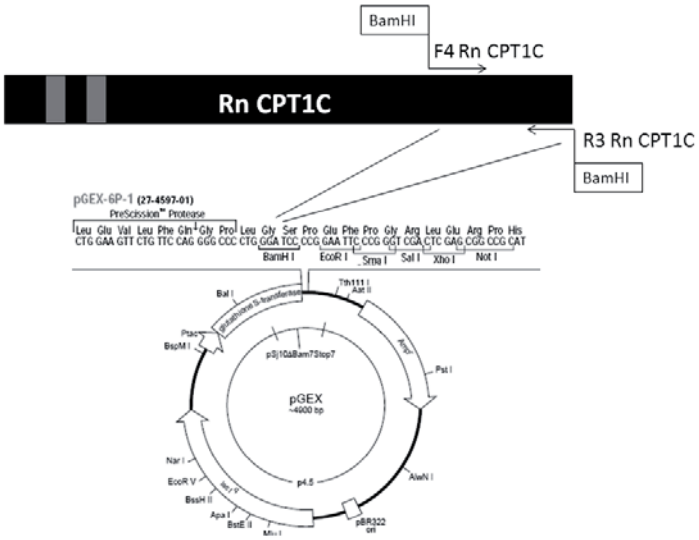

Figure 24. Cloning into pGEX-6P-1 vector. C-terminal 115 amino acids of rat CPT1C (2056-2406bp) were cloned into BamHI site of pGEX-6P-1. Rat CPT1C whole length cDNA sequence is shown in black and transmembrane domains are highlighted in gray.

In preliminary studies, a low yield of recombinant protein was recovered, so the first step for optimization was to evaluate the bacterial strain more suitable for the expression of the fusion protein and the colony expressing it in higher amounts. As long as both colonies of BL21 were showing high expression levels, this strain was selected for the expression (Figure 25a).

The second step was to optimize cell lysis conditions using either enzymatic cell lysis only, or enzymatic lysis and ultrasonication together. At this point, the conclusion was that sonication plus enzymatic cell lysis substantially increased the recovery of soluble protein but the recombinant protein was still present mainly in inclusion bodies (insoluble aggregates that are failed folding intermediates of the overexpressed protein) (see Figure 25b). Therefore, different approaches for increasing soluble expression were tested (including increased aireation, lower growth temperature, induction at lower

cell densities of the culture, modification of IPTG concentrations or induction for shorter periods of time) without achieving any increase in soluble recombinant protein.

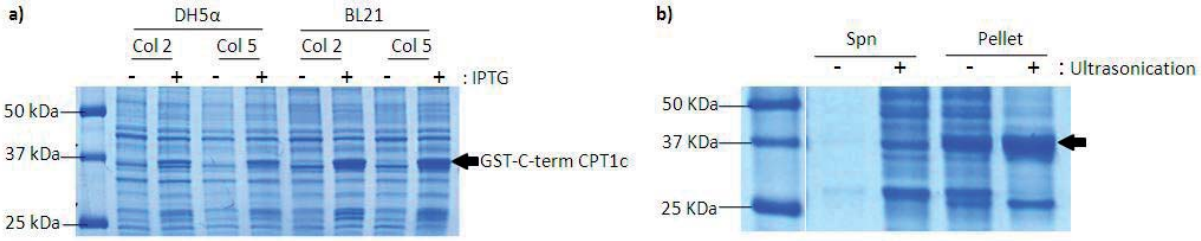

Figure 25. a) GST-Cterm CPT1C expression in different colonies and strains. Two colonies and two *E. coli* strains (DH5α and BL21) were explored for optimizing protein expression. GST-Cterm CPT1C shows a molecular weight of approx. 37 kDa (25 kDa of GST and 12 kDa of the 115 last residues of CPT1C). The black arrow points the band corresponding to the expressed GST-Cterm CPT1C in all gels of this section. **b) Cell lysis in different conditions**. Induced cultures were lysed using a breaking buffer (containing lysozyme) and with or without an additional step of 3 cycles of ultrasonication of 45 s each. After these treatments, suspensions were centrifuged at 13,000 x g for 10 min at 4°C and samples from the supernatant ("spn") and the pellet were loaded.

Given the fact that no expression conditions reached higher levels of soluble recombinant protein, solubilization of the protein from the inclusion bodies was tested. A common detergent like 1% Triton X-100 was first tested but the protein still remained in inclusion bodies, as shown in the lane corresponding to the pellet in Figure 26a. Therefore other denaturants like 6 M guanidine hydrochloride or 2-6 M urea were used. Although it was possible to solubilize a greater amount of protein (Figure 26b), it precipitated in the posterior dialysis process (to eliminate denaturants from the sample) making it impossible to recover enough amount of purified soluble protein for antibody production. Therefore another approach for producing antibodies against CPT1C was needed.

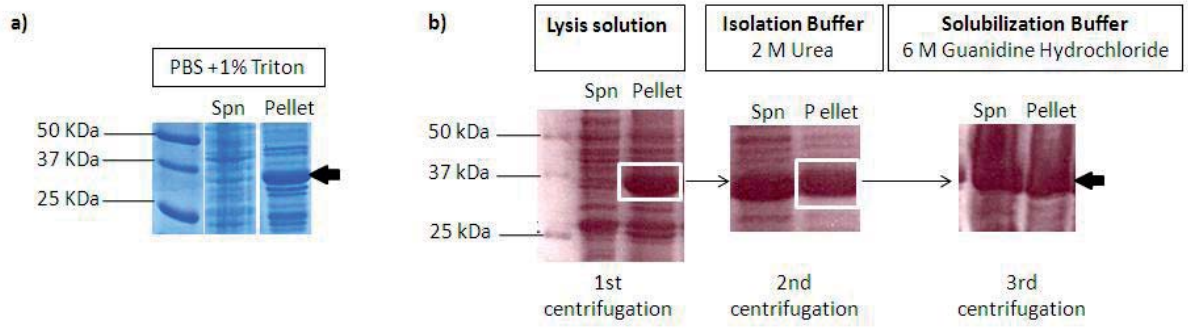

Figure 26. (a) Solubilization of inclusion bodies with Triton X-100. After cell lysis, the pellet was resuspended in PBS containing 1% Triton X-100, incubated for 10 min at 37°C with agitation and centrifuged. Samples from the supernatant and the pellet are shown in the gel.N**b) Solubilization of inclusion bodies with Urea and Guanidine hydrochloride.** The figure shows how the protein was partly solubilized when the pellet from cell lysis (1st centrifugation) was treated with 2 M urea and centrifuged (2nd centrifugation). Subsequently, the pellet obtained after urea treatment was resuspended and ultrasonicated in 6 M Guanidine hydrochloride, recovering half of the remaining amount of protein in the soluble fraction or supernatant (3rd centrifugation).

Finally, a strategy similar to that used by Wolfgang et al., 2006 was performed. Their strategy had already shown to be an effective approach for producing specific antibodies to CPT1C. Hence, rabbits were immunized with a synthesized peptide containing the last 15 amino acids of the *Mus musculus*

sequence of CPT1C, as shown in Figure 27a. This peptide was N-terminally conjugated to KLH to enhance immunogenicity. Polyclonal antibodies were affinity purified from rabbit sera by using the same peptide.

The antibody specificity was tested in cultured cell extracts overexpressing CPT1A or CPT1C. Cross-reactions were discarded by reprobing the membranes with CPT1A antibody (Figure 27b).

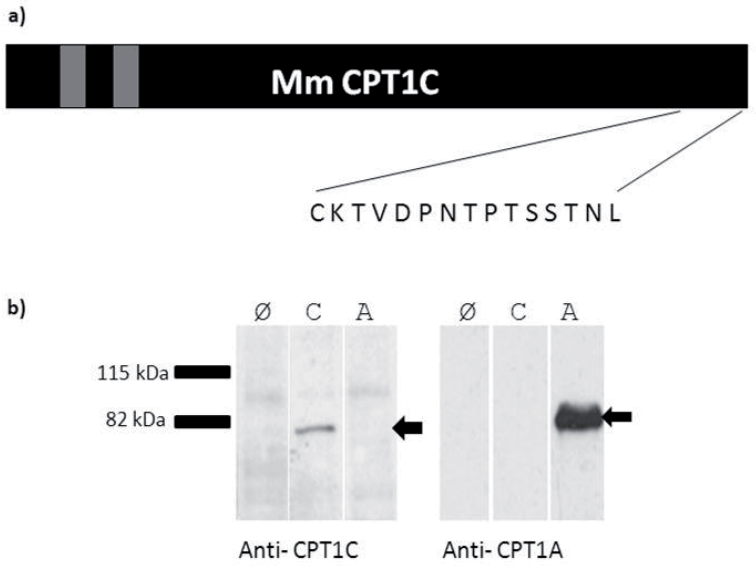

Figure 27. **(a) Petide synthesis for antibody production**. Schematic protein sequence of mouse CPT1C is shown in a black square (predicted transmembrane domains are in gray) and the last 15 amino acids of the sequence used to synthesize the peptide for antibody production is written in the single letter code for amino acids. **(b) Testing of the raised antibody to the C-terminal end of CPT1C**. Samples from HEK293T cells expressing empty pIRES (Ø), pIRES-CPT1C (c) or pIRES-CPT1A (a), were lysed and mitochondrial fractions were separated. Immunoblotting with the obtained anti-CPT1C antibody and reprobing the same membrane with anti-CPT1A, showed no cross-reaction among both antibodies. The arrows point the proteins specifically recognized by each antibody.

6.2 Antibody to N-terminal CPT1C: Anti-CPT1C N-terminus

A polyclonal antibody to the N-terminal region of CPT1C was also generated with a similar strategy. A peptide of 17 amino acids from the *Mus musculus* sequence of CPT1C, containing residues from Leucine 11 to Valine 27, was synthesized for immunization. This peptide was predicted to be highly antigenic and was substantially different from CPT1A sequence within the same region. Moreover, the antibody would potentially recognise also the same epitope from rat CPT1C, as it only differs in 1 residue from the synthesized peptide (see Figure 28).

The peptide was N-terminally conjugated to KLH to enhance immunogenicity. Rabbits were immunized and antibodies were affinity purified from rabbit sera by using the same peptide.

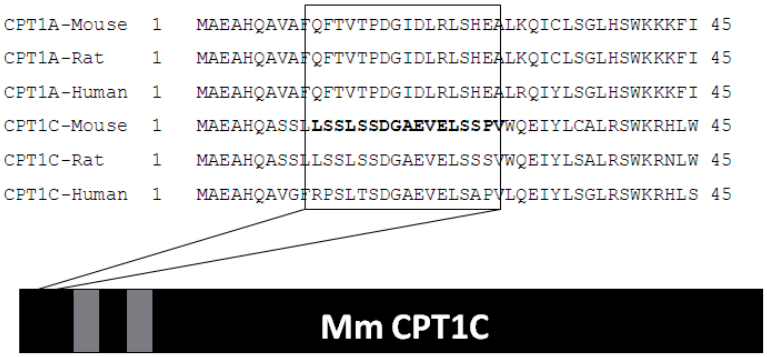

Figure 28. Peptide synthesis for N-terminal antibody production. First 45 residues of human, mouse and rat CPT1C and CPT1A sequences are shown in the figure. The square outlines the comparison of the region chosen for peptide synthesis. The sequence of the 17 aa peptide used for rabbit immunization is highlighted in bold.

The antibodies obtained (anti-CPT1C N-terminus) were tested on yeast extracts from *S. cerevisiae* transformed either with pEG(KG) empty vector (which expresses GST protein) or pEG(KG)-CPT1C (which expresses GST-CPT1C fusion protein), showing specific recognition of CPT1C, as shown in Figure 29.

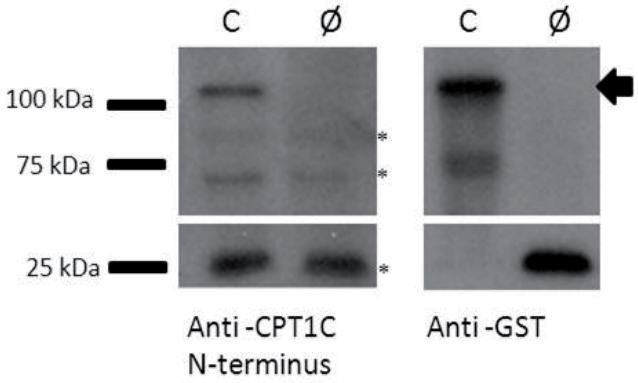

Figure 29. Testing of the antibody to CPT1C N-terminus. Mitochondrial fraction of yeast extracts expressing either GST-CPT1C (lane shown as "C") or empty pEG(KG) (lane shown as "Ø") were obtained. Upper image: GST-CPT1C (band marked with a black arrow) was detected by Western blot using anti-CPT1C N-terminus and anti-GST antibodies. GST-CPT1C shows a molecular weight of approximately 115 kDa (corresponding to the addition of 90 kDa from CPT1C and 25 kDa from GST). Bottom image: expressed GST from the empty vector showed a unique band when the membranes were probed with anti-GST antibody. (*) Unspecific bands.

RESULTS

1. CPT1C STRUCTURAL MODEL

In order to determine whether CPT1C was an enzyme with the structural characteristics that enabled its activity, and taking advantage of the existing model of CPT1A (Morillas et al., 2001; Morillas et al., 2004; López-Viñas et al., 2007), the 3-D structure of CPT1C has been constructed by homology modeling.

A multiple amino acid sequence alignment of the different isoforms of CPT1 from human, mouse and rat is shown in Figure 30. A ribbon picture of the final model of CPT1C, including the putative location of the carnitine and palmitoyl-CoA ligands, is shown in Figure 31A and 31B. The main part of this theoretical model of CPT1C tridimensional structure (from residue Pro^{162} to Gly^{764}) was calculated through computational techniques based on the homology with other members of carnitine/choline acyltransferases (CAT, COT and CPT2) of known structure (Jogl and Tong, 2003; Wu et al., 2003; Jogl et al., 2005; Hsiao et al., 2006). The structure of the N-terminal domain (residues from Leu^{10} to Phe^{50}) is based on theoretical calculations such as folding prediction and molecular docking, demonstrated experimentally for CPT1A (López-Viñas et al., 2007).

Residues within 4 Å from both substrates were identified as residues contacting them (blue asterisks in Figure 30). When identified, the homology with the same amino acid positions in CPT1A and CPT1B sequence on the alignment was analyzed. All residues implicated in carnitine binding are well conserved. Residues involved in palmitoyl-CoA binding are mostly conserved, with some conservative and semi-conservative changes which do not apparently influence the activity of this isozyme.

It is important to notice that residues that had been shown to be involved in the catalysis of the reaction in CPT1A are well conserved in CPT1C sequence. This is the case of the catalytic His^{473} and Ala^{381}, which occupy position 479 and 385 in the alignment (highlighted with a red and a green asterisk in Figure 30), respectively. These residues had previously shown that when mutated, the activity was totally abolished (in the case of H473A) or strongly reduced (in the case of A381D) (Morillas et al., 2001).

Figure 30 (next page). Multiple sequence alignment of several carnitine palmitoyltransferases. The amino acid sequences of human, mouse and rat CPT1A, CPT1B and CPT1C were aligned as described in the Experimental procedures section 5.1. Colouring of similar residues is performed according to average BLOSUM62 score: identical residues, corresponding to high values in BLOSUM62 score, are coloured in cyan, semi-conserved residues, with a score of 1.5, are coloured in midblue and residues showing lower scores, below 0.5, are coloured in lightgray. The catalytic His^{473} and Ala^{381} are highlighted with a red and green asterisk. The conservative and semi-conservative changes of residues contacting carnitine and palmitoyl-CoA are higlighted with a blue asterisk.

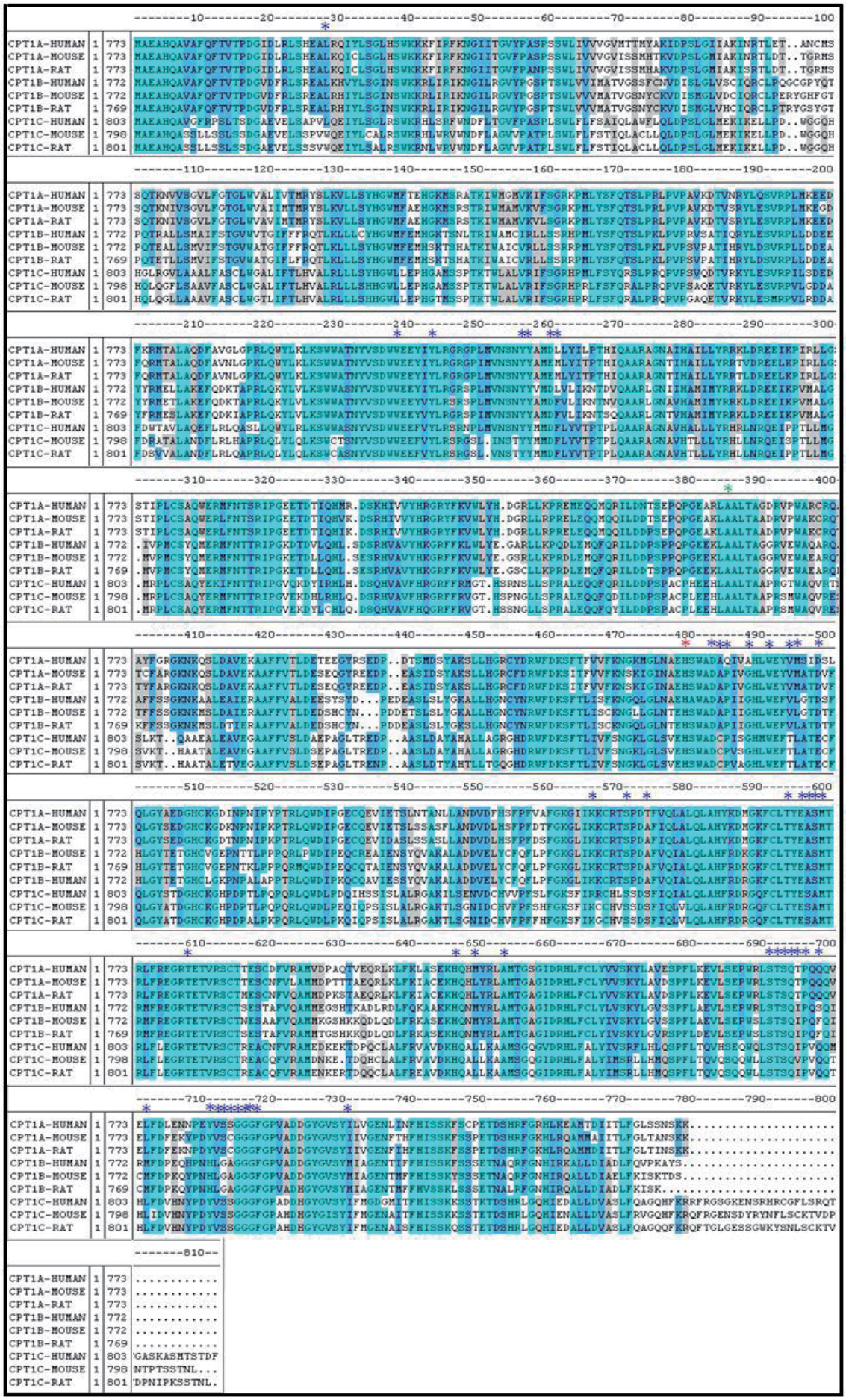
CPT1A-HUMAN
CPT1A-MOUSE
CPT1A-RAT
CPT1B-HUMAN
CPT1B-MOUSE
CPT1B-RAT
CPT1C-HUMAN
CPT1C-MOUSE
CPT1C-RAT

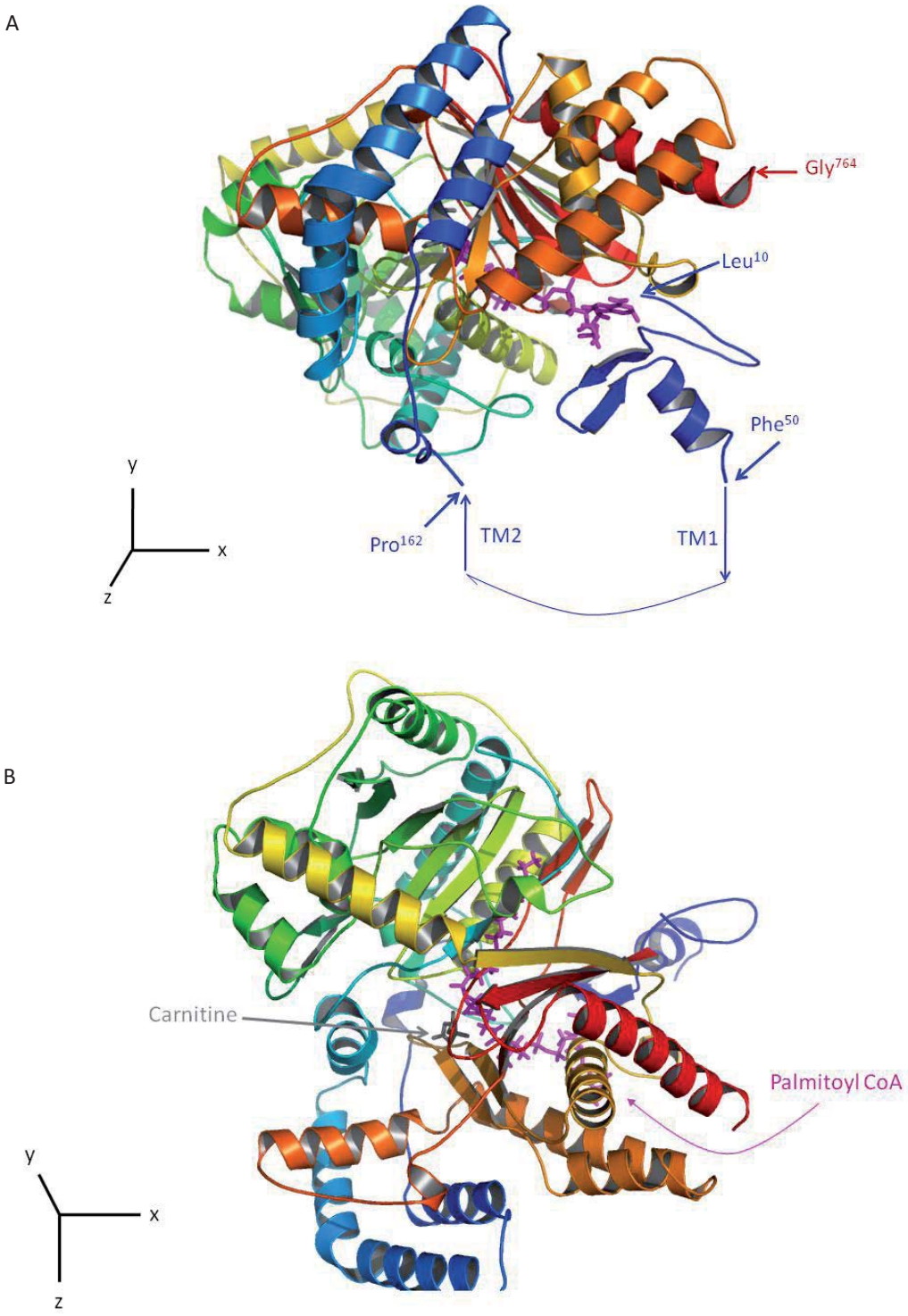

Figure 31. Structural model of rat CPT1C. A proposed model for CPT1C is shown in the ribbon plot representation. The putative sites for carnitine (white) and palmitoyl-CoA (magenta) are indicated. **(A)** A frontal view of the model in which residues flanking the modeled region have been highlighted (regions modeled: from Leucine 10 to Phenylalanine 50 (in blue) and from Proline 162 to Glycine 764). In this model the hypothetic position of transmembrane domains 1 and 2 (TM1, TM2), and the loop region between them, have been represented by blue arrows. **(B)** A top view of the model.

Looking at the 3-D model, the residues important for catalysis and the residues forming the channel where substrates are fitted have the same spatial distribution as in CPT1A model (Figure 32).

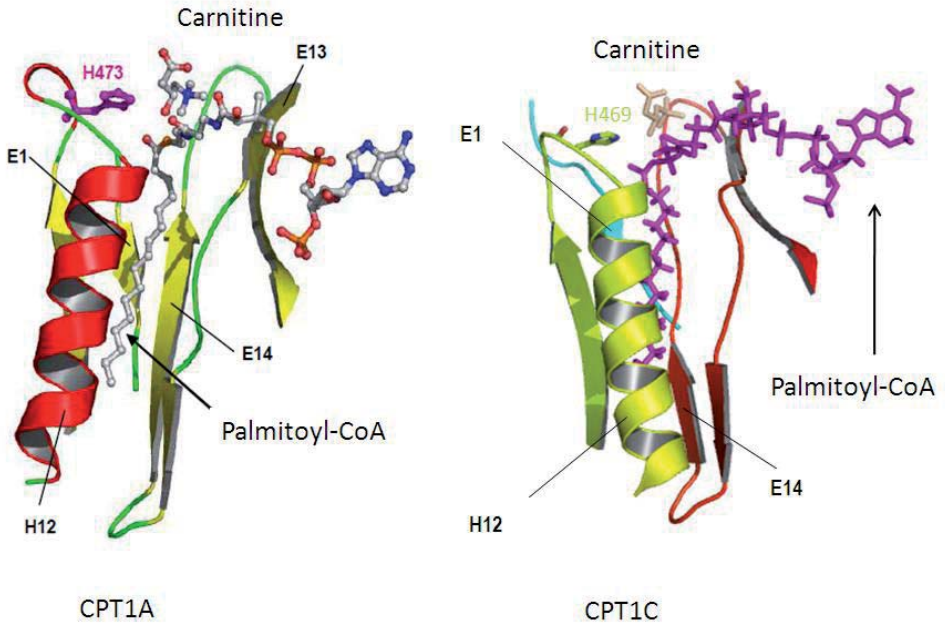

Figure 32. Comparison of residues forming the hydrophobic channel where palmitoyl-CoA accommodates in CPT1A and CPT1C models. Relative position of the hydrophobic channel for docking palmitoyl-CoA, formed by alpha helix 12 and the beta sheet 14. Catalytic histidine and carnitine are also shown.

The data provided by this 3-D structural model of CPT1C suggest that this isozyme would be able to catalyze the conversion of palmitoyl-CoA into palmitoylcarnitine. Therefore, the first experimental aim of this study was to determine the kinetic parameters of this isozyme.

2. CPT1 ENZYMATIC ACTIVITY

The first aim of this study, with regard to the 3-D model, was to characterize the functional properties of CPT1C. Given the fact that there is a high sequence similarity between CPT1A and CPT1C at the protein level, CPT1C was predicted to catalyze the same reaction as that of CPT1A.

Preliminary results from our group had shown a significant increase in palmitoylcarnitine levels in mammalian cell extracts overexpressing CPT1C, suggesting that CPT1C had carnitine palmitoyltransferase activity and that palmitoyl-CoA was a substrate for this isoenzyme. Considering that mammalian cells have endogenous CPT1 activity, it makes this model inappropriate to study the enzymatic activity of CPT1C.

In order to characterize the functional properties of CPT1C, heterologous expression in the yeast *Saccharomyces cerevisiae,* which lacks CPT1 activity, was performed. This model had

been used previously to characterize similar enzymes (Zhu et al., 1997; Cohen et al., 1998; Prip-Buus et al., 1998; Morillas et al., 2002)

2.1 CPT1C activity in yeast mitochondria

The full length cDNA of rat CPT1C was previously cloned in our group, into a yeast expression vector called pYES2 (pYES-CPT1C). This vector has been designed for heterologous expression of the protein of interest in *S. cerevisiae* under the control of the GAL1 promoter. As a positive control, full length cDNA of rat CPT1A had also been cloned into the same vector (pYES-CPT1A). The empty pYES2 vector was used as a negative control and the values obtained from the empty vector in the assays, as well as blank values, were subtracted from all samples.

After expressing the different constructs in *S. cervisiae* W303-1A strain, cells were recovered, lysed and mitochondrial extracts were obtained. Then, CPT1 activity was determined by the radiometric method previously described by Morillas et al., 2000. The substrates were 50 µM palmitoyl-CoA and 400 µM L-[methyl-^{3}H] carnitine, and ^{3}H-palmitoylcarnitine was the product to determine. From 15 to 80 µg of protein from mitochondrial fractions were assayed for 5 min at 30°C, and specific activity was calculated (Figure 33). To verify the expression of the transformed plasmids, Western blot of assayed fractions was performed (bands corresponding to each sample immunoblotted with the corresponding antibodies are shown in Figure 33).

No CPT1C specific activity was found, although the expressed proteins were detected as shown in Figure 33, suggesting that the conditions for determining CPT1A activity were not suitable for CPT1C activity. Therefore, appropriate conditions for CPT1C activity assay need to be established.

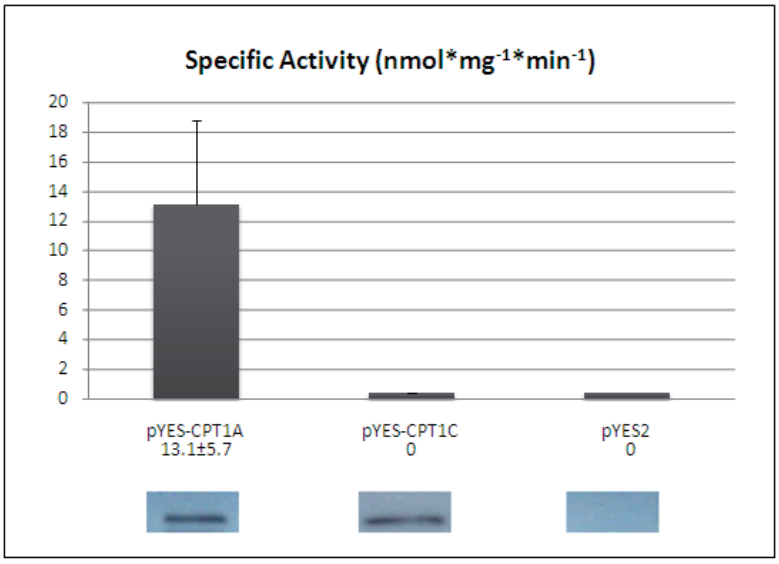

Figure 33. CPT1C activity in yeast mitochondria. Mitochondrial fractions isolated from *S. cerevisiae* expressing empty pYES2, pYES-CPT1A and pYES-CPT1C were assayed for CPT1 activity as described in Experimental procedures. Values are expressed as means of three separate experiments performed in duplicate ± standard deviation. Immunoblots of fractions assayed performed with anti-CPT1A (on the left) or anti-CPT1C (in the middle) antibodies, or both (on the right).

2.2 CPT1 assay in different conditions

As established conditions for CPT1A activity assay did not show catalytic activity for CPT1C, the conditions of the activity assay were changed.

To test the hypothesis whether CPT1C had a lower enzymatic activity than CPT1A, the reaction was performed for longer periods of time. No substantial increases in the specific activity were observed while CPT1A activity gradually decreased. At 20 minutes of reaction an activity of 0.2 nmol palmitoylcarnitine*min^{-1}*mg^{-1} prot for CPT1C was observed, which cannot be taken into account because this value is within the standard deviation of blank samples in the radiometric method (see Figure 34A and 34B).

Then the effect of temperature in the reaction was tested. Increasing the assay temperature to 37°C increased CPT1A activity but had no effect on CPT1C activity (Figure 34C and 34D).

To study whether CPT1C was an enzyme with a higher K_m for palmitoyl-CoA than CPT1A, palmitoyl-CoA concentration was increased by 5 fold showing a great decrease in CPT1A activity and no CPT1C specific activity (values obtained were under the limit of detection for this technique) (seeFigure 34C and values in Figure 34D).

With all these negative results on CPT1C activity, and considering that CPT1C contains all the catalytic residues within its catalytic core, a new hypothesis was postulated: maybe CPT1C had some structural features especially in the N- or C-terminus (which are more divergent) that would block its own ability to catalyze the same reaction that CPT1A does. To test this hypothesis, a chimeric construct was generated.

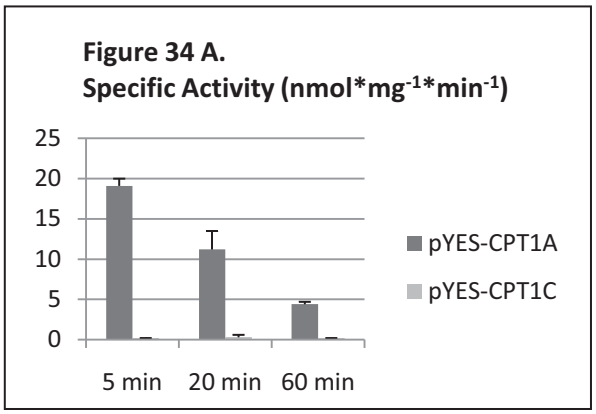

	pYES-CPT1A	pYES-CPT1C
5 min	19.1±0.9	0
20 min	11.2±2.3	0.2±0.3
60 min	4.4±0.3	0

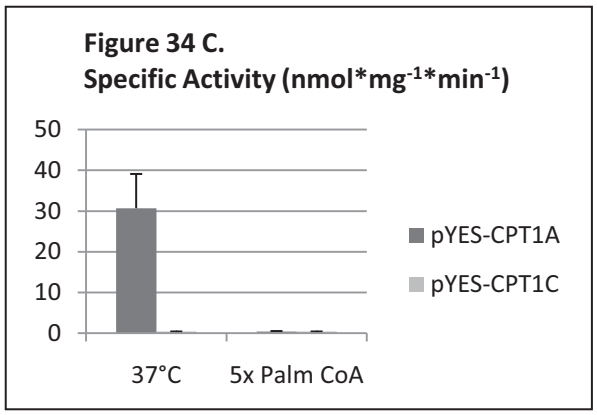

Figure 34 D.	pYES-CPT1A	pYES-CPT1C
37°C	30.6±8.4	0
5x Palm CoA	0.4±0.1	0.2±0.3

Figure 34. Study of CPT1C specific activity under different conditions. **(A) Determination of the activity at different times**. Mitochondrial fractions isolated from *S. cerevisiae* expressing empty pYES2, pYES2-CPT1A and pYES2-CPT1C were assayed for CPT1 activity for 5, 20 and 60 min. **(B)** Table of values represented in previous graph. Values are expressed as mean ± standard deviation of a single experiment performed in triplicate. **(C) Determination of the activity at a different temperature and at greater substrate concentration**. The same fractions were assayed for CPT1 activity in the different conditions described in the text, shown in the graph as: 37°C (assay performed at 37°C) and 5x palmitoyl-CoA (assay performed with 250 µM of the substrate palmitoyl-CoA in the reaction mix). **(D)** Table of values represented in previous graph are expressed as mean ± standard deviation (n=4).

2.3 Chimeric construct

Catalytic residues of CPT1A are conserved in CPT1C and they are located in the central part or core, of the protein sequence. Furthermore, CPT1C C-terminus is the most divergent region when compared to CPT1A and CPT1B sequences, and one can speculate that this region is responsible for an inhibitory effect. Therefore, it was hypothesized that a chimeric protein containing CPT1C core fused to N- and C-terminal domains of CPT1A sequence would be active. This chimera was engineered in pYES2 vector (pYES·ACA) as shown in Figure 35A. If this construct was to show some activity, it could be concluded that the mentioned structural domains of CPT1C sequence were inhibiting its ability to catalyze this enzymatic reaction.

CPT1 activity was determined by the radiometric method in the usual conditions (Morillas et al., 2000), for 4 minutes, on mitochondrial fractions from yeast expressing empty pYES, pYES-CPT1A and pYES·ACA. The results show a specific activity for pYES·ACA of 1.3 ± 1.5 nmol palmitoylcarnitine *min^{-1}*mg^{-1} prot but with high variability between experiments as showed by the value of the standard deviation (see results of mitochondrial fraction in Figure 35B and 35C). These results suggested that CPT1C catalytic core was less active than that of CPT1A, and that CPT1C defective activity is not due to either N- or C-terminal tail.

Preliminary results from our group showed the presence of CPT1C overexpressed protein also in the microsomal fraction of yeast extracts. Hence, this fraction was assayed for CPT1 activity in yeast expressing either empty pYES, pYES-CPT1A, pYES-CPT1C or pYES·ACA.

No substantial enzymatic activity at 4 or 10 min could be found in microsomal fractions of any construct (see Figure 35B and 35C). Residual CPT1A activity in microsomal fractions might be due to mitochondrial contamination.

A.

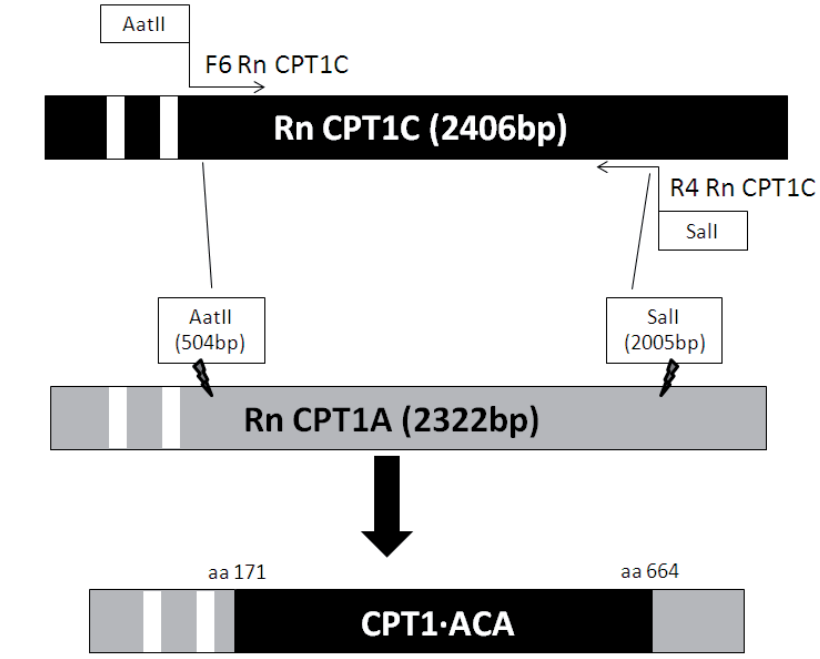

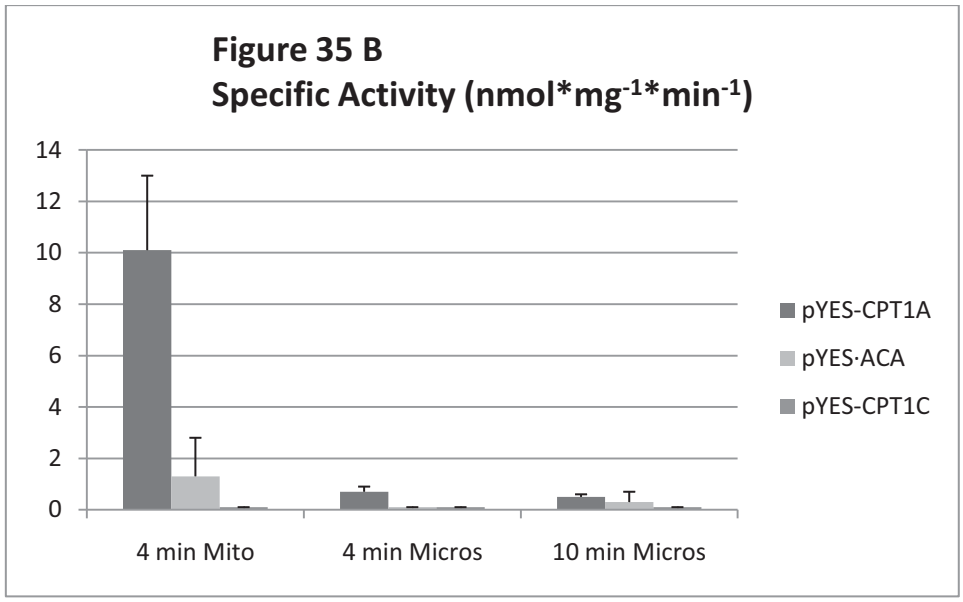

Figure 35 C.	pYES-CPT1A	pYES·ACA	pYES-CPT1C
4 min Mito	10.1±2.9	1.3±1.5	0
4 min Micros	0.7±0.2	0	0
10 min Micros	0.5±0.1	0.3±0.4	0

Figure 35. Study of the specific activity shown by catalytic core of CPT1C in CPT1 assay. **(A) Cloning strategy for creating pYES·ACA**. A chimera containing the catalytic core of rat (Rn) CPT1C and N- and C-terminus of rat (Rn) CPT1A in pYES2 was constructed (Cloning details in Experimental Procedures 1.7 section). **(B and C) Activity assay of pYES·ACA and microsomes**. **(B)** Mitochondrial and microsomal fractions isolated from *S. cerevisiae* expressing empty pYES, pYES-CPT1A and pYES-CPT1Aca were assayed. **(C)** Table of values represented in previous graph expressed as mean specific activity ± standard deviation of n=4.

To verify the expression of all the transformed proteins in all assays, Western blot of the fractions assayed were performed. See a representative Western blot in Figure 36. As shown in the figure, CPT1A is mainly expressed in mitochondria but CPT1C is expressed in both fractions (mitochondrial and microsomal).

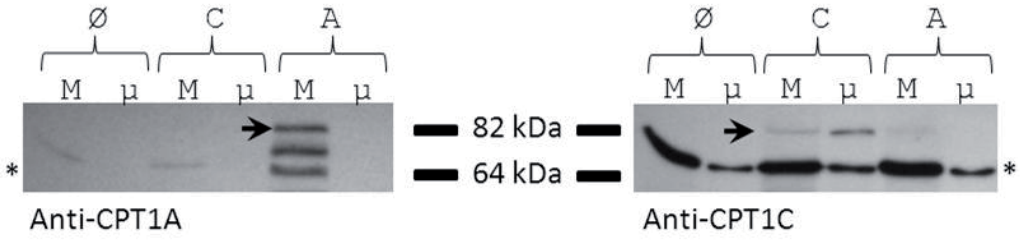

Figure 36. Representative Western blot of mitochondrial (M) and microsomal (µ) fractions isolated from *S. cerevisiae* expressing empty pYES (Ø), pYES-CPT1C (C), pYES-CPT1A (A) and pYES·ACA (ACA), subjected to immunoblotting using anti-CPT1A and anti-CPT1C antibodies. The arrow indicates the band corresponding to the overexpressed protein. Multiple bands on mitochondrial extracts of CPT1A might be due to proteolysis. Asterisk shows unspecific band. 80 µg of protein were loaded per lane.

Taken together, these results suggest that CPT1C expressed in yeast has no activity or very low. It could be due to several reasons:

1) The assay conditions are not the adequate ones for optimal activity of CPT1C isolated from yeast.
2) The optimal substrate for the reaction is other than those previously tested.
3) Yeast cells lack some specific modifications that are present in mammalian cells.
4) Improper folding of the protein expressed in yeasts (not very plausible because the same heterologous expression method has been used to characterize CPT1A enzymatic parameters).
5) The values of specific activity for CPT1C found here are below the limit of detection of the radiometric method, suggesting that a more sensitive method needs to be developed in order to characterize the functional properties of CPT1C.

3. SUBCELLULAR LOCALIZATION

Although CPT1A and CPT1B are known to be mitochondrial enzymes, results from our group pointed to CPT1C being expressed in an organelle other than mitochondria (see Westrern blot in Figure 36).

To study the intracellular localization of CPT1C, different strategies were designed. One approach was to transiently transfect different cell lines with CPT1C fused to EGFP at the C-terminal end, and subsequently perform immunofluorescence co-localization experiments on the same cells with different specific organelle markers. Another approach was to determine the intracellular localization of endogenous CPT1C in neuronal primary cultures using anti-CPT1C antibodies.

3.1 CPT1C and CPT1A show different intracellular distribution

The first approach was to use the EGFP fusion protein strategy to detect CPT1C localization. It is well known that in many proteins, the signal sequence targeting the protein to its specific organelle is located in the N-terminal region of the protein. Hence, fusion proteins containing the EGFP moiety at the C-terminal end of the desired protein sequence were engineered.

Full length cDNAs of rat CPT1A and CPT1C (omitting nucleotides corresponding to the stop codon) were cloned into pEGFP-N3 vector (a mammalian expression vector which encodes EGFP fused to the C-terminal end of the sequence cloned into the MCS). These constructs expressed the two fusion proteins schematized on Figure 37.

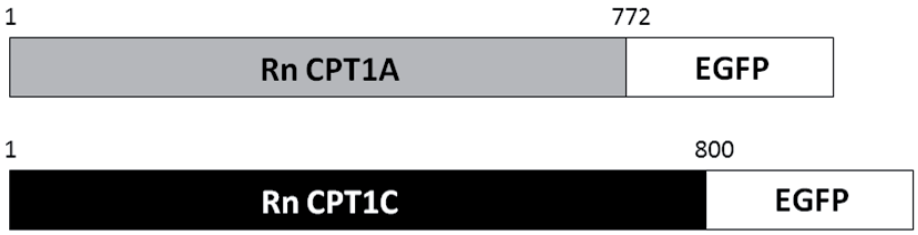

Figure 37. Schematic representation of EGFP fusion proteins expressed from the pEGFP-N3 plasmid constructs. The gray square represents rat (Rn) CPT1A sequence and the black one represents that of rat CPT1C. White squares represent EGFP protein. Numbers indicate amino acid positions of the corresponding CPT1 proteins.

Lipofectamine reagent was used to transiently transfect both plasmids in different cell lines. This strategy allows the visualization of the fluorescent pattern shown by the protein fused to EGFP.

The first step was to transfect CPT1A and CPT1C in SH-SY5Y, a cell line with neural characteristics (derived from a human bone metastatic neuroblastoma). The pattern of transfected constructs at different times after transfection was analysed. The first finding was that CPT1C showed a totally different pattern compared to that of CPT1A, and it was the same at all times studied (see Figure 38). Afterwards, a non-neuronal cell line like HEK293T (derived from human embryonic kidney) was also transfected showing the same differential pattern at 48 h after transfection (Supplemental data, Figure S1). This lineage was tested because it has higher transfection efficiencies making it more suitable for possible future experiments. In both cases, fluorescent CPT1A was expressed in punctuate or discrete filamentous manner, while fluorescent CPT1C showed a reticular pattern.

To confirm these results in primary cultures, the same constructs were transfected in human primary cultures of fibroblasts available in our lab from previous work. 48h after transfection the pattern was analyzed and the same distributions were observed (Supplemental data, Figure S1). These plamids were also transfected in neuronal primary cultures showing distinct patterns (Supplemental data, Figure S1).

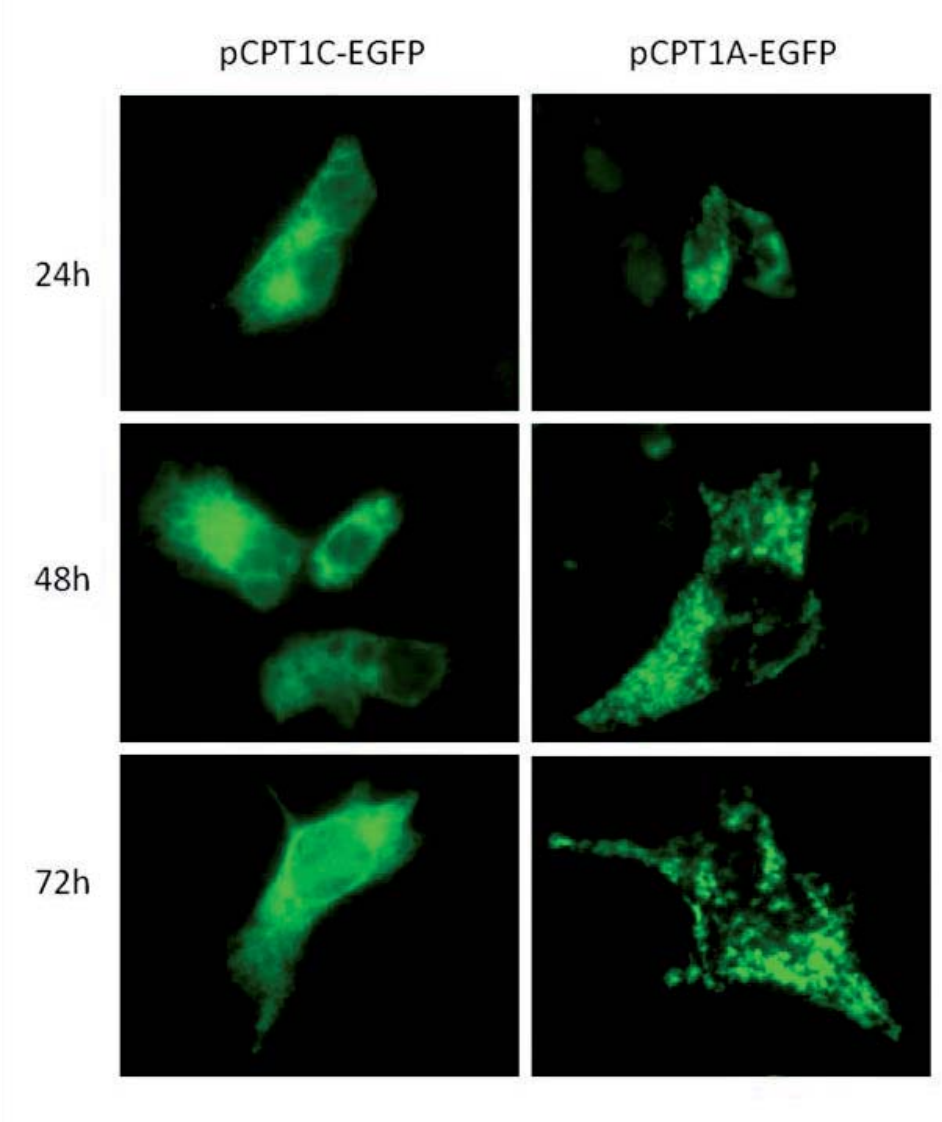

Figure 38. Fluorescence pattern shown by pCPT1A-EGFP and pCPT1C-EGFP. SH-SY5Y cells were transiently transfected with Lipofectamine 2000 reagent with pCPT1A-EGFP and pCPT1C-EGFP constructs and fluorescence was visualized at different times after transfection (24h, 48h and 72h, as shown in the figure). Images were taken with 1000x magnification in a Leica DM/IRB fluorescence microscope.

All these results suggested that CPT1A was located in the mitochondrial outer membrane as previously described (Broadway et al., 2003) and that CPT1C might be located in the endoplasmatic reticulum (ER). Therefore, the next step was to directly demonstrate these apparent localizations.

3.2 CPT1C is localized in the endoplasmic reticulum of neurons

Co-localization studies were performed with MitoTracker, a potential-sensitive dye that accumulates in mitochondria, and with anti-calnexin, an ER integral protein. These studies were carried out on fibroblasts, SH-SY5Y or HEK293T cells transiently expressing fluorescent CPT1A and CPT1C. Figure 39A clearly shows that CPT1C is localized in the ER membrane, but not in mitochondria. In contrast, CPT1A is localized in mitochondria, as previously described in other cells (Broadway et al., 2003) (Figure 39B). The slight co-localization of CPT1A with anti-calnexin and that of CPT1C with Mitotracker, may be due to the contact sites between the ER membrane and the mitochondrial outer membrane, known as mitochondrial- associated membranes (Rusiñol et al., 1994; Wang et al., 2000; Bionda et al., 2004; Goetz and Nabi, 2006).

To assess whether either isoform is localized in peroxisomes (other organelles implicated in fatty acid oxidation) co-localization studies were performed with anti-PMP70, a peroxisomal membrane protein. No major co-localization was observed between PMP70 and CPT1C or CPT1A. The slight co-localization of CPT1C or CPT1A with PMP70 may be due to a residual localization of the overexpressed proteins in peroxisomes (Figure 39C). The same experiments were performed with SH-SY5Y cells, PC12 cells and HEK293T cells with same results.

Figure 39 (next page). Co-localization studies of CPT1C in mitochondria, ER and peroxisomes. **(A)** Fibroblasts were transfected with pCPT1C-EGFP or pCPT1A-EGFP and incubated with anti-calnexin as primary antibody. **(B)** Fibroblasts transfected with the same plasmids were stained with Mito-Tracker. **(C)** HEK293T cells transfected with the same constructs were incubated with anti-PMP70 as primary antibody. (Images were taken with a fluorescent or a confocal microscope.)

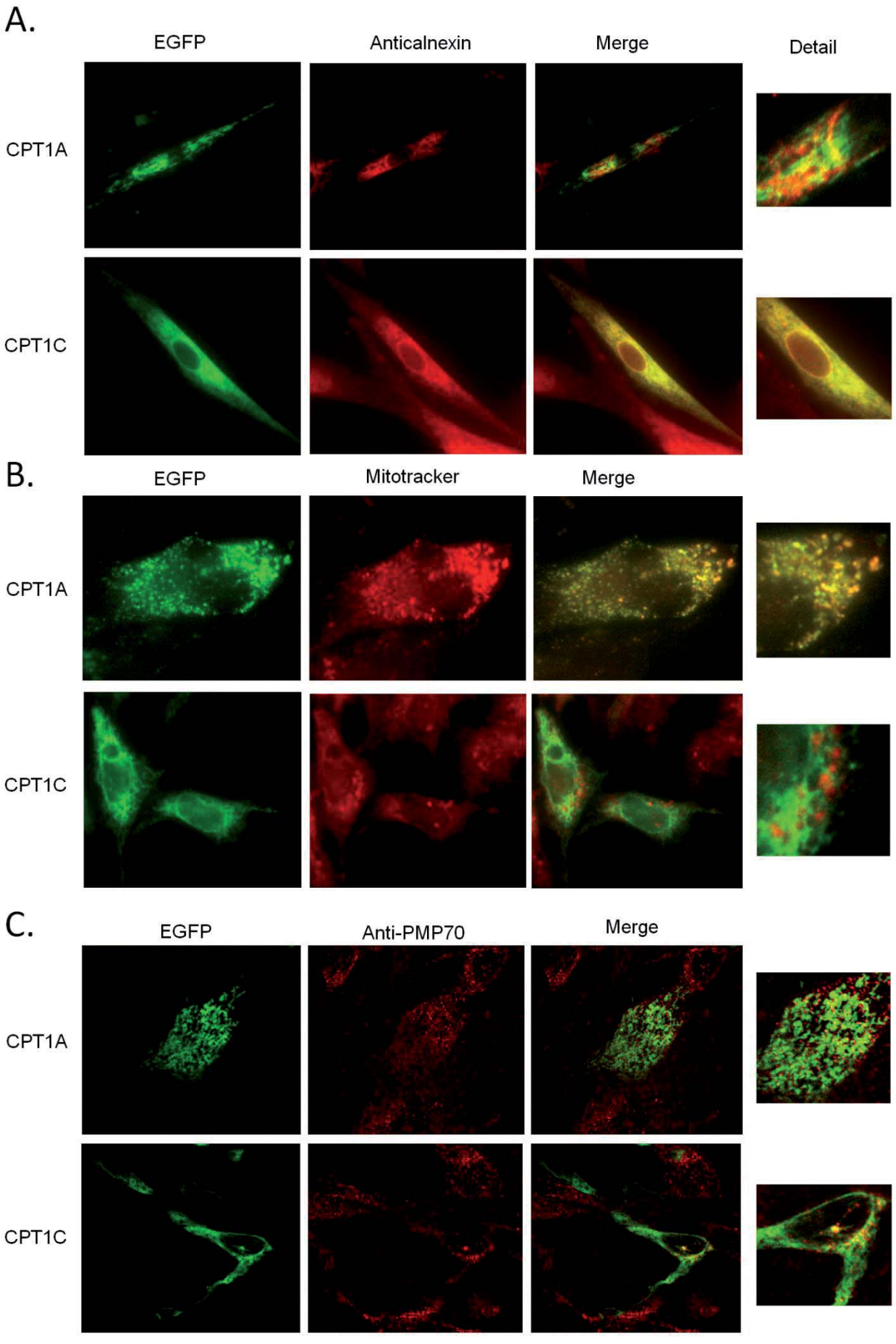
A.
EGFP
Anticalnexin
Merge
Detail
CPT1A
CPT1C
B.
EGFP
Mitotracker
Merge
CPT1A
CPT1C
C.
EGFP
Anti-PMP70
Merge
CPT1A
CPT1C

The next step was to confirm the ER localization of the endogenous protein in neuronal primary cultures. With this aim we obtained mice cortical primary cultures, from E16 embryos and cells were cultured for 6 days. After that period, cells were fixed and immunodetections with anti-CPT1C antibody and with anti-calreticulin (another ER marker) were performed. Figure 40 shows total co-localization of these two proteins in cortical neurons. Staining of CPT1C can be observed in the cell body and in neuronal projections, which indicates that CPT1C is expressed in the rough (mainly localized at the neuronal body) and smooth endoplasmic reticulum (observable in all the structures of the neuron) (Rolls et al., 2002).

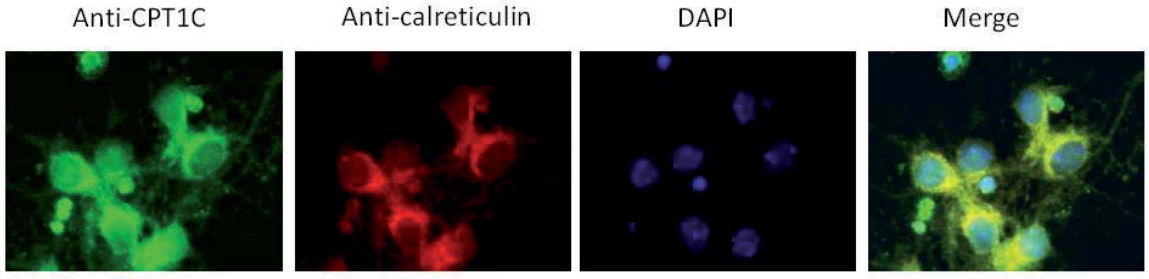

Figure 40. Immunodetection of endogenous CPT1C in neurons. Immunocytochemistry using anti-CPT1C (in green) and anti-calreticulin (in red) antibodies was performed. Nucleus are in blue from DAPI staining. Cells were visualized with 40x objective in a fluorescent microscope.

These results confirmed CPT1A localization in mitochondria and demonstrated that CPT1C is localized to the ER membrane. Therefore, the next aim was to elucidate the region responsible for this specific localization.

3.3 The N-terminus of CPT1C targets it to the endoplasmic reticulum

Key residues directing CPT1A isoform to mitochondria have been described (Cohen et al., 1998; Cohen et al., 2001). Given the fact that some of these residues were divergent in CPT1C sequence (see Figure 7 in section 2.2 of the Introduction), the next objective was to elucidate whether the same region was responsible for ER targeting of CPT1C isoform.

With this aim, two chimeric plasmids were constructed. One encoding the two trans-membrane domains and the mitochondrial import signal described by the Prip-Buus group (Cohen et al. 2001) of CPT1A gene, fused to the rest of the sequence of CPT1C, and vice versa. The recombinant plasmids were called pCPT1·AC-EGFP and pCPT1·CA-EGFP, respectively (see Figure 41A).

SH-SY5Y cells were transiently transfected with these constructs and cells were visualized in a fluorescent microscope (Figure 41B).

CPT1C and CPT1·CA showed the same reticular pattern, suggesting that they are localized in ER. CPT1A and CPT1·AC showed the same punctuate or filamentous pattern described for the

mitochondrial localization as shown in Figure 41B. The same experiments in primary cultures of fibroblasts were performed with the same results (Supplemental data, Figure S2).

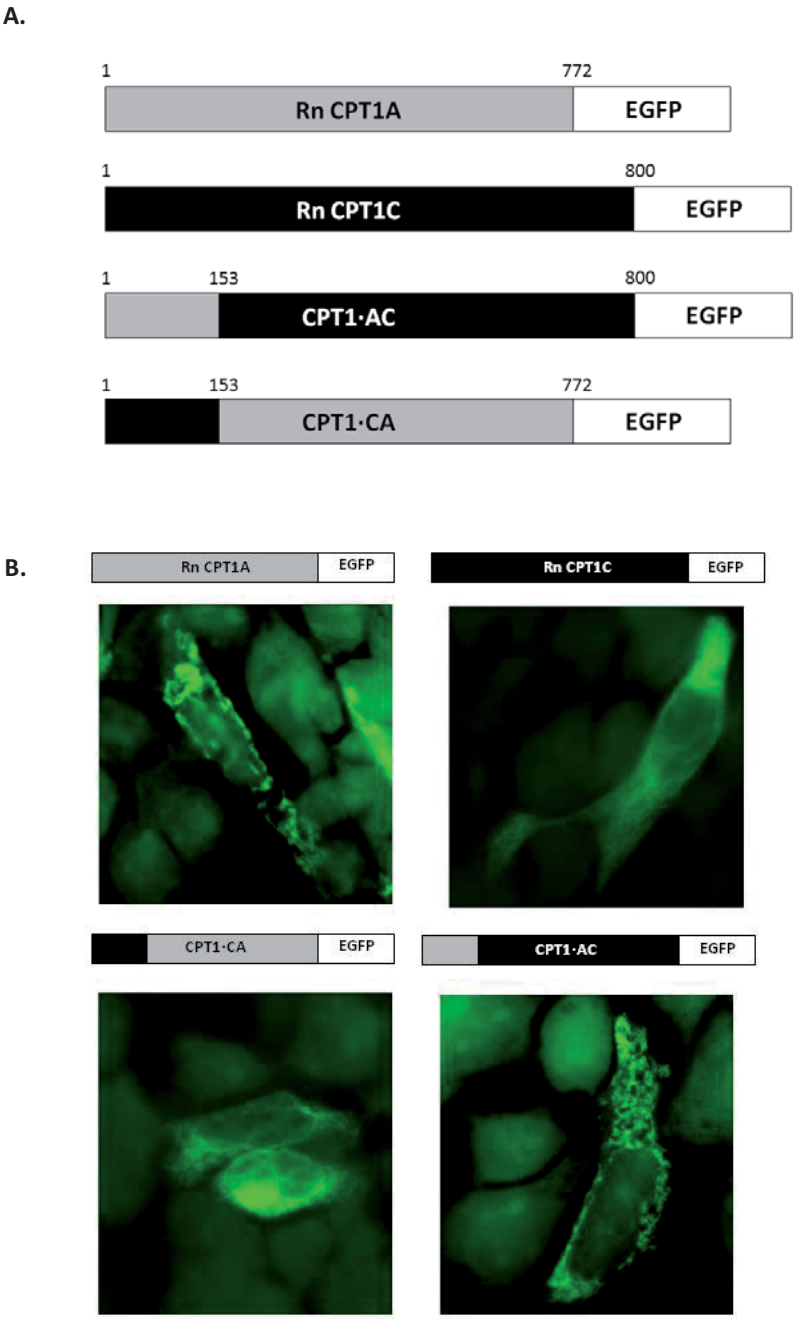

Figure 41. **Subcellular localization of fusion proteins CPT1A-EGFP, CPT1C-EGFP, CPT1·CA-EGFP, and CPT1·AC-EGFP in cultured cells.** (In gray, rat (Rn) CPT1A protein sequence; in black, rat (Rn) CPT1C sequence; in white: EGFP) **(A)** Schematic representation of chimeric proteins obtained. CPT1·CA-EGFP contains the first 153 aa of CPT1A replaced by the same region of CPT1C, and vice versa for CPT1·AC-EGFP. For detailed description of cloning strategy and primers used see Expermiental Procedures 1.7. **(B)** SH-SY5Y human neuroblastoma cells were transfected with the different plasmids. 48 h after transfection, cells were visualized in a fluorescence microscope (1000x magnification).

These results suggested that the exchange of N-terminal ends between the two CPT1 isoforms swapped the intracellular localization of the recombinant chimeric proteins, suggesting that within this region of CPT1C is contained a putative microsomal targeting signal responsible for ER localization, or that the lack of a specific mitochondrial targeting signal directs the protein to microsomes by default.

These results also suggested that ER localization for CPT1C was specific and not due to aberrant localization of the over-expressed protein.

Taken together all these results lead to the conclusion that CPT1C is localized to ER membrane of neurons and that the specific sequence of CPT1C N-terminal domain drives the protein to this localization.

Many ER targeted proteins remove their signal peptide after the insertion in the ER. Given the fact that in SDS-PAGE gels, CPT1C shows a molecular weight lower than that predicted from its amino acid sequence, we wanted to confirm whether there is a processing of the N-terminal region of CPT1C, or not. Therefore, the next aim of this study was to clarify this issue.

4. CPT1C N-TERMINUS PROCESSING

To elucidate if there is a processing of the N-terminus of the endogenous CPT1C, we used the antibody to N-terminal region of CPT1C (produced and tested in our laboratory as described in Experimental procedures 6.2 of this manuscript, Figure 29) on brain extracts from wild type (WT) and knockout (KO) mice (that do not express CPT1C protein). In our group a CPT1C KO mouse model has been developed and is being studied (P. Carrasco and N. Casals, unpublished results).

Antibodies to C-terminus of CPT1C were used to confirm the presence or absence of this protein in each extract. As shown in Figure 42, N-terminal antibody did not detect CPT1C, suggesting that there is a processing of this region of the protein.

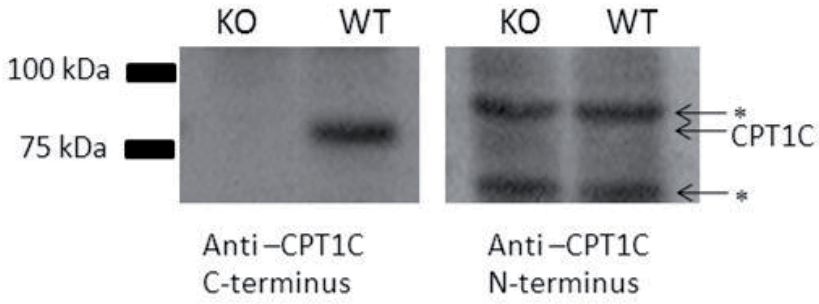

Figure 42. **Western blot of brain extracts probed with either anti-CPT1C C-terminus or anti-CPT1C N-terminus antibodies.** Arrows point different bands detected: two are unspecific bands (*) and the other band corresponds to the expressed CPT1C in wild type mice (WT). Knockout mice have been obtained in our laboratory and they have shown not to express CPT1C, therefore brain extracts from these knockout mice (KO) were used as negative controls in this study. The N-terminus antibody had already been tested (see Experimental procedures 6.2, Figure 29). 100 µg of protein were loaded in each lane.

Thus far the subcellular localization of the protein, the region responsible for this location and possible modifications within it have been demonstrated. The next aim of this study was to elucidate if the predicted catalytic region of CPT1C is facing towards the cytoplasm or the lumen of the ER.

5. CPT1C MEMBRANE TOPOLOGY

As previously demonstrated, CPT1C is localized in the endoplasmic reticulum membrane. From sequence analysis two domains are predicted to be transmembrane, implying two possible topologies for CPT1C. Therefore, the predicted catalytic core of the enzyme can either be facing the cytoplasm or the ER lumen with different physiological consequences.

5.1 Prediction of membrane topology

The residues from the region containing the N terminus and two membrane-spanning regions of CPT1A are mainly equivalent to those found in CPT1C, which suggests that CPT1C most likely adopts the same membrane topology described for CPT1A (Fraser et al. 1997), with C- and N-terminal segments exposed on the cytosolic side of the membrane. To verify this hypothetical topology, we used two transmembrane topology prediction servers: **TMHMM version 2.0** (http://www.cbs.dtu.dk/services/TMHMM/) (Sonnhammer et al., 1998; Krogh et al., 2001; Moller et al., 2001) and **HMMTOP version 2.0** (http://www.enzim.hu/hmmtop/) (Tusnády and Simon, 1998; Tusnády and Simon, 2001), both using hidden Markov model (HMM). TMHMM is based on the "positive inside rule". This rule predicts that domains with a high amount of positive residues tend to be facing the cytosol. HMMTOP also incorporates preliminary experimental information into the topology prediction thus increasing the prediction accuracy of the method.

The predictions obtained for the catalytic core of CPT1A and CPT1C sequence of various species are summarized in the following table (Table 5 and Supplemental data, Figure S3A and S3B). In all cases, the orientation of the catalytic domain resulted to be the lumen of the corresponding organelle.

	CPT1A			CPT1C		
	Rat	Mouse	Human	Rat	Mouse	Human
TMHMM	lumen	lumen	lumen	lumen	lumen	lumen
HMMTOP	lumen	lumen	lumen	lumen	lumen	lumen

Table 5. Orientation of C-terminal domain of rat, mouse and human CPT1A and C obtained from two prediction servers: TMHMM and **HMMTOP** version 2.0. "Lumen" indicates the intraorganellar orientation of the C-terminal domain. In CPT1A "lumen" corresponds to mitochondrial intermembranous space, and in CPT1C it corresponds to the lumen of the ER.

The topology of rat CPT1A has already been experimentally demonstrated (Fraser et al., 1997) and the orientation of the catalytic core is the opposite from the predicted with these bioinformatic tools. Therefore the topology of CPT1C in the ER membrane needed to be experimentally demonstrated.

5.2 The catalytic region of CPT1C is facing the cytoplasm

It is well known that glycosylation of membrane and secretory glycoproteins occur only on the luminal side of the ER and Golgi apparatus (R. Kornfeld and S. Kornfeld, 1985). The co-translational attachment of N-linked oligosaccharides to nascent polypeptide chains occurs on asparagine residues in the sequence Asn-*X*-Ser/Thr, where *X* can be any amino acid except proline (R. Kornfeld and S. Kornfeld, 1985). One approach to defining the topology of an integral protein is to detect N-linked oligosaccharides within it (Chang et al. 1994; Schinkel et al. 1993). The feasibility of this strategy was indicated in its previous successful application to the testing of topological models of integral membrane proteins such as 3-hydroxy-3-methyl-glutaryl-CoA reductase (HMGCR) (Olender and Simon, 1992), cystic fibrosis transmembrane conductance regulator (CFTR) (Chang et al., 1994) and multidrug resistance protein (MRP) (Hipfner et al. 1997).

To elucidate CPT1C membrane topology, the potential glycosylation pattern was analysed. Different constructs with N-glycosylation sites introduced in the multiple domains of CPT1C were created and deglycosylation assays on microsomes from cells transfected with the different constructs were performed.

We used NetNGlyc server (http://www.cbs.dtu.dk/services/NetNGlyc) to find potential N-glycosylation sites in CPT1C. Endogenous Asn-*X*-Ser/Thr sequences were identified for rat, mouse and human CPT1C. These endogenous sites were all located in the core region of CPT1C contained in the predicted catalytic domain (see Figure 43A). Some of these sites (Asn^{250} and Asn^{311}) were potentially exposed to the action of oligosaccharyltransferases, as predicted from our theoretical model of CPT1C structure (Figure 43A). Additional N-glycosylaiton sites were introduced at amino acid positions 22 and 86, located in the N-terminal region (region prior to the first predicted transmembrane domain) and the loop region (region between the two predicted transmembrane domains) respectively (shown in Figure 43B). All sequences were cloned into pIRES vector obtaining the constructs: pIRES-Nterm, pIRES-Loop and pIRES-CPT1C (see description and scheme in Figure 43B).

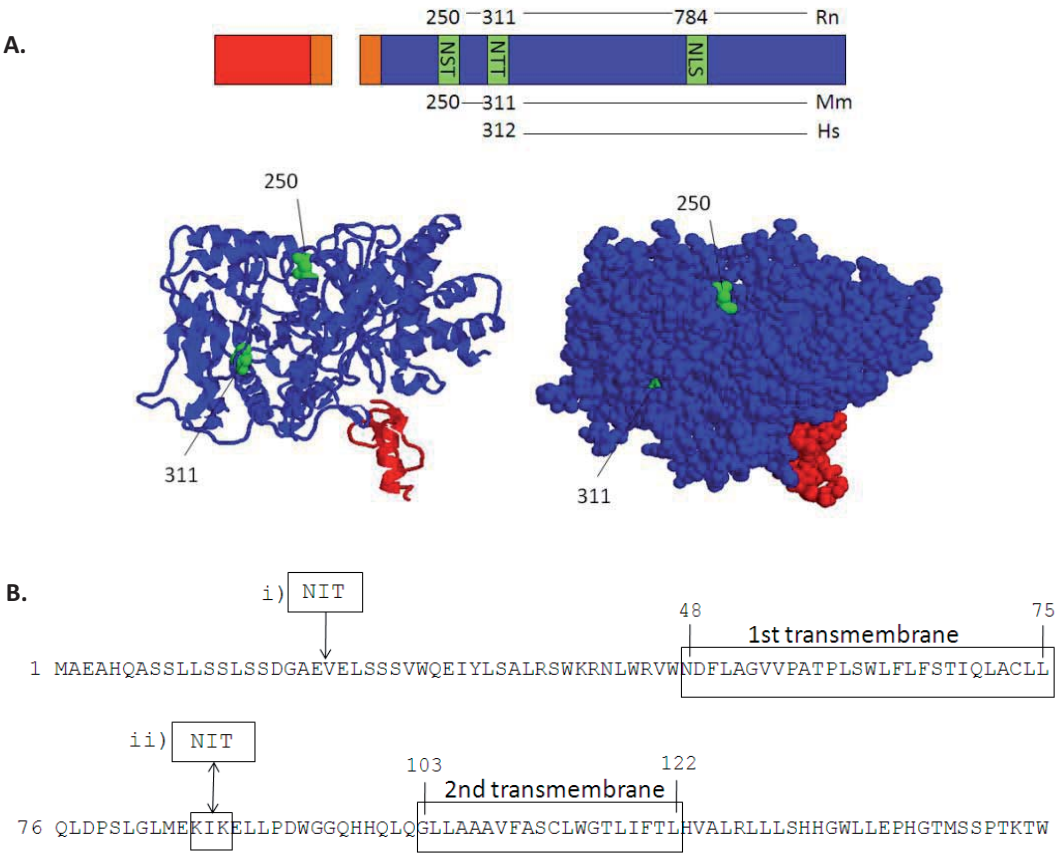

Figure 43. (A) 3-D Theoretical model of CPT1C showing putative glycosylation sites. Sites potentially exposed to the action of oligosaccharyltransferases are shown in green, and their respective amino acid positions are numbered on rat (Rn), mouse (Mm) or human (Hs) CPT1C sequences. **NST:** Asn-Ser-Thr, **NTT:** Asn-Thr-Thr and **NLS:** Asp-Leu-Ser. The structure of the N-terminal domain (in red), the transmembrane domains (in brown) and region after transmembrane domains (in blue) are shown. C-terminal tail of CPT1C (residues that lack in CPT1A sequence) and the loop region (between transmembrane segments) are not shown in this model. **(B) Amino acid sequence of 150 first residues of rat CPT1C sequence.** Overview of the strategy used for introducing glycosylation sites at the N-terminal and loop region of CPT1C. **pIRES-Nterm** (i) incorporates a whole glycosylation site (**NIT**: Asn-Ile-Thr) and **pIRES-Loop** (ii) creates a glycosylation site (NIT) by replacing two nucleotides using site-directed mutagenesis. Predicted positions of both transmembrane regions are also shown. For cloning details see Experimental procedures 1.7.

Using Metafectene reagent, HEK293T cells were transiently transfected with either empty pIRES, pIRES-Nterm, pIRES-Loop or pIRES-CPT1C, with an efficiency of approximately 80-90% (Figure 44A). After 48 hours of transfection cells were lysed, microsomal fractions were recovered and deglycosylation assays were performed using Peptide-N- glycosidase F (PNGase F) following manufacturer's recommendations. This enzyme releases asparagine-linked oligosaccharides from glycoproteins by hydrolyzing the amide of the asparagine side chain producing a decrease in the molecular weight of the protein and in consecuence, an increased mobility in gel electrophoresis. As a positive control for the deglycosylation assay we used bovine pancreatic Ribonuclease B (RNase B) which is a glycoprotein that contains a single glycosylation site at Asn^{34} (see figure 44B).

As shown in Figure 44C only microsomes from cells transfected with pIRES-Loop showed a decrease of 2.5 kDa when treated with the deglycosylating enzyme PNGase F. No band corresponding to CPT1C was detected in cells transfected with empty pIRES, as HEK293T cells do not express CPT1C.

Contrary to what was predicted using the bioinformatic tools, this result supports a model in which the N-terminal and the catalytic domains of CPT1C might be facing the cytoplasm, and the loop region is probably facing the lumen of ER.

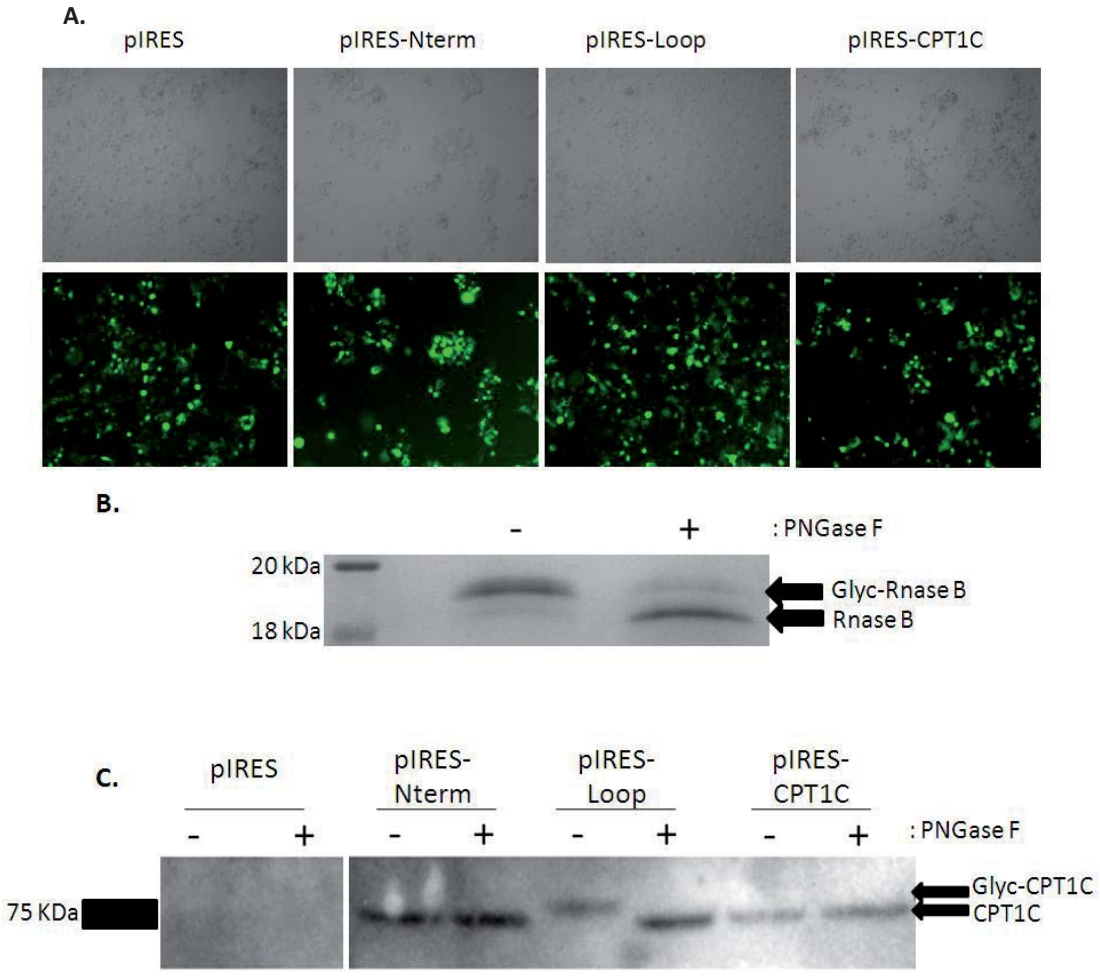

Figure 44. Experimental demonstration of CPT1C membrane topology. (A) Transfection efficiency. 48h after transfection approx. 80-90% of the HEK293T cells showed green fluorescence from the expression of the EGFP encoded in pIRES vectors. Images were taken with 40x magnification in a fluorescence microscope either with white light (upper images) or filter for green fluorescence (bottom images). **(B) Positive control of deglycosylation assay**. RNase B was treated with or without PNGase F showing a mobility shift. Arrows point bands corresponding to glycosylated RNase B ("Glyc-RNAase B", 16 kDa) and the deglycosylated form ("RNase B", 13 kDa) in a 15% SDS-PAGE gel stained with Blue Coomassie. **(C) Deglycosylation assay**. Immunoblotting with CPT1C antibody of microsomal fractions treated either with (+) or without (-) PNGase F and separated in 8% SDS-PAGE. Band corresponding to glycosylated form of CPT1C is indicated by an arrow and named as "Glyc-CPT1C". Bands corresponding to non-glycosilated CPT1C are named "CPT1C".Only microsomes expressing pIRES-Loop showed a mobility shift.

6. CPT1C PARTNERS

At this point of the work, CPT1C function had not been clarified yet. Therefore, the next aim of this study was to open new lines of research that would deal with the function of this interesting neuron-expressed protein in the future.

An important clue in protein function is the interaction networks where the protein is involved. The knowledge of such protein-protein interactions might help elucidating the cellular processes where CPT1C participates. One approach for detecting protein interactions *in vivo* is the yeast two hybrid system (Y2H) (Fields and Song, 1989), hence a Y2H assay was performed with CPT1C as the bait protein, and a human brain cDNA library, as the prey potential binding partners.

The design of the bait protein is a key element in the development of the Y2H assay. As the catalytic core has been shown to be facing the cytoplasm, this domain is potentially capable of interacting with other proteins. Hence, the CPT1C used as the bait contained the catalytic core. Transmembrane domains were excluded from the bait, as they could retain the protein in its target organelle and would not let it go to the nucleus were the interaction can be detected in this system. Moreover, given the fact that the N-terminal domain of the protein has been suggested to be proteolyzed, this domain was not present in the bait, either (Figure 45).

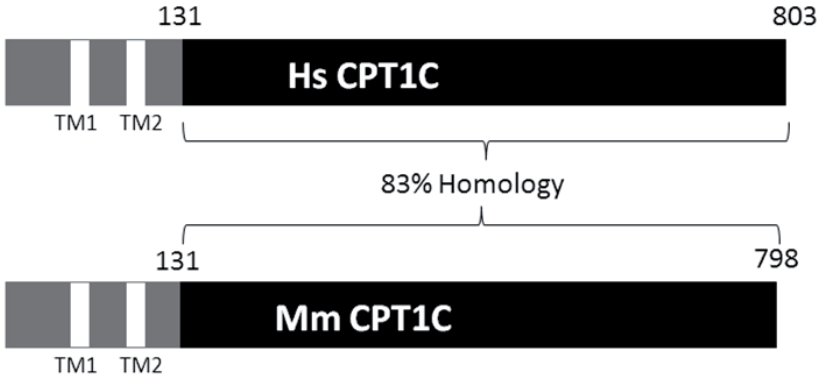

Figure 45. Schematic representation of the CPT1C fragment used as bait. Human (Hs) and mouse (Mm) protein containing amino acids from 131 to the end of the protein sequence was cloned into pGBT9 for the Y2H assay (region in black).For cloning details see Experimental procedures 1.7 section. Transmembrane domains and region shaded in gray were excluded from the bait. It also shows the homology among the fragments used as baits.

The interacting partners were identified by colony PCR analysis, sequencing and BLAST/GenBank databases searches. Later on, new experiments will have to be designed to confirm the validity of the most meaningful findings from this Y2H.

6.1 Library transformation and screening

A human fetal brain (HFB) cDNA library was screened with human CPT1C (fragment encoding amino acids 131-803) in Y2H system.

35 independent $Ade^+/His^+/Leu^+/Trp^+$ colonies were isolated from $3x10^5$ transformants. These colonies were stricked on SD/-Ade/-His/-Leu/-Trp/ X-α-gal plates to confirm the interaction through a blue/white colony test (see Figure 46A) resulting in 30 blue colonies. The plasmids from these blue positive colonies were amplified using colony PCR analysis (except 2 clones that could not be amplified in any conditions tested) (see Figure 46B).

A.

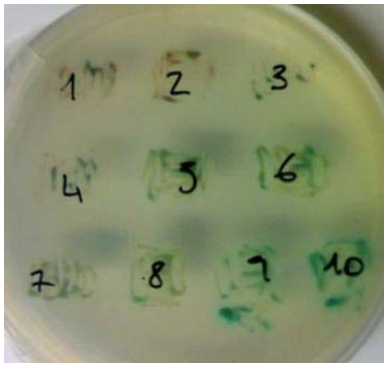

B.

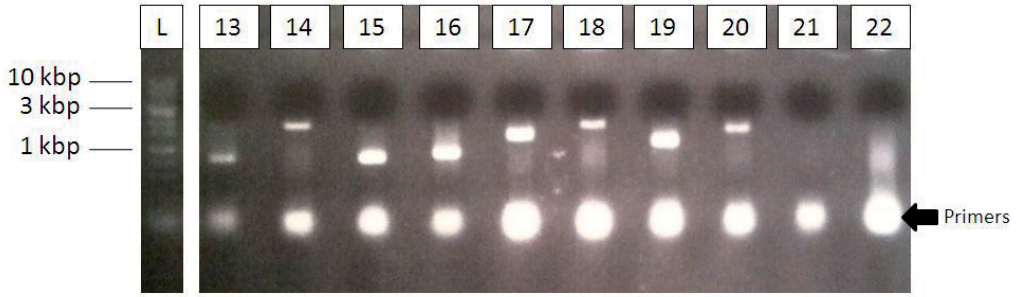

Figure 46. Example of the results obtained from the Y2H screening. (A) Blue/white colony test. Image of the first 10 colonies streaked on SD/-Ade/-His/-Leu/-Trp/X-α-gal plates. **(B) Amplicons obtained from positive colonies.** Positive colonies were PCR amplified using primers: 5' AD-insert screening amplimer and 3' AD-insert screening amplimer (primer sequences specified in Experimental procedures 2.2.6 section, Figure 23).

The amplified fragments were excised from the gel for direct sequencing with activation domain primers (primers described in Experimental procedures 2.2.6 section, Figure 23). Then BLAST database searches were performed looking for similarities with *H. sapiens* sequences in GenBank. The results obtained were:

- 14 different clones showed high similarity (98-100% homology) in BLAST searches of oligonucleotides and amino acids sequences, with 13 different proteins from GenBank. Two of them matched the same nucleotide sequence, the full length cDNA of Dynactin 3.

- 6 clones had the insert in the prey plasmid from the cDNA library with an altered open reading frame.
- 4 clones matched with 3' UTR sequences of different genes.
- 4 clones matched sequences contained in introns.

A screening with the same library but using the equivalent mouse sequence of CPT1C (aa 131-798) was performed looking for internal consistency of the screening and looking for meaningful interactions of endogenous CPT1C.

In this screening 93 independent $Ade^+/His^+/Leu^+/Trp^+$ colonies were isolated from $9x10^4$ transformants. These colonies were stricked on SD/-Ade/-His/-Leu/-Trp/X-α-gal plates resulting in 32 blue colonies. The plasmids from these blue positive colonies were amplified using colony PCR analysis (except 5 clones that could not be amplified in any conditions tested) and sequenced. BLAST database searches were performed and similarities with *H. Sapiens* sequences in GenBank were analyzed. The results obtained were:

- 19 different clones showed high similarity with 19 different proteins from GenBank. Two of them matched the same nucleotide sequence, the full length cDNA of Proteasome subunit 4.
- 6 clones coincided with 3' UTR sequences of different genes.
- 2 clones matched sequences contained in introns.

Any of the proteins found in this second screening coincided with those of the first screening. Therefore, any of the binding partners found was a clear candidate for a real interaction *in vivo*. Consequently, a deeper understanding of each of the candidates was necessary to detect an interacting partner that was worth further study.

A percentual representation of each set of results is displayed in Supplemental data, Figure S4.

6.2 Analysis of putative positive clones

The subcellular location, tissue distribution, conserved domains and functional features of each of the positive clones were studied. In the next tables interacting proteins are shown ordered mainly by subcellular locations or common domains present in these proteins. Nuclear proteins or intraorganellar proteins would not be good candidates for real interactions.

Thirteen interacting proteins in the screening performed with HFB cDNA library and human sequence of CPT1C are shown in the next table (Table 6).

Gene abbreviation	Gene name	aa positions of inserted fragment	Localization	Expression	Relevant information
DCTN3	Dynactin 3 (p22), isoform 1	aa 1--> 187 (stop)	Cytoplasm, centrosome during interphase and to kinetochores and to spindle poles throughout mitosis.	Ubiquitous	This gene encodes the smallest subunit of dynactin, a macromolecular complex consisting of 10 subunits ranging in size from 22 to 150 kD. Dynactin binds to both microtubules and cytoplasmic dynein. It is involved in a diverse array of cellular functions, including ER-to-Golgi transport, the centripetal movement of lysosomes and endosomes, spindle formation, cytokinesis, chromosome movement, nuclear positioning, and axonogenesis. This subunit, like most other dynactin subunits, exists only as a part of the dynactin complex. It is primarily an alpha-helical protein with very little coiled coil, and binds directly to the largest subunit (p150) of dynactin. Moreover, a missense mutation at the conserved microtubule-binding domain of p150glued, a major component of dynein/dynactin complex, has been linked to an autosomal dominant form of motor neuron disease (MND) (Lai et al., 2007).
DNAJB6	DnaJ (Hsp40) homolog, subfamily B, member 6, isoform b	aa54--->241 (stop)	Cytoplasm, perinuclear region. Nucleus	Ubiquitous (high levels brain and testis)	This gene encodes a member of the DNAJ protein family. DNAJ family members are characterized by a highly conserved amino acid stretch called the 'J-domain' and function as one of the two major classes of molecular chaperones involved in a wide range of cellular events, such as protein folding and oligomeric protein complex assembly. This family member is highly enriched in the central nervous system. It regulates Hsp70 ATPase activity and may also play a role in polyglutamine aggregation in specific neurons (Chuang et al., 2002).
PKM2	Pyruvate kinase, muscle, isoform M1	aa425-->531 (stop) fragment equivalent in all three isoforms	Cytoplasm. Nucleus.	Lung Proliferating cells (embryonic and cancer cells)	This gene encodes a protein involved in glycolysis. The encoded protein is a pyruvate kinase that catalyzes the transfer of a phosphoryl group from phosphoenolpyruvate to ADP, generating ATP and pyruvate. This protein has been shown to interact with thyroid hormone and may mediate cellular metabolic effects induced by thyroid hormones.
BTBD1	BTB (POZ)domain containing 1, isoform 2	aa112--> 385 (stop)	Cytoplasm	Ubiquitous	The N-terminus of the protein contains a proline-rich region and a BTB/POZ domain (broad-complex, Tramtrack and bric a brac/Pox virus and Zinc finger), both of which are typically involved in protein-protein interactions. BTBD1 function

					has not been characterized yet, but its co-localization with an E3 ubiquitin ligase, suggests its involvement in protein degradation by the ubiquitin/proteasome pathway (Pisani et al., 2007).
RNF40	Ring finger protein 40(also known as Staring)	aa2-->1001 (stop)	Cytoplasm	Ubiquitous	The protein encoded by this gene contains a RING finger, a motif known to be involved in protein-protein and protein-DNA interactions. This protein was reported to interact with the tumor suppressor protein RB1. Studies of the rat counterpart suggested that this protein may function as an E3 ubiquitin-protein ligase, and may facilitate the ubiquitination and degradation of syntaxin 1, which is an essential component of the neurotransmitter release machinery (Chin et al., 2002).
TICAM1	toll like receptor adaptor molecule 1	aa400-->712 (stop)	Cytoplasm	Ubiquitous	(aa300-527) **TIR domain**: is an intracellular signalling domain that mediates protein-protein interactions between the Toll-like receptors (TLRs) and signal-transduction components. When activated, TIR domains recruit cytoplasmic adaptor proteins. TICAM1 is a Toll/IL1R (TIR) domain-containing adaptor molecule that specifically interacts with TLR3, and activates nuclear factor kappa-B (NFκB).
CRYL1	Crystallin, lambda 1	aa38-->319 (stop)	Cytoplasm	Ubiquitous	The uronate cycle functions as an alternative glucose metabolic pathway, accounting for about 5% of daily glucose catabolism. The product of this gene catalyzes the dehydrogenation of L-gulonate into dehydro-L-gulonate in the uronate cycle. The enzyme requires NAD(H) as a coenzyme, and is inhibited by inorganic phosphate. This enzyme shows 22% sequence identity with 3-hydroxyacyl-CoA dehydrogenase (HAD: involved in fatty acid metabolic processes) of the oxidoreductases in the protein databases (Ishikura et al., 2005).
MSTO1	misato homolog 1 (Drosophila)	aa288-->570 (stop)	Mitochondria outer membrane	Ubiquitous	(aa153 – 564) **Misato domain**: Human Misato shows similarity with Tubulin/FtsZ family of GTPases and is localized to the the outer membrane of mitochondria. Available results indicate that human Misato has a role in mitochondrial distribution and morphology and that its unregulated expression leads to cell death (Kimura and Okano, 2007).
NDUFB9	NADH dehydrogenase (ubiquinone) 1 beta	aa7-->179 (Stop)	Mitochondria inner membrane	Ubiquitous	(aa14 – 77) **Complex 1 protein (LYR family) domain**: Proteins in this family have been identified as a component of the higher eukaryotic NADH complex. In yeast, an

	subcomplex, 9				homologous protein has been shown to play a role in Fe/S cluster biogenesis in mitochondria. The exact function of this protein has not been characterized yet.
BCAS2	Breast carcinoma amplified sequence variant 2	aa1-->225 (stop)	Nucleus, nucleolus	Ubiquitous	(aa10-215) **Breast carcinoma amplified sequence 2 (BCAS2) domain**: This family consists of several eukaryotic sequences of unknown function. BCAS2 is a putative spliceosome associated protein. The exact function of this protein has not been characterized yet.
NCAPH2	kleisin beta, isoform CRA-Cnon-SMC condensin II complex, subunit H2, isoform 2	aa304--->605 (stop)	Nucleus	Ubiquitous	Condensin complexes I and II play essential roles in mitotic chromosome assembly and segregation. Both condensins contain 2 invariant structural maintenance of chromosome (SMC) subunits, SMC2 (MIM 605576) and SMC4 (MIM 605575), but they contain different sets of non-SMC subunits. NCAPH2 is 1 of 3 non-SMC subunits that define condensin II (Ono et al., 2003).
CXXC1	CXXC finger 1 (PHD domain)	aa53--> 660 (stop)	Nucleus	Ubiquitous	Proteins that contain a CXXC motif within their DNA-binding domain, such as CXXC1, recognize CpG sequences and regulate gene expression (Carlone and Skalnik, 2001).
UBAP2L	ubiquitin associated protein 2-like , isoform a	aa801--->1087 (stop)	?	Ubiquitous	No conserved domains in the region of the insert. The exact function of this protein has not been characterized yet.

Table 6. List of interacting proteins obtained from positive clones in a Y2H screening of human CPT1C with a human fetal brain (HFB) cDNA library.

Eighteen interacting proteins in the screening performed with HFB cDNA library and mouse sequence of CPT1C are shown in the next table (Table 7).

Gene abbrevi-ation	Gene name	aa positions of inserted fragment	Localiza-tion	Expression	Relevant information
PSMB4	proteasome subunit, beta type 4	aa1 → 264(stop)	Cytoplasm. Nucleus	Ubiquitous	The proteasome is a multicatalytic proteinase complex with a highly ordered ring-shaped 20S core structure. The core structure is composed of 4 rings of 28 non-identical subunits; 2 rings are composed of 7 alpha subunits and 2 rings are composed of 7 beta subunits. Proteasomes are distributed throughout eukaryotic cells at a high concentration and cleave peptides in an ATP/ubiquitin-dependent process in a non-lysosomal pathway. An essential function of a

					modified proteasome, the immunoproteasome, is the processing of class I MHC peptides. This gene encodes a member of the proteasome B-type family, also known as the T1B family, which is a 20S core beta subunit.
FANCL	Fanconi anemia complementation group L	aa194→375(stop)	Cytoplasm. Nucleus	Ubiquitous	The Fanconi anemia complementation group (FANC) currently includes FANCA, FANCB, FANCC, FANCD1 (also called BRCA2), FANCD2, FANCE, FANCF, FANCG, FANCI, FANCJ (also called BRIP1), FANCL, FANCM and FANCN (also called PALB2). Fanconi anemia is a genetically heterogeneous recessive disorder characterized by cytogenetic instability, hypersensitivity to DNA crosslinking agents, increased chromosomal breakage, and defective DNA repair. This gene encodes the protein for complementation group L and displays E3 ubiquitin ligase activity, probably on monoubiquitination of FANCD2 thus activating its ability to repair DNA damage (Meetei et al., 2003; Gurtan et al., 2006; Ling et al., 2007).
PELI1	pellino homolog 1(Drosophila)	aa300→418(stop)	Cytoplasm	Ubiquitous	Pellino proteins are E3 ubiquitin ligases involved in signaling events downstream of the Toll and Interleukin-1 receptors, key initiators of innate immune and inflammatory responses. Pellino1 is ubiquitously expressed, with low levels of expression in brain (Jiang et al., 2003). Their phosphorylation induces their E3 ligase activity. It has been reported that Pellino proteins interact with IRAK proteins, polyubiquitinating them in different Lysine residues, resulting in signaling events (NF-κB activation) or in proteasome degradation. Pellino proteins are also autoubiquitinated for their proteasomal degradation, probably terminating the signaling cascade. (Choi et al., 2006; Butler et al., 2007; Lin et al., 2008; Moynagh, 2009).
NPLOC4	nuclear protein localization 4 homolog (*S. cerevisiae*)	aa476→608(stop)	Cytoplasm Endoplasmic reticulum. Nucleus.	Expressed at highest levels in brain, heart, skeletal muscle, kidney and fetal liver	Ufd1-Npl4 is an heterodimer that binds an ATPase (p97/VCP), promoting the retrotranslocation of emerging ER proteins, their ubiquitination by associated ligases and handling to the 26S proteasome for degradation in a process known as ERAD (ER-associated degradation). (Ye et al., 2003; Lass et al., 2008)
SNX9	sorting nexin 9	aa335→595(stop)	Plasma membrane. Cytoplasm (endocytosis)	Ubiquitous (present in presynaptic terminals of CNS)	This gene encodes a member of the sorting nexin family. Members of this family contain a phox (PX) domain, which is a phosphoinositide binding domain, and are involved in intracellular trafficking. This protein contains a SH3 domain near its N-terminus. SNX9binds strongly to dynamin (a GTPase participating in the separation of vesicles from the originating membrane in chlatrin mediated

					endocytosis) and activates also other members (like N-WASP) important for coordinating actin polymerization with vesicle release (Lundmark and Carlsson, 2009). It has been shown that SNX9 is expressed in presynaptic terminals and coordinates synaptic vesicle endocytosis (Shin et al., 2007).
DLL3	delta-like 3 (Drosophila) isoform 1	aa148→618(stop)	Golgi apparattus membrane		This gene encodes a member of the delta protein ligand family. This family functions as Notch ligands that are characterized by a DSL domain, EGF repeats, and a transmembrane domain. Mutations in this gene cause autosomal recessive spondylocostal dysostosis 1. It has been described that DLL3 has a distinct intracellular localization (the Golgi network) than that of DLL1, suggesting a new specific role for this isoform, yet undefined (Geffers et al., 2007).
BCAN	Brevican isoform 1	aa602→911(stop)	Secreted, extracellular space, extracellular matrix (Ranvier nodes)	Highly expressed in brain	(aa652-682) **EGF-CA. Calcium-binding EGF-like domain:** present in a large number of membrane-bound and extracellular (mostly animal) proteins. Many of these proteins require calcium for their biological function and calcium-binding sites have been found to be located at the N-terminus of particular EGF-like domains; calcium-binding may be crucial for numerous protein-protein interactions. Brevican is known to be an abundant extracellular matrix component in the adult brain. It is present at the nodes of Ranvier on myelinated axons with a particular large diameter in the central nervous system (Bekku et al., 2009).
GCA	Grancalcin, EF-hand calcium binding protein	aa1→217(stop)	Cytoplasm. Cytoplasmic granule membrane; Peripheral membrane protein.	Neutrophils and macropha-ges. Bone marrow	This gene product, grancalcin, is a calcium-binding protein abundant in neutrophils and macrophages. It belongs to the penta-EF-hand subfamily of proteins which includes sorcin, calpain, and ALG-2. Grancalcin localization is dependent upon calcium and magnesium. In the absence of divalent cation, grancalcin localizes to the cytosolic fraction; with magnesium alone, it partitions with the granule fraction; and in the presence of magnesium and calcium, it associates with both the granule and membrane fractions, suggesting a role for grancalcin in granule-membrane fusion and degranulation. It has been shown that genes included in a susceptibility locus for type 1 diabetes on chromosome 2q24.3 (including: IFIH1 interferon induced helicase, GCA grancalcin or the potassium channel KCNH7) are potential candidates implicated in the pathogenesis of autoimmune diseases such as type 1 diabetes or multiple sclerosis, although strong linkage disequilibrium in the region hampered further localization of the

					etiologic gene (Martinez, A. et al., 2008).
WDR6	WD repeat domain 6 protein	aa982→1 151 (stop)	Cytoplasm.	Ubiquitous	This gene encodes a member of the WD repeat protein family. WD repeats are minimally conserved regions of approximately 40 amino acids typically bracketed by gly-his and trp-asp (GH-WD), which may facilitate formation of heterotrimeric or multiprotein complexes. The encoded protein interacts with serine/threonine kinase 11, and is implicated in cell growth arrest.
BAT2	HLA-B associated transcript-2	aa1874→ 2157 (stop)	Cytoplasm. Nucleus	Limited to cell-lines of leukemic origin	A cluster of genes, BAT1-BAT5, has been localized in the vicinity of the genes for TNFα and TNFβ. These genes are all within the human major histocompatibility complex class III region. This gene has microsatellite repeats which are associated with the age-at-onset of insulin-dependent diabetes mellitus (IDDM) and possibly thought to be involved with the inflammatory process of pancreatic beta-cell destruction during the development of IDDM. This gene is also a candidate gene for the development of rheumatoid arthritis.
ZMYM 3	zinc finger MYM-type protein 3, isoform 1	aa769→1 370 (stop)	Nucleus. Cytoplasm.	Ubiquous (most abundant in brain)	This gene is located on the X chromosome and is subject to X inactivation. It is highly conserved in vertebrates and most abundantly expressed in the brain. The encoded protein is a component of histone deacetylase-containing multiprotein complexes that function through modifying chromatin structure to keep genes silent. A chromosomal translocation (X; 13) involving this gene is associated with X-linked mental retardation.
hnRNP H3	heterologous nuclear ribonucleoprotein H3 (2H9), isoform a	aa25→ 346(stop)	Nucleus	Ubiquitous	This gene belongs to the subfamily of ubiquitously expressed heterogeneous nuclear ribonucleoproteins (hnRNPs). The hnRNPs are RNA binding proteins and they complex with heterogeneous nuclear RNA (hnRNA). These proteins are associated with pre-mRNAs in the nucleus and appear to influence pre-mRNA processing and other aspects of mRNA metabolism and transport. While all of the hnRNPs are present in the nucleus, some seem to shuttle between the nucleus and the cytoplasm. The hnRNP proteins have distinct nucleic acid binding properties. The protein encoded by this gene has two repeats of quasi-RRM domains that bind to RNAs. It is localized in nuclear bodies of the nucleus. This protein is involved in the splicing process and it also participates in early heat shock-induced splicing arrest by transiently leaving the hnRNP complexes. Several alternatively spliced transcript variants have been noted for this gene; however,

					not all are fully characterized.
hnRNPM	heterologous nuclear ribonucleoprotein	aa511→730(stop) insert common in both isoforms	Nucleus	Ubiquitous	This gene belongs to the subfamily of ubiquitously expressed heterogeneous nuclear ribonucleoproteins (hnRNPs). This protein also constitutes a monomer of the N-acetylglucosamine-specific receptor which is postulated to trigger selective recycling of immature GlcNAc-bearing thyroglobulin molecules. Multiple alternatively spliced transcript variants are known for this gene but only two transcripts have been isolated.
TPP1	tripeptidyl peptidase 2 preproprotein	aa446→572(stop)	Lysosomes	Ubiquitous	This gene encodes a member of the sedolisin family of serine proteases. The protease functions in the lysosome to cleave N-terminal tripeptides from substrates, and has weaker endopeptidase activity. It is synthesized as a catalytically-inactive enzyme which is activated and auto-proteolyzed upon acidification. Mutations in this gene result in late-infantile neuronal ceroid lipofuscinosis, which is associated with the failure to degrade specific neuropeptides and a subunit of ATP synthase in the lysosome.
CTSB	Cathepsin B preproprotein	aa91→240(stop)	Lysosomes	Ubiquitous	The protein encoded by this gene is a lysosomal cysteine proteinase composed of a dimer of disulfide-linked heavy and light chains, both produced from a single protein precursor. It is also known as amyloid precursor protein secretase and is involved in the proteolytic processing of amyloid precursor protein (APP). Incomplete proteolytic processing of APP has been suggested to be a causative factor in Alzheimer disease, the most common cause of dementia. Overexpression of the encoded protein, which is a member of the peptidase C1 family, has been associated with esophageal adenocarcinoma and other tumors. At least five transcript variants encoding the same protein have been found for this gene.
ARID1A	AT rich interactive domain 1A, isoform a	aa1231→2285 (stop)	Nucleus	Ubiquitous	This gene encodes a member of the SWI/SNF family, whose members have helicase and ATPase activities and are thought to regulate transcription of certain genes by altering the chromatin structure around those genes. The encoded protein is part of the large ATP-dependent chromatin remodeling complex SNF/SWI, which is required for transcriptional activation of genes normally repressed by chromatin. It possesses at least two conserved domains that could be important for its function. First, it has a DNA-binding domain that can specifically bind an AT-rich DNA sequence known to be recognized by a SNF/SWI complex at the beta-globin locus. Second, the C-terminus of the protein can stimulate

					glucocorticoid receptor-dependent transcriptional activation. It is thought that the protein encoded by this gene confers specificity to the SNF/SWI complex and may recruit the complex to its targets through either protein-DNA or protein-protein interactions. Two transcript variants encoding different isoforms have been found for this gene.
ANKS3	Ankyrin repeat and sterile alpha motif domain containing 3	aa467→656(stop)	?	?	(aa426-485) **Sterile alpha motif (SAM):** Widespread domain in signalling and nuclear proteins. In EPH-related tyrosine kinases, appears to mediate cell-cell initiated signal transduction via the binding of SH2-containing proteins to a conserved tyrosine that is phosphorylated. In many cases mediates homodimerization. The exact function of this protein has not been characterized yet.
WDR 73	WD repeat domain 73	aa215→378(stop)	?	?	No domains described for this protein. The exact function of this protein has not been characterized yet.

Table 7.List of Interacting proteins obtained from positive clones in Y2H screening of mouse CPT1C with a human fetal brain (HFB) cDNA library.

All these diverse proteins found in the Y2H screening need to be further tested in order to clarify real CPT1C interacting partners and their significance. This will help learning more about the intracellular processes where CPT1C might participate, giving new insights into its function.

DISCUSSION

Since CPT1C was first characterized (Price et al., 2002), the specific function of this brain expressed isoform has not been revealed. In this study we aimed to characterize it at the molecular level in order to gather information that could approach us in finding out its physiological function. With this aim a 3-D structure of the protein has been modeled, its kinetic parameters have been determined and its subcellular location and membrane topology have been revealed. Furthermore, a Y2H assay has been performed to elucidate whether CPT1C was able to interact with other proteins in order to give some light on the cellular pathways where CPT1C might be involved.

The results obtained in this study lead to the concept that CPT1C has a completely different function from that of the other two known isoforms (CPT1A and CPT1B). This hypothesis is supported mainly by two facts: 1) this new CPT1 isozyme is located to the ER membrane in spite of the outer mitochondrial membrane which is the known location for the other isoforms, and 2) results published by our group (Sierra et al., 2008) show that CPT1C is not involved in the oxidation of palmitate (overexpression of CPT1C in mammalian cells does not increase the oxidation rate of palmitate, whereas CPT1A did) (see Figure 47). Therefore, CPT1C function might not be related to producing energy from fatty acids but, probably has a role linked to ER specific functions.

	$[^{14}C]CO_2$ production
	nmol/mg/h
Empty pIRES	6.1 ± 0.9
pIRES-CPT1c	5.7 ± 0.7
pIRES-CPT1a	9.2 ± 2.1

Figure 47. **Palmitate oxidation in PC12 cells overexpressing CPT1C.** 48h after transfection of cultured cells with pIRES-CPT1C, pIRES-CPT1A or empty pIRES, cells were incubated for 2 h with [1-^{14}C] palmitate. Palmitate oxidation to CO_2 was determined. Data are presented as mean ± standard error of the mean of three independent experiments. Data for CPT1A are significantly different from control cells ($p<0.05$). (From Sierra et al., 2008)

We will first briefly discuss the molecular role of CPT1C regarding to its catalytic activity and subcellular localization. From the Y2H results, we will also speculate its participation in other pathways, and finally, its physiological function will be discussed based on the gathering of our published and non-published results together with the present literature.

1. CATALYTIC ACTIVITY

From the activity assays on yeast mitochondria expressing CPT1C, it was concluded that CPT1C had no catalytic activity in this system. This can be due to different hypothesis:

1. In the yeast expression system, CPT1C is folded into a non-active conformational state.
2. The method for detecting enzymatic activity is not sensitive enough to detect CPT1C activity.
3. The yeast expression system lacks something (i.e. interacting partners) necessary for CPT1C enzymatic activity, which might only be present in the physiological environment of the protein.

The first hypothesis is fairly improbable because of the high sequence similarity of CPT1C to the other isoforms (CPT1A and CPT1B) that have been kinetically characterized in this expression system (Zhu et al., 1997; de Vries et al., 1997; Prip-Buus et al., 1998), but it cannot be discarded.

In order to verify the second hypothesis, our group developed an HPLC-MS/MS method for determining CPT1C catalytic activity (Jáuregui et al., 2007). This newly developed HPLC based method produces reliable and accurate measurements of palmitoylcarnitine concentrations in biological samples with a sensitivity limit of 0.48 ng/ml, which corresponds to a specific activity of 0.0045 nmol·mg^{-1}·min^{-1} in our CPT1 assay conditions. In the radiometric assay, the sensitivity limit (calculated as the standard deviation of ten blank points) corresponds to a specific activity of 0.4 nmol·mg^{-1}·min^{-1}. It indicates that the chromatographic method is 100 times more sensitive than the radiometric. Using the chromatographic method no activity on yeast extracts expressing CPT1C was detected, discarding the second hypothesis.

To test the third hypothesis, other members from our group assayed microsomal fractions (as increasing evidences showed this subcellular localization) of mammalian cultured cells overexpressing CPT1C and concluded that: 1) CPT1C catalyzes the transesterification reaction between palmitoyl-CoA and acylcarnitine esters and that 2) CPT1C is an enzyme 100 times less active than the liver isoform (CPT1A) (Figure 48).

Cells	Plasmid transfection	*n*	Activity	*p*	Absolute increase	Percent increase
			nmol palmitoylcarnitine/ mg/min			*%*
PC12	Control	7	1.37 ± 0.81	<0.05		
	CPT1c	7	1.94 ± 0.96	<0.05	0.57	41.6
293	Control	9	0.22 ± 0.11	<0.05		
	CPT1c	9	0.35 ± 0.18	<0.05	0.13	59

Figure 48. **Carnitine palmitoyltransferase activity in PC12 and HEK293T cells:** Cells were transfected with pIRES-CPT1C or empty vector pIRES (control cells). 48 h after transfection, cells were collected and 40 mg of microsomal fraction was assayed for CPT1 activity. The palmitoylcarnitine formed in the assay was determined by HPLC-mass chromatography. Activity is presented as the mean ± standard error of the mean. Wilcoxon test for non-parametric paired samples was used. *n* =number of experiments. Absolute and percent increases in CPT1C activity are compared to control cells. (From Sierra et al., 2008).

These results confirmed the third hypothesis leading to the conclusion that CPT1C needs specific conditions or environment (provided by mammalian cells) for achieving catalytic activity. The special conditions or environment could be: a) activating or interacting proteins present in mammalian cells and absent from yeast, or b) specific modifications produced in mammalian cells, like changes in membrane potential. The low CPT1C activity can suggest that this enzyme is involved in biosynthetic pathways (rather than catabolic ones), or in signaling pathways acting as a metabolic sensor (discussed below).

In fact, the specific activity found for CPT1C is surprisingly low since CPT1C contains all of the key residues known to be important for CPT1A catalytic activity. Moreover, information obtained from the tridimensional structure model shows that CPT1C can potentially catalyze the same reaction with similar kinetic characteristics, despite some conservative amino acid changes and some semi-conservative.

Taking into account all this information, it can be hypothesized that in certain conditions (still undetermined) CPT1C could increase its catalytic activity to levels similar to those shown by the other isoforms (CPT1A and CPT1B).

2. SUBCELLULAR LOCALIZATION

The initial notion that CPT1C is localized in mitochondria stems from an observation of CPT1C protein in mitochondrial fraction of brain (Price et al., 2002). Although CPT1C was also found in the microsomal fraction of brain extracts, as revealed by Western blot experiments, the authors attributed this to contamination problems in the cellular fractioning process.

Later, Dai and colleagues concluded that CPT1C co-localizes with MitoTracker (Dai et al., 2007), although the images did not show perfect matching and co-localization studies were not performed with any ER marker (Figure 49).

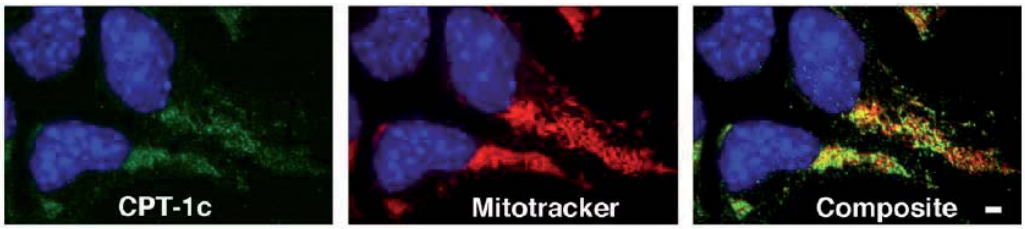

Figure 49. **Co-localization of CPT1C with a mitochondrial marker.** Mouse hypothalamic GT1-7 neurons in cell culture were immunostained with anti-CPT1C antibody and MitoTracker. CPT1C immunoreactivity (green) overlaps MitoTracker fluorescence (red); the composite image shows that CPT1C is closely associated with mitochondria (yellow). Bar: 5 µm. (From Dai et al., 2007).

In contrast, subcellular localization experiments performed in this study clearly demonstrate that CPT1C is localized in the ER membrane. The fusion protein CPT1C-EGFP showed a clear reticular pattern and a completely different distribution than that observed for CPT1A-EGFP. This pattern was maintained over time after transfection in transiently transfected cells as well as in stably transfected PC12 cells (results not shown). Moreover, in this study co-localization experiments with ER markers were performed for the first time, showing a total overlap in different cell types. We also performed localization studies of chimeric proteins, evidencing

that the exchange of the N-terminus (which contains the mitochondrial targeting signal in CPT1A) of both isoforms (CPT1A and CPT1C) can swap their targeting, suggesting that the specific sequence of the first 150 aa of CPT1C targets the protein to the ER. Additionally, subcellular fractioning of mouse and rat brain homogenates showed immunodetection of CPT1C mainly in the microsomal fraction (Sierra et al., 2008) confirming all previous results and discarding that ER location was an artifact due to overexpression (Figure 50).

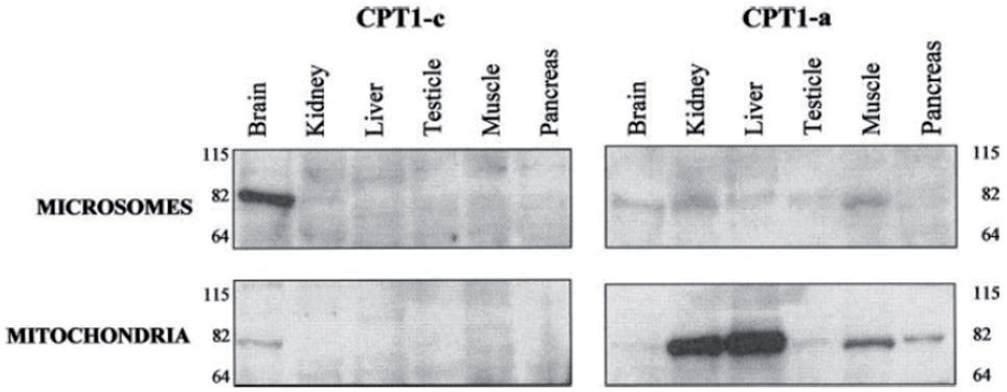

Figure 50. **Western blot of CPT1C in mitochondrial and ER cell fractions from different tissues of adult mouse.** 60 µg of protein cell fraction was run in each line. The same membranes were incubated with anti-CPT1C and anti-CPT1A antibodies. (From Sierra et al., 2008)

Our subcellular localization experiments also showed a slight co-localization with mitochondrial markers (like in Dai et al., 2007) and it might be the result of the expression of this protein in a structure called mitochondrial associated membranes or MAMs (for contact sites between ER membrane and the outer mitochondrial membrane). MAMs have been shown to be enriched in phospholipid biosynthetic enzymes and have been related to the transference of calcium ions from the ER to the mitochondria (Rusiñol et al., 1994; Wang et al., 2000; Goetz and Nabi, 2006).

The new localization of a CPT1 isozyme suggests its involvement in ER related functions. Moreover, its topology in the membrane facing its N- and C-terminal ends towards the cytoplasm implies that the product of the reaction catalyzed by CPT1C is delivered to the cytoplasmic space, therefore suggesting that its function can also be related to the delivery of palmitoylcarnitine in this space for subsequent transport through intracellular membranes (the ER membrane included). The reaction catalyzed by CPT1C might influence the concentration of its substrates or products in microenvironments related to its activity. Therefore, CPT1C would regulate palmitoyl-CoA/palmitoylcarnitine levels in microdomains within the neuron.

Herein, the three main functions in which CPT1C might be potentially involved are proposed.

a) CPT1C DOWNREGULATES PHOSPHOLIPID SYNTHESIS

One of the main biosynthetic pathways related to the cytoplasmic face of the ER is the synthesis of phospholids which are the major structural lipids in eukaryotic membranes (some phospholipids contain palmitate in their hydrophobic portion). Phospholipid synthesis takes place in the cytosic side of the ER membrane and begins with the

esterification of two acyl-CoAs to the phosphorylated glycerol backbone, forming phosphatidic acid, whose two long hydrocarbon chains anchor the molecule to the membrane. Subsequent enzymatic reactions synthesize the large array of phospholipids. Phospholipids are important constituents of membranes, and in neurons, phospholipid synthesis increases during neurite outgrowth (Araki and Wurtman, 1997). Phospholipid composition also determines membrane fluidity and shape, important for chlatrin-mediated endocytosis in synaptic vesicle recycling (Marza and Lesa, 2006; Darios and Davletov, 2006; Ben Gedalya et al., 2009).

We propose that, when active, CPT1C present in neurons would downregulate the synthesis of phospholipids, by decreasing the amount of one of its substrates (through the conversion of palmitoyl-CoA into palmitoylcarnitine) (Figure 51). The reduced amount of phospholipids containing palmitate could locally alter membrane fluidity or shape, or even the recruitment of proteins involved in synaptic vesicle trafficking, producing changes in synaptic transmission at those locations.

In addition, synaptic vesicles (SV) are especially rich in phospholipids containing polyunsaturated fatty acids (PUFAs) and they seem to be involved in neurotransmission and/or in SV biogenesis, in a mechanism not clear yet (Marza and Lesa, 2006). Therefore, it could be also speculated that CPT1C activity would decrease the incorporation of palmitate into phospholipids in microdomains, thus favoring the incorporation of PUFAs for the correct formation of SV. This speculative mechanism for CPT1C in controlling the composition of phospholipids in SV, would be common to all neurons, and would have different consequences in the different regions of the brain depending on the importance of this mechanism in each nucleus or area.

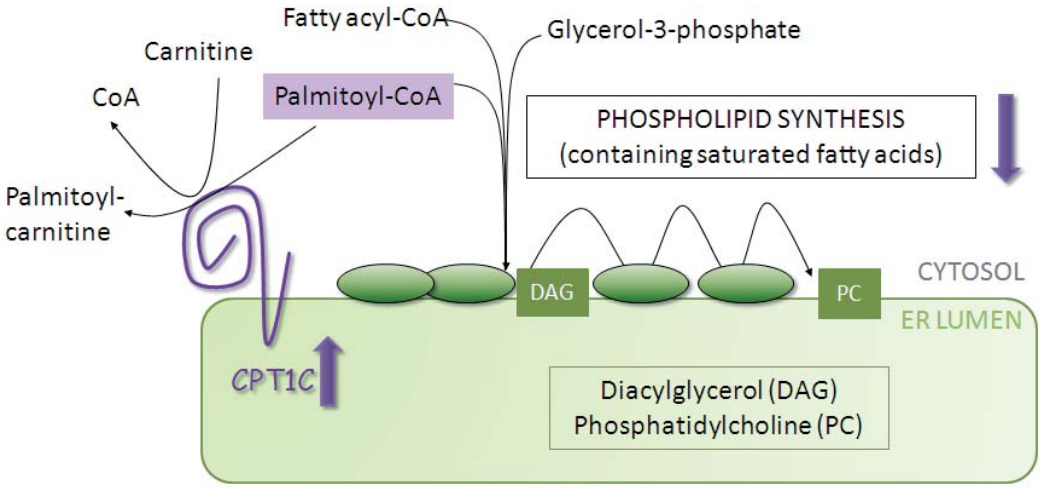

Figure 51. CPT1C activity decreases phospholipid synthesis. Phospholipid synthesis takes place at the interface between ER membrane and the cytosol and is catalyzed by membrane-associated enzymes (green ovals). At the beginning, two fatty acids from fatty acyl-CoA (one of them can be palmitoyl-CoA) are esterified to the phosphorylated glycerol backbone, forming phosphatidic acid, whose two hydrocarbon chains anchor the molecule to the membrane. Then, a phosphatase converts phosphatidic acid into diacylglycerol (DAG). A polar head group is then transferred to the exposed hydroxyl group thus forming phospholipids like phosphatidylcholine (PC). CPT1C would be able to decrease the amount of palmitoyl-CoA available for its incorporation into newly synthesized phospholipids.

b) CPT1C REDUCES THE *DE NOVO* SYNTHEIS OF CERAMIDE AND SPHINGOLIPIDS

The *de novo* synthesis of ceramide is performed in the ER and possibly in ER-associated membranes, such as the perinuclear membrane and mitochondria-associated membranes. Ceramide is considered the central molecule in sphingolipid metabolism which takes place in multiple subcellular localizations. Ceramide can also be formed from the hydrolysis of sphingomyelin, cerebrosides or from sphingosine by the action of different enzymes (Ogretmen and Hannun, 2004; Hannun and Obeid, 2008). In neurons, *de novo* synthesis of ceramide has been suggested to be involved in axonal and dendritic development of hippocampal neurons and Purkinje cells (Buccoliero and Futerman, 2003). In contrast, increases in ceramide levels have also been reported to sensitize neurons to excitotoxic damage and promote apoptosis, both characteristics present in many neurodegenerative disorders (Haughey et al., 2004; Jana et al., 2009).

Sphingolipids (like ceramide, dihydroceramide, ceramide-1-phosphate, sphingosine, sphingosine-1-phosphate, glucosylceramide, lyso-sphingomyelin) are bioactive lipid species with roles in the regulation of cell growth, death, senescence, adhesion, migration, inflammation, angiogenesis and intracellular trafficking. It has been recently shown that sphingosine, a releasable backbone of sphingolipids, activates synaptobrevin in synaptic vesicles to form the SNARE complex implicated in membrane fusion (Darios et al., 2009), thus providing new roles for sphingolipids in neurotransmission. Moreover, sphingolipids have also important roles in the regulation of the fluidity and subdomain structure of the lipid bilayer, especially lipid rafts. Lipid rafts are membrane platforms that have been shown to function in membrane signaling and trafficking (Ogretmen and Hannun, 2004; Lingwood and Simons, 2010). In specific regions of neurons, such as the growth cone, lipid rafts are involved in axon growth and guidance through their ability to capture and reorganize the cytoskeletal machinery (Kamiguchi, 2006).

The *de novo* synthesis of ceramide begins with the condensation of palmitate (from palmitoyl-CoA) and serine to form 3-keto-dihydrosphingosine through the action of serine-palmitoyltransferase (SPT), an enzyme located in the ER membrane. In this context, CPT1C could be decreasing the amount of the substrate palmitoyl-CoA for the synthesis of ceramide, thus down-regulating the whole pathway and resulting in lower levels of *de novo* ceramide production (Figure 52). In fact, unpublished results from our group showed that the *de novo* ceramide production decreased by approximately 20% when CPT1C was overexpressed in PC-12 and HEK293T cells. Conversely, CPT1C overexpression in these cell lines did not show variations in total ceramide levels, suggesting that CPT1C effect is mediated specifically by the regulation of the *de novo* ceramide synthesis (A. Sierra and N. Casals, unpublished results). These results shuggest that the regulation of *de novo* ceramide synthesis can be directed by the amount of palmitate incorporated to this pathway in neurons, which could be the role for CPT1C, thus affecting processes such as neurotransmission or axonal/dendritic development.

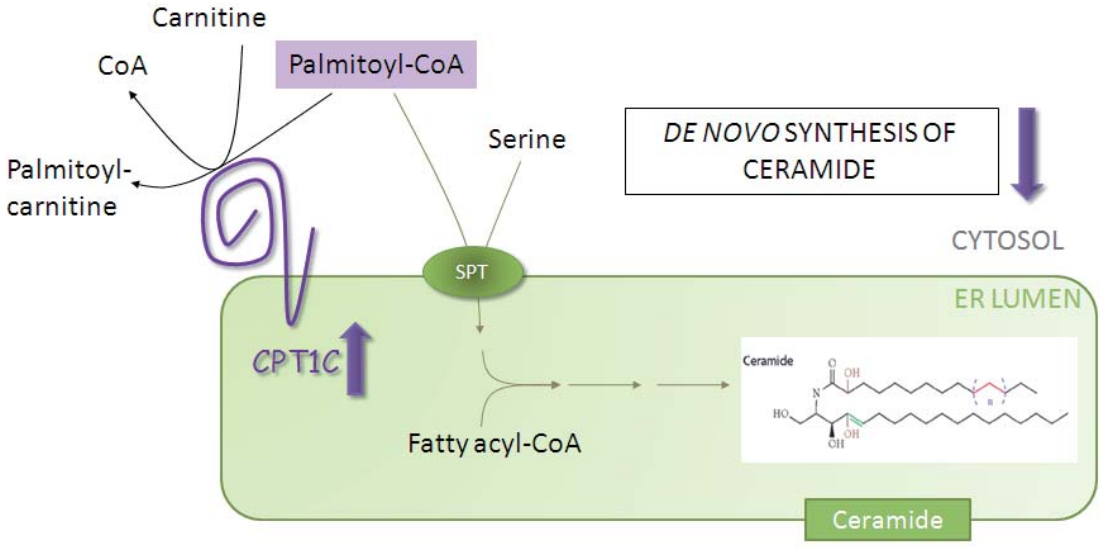

Figure 52. CPT1C decreases de *novo* synthesis of ceramide. This pathway has been shown to be decreased in a ≈20% when overexpressing CPT1C in HEK293T or PC12 cells (A. Sierra and N. Casals, unpublished results). Since ceramide synthesis begins with the condensation of palmitoyl-CoA and serine through the action of serine-palmitoyltransferase (SPT), an enzyme located in the ER membrane, the presence of CPT1C in this same location could decrease the amount of substrate (palmitoyl-CoA) available for this pathway, thus lowering ceramide levels produced.

c) CPT1C DOWNREGULATES PROTEIN PALMITOYLATION

Unpublished results from our group from the study of the KO mice for CPT1C suggest a role for this new isozyme in the formation of new memories, learning and motor coordination (P. Carrasco and N. Casals, unpublished results). These alterations seem to have an underlying mechanism with regard to neurotransmission. In this context, a posttranslational modification named palmitoylation could be the link.

Palmitoylation consists on the addition of a palmitate to a cysteine residue of the target protein, through the formation of a thioester bond. Incorporation of palmitate or other fatty acids into proteins is usually performed by a series of enzymes generally named palmitoyl-acyl transferases (PATs). Specifically, the family of enzymes identified as palmitoylating is named DHHC (Asp-His-His-Cys) because of the presence of this domain within a region especially rich in cysteine residues, important for the catalysis of the reaction. The sequence DHHC is found in a region within a Zinc finger domain (which is one of the domains present in many proteins found to interact with CPT1C in the Y2H assay). These enzymes use as a substrate for the reaction a palmitoyl-CoA and they have been found to be located in association with the ER membrane, the Golgi, secretion vesicles and the plasma membrane. Many enzymes of this family (which consists of 23 members) are expressed in the brain. The incorporation of lipids to proteins facilitates their targeting to membranes, resulting in changes in the subcellular localization of the target protein and/or changes in its function. It has also been shown that palmitoylation of transmembrane proteins regulates their processing and their targeting into membrane domains like lipid rafts. Much work on this issue is being performed, and it has already shown that many neuronal proteins incorporate this modification reversibly and that it has a very important

role in the regulation of synaptic transmission and neuronal development (proteins such as synaptotagmin, synaptobrevin, SNAP25, PSD95, GluR4 and 6, among others have been shown to be reversibly palmitoylated). Moreover, some enzymes of the DHHC family have been related to diseases like schizophrenia, X-linked mental retardation and Huntington disease (El-Husseini and Bredt, 2002; Ohno et al., 2006; Linder and Deschenes, 2007; Fukata and Fukata, 2010).

Although in the Y2H assay no palmitoylating protein has been found to interact with CPT1C, different proteins containing Zinc finger domains in fact did interact with CPT1C. As DHHC members are transmembrane proteins (Figure 53), it is possible that interactions with this kind of proteins has not been detected in this system. An interaction with such a protein would suggest a role for CPT1C in regulating the pool of the substrate available for the palmitoylating reaction.

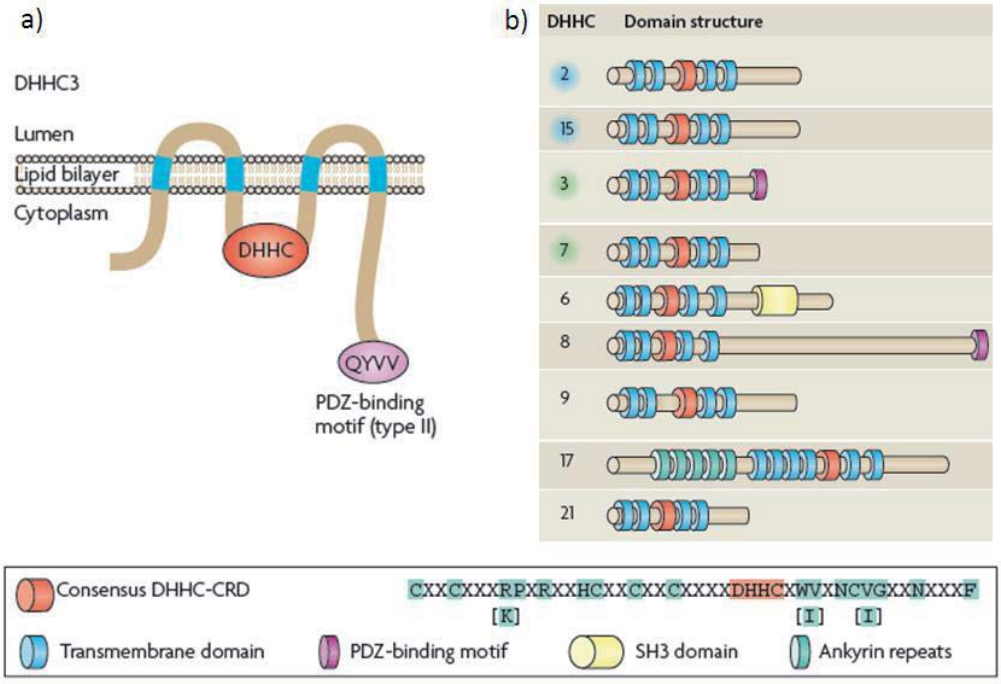

Figure 53. DHHc-type palmitoylating enzyme family. a) DHHC3, a representative DHHC (Asp-His-His-Cys) protein, has four transmembrane domains and a conserved cysteine-rich domain (CRD) containing a DHHC motif in the cytoplasmic loop. The DHHC sequence is essential for palmitoylating activity. DHHC3 also has a PDZ-binding motif at its carboxy-terminus. B) **Domain structures in DHHC enzymes.** Besides a DHHC core domain, each DHHC protein has individual protein–protein-interacting domains such as a PDZ-binding motif, an SH3 domain and ankyrin repeats. Blue and green backgrounds show the DHHC2/15 and DHHC3/7 subfamilies, respectively. DHHC proteins have distinct but overlapping substrate specificity, and several DHHC proteins are associated with human diseases. In the amino-acid sequence of the consensus DHHC-CRD, letters shown in red and green represent conserved sequences of the DHHC motif and CRD, respectively; X represents any amino acid. (Modified from Fukata and Fukata, 2010)

A speculative model could be proposed where CPT1C would decrease the amount of palmitoyl-CoA available for palmitoylating other proteins (Figure 54). This would be performed in situations where CPT1C catalytic activity could be increased by signaling pathways or conditions yet to be determined, giving rise to a new level of regulation in the reversible palmitoylation of synaptic proteins. This regulatory mechanism could affect synaptic transmission in processes such as creation of new memories, learning or even motor coordination.

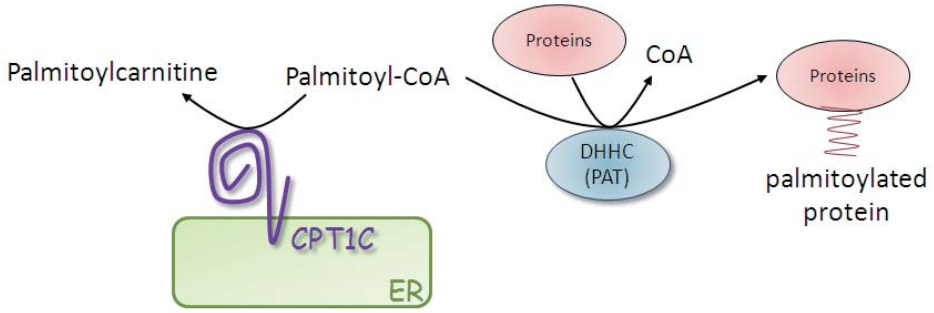

Figure 54. Theoretical participation of CPT1C in regulating palmitoyl-CoA pool available for protein palmitoylation through DHHC protein acyltransferases. PAT/DHHC involved in palmitoylation have distinctive subcellular localizations, contributing to compartmentalized regulation of substrate proteins in the polarized neuron. Some of them are in the ER membrane, in the Golgi complex in the cell body of neurons, some in small vesicle-like structures in dendrites, the cell body or axon terminals.

3. INTERACTING PROTEINS

To find out where to focus future experiments that can reveal CPT1C physiological function, a Y2H assay was performed. We have studied the bibliography and Gene Home information on the positive clones described in Tables 6 and 7 shown in the Y2H assay results (see Results section 6.2). It is important to notice that discussion from these results is merely speculative, since these interactions have not yet been tested *in vivo*.

Since the Y2H for membrane proteins was not set up yet at the time of this study, the Y2H for soluble proteins had to be used. As CPT1C is a membrane protein we had to decide the best "bait" for performing the Y2H screening and obtaining the most meaningful interactions. In this study we have shown that CPT1C is a polytopic membrane protein with two transmembrane domains, the short N-terminal and the long C-terminal ends facing the cytosol, and the domain between transmembrane segments (loop region) facing the lumen of the ER. The C-terminal segment showed different characteristics that apparently made it more prone to physiologically interesting protein interactions:

- The C-terminal domain is the longest fragment.
- The C-terminal domain contains the catalytic core.
- The C-terminal domain is facing the cytosol where many proteins can interact and link CPT1C to multiple cellular pathways also located in the cytosol.
- Our results show that the N-terminus of the protein is excised.

Thus, we decided to use the cytosolic C-terminal domain as the "bait", assuming some false negative results due to: 1) interactions among the N- and C-terminal domains affect the conformation of the protein and are important for determining some kinetic parameters of CPT1A and CPT1B (López-Viñas et al., 2007; Zammit, 2008). If these interactions are also found in CPT1C, the 3-D conformation of the protein with the C-terminus alone or in its physiological environment (interactions between N/C-termini) could markedly differ and interactions specific to this region would be lost; 2) Interactions specific to the N-terminus or to the loop region could never be found with our strategy.

Considering that our bait is the cytosolic domain of the protein, interacting proteins found in the Y2H assay which are located in the lumen of organelles like lysosomes, nucleus, or the inner mitochondrial membrane are more likely to be artefactual, as well as secreted proteins. In consequence, proteins like NDUFB9, BCAS2, NCAPH2, CXXC1, hnRNP H3, hnRNP M, ARID1A, TPP1, CTSB and BCAN were assumed as false positives. Additionally, proteins known not to be expressed in the brain were not taken into account (like GCA). Moreover, the laboratory of Erica Golemis provides a list of the most common false positives found in a Y2H assay (http://www.fccc.edu/research/labs/golemis/InteractionTrapInWork.html). Among them we find subunits of the proteasome, heat shock proteins and Zinc finger proteins. Hence, PSMB4 and DNAJB6 were also discarded.

From the interaction of CPT1C with different E3 ubiquitin ligases (FANCL, PELI1, RNF40 and indirectly BTBD1) one can get the idea that CPT1C could be itself ubiquitinated. On the contrary, our preliminary results (Supplemental data, Figure S5) show that CPT1C is not ubiquitinated, hence, these proteins were also discarded.

The rest of the positive clones have some functional common characteristics so we have grouped them in four functionally different groups (summarized in the next table), and a brief overview on each of the interacting partners and the possible implication of the interaction with CPT1C is speculated.

Function	Interacting partners
Protein degradation	NPLOC4 or Npl4
Membrane trafficking and cell structure	DCTN3, SNX9, MSTO1.
Metabolism	PKM2, CRYL1
Signal transduction	WDR6 (discussed in the next section)

a) Protein degradation

One of the most studied functions of the ER is its participation in the synthesis of secretory and membrane proteins. It is also well known that the proper folding of these newly synthesized proteins is achieved in the ER with the help of chaperones and other proteins present in the lumen of ER. When proper folding is not achieved, these unfolded proteins are transported from the ER lumen into the cytosol (process known as retrotranslocation) for their subsequent degradation in the ubiquitin/proteasome

pathway, by a process known as endoplasmic reticulum associated degradation (ERAD). ERAD is impaired in acute disorders and degenerative diseases of the brain (Paschen, 2003), such as Huntington disease (Duennwald and Lindquist, 2008).

Results obtained from the Y2H assay showed interaction of CPT1C with one of the components implicated in ERAD, named Npl4. This protein is part of the complex (p97-Ufd1-Npl4) that recognizes retrotranslocated proteins and couples them to their ubiquitilation. The receptor that recruits the p97-Ufd1-Npl4 complex is still unknown (Ye et al., 2003; Hitchcock et al., 2003; Pye et al., 2007; Lass et al., 2008). We speculate that CPT1C is the membrane receptor in the ER membrane of neurons; therefore CPT1C would recruit the complex where Npl4 is involved.

RNA interference of Npl4 on HeLa cells induces proteasome degradation of Ufd1. It does not induce unfolded protein response (rather it decreases α-TCR levels, a typical ERAD substrate); but it is associated with a 2-fold increase in the levels of polyubiquitinated proteins (Nowis et al., 2006). Preliminary results (Supplemental data, Figure S5) don't show any increase in the general polyubiquitination protein pattern or levels in brain homogenates from KO mice when compared to WT. Despite this, levels of Ufd1 and α-TCR (or other unfolded protein response markers) should be determined in cultured neurons from WT and KO mice to further assess the veracity of this interaction.

b) Membrane trafficking and cell structure

Dynactin 3 (DCTN3) is the smallest subunit of dynactin, a macromolecular complex consisting of 10 subunits ranging in size from 22 to 150 kD. Dynactin binds to both microtubules and cytoplasmic dynein. It is involved in a diverse array of cellular functions, including ER-to-Golgi transport, the centripetal movement of lysosomes and endosomes, spindle formation, cytokinesis, chromosome movement, nuclear positioning, and axonogenesis (Grabham et al., 2007). DCTN3 binds directly to the largest subunit (p150) of dynactin. A specific mutation in this subunit has been linked to an autosomal dominant form of motor neuron disease (Lin et al., 2007). The fact that this subunit is a very small and inaccessible part of the dynactin complex suggests that an interaction with CPT1C is rather improbable. Still it could be interesting to determine whether CPT1C is present in dendritic spines and to clarify whether dynactin 3 participates in its transport to this location.

Sorting nexin 9 (SNX9) has been shown to be expressed in presynaptic terminals and to coordinate synaptic vesicle endocytosis (Shin et al., 2007). The effect of knocking down endogenous SNX9 (with siRNA) on hippocampal neurons resulted in a slowing down of the synaptic vesicle endocitosys (Shin et al., 2007). The presence of CPT1C in presynaptic terminals needs to be evaluated and the effect of knocking down CPT1C on synaptic vesicle endocytosis should be studied to better understand this interaction.

The interaction of CPT1C with a protein involved in mitochondrial distribution and morphology (Misato or MSTO1), and the fact that CPT1C seems to be expressed in MAMs also, suggests that it should be elucidated whether CPT1C can participate in mitochondrial modeling. Silencing of Misato in HeLa cells resulted in the disappearance of the filamentous mitochondrial network and in mitochondrial fragmentation (Kimura and Okano, 2007). Therefore, it would be interesting to study whether the mitochondrial

distribution and morphology of cultured neurons or brain slices from KO mice for CPT1C is altered.

c) Metabolism

PKM2 is a pyruvate kinase that catalyzes the transfer of a phosphoryl group from phosphoenolpyruvate to ADP, generating ATP and pyruvate. Increased oxidation and decreased activity of this enzyme was reported in human brain samples of cases with mild cognitive impairment (Poon et al., 2006; Butterfield and Sultana, 2007; Reed et al., 2008). The finding that proteins involved in glucose metabolism are oxidized proteins suggests disturbances in memory formation and memory retrieval (Butterfield and Sultana, 2007). Preliminary results from the study of the phenotype shown by our model of the knockout mice for CPT1C, shows that these mice have impaired memory and ability for learning, thus suggesting that the interaction of CPT1C with PKM2 should be further studied.

4. HYPOTHESIS ON CPT1C PHYSIOLOGICAL FUNCTION IN MAMMALIAN BRAIN

The different approaches proposed in this work were all focused on finding new clues to elucidate the physiological function of CPT1C. The low catalytic activity found for CPT1C suggests that this new isozyme could be acting as a molecular sensor of some metabolites. In fact, the last results published have been obtained from the study of CPT1C KO mice and they support a role for CPT1C as an energy-sensing target in the hypothalamus (Wolfgang et al., 2006; Gao et al., 2009). Preliminary results obtained in our group from the study of a new CPT1C KO mouse model, support these findings and also show other alterations like learning and memory deficiencies and motor problems (P. Carrasco and N. Casals, unpublished results). These results though, suggest that CPT1C function might be involved in functions more common to all neurons. Nevertheless, the specific mechanisms revealed by the study of CPT1C function in hypothalamic neurons might provide a model for stablishing the physiological function of CPT1C in other neuronal cell types.

We will now discuss the possible molecular pathway in which CPT1C might participate. Two main hypotheses are proposed implicating CPT1C downstream or upstream of malonyl-CoA.

4.1 Downstream involvement of CPT1C in feeding behaviour

Lane and colleagues revealed that CPT1C knockout mice have lower body weight and food intake (See Introduction, section 3, Figure 8), and also exhibit decreased rates of fatty acid oxidation in peripheral tissues when fasted (Wolfgang et al., 2006). These results were confirmed by a new CPT1C KO mice model developed by Gao et al., (See Introduction, section 3, Figure 10) (Gao et al., 2009). Paradoxically, CPT1C KO mice fed a high-fat diet are more susceptible to obesity. All these findings indicate that CPT1C is necessary for the regulation of energy homeostasis (Wolfgang et al., 2006; Gao et al., 2009).

Current evidence suggests that hypothalamic fatty acid metabolism may play a role in regulating food intake. Hypothalamic nuclei are responsible for integrating multiple signals (informing about energy status from different peripheral tissues) and for responding to changes in energy status by altering the expression of specific neuropeptides (orexigenic: NPY, AgRP and anorexigenic: POMC, CART) to adjust food intake to whole-body energy demands (López et al., 2008).

Different observations have implicated malonyl-CoA (an intermediate in fatty acid synthesis) as an indicator of energy status in hypothalamic neurons. Levels of malonyl-CoA are determined by the complex interplay of enzymes (AMPK, ACC, MCD and FAS) that are responsive to nutrient availability. In fact, malonyl-CoA levels are dynamically regulated by fasting and feeding, and alter subsequent feeding behaviour by altering the expression of neuropeptides that regulate food intake and energy expenditure. As CPT1C binds malonyl-CoA with a K_D of ≈0.3 μM that lies within the dynamic range of hypothalamic malonyl-CoA concentration in fasted and refed states (≈0.1-1.4 μM respectively), it is possible that CPT1C is a downstream target of malonyl-CoA (Figure 55). Therefore, CPT1C would be inhibited in conditions of energetic availability when malonyl-CoA levels are high, and CPT1C would be active when energy is scarce and malonyl-CoA levels are low. What is not known is the enzymatic role of CPT1C or how it is linked to a downstream regulatory target that controls food intake and/or energy expenditure (reviewed in Wolfgang and Lane, 2006). We speculate that CPT1C, depending on energy status, is regulating ceramide and/or sphingolipid synthesis thus affecting lipid raft formation which is important for synaptic transmission. It can also be speculated that modulation of CPT1C activity is regulating protein palmitoylation which is important for synaptic plasticity.

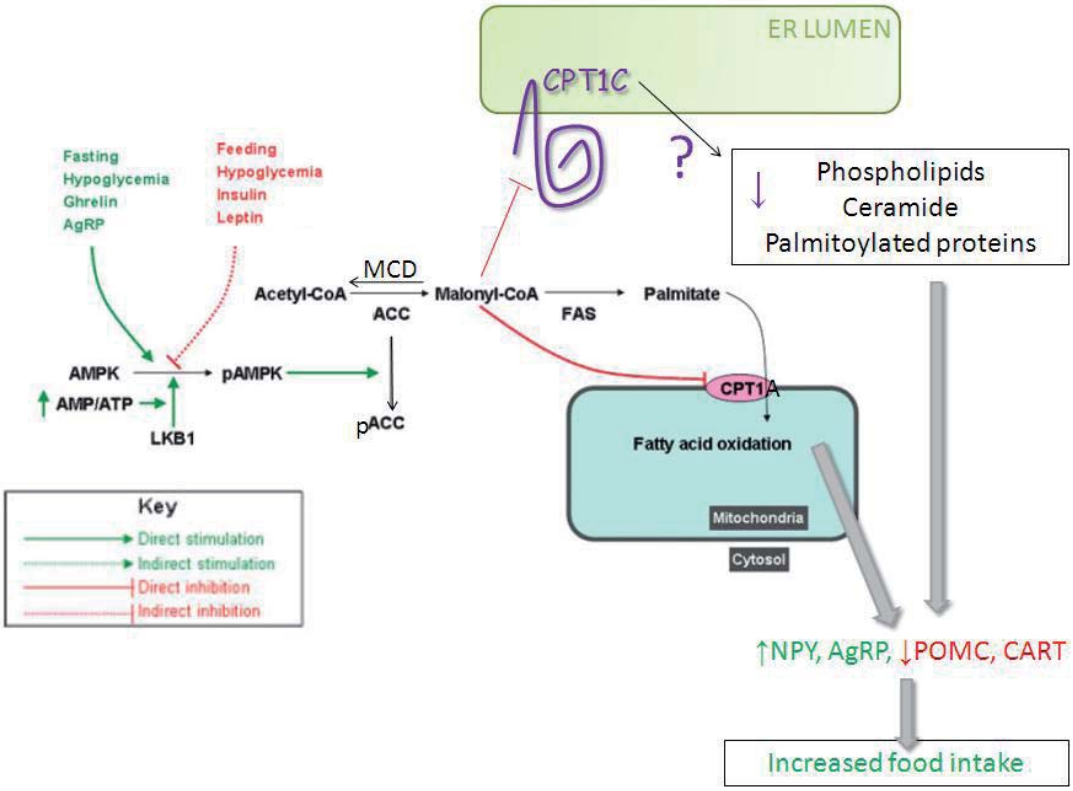

Figure 55. Downstream involvement of CPT1 activity in the regulation of food intake. In the hypothalamus, positive energy balance signals inhibit AMPK phosphorylation, whereas negative energy balance signals stimulate AMPK phosphorylation and activation. AMPK phosphorylation induces inactivation of ACC thus decreasing malonyl-CoA levels which in turn promotes CPT1A (increasing fatty acid oxidation) and maybe CPT1C activity. We hypothesize that CPT1C increased activity can potentially effect phospholipid or *de novo* ceramide synthesis, or even alter levels of palmitoylated proteins. Through a yet unknown mechanism these effects would mediate expression of orexigenic and anorexigenic neuropeptides and therefore lead to modifications in food intake. (Modified from López et al., 2007).

4.2 Upstream involvement of CPT1C in feeding behaviour

Results obtained from the Y2H assay show that CPT1C can interact with a protein (WDR6) that interacts with LKB1 (Xie et al., 2007). LKB1 is an AMPK kinase that when active, phosphorylates threonine 172 on AMPK (Jansen et al., 2009). AMPK is an intracellular energy sensor that maintains the energy balance within the cell and plays a role in the regulation of feeding (Andersson et al., 2004). It has also been shown that AMPK phosphorylates ACC in the hypothalamus leading to increased food intake (Kim et al., 2004).

From this interaction (CPT1C with WDR6) we speculate two possibilities:

a) CPT1C ACTS RECRUITING ENZYMES INVOLVED IN THE REGULATION OF FOOD INTAKE

WDR6 is a member of the WD repeat protein family. WD repeats are minimally conserved regions of approximately 40 amino acids typically bracketed by Gly-His and Trp-Asp (GH-WD), which may facilitate formation of heterotrimeric or multiprotein complexes. Therefore, the interaction of CPT1C with this protein could mediate the formation of a multiprotein complex.

Since CPT1C has been shown to be an enzyme with very low catalytic activity, we speculate that CPT1C with WDR6 could be recruiting LKB1, AMPK and ACC close to the ER or MAMs. In MAMs malonyl-CoA levels could influence CPT1A activity, and subsequently regulate food intake through a yet unknown mechanism.

In this hypothetic model, CPT1C would be acting upstream of malonyl-CoA, recruiting the enzymatic machinery necessary for modulating the levels of this intermediate metabolite that regulates feeding behaviour (Figure 56).

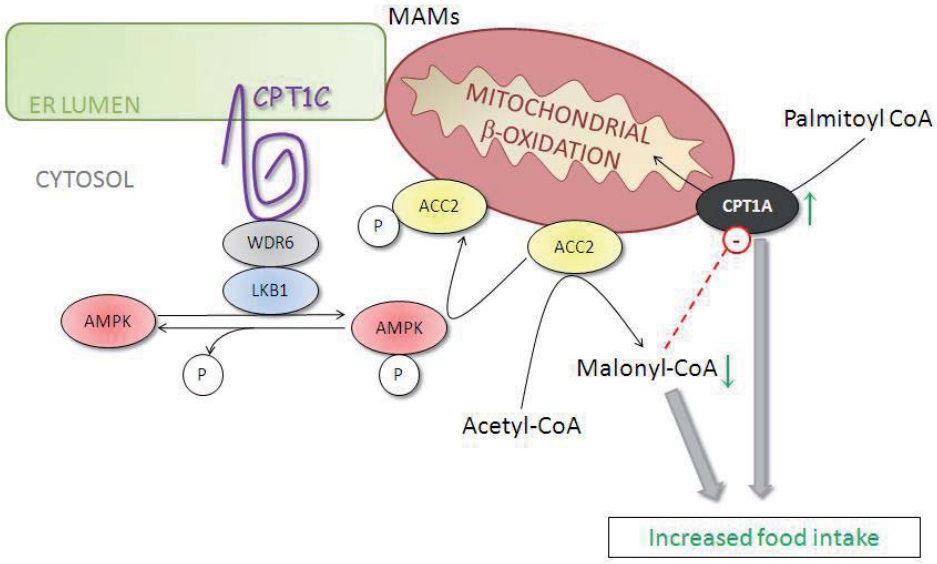

Figure 56. CPT1C acts recruiting enzymes involved in the regulation of food intake. In this model, CPT1C would act recruiting the machinery involved in AMPK phosphorylation close to its target enzyme, ACC2, for the modulation of malonyl-CoA levels and CPT1A activity. Through yet unknown mechanisms malonyl-CoA levels and CPT1A activity would lead to changes in the expression of orexigenic and anorexigenic neuropeptides mediating feeding behaviour.

b) INCREASED CPT1C ACTIVITY COULD DECREASE MALONYL-CoA LEVELS INVOLVING THE *DE NOVO* SYNTHESIS OF CERAMIDE

The treatment of endothelial cells with palmitate resulted in increases in the *de novo* synthesis of ceramides and in the activation of protein phosphatase PP2A activity. PP2A activation decreases AMPK phosphorylation/activation and thus activates ACC that produces increases in malonyl-CoA levels (Wu et al., 2007).

Considering that CPT1C seems to have the potential for higher specific activity (as shown from the results obtained in the 3-D structural model) we propose a new hypothesis on the involvement of CPT1C in the regulation of feeding behaviour. We speculate that situations of low CPT1C activity in the hypothalamus would produce an increase in the *de novo* synthesis of ceramide, through increases in palmitoyl-CoA levels in microdomains [supported by unpublished results from our group (A. Sierra and N. Casals, unpublished results), which have shown a ≈20% decrease in ceramide levels, from *de novo* synthesis, when CPT1C was overexpressed in PC12 and HEK293T cells]. Increased ceramide levels would activate PP2A and consequently AMPK would be dephosphorylated and inactivated. Inactivation of AMPK would increase ACC activity producing increases in malonyl-CoA levels, which in turn would inhibit, in a larger extent, CPT1 activity. The

increase in malonyl-CoA levels and the inhibition of CPT1 activity, would mediate a decrease in food intake by modifying the expression of hypothalamic neuropeptides. Conversely, increases in CPT1C activity (in conditions still undetermined) would lead to a decrease in malonyl-CoA levels, producing increases in food intake (Figure 57). This hypothesis implicates that CPT1C activity could be regulated through unknown mechanisms, maybe involving other interacting partners.

Taking into account the hypothesis presented here, the decrease in food intake of the KO mice would be due to increased palmitoyl-CoA levels leading to increases in the *de novo* synthesis of ceramides. This hypothesis places CPT1C upstream of the malonyl-CoA signal and involves ceramides in the regulation of feeding behaviour.

It is also very likely that CPT1C is involved both upstream and downstream of the pathway providing a positive feedback in this regulatory mechanism (Figure 57).

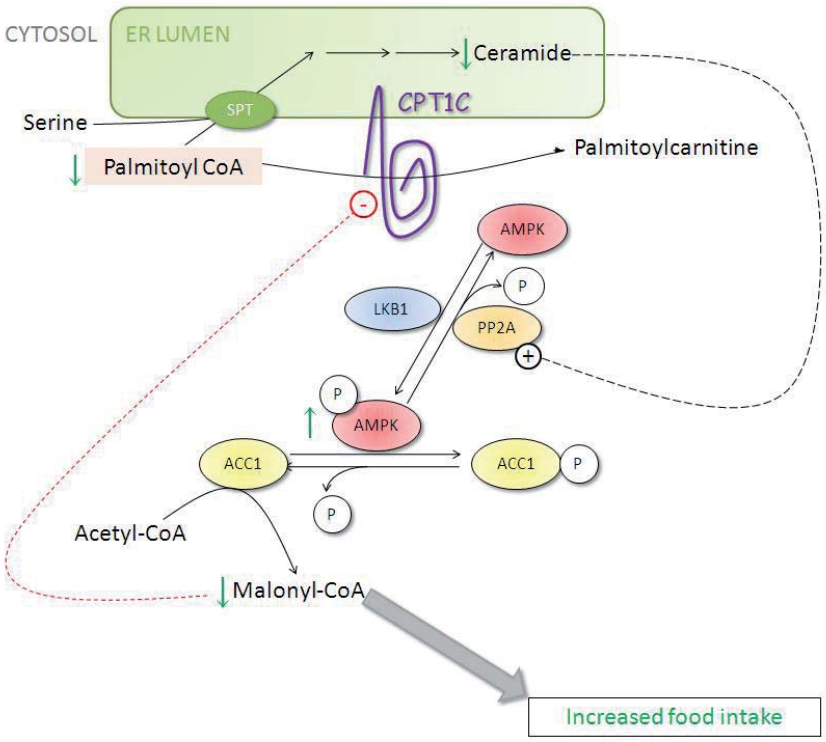

Figure 57. Increased CPT1C activity could decrease malonyl-CoA levels involving the *de novo* synthesis of ceramide. In situations leading to increased CPT1C activity, *de novo* ceramide production would be decreased allowing AMPK phosphorylation. Therefore, ACC1 activity would be decreased, reducing malonyl-CoA levels which in turn would lead to continuous activation of CPT1C and to increased food intake through the regulation of orexigenic and anorexigenic neuropeptides.

All these speculative mechanisms have to be further studied and are presented here with the aim of opening new lines of research for future experiments that will hopefully clarify the physiological role of this interesting neuron- expressed protein.

In summary, we hypothesize that CPT1C activity can be modulated through interacting partners or through a specific metabolic context. We also propose that CPT1C mainly affects palmitoyl-CoA levels in microdomains (determined domains of ER or even MAMs) for further regulating either: 1) *de novo* synthesis of ceramide or, 2) phospholipids synthesis (especially

saturated fatty acids versus PUFA containing phospholipids) or, 3) protein palmitoylation. These potential effects in hypothalamic neurons would involve CPT1C in the regulation of feeding behaviour, and in other brain regions they would affect the learning process or motor abilities.

CONCLUSIONS

1. The data provided by the 3-D structural model of CPT1C suggest that this isozyme is able to catalyze the conversion of palmitoyl-CoA into palmitoylcarnitine. The catalytic residues are conserved and residues contacting both substrates, palmitoyl-CoA and carnitine, are all equivalent to those found for CPT1A.

2. Expression of rat CPT1C in *Saccharomyces cerevisiae* yields no catalytic activity when testing different conditions (longer periods of time, increased temperature, increased substrate concentration, testing of microsomal fraction or chimeric protein CPT1·ACA). Thus, the yeast expression system is not suitable for studying CPT1C enzymatic activity because yeast lacks some factor that is present in mammalian cells.

3. Endogenous and overexpressed CPT1C is basically localized in the endoplasmic reticulum of mammalian cells (HEK293T, PC12, SH-SY5Y, primary cultures of fibroblasts and neurons). Some evidences indicated that CPT1C could also be found, in lower amounts, in mitochondrial associated membranes (MAMs).

4. The specific sequence of CPT1C N-terminal domain (first 150 amino acids) drives the protein to the endoplasmic reticulum.

5. The N-terminal end of endogenous CPT1C in wild type mouse brain is processed (at least until Val^{27}) and is not detected in mouse brain cortex lysates

6. The N- and C-terminal domains of CPT1C are facing the cytosolic side of the endoplasmic reticulum membrane, whereas the loop domain is facing the endoplasmic reticulum lumen.

7. The data provided by the yeast two-hybrid assay do not indicate a unique binding partner of CPT1C. Instead the assay retrieved proteins involved in different functions: protein degradation, membrane trafficking, cell structure, signal transduction and metabolism.

SUPPLEMENTAL DATA

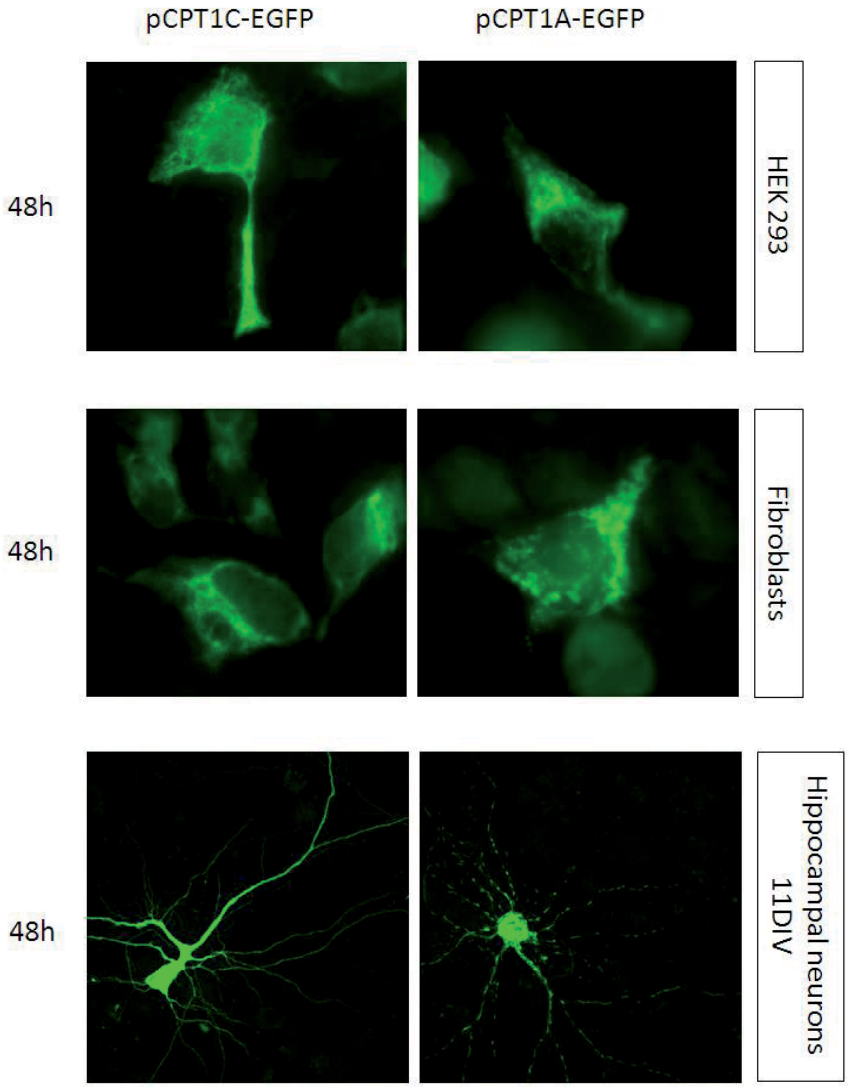

Figure S1. Fluorescence pattern shown by pCPT1A-EGFP and pCPT1C-EGFP. HEK293, primary cultures of fibroblasts or hippocampal neurons were transiently transfected with Lipofectamine 2000 reagent with pCPT1A-EGFP and pCPT1C-EGFP constructs and fluorescence was visualized at 48h after transfection. Images were taken with 1000x magnification in a Leica DM/IRB fluorescence microscope.

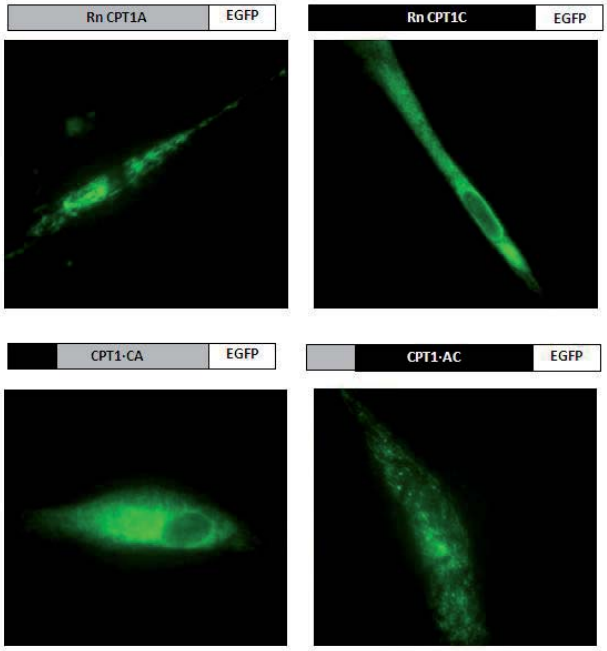

Figure S2. **Subcellular localization of fusion proteins CPT1A-EGFP, CPT1C-EGFP, CPT1·CA-EGFP, and CPT1·AC-EGFP in cultured cells.** (In gray, CPT1A sequence; in black, CPT1C sequence; in white: EGFP). Primary cultures of fibroblasts were transfected with the different plasmids. 48 h after transfection, cells were visualized in a fluorescence microscope (1000x magnification).

A

TMHMM 2.0

CPT1A *Mus musculus* (773aa)

Sequence	TMHMM2.0	outside	1	48
Sequence	TMHMM2.0	TM	49	71
Sequence	TMHMM2.0	inside	72	103
Sequence	TMHMM2.0	TM	104	126
Sequence	TMHMM2.0	outside	127	773

CPT1A *Rattus norvegicus* (773aa)

Sequence	TMHMM2.0	inside	1	103
Sequence	TMHMM2.0	TM	104	126
Sequence	TMHMM2.0	outside	127	773

CPT1A *Homo sapiens* (803aa)

Sequence	TMHMM2.0	outside	1	61
Sequence	TMHMM2.0	TM	62	84
Sequence	TMHMM2.0	inside	85	103
Sequence	TMHMM2.0	TM	104	126
Sequence	TMHMM2.0	outside	127	773

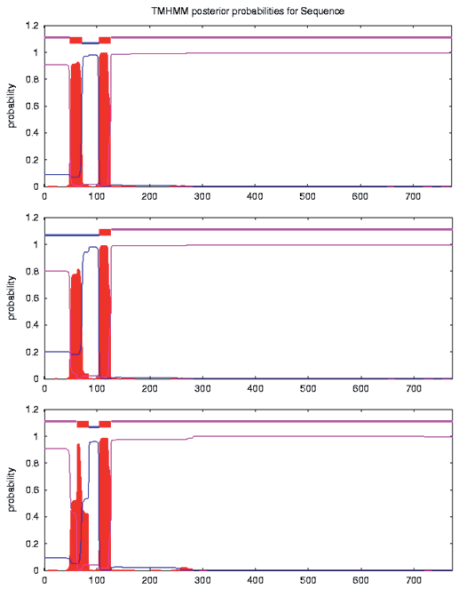

CPT1C *Mus musculus* (798 aa)

Sequence	TMHMM2.0	inside	1	103
Sequence	TMHMM2.0	TM	104	126
Sequence	TMHMM2.0	outside	127	798

CPT1C *Rattus norvegicus* (801 aa)

Sequence	TMHMM2.0	inside	1	103
Sequence	TMHMM2.0	TM	104	126
Sequence	TMHMM2.0	outside	127	801

CPT1C *Homo sapiens* (803 aa)

Sequence	TMHMM2.0	outside	1	52
Sequence	TMHMM2.0	TM	53	75
Sequence	TMHMM2.0	inside	76	103
Sequence	TMHMM2.0	TM	104	126
Sequence	TMHMM2.0	outside	127	803

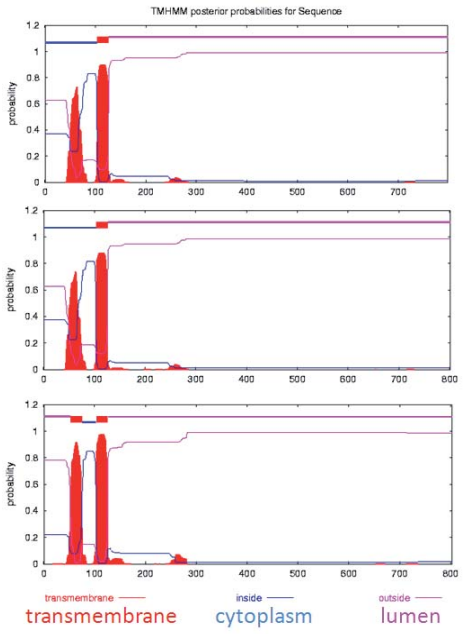

Figure S3A. Bioinformatic topology prediction: A) **Prediction with TMHMM 2.0**: Here are shown the plots for CPT1A and CPT1C from different species specified in each case. "Inside" shows the amino acid segment oriented towards the cytoplasmic side of the membrane of the corresponding organelle (blue segments).; "TM" refers to amino acid segments predicted to be intramembrane (red segments in the graph plot); "Outside" expresses the amino acid residues in the fragment facing the opposite side of the membrane (pink segments in the graph).

B

HMMTOP 2.0

CPT1C *Mus musculus* (798aa)

N-terminus: IN (cytoplasm)
Number of transmembrane domains: 3
Transmembrane helices: 50-72
103-122
135-154

CPT1C *Rattus norvegicus* (801aa)

N-terminus: IN (cytoplasm)
Number of transmembrane domains: 1
Transmembrane helices: 50-69

CPT1C *Homo sapiens* (803aa)

N-terminus: IN (cytoplasm)
Number of transmembrane domains: 3
Transmembrane helices: 50-72
103-122
141-158 o

CPT1A *Mus musculus* (773aa)

N-terminus: OUT (lumen)
Number of transmembrane domains: 2
Transmembrane helices: 50-73
104-122

CPT1A *Rattus norvegicus* (773 aa)

N-terminus: OUT (lumen)
Number of transmembrane domains: 2
Transmembrane helices: 56-79
110-128

CPT1A *Homo sapiens* (773aa)

N-terminus: OUT (lumen)
Number of transmembrane domains: 2
Transmembrane helices: 49-73
104-122

Figure S3B. Bioinformatic topology prediction: B) Prediction with HMMTOP 2.0: Summarized plot of the results obtained with this program for the different sequences highlighted in bold. "N-terminus" indicates the orientation of the N-terminal fragment of the protein. "Transmembrane helices" indicates the residues flanking transmembrane domains.

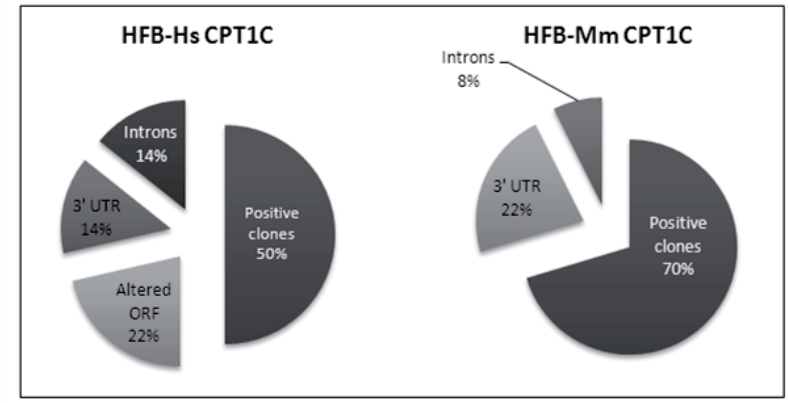

Figure S4. Herein represented are percentual values corresponding to the Y2H performed with HFB (human fetal brain cDNA Library) and: **a)** Hs CPT1C [human CPT1C sequence (aa131-803)] that resulted in 28 colonies growing in SD/-Ade/-His/-Leu/-Trp/X-α-gal plates or **b)** MmCPT1C [mouse CPT1c sequence (aa131-803)] that resulted in 32 colonies growing in the same plates. "Positive clones" represent sequences that matched proteins in GeneBank searches in the correct reading frame and with homologies higher thant 98%. "Introns" correspond to amplicons that matched introns sequences in GeneBank. "3' UTR" is for sequences that matched 3' UTR regions of different genes. Some positive clones had an altered open reading frame in the sequence inserted in the cDNA library ("Altered ORF"), giving rise to expressed proteins that could interact with the bait but matched no protein in BLAST searches.

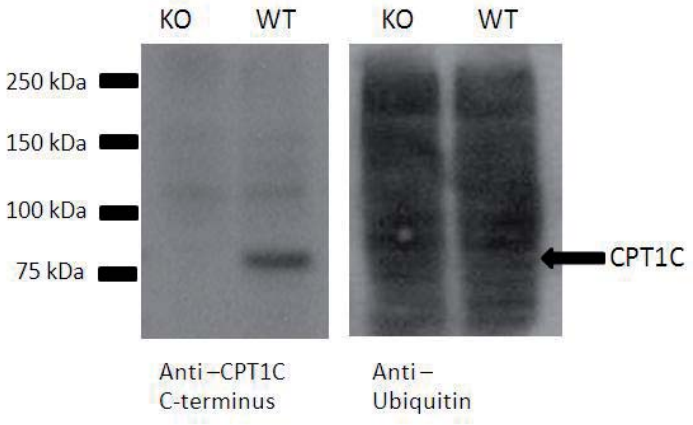

Figure S5. Western blot with an anti-Ubiquitin antibody. Brain extracts of KO and WT mice. The WB shows that in the WT brain extracts there is CPT1C present (immunoblotting with antibody anti-CPT1C) but at the same heigh there is no band when the same membrane is probed with an anti-ubiquitin antibody (1:1000). The WB also shows that there are no differences in the pattern or general intensity of ubiquitinated proteins among WT or KO mice. (Antibody anti-Ubiquitin, sc-8017, Santa Cruz Biotechnology).

RESUM
(en català)

INTRODUCCIÓ

EL SISTEMA CARNITINA PALMITOILTRANSFERASA

El sistema de les carnitina palmitoiltransferases (CPT) permet l'entrada d'àcids grassos de cadena llarga a la matriu mitocondrial (on seran beta-oxidats) gràcies a un seguit de transesterificacions realitzades per diferents enzims (Kerner i Hoppel, 2000). El primer enzim d'aquest sistema és la carnitina palmitoiltransferasa 1, CPT1, que és una proteïna que es localitza a la membrana mitocondrial externa i que catalitza la transesterificació d'àcids grassos des del CoA a la carnitina. El producte format pot atravessar la membrana interna amb l'ajuda d'una carnitina-acilcarnitina translocasa (CACT). Posteriorment, CPT2, que es troba a la cara luminal de la membrana mitocondrial interna, reverteix la reacció de CPT1, retransferint el grup CoA a l'àcid gras. És aleshores quan l'acil-CoA entra a la beta-oxidació i acaba produint acetil-CoA (Zammit, 2008; Rufer et al., 2009).

La reacció catalitzada per CPT1 és el principal punt de control de la beta-oxidació per la seva capacitat de ser inhibit pel malonil-CoA, que és un intermediari de la biosíntesi d'àcids grassos(McGarry i Foster, 1980). La reacció catalitzada per CPT1 no és només important pel control de la beta-oxidació, sino que també determina la disponibilitat d'acil-CoA de cadena llarga per altres processos com ara la síntesi de lípids complexos.

En mamífers, l'enzim CPT1 existeix en almenys tres isoformes:

- **CPT1A,** també es coneix com la isoforma de fetge o isoforma L (L-CPT1). És la isoforma que s'expressa més ubiquament i no només es troba a les mitocòndries del fetge sino que també s'expressa al pàncrees, als ronyons, pulmons, melsa, intestí, cervell i ovaris (Esser et al., 1993; Britton et al. 1995; McGarry and Brown, 1997).
- **CPT1B,** també es coneix com la isoforma del múscul (M-CPT1). Es va identificar primer a les mitocòndries del múscul esquelètic i cardíac, però també es troba al teixit adipós i als testicles (Yamazaki et al., 1995; Esser et al., 1996).
- **CPT1C** s'ha descrit recentment i s'ha trobat que és una proteïna d'expressió exclusiva al cervell. Aquesta nova isoforma presenta una alta homologia de seqüència amb les altres isoformes però la seva funció és encara ara desconeguda (Price et al., 2002).

CPT1A i CPT1B

Aquestes dues isoformes es coneixen molt bé ja que s'han estudiat molt des que van ser clonades per primera vegada. Tot i que la identitat en la seqüència d'aminoàcids entre les isoformes és alta (62%), ambdós isoenzims presenten característiques

cinètiques i regulatòries diferents: CPT1A presenta una major afinitat pel substrat carnitina i té menor afinitat per l'inhibidor fisiològic malonil-CoA que la isoforma de múscul (Esser et al., 1996; McGarry and Brown, 1997; Zammit, 2008). La diferent afinitat per l'inhibidor reversible de l'enzim probablement està implicada en la regulació diferencial de la beta-oxidació en el múscul en comparació amb el fetge.

Totes dues isoformes es localitzen a la membrana mitocondrial externa amb dos dominis transmembrana (TM1 i TM2) i amb els extrems N- i C-terminals orientats cap a la cara citoplasmàtica (Fraser et al., 1997). També s'ha demostrat que residus d'entre els primers 150 aminoàcids del domini N-terminal (inclou els dos dominis transmembrana i una regió una mica més cap avall), contenen informació clau per dirigir l'enzim a la seva localització (Cohen et al., 1998; Cohen et al., 2001).

També estan molt ben caracteritzats els residus importants per a l'activitat catalítica i per a la sensibilitat al malonil-CoA i s'han predit estructures tridimensionals en base als cristalls existents de la carnitina aciltransferasa (CAT), carnitina octanoiltransferasa (COT) i carnitina palmitoiltransferasa 2 (CPT2) (López-Viñas et al, 2007).

REGULACIÓ FISIOLÒGICA PER MALONIL-CoA AL FETGE I AL MÚSCUL

Els enzims CPT1A i CPT1B estan estretament regulats pel seu inhibidor fisiològic, el malonil-CoA, i representen la reacció enzimàtica més important en la regulació de la beta-oxidació mitocondrial d'àcids grassos (McGarry i Foster, 1980). Aquest procés permet a la cèl·lula senyalitzar la disponibilitat de lípids i carbohidrats al fetge, cor, múscul esquelètic i les cèl·lules β del pàncrees (Zammit, 1999).

Al fetge, el malonil-CoA és el metabòlit que assegura que l'oxidació i la biosíntesi d'àcids grassos no es produeixin alhora. En el cas d'ingesta de carbohidrats (quan la insulina és alta) s'incrementa la concentració de malonil-CoA, es suprimeix l'activitat CPT1 i els nous acils-CoA de cadena llarga es dirigeixen a formar productes d'esterificació (triacilglicerols, TAG). En canvi, en situació de dejuni (baixa insulina), disminueix el flux de la glicòlisi, cauen els nivells de malonil-CoA i s'atura la síntesi de nous àcids grassos. En aquest context, CPT1 està activada i els àcids grassos lliures circulants s'incorporen directament a la beta-oxidació i s'accelera la producció de cossos cetònics (McGarry and Foster, 1980; McGarry et al., 1989).

En els teixits no lipogènics com el múscul cardíac i esquelètic, el malonil-CoA actua com a senyalitzador. En dejuni, els nivells de malonil-CoA són baixos i s'incrementa l'activitat CPT1 entrant àcids grassos a la mitocòndria i produint una alta taxa oxidativa al múscul. Per altra banda, la inhibició de CPT1 que es produeix quan els nivells de malonil-CoA pugen (en alimentació) fa caure la taxa de beta-oxidació (McGarry et al., 1983; Wolfgang and Lane, 2006).

S'ha vist que el múscul expressa una forma de acetil-CoA carboxilasa (ACC2, l'enzim que sintetitza el malonil-CoA) que es troba unida a la cara citosòlica de la membrana mitocondrial externa, i expressa molt poc o gens de sintasa d'àcids grassos (FAS) que eliminaria el malonil-CoA incorporant-lo a nous àcids grassos formats per aquest enzim. En canvi, el múscul si que expressa en abundància l'enzim malonil-CoA descarboxilasa (MCD) que seria l'enzim que disminuiria els nivells de malonil-CoA en aquest teixit (McGarry and Foster, 1980). Per tant el flux de síntesi i degradació de malonil-CoA media el potencial oxidatiu dels greixos al múscul (Wolfgang and Lane, 2006).

CPT1C: UNA NOVA ISOFORMA

Realitzant cerques *in silico* en bases de dades basant-se en la seqüència de nucleòtids o de la proteïna CPT1A humana es va identificar un nou gen, al que es va designar CPT1C degut a l'alta similitud que presentava envers les altres isoformes de CPT1 (Price et al., 2002). El nou enzim però conté un extrem C-terminal més llarg (uns 30 aminoàcids més) que les altres isoformes. Analitzant en detall les dades de l'homologia de la nova isoforma amb les ja conegudes es va determinar que CPT1C era més similar a CPT1A que a CPT1B.

El que no s'ha trobat és la forma ortòloga d'aquest enzim en altres espècies que no siguin mamífers, mentres que les altres isoformes s'expressen en organismes com ocells, peixos, rèptils, amfibis o insectes. Això suggereix una funció específica per aquesta isoforma, pròpia de cervells més desenvolupats (Price et al., 2002; Sierra et al., 2008).

Estudis d'expressió indiquen que CPT1C es localitza exclusivament al sistema nerviós central i es troba distribuït homogèniament a totes les àrees (hipocamp, còrtex, hipotàlem, cerebel i altres). El patró d'expressió d'aquest nou enzim s'assembla més al patró d'enzims com FAS o ACC1 (enzims relacionats a la biosíntesi de greixos) que a la d'enzims com CPT1A o ACC2 (més relacionats a la beta-oxidació) (Price et al., 2002; Sorensen et al., 2002; Dai et al., 2007).

Analitzant la seqüència d'aminoàcids veiem que tots els residus importants per dur a terme l'activitat carnitina aciltransferasa estan conservats a CPT1C, així com el lloc d'unió al malonil-CoA. Tot i això, quan s'han realitzats assaigs d'activitat CPT1 (pel mètode radiomètric) no s'ha trobat activitat ni assajant altres substrats (diversos acils-CoA que són bons substrats de CPT1A i/o CPT1B). Podria ser que la cua C-terminal de CPT1C allargada obstaculitzés l'activitat de l'enzim.

Pel que fa a la localització subcel·lular de CPT1C, i tenint en compte l'alta homologia de seqüència amb les altres isoformes, s'ha proposat que CPT1C tindria la mateixa

localització intracel·lular, és a dir, a la membrana mitocondrial externa, i amb la mateixa topologia que les altres isoformes (Price et al., 2002).

FUNCIÓ FISIOLÒGIA DE CPT1C

Per aclarir el paper d'aquest isoenzim en l'homeòstasi energètica, dos grups han obtingut ratolins amb una delecció dirigida del gen de CPT1C i han publicat els seus resultats (Wolfgang et al., 2006; Gao et al., 2009).

En el primer model de kcnock-out (KO) desenvolupat al grup del Dr. Lane, els ratolins KO no mostraven anormalitats aparents del desenvolupament ni alteracions en la mida dels òrgans. Tampoc hi havia diferències en la temperatura corporal quan se'ls compara amb els seus germans salvatges (WT). El que si es va observar, és que quan són alimentats amb una dieta de laboratori normal (standard chow, SC) els ratolins KO mostraven una disminució en el pes corporal d'aproximadament el 15% i una disminució de la ingesta propera al 25% (Wolfgang et al., 2006).

En canvi, en sotmetre'ls a una dieta rica en greixos (high fat diet, HFD), els ratolins KO per CPT1C són més susceptibles a obesitat (guanyen més pes tot i que mengin menys), esdevenen mitjanament resistents a la insulina i mostren un menor consum energètic als teixits perifèrics (Wolfgang and Lane, 2006).

Wu i col·laboradors van desenvolupar un nou model de ratoilns KO per CPT1C (Gao et al., 2009). Aquests ratolins mostraven un fenotip molt similar al descrit anteriorment. A més, van trobar que l'expressió dels gens que promouen la beta-oxidació al fetge i al múscul estaven molt disminuïda en els ratoilns KO sotmesos a una dieta rica en greixos respecte als nivells d'expressió observats pels ratolins WT en les mateixes condicions d'alimentació. També van veure que l'activitat CPT1 i l'oxidació de palmitat estaven disminuïts en els ratolins KO respecte els WT (Figura 10).

També s'ha vist que la sobreexpressió de CPT1C a l'hipotàlem és suficient per protegir els ratolins KO del guany de pes corporal quan se'ls alimenta amb una dieta rica en greixos (Dai et al., 2007).

Tots aquests resultats indiquen que CPT1C podria tenir un paper protector davant dels efectes d'una dieta rica en greixos i que CPT1C és necessari per regular l'homeòstasi energètica.

IMPLICACIÓ DE L'ACTIVITAT CPT1 EN EL CONTROL DE LA INGESTA

Els nuclis hipotalàmics integren diferents senyals (hormonals i neuronals) que informen de l'estat energètic dels teixits perifèrics i que responen a la informació rebuda modificant l'expressió de determinats neuropèptids (NPY, AgRP, POMC, CART)

que ajusten la ingesta alimentària als requeriments energètics de l'organisme (López et al., 2008).

La restricció de la ingesta porta a l'activació d'una subpoblació de neurones en les quals s'indueix l'expressió de pèptids hipotalàmics orexigènics: neuropèptid Y (NPY) i l'"aguti related protein" (AgRP), i es disminueix l'expressió dels pèptids anorexigènics: proopiomelonocortina (POMC) i el trànscrit regulat per cocaïna-amfetamina (CART). Aquests canvis, combinats, provoquen un augment de la ingesta i una reducció de la despesa energètica. En realimentació, s'esdevé la resposta inversa (Hu et al., 2003).

Les neurones han desenvolupat mecanismes que els permeten monitoritzar la disponibilitat energètica a l'espai extracel·lular. Un d'ells s'activa quan la relació AMP/ATP augmenta (per exemple, durant el dejuni) i implica l'activació de la quinasa depenent d'AMP (AMPK). S'ha vist que la inducció sostinguda de l'activitat AMPK és suficient per induir la ingesta i porta a obesitat, i a la inversa; aquests canvis en l'activitat AMPK vénen acompanyats de canvis en l'expressió de pèptids hipotalàmics (Kim et al., 2004, Minokoshi et al., 2004).

L'activació de l'AMPK afecta l'estat de fosforilació de l'acetil-CoA carboxilasa, ACC. Quan ACC és fosforilada s'inactiva i deixa de catalitzar la reacció de formació de malonil-CoA, reduint així els nivells d'aquest metabòlit intermediari que deixarà d'inhibir l'activitat CPT1 mitocondrial i s'activarà l'entrada d'àcids grassos a la mitocòndria on seran beta-oxidats (Kahn et al., 2005, López et al., 2007). De fet s'ha vist que la inhibició tant farmacològica com genètica de l'activitat CPT1 hipotalàmica porta a una disminució de la ingesta i a una pèrdua de pes (Obici et al., 2003). Pel que es pot deduir que la taxa d'oxidació de greixos en determinades neurones hipotalàmiques informa de la disponibilitat de nutrients a l'hipotàlem que modularà el comportament alimentari i l'entrada endògena de nutrients a la sang (Obici et al., 2003).

Algunes senyals hormonals, com la leptina o la grelina, actuen per aquesta mateixa via (l'eix hipotalàmic AMPK/malonil-CoA/CPT1) però amb efectes contraris (Figura 12) (Minokoshi et al., 2004; Gao et al., 2007; Wolfgang et al., 2007; López et al., 2008).

OBJECTIUS

Objectiu general:

Determinar la funció fisiològica de CPT1C.

Objectius específics:

1. Identificar *in silico* els residus que puguin alterar l'activitat enzimàtica de CPT1C a través de la construcció d'un model de l'estructura 3-D utilitzant el modelat per homologia.
2. Determinar les característiques cinètiques de l'enzim expressant la proteïna en llevats.
3. Estudiar la localització subcel·lular de CPT1C.
4. Determinar la topologia a la membrana d'aquesta proteïna.
5. Identificar proteïnes que puguin interaccionar amb CPT1C.

RESULTATS I DISCUSSIÓ

MODEL ESTRUCTURAL 3-D

Es va construir el model 3-D de l'estructura de CPT1C (utilitzant el modelat per homologia) a partir del model existent de CPT1A (Morillas et al., 2001; Morillas et al., 2004; López-Viñas et al., 2007), per determinar si la nova isoforma contenia les propietats estructurals necessàries per dur a terme la mateixa reacció enzimàtica que CPT1A.

Es van analitzar els residus en contacte amb ambdós substrats (es considera que els residus a una distància igual o inferior a 4 Å estan en contacte). Un cop identificats es va buscar la homologia en la mateixa posició en els alineaments amb CPT1A i CPT1B. Tots els residus implicats en la unió a la carnitina estaven ben conservats. Els residus implicats en la unió del palmitoil-CoA estaven majoritàriament ben conservats amb alguns canvis semi-conservatius que no semblaria que interferissin l'activitat de l'enzim (Figura 31). Els residus implicats en la catàlisi també estaven ben conservats (His^{473} i Ala^{381}) (Figura 30).

Aquestes prediccions fan pensar que l'enzim CPT1C hauria de ser capaç de catalitzar la mateixa reacció que CPT1A.

ACTIVITAT ENZIMÀTICA DE CPT1C

Degut a què resultats preliminars del nostre grup havien mostrat certa activitat CPT1C (en expressar la proteïna en cèl·lules de mamífer s'havia observat un increment en la

quantitat de palmitoilcarnitina formada) ens vam plantejar de determinar les característiques cinètiques de l'enzim utilitzant el sistema d'expressió heteròloga dels llevats. Els llevats representen un organisme ideal per determinar l'activitat dels enzims CPT1 ja que no contenen aquest enzim endògenament. A més aquest sistema ja s'ha emprat anteriorment per caracteritzar enzims similars (Zhu et al., 1997; Cohen et al., 1998; Prip-Buus et al., 1998; Morillas et al., 2002).

Es van utilitzar vectors d'expressió en llevats (pYES2) sota el control del promotor GAL1. Es van clonar les respectives isoformes CPT1C i CPT1A (com a control positiu de l'activitat) en aquests plasmidis. L'expressió del plasmidi buit s'utilitzava com a control negatiu de l'assaig.

Després d'expressar els diferents constructes en la soca W303-1A de *S. cervisiae* s'obtenien les fraccions mitocondrials i el mateix dia es determinava l'activitat CPT1 utilitzant el mètode radiomètric (Morillas et al., 2000). Els substrats eren: palmitoil-CoA a 50 µM i L-[metil-^{3}H] carnitina a 400 µM. El producte que es quantificava era la ^{3}H-palmitoilcarnitina. S'assajaven de 15 a 80 µg de proteïna de les fraccions mitocondrials durant 5 min a 30°C i es calculava l'activitat específica. D'aquesta manera no es va trobar activitat específica CPT1C (Figura 33), fet que suggeria que potser les condicions posades a punt per assajar l'activitat CPT1A no es corresponien amb les necessàries per determinar l'activitat CPT1C.

Per comprovar que CPT1C no tingués una velocitat de catàlisi menor que la CPT1A es van assajar a temps més llargs (fins 60 min). L'activitat observada per CPT1C era de 0.2 nmol palmitoilcarnitina*min^{-1}*mg^{-1} prot, que no es pot tenir en compte ja que queda dins la desviació estàndard dels blancs de la reacció en el mètode radiomètric. Després es va determinar l'efecte de la temperatura en la reacció i es va pujar de 30 a 37°C. Així es va incrementar l'activitat CPT1A però no va tenir cap efecte en la de CPT1C. També es va voler comprovar la hipòtesi que CPT1C fos un enzim amb una K_m pel palmitoil-CoA més gran que la de CPT1A augmentant la concentració d'aquest substrat 5 vegades però tampoc es va observar un increment en l'activitat CPT1C (Figura 34).

Tenint en compte que els residus important per la catàlisi estan conservats i es troben a la part central de la proteïna, i que les regions més diferents a les altres isoformes són la regió N- i C-terminal que podrien produir un efecte inhibidor en l'activitat de CPT1C, es va assajar l'activitat d'una proteïna quimèrica que contenia el nucli catalític de CPT1C però els extrems de CPT1A. La quimera tampoc va mostrar ser activa, fet que suggereix que el nucli catalític de CPT1C té menor capacitat de catalitzar la reacció que el de CPT1A (Figura 35).

També es va assajar l'activitat en la fracció microsomal (en diferents condicions) sense obtenir tampoc valors apreciables d'activitat CPT1C (Figura 35).

Tots aquests resultats suggereixen que la proteïna CPT1C expressada en llevats no és activa o té molt baixa activitat. Això es pot atribuir a diferents hipòtesi:

1. Un incorrecte plegament de la proteïna en expressar-la en llevats. Aquesta causa no sembla molt probable ja que aquest sistema d'expressió s'ha utilitzat prèviament per caracteritzar els paràmetres cinètics de CPT1A (Zhu et al., 1997; de Vries et al., 1997; Prip-Buus et al., 1998).
2. Els valors d'activitat específica trobats estan per sota del límit de detecció del mètode radiomètric, suggerint que cal desenvolupar un mètode detecció més acurat per determinar les característiques funcionals de CPT1C. Per a testar aquesta hipòtesi, el nostre grup va desenvolupar un mètode cromatogràfic (HPLC-MS/SM) per determinar l'activitat de CPT1C (Jáuregui et al., 2007). Amb aquest nou mètode s'obtenen mesures de concentracions de palmitoilcarnitina amb un límit de sensibilitat de 0,48 ng/ml, que corresponen a una activitat específica de 0,0045 nmol·mg^{-1}·min^{-1} amb les nostres condicions d'assaig CPT1. En el mètode radiomètric el límit de sensibilitat es correspon a una activitat de 0,4 nmol·mg^{-1}·min^{-1} (es calcula mesurant la desviació estàndard de deu mesures de blancs de la reacció). Això indica, que el mètode cromatogràfic és 100 vegades més sensible que el radiomètric. Utilitzant aquest mètode no es va detectar activitat en llevats que expressaven CPT1C, descartant així la segona de les causes.
3. El substrat òptim per la reacció és diferent dels que ja s'han testat anteriorment.
4. Al sistema dels llevats mancaria alguna modificació de la proteïna que sí que es podria produir en un sistema d'expressió en cèl·lules de mamífer. Per verificar aquesta hipòtesi, el nostre grup va assajar fraccions subcel·lulars de cèl·lules de mamífer en cultiu (HEK293T i PC-12) que sobreexpressaven CPT1C. Dels resultats obtinguts es va concloure que: 1) CPT1C catalitzava la reacció de transesterificació entre el palmitoil-CoA i els èsters d'acilcarnitina i que 2) CPT1C és un enzim 100 vegades menys actiu que la isoforma de fetge (CPT1A) (Figura 48), confirmant aquesta quarta hipòtesi i descartant la tercera. En conclusió, l'enzim CPT1C necessita unes condicions especials o un ambient concret proveït per les cèl·lules de mamífer i absent en llevats. Aquestes condicions o ambient determinat podrien ser: a) presència de determinades proteïnes activadores o interaccionants, presents en cèl·lules de mamífer, o bé b) modificacions específiques que es podrien produir en cèl·lules de mamífer com poden ser canvis en el potencial de membrana. Per altra banda, la baixa activitat de CPT1C suggereix que aquest enzim estaria implicat més aviat en vies biosintètiques (més que en catabòliques) o en vies de transducció en les que podria actuar com a sensor metabòlic. Pel que es pot concloure de la

informació obtinguda del model 3-D, CPT1C hauria de poder catalitzar la reacció de manera equivalent a com ho fa CPT1A. Podria ser que en determinades condicions (encara desconegudes) CPT1C presentés valors més alts d'activitat.

LOCALITZACIÓ SUBCEL·LULAR

Tot i que CPT1A i CPT1B es sap que són enzims mitocondrials, resultats del nostre grup apuntaven una nova localització per CPT1C.

Per a determinar la localització subcel·lular de l'enzim es van dur a terme dues aproximacions:

- Es van transfectar transitòriament diferents tipus cel·lulars (SH-SY5Y, HEK293T, Fibroblastes, PC-12) amb una construcció que portava la proteïna CPT1C fusionada a EGFP per l'extrem C-terminal de CPT1C (pCPT1C-EGFP). Es va fer el mateix per CPT1A (pCPT1A-EGFP). Es va poder observar que les dues isoformes presentaven distribucions subcel·lulars ben diferenciades (Figura 38). Mentre que CPT1A mostrava un patró filamentós o granular, CPT1C presentava un patró més aviat reticular. Posteriorment es van realitzar experiments de co-localització amb diferents marcadors subcel·lulars (de mitocòndria, reticle endoplasmàtic i peroxisomes) sobre les cèl·lules transfectades (Figura 39). Es va concloure que CPT1C es localitzava a la membrana del reticle endoplasmàtic (RE). També es podia observar certa coincidència amb el marcador mitocondrial que es va atribuir a una possible localització de la proteïna en els punts de contacte entre la membrana del RE i la membrana mitocondrial externa (coneguts com membranes associades a mitocòndries, MAM).
- Es va determinar la localització de la proteïna endògena realitzant dobles immunocitoquímiques sobre cultius primaris de neurones amb anticossos contra la proteïna CPT1C i contra un marcador de reticle (calreticulina), mostrant una co-localització total d'ambdues senyals (Figura 40).

Els resultats obtinguts demostren clarament que CPT1C es localitza a la membrana del RE. Posteriorment al nostre grup es van realitzar fraccionaments subcel·lulars d'homogenats de cervell de ratolí i de rata que van mostrar la immunodetecció de CPT1C en la fracció microsomal (Sierra et al., 2008) confirmant els resultats d'aquest estudi (Figura 50).

Aquesta nova localització d'un enzim CPT1 suggereix la seva implicació en funcions relacionades amb el RE. De fet, resultats publicats pel nostre grup (Sierra et al., 2008) demostren que l'enzim CPT1C no estaria implicat en l'oxidació de palmitat, ja que la sobreexpressió de CPT1C en cèl·lules de mamífer en cultiu no incrementa la taxa

d'oxidació del palmitat, mentre que la transfecció de CPT1A sí que l'incrementa, descartant així la seva implicació en la beta-oxidació.

L'EXTREM N-TERMINAL DE CPT1C DIRIGEIX LA PROTEÏNA AL RE

S'han descrit els residus responsables de dirigir la proteïna CPT1A a la mitocòndria (Cohen et al., 1998; Cohen et al., 2001). Com que alguns d'aquests residus diferien en comparar-los amb els presents a la nova isoforma, vam voler aclarir si la mateixa regió de la proteïna era responsable del direccionament diferencial.

Per a fer-ho es van construir dos plasmidis quimèrics. Un que codificava la regió N-terminal amb els dos dominis transmembrana i la senyal d'import a la matriu mitocondrial (descrita a Cohen et al. 2001) de la isoforma CPT1A fusionat a la resta del gen de CPT1C i a EGFP, i a la inversa (a aquests plasmidis se'l va anomenar pCPT1·AC-EGFP i pCPT1·CA-EGFP).

Es van transfectar transitòriament cèl·lules SH-SY5Y amb els diferents plasmidis (pCPT1C-EGFP, pCPT1A-EGFP, pCPT1·AC-EGFP, i pCPT1·CA-EGFP) i es va observar un canvi de localització en intercanviar els extrems N-terminals d'ambdues proteïnes (Figura 41).

Aquest resultat suggereix que dins de la seqüència de l'extrem N-terminal de CPT1C hi ha algun tipus de senyal que dirigeix la proteïna al RE, o bé que la manca de senyals de direccionament a la mitocòndria fan que la proteïna es localitzi al RE per defecte.

PROCESSAMENT DE L'EXTREM N-TERMINAL

Moltes proteïnes de RE eliminen el pèptid senyal després de la seva inserció al RE. Com que el pes molecular observat per la proteïna en separar-la en gels de SDS-PAGE era inferior al predit segons la seva seqüència d'aminoàcids, vam voler confirmar si CPT1C patia un processament d'aquesta regió.

Vam utilitzar un anticòs contra l'extrem N-terminal de CPT1C (anticòs produït pel nostre grup i que s'havia mostrat efectiu en reconèixer per Western blot la proteïna CPT1C expressada en el sistema de llevats, veure l'apartat 6.2 dels Procediments experimentals) en extractes de cervell obtinguts de ratolins salvatges (WT) i KO per CPT1C (Figura 42).

Vam veure que l'anticòs no reconeixia la proteïna en aquests extractes, fet que suggeria que aquesta regió de la proteïna és processat.

TOPOLOGIA A LA MEMBRANA

Ja havíem demostrat que CPT1C es localitzava a la membrana del RE. Com que de l'anàlisi de la seqüència d'aminoàcids es prediuen dos dominis transmembrana, es

podrien considerar dos possibles topologies. El fet que el domini catalític s'orienti cap al citoplasma o cap a la llum del RE tindria diferents implicacions fisiològiques. Vam comprovar experimentalment la topologia ja que els programes bioinformàtics predeien una topologia incorrecta per CPT1A.

És ben conegut que les proteïnes de membrana durant la seva traducció al RE poden incorporar N-glicosilacions (Chang et al. 1994; Schinkel et al. 1993). Aquesta glicosilació en els polipèptids naixents es produeix a la llum del RE en residus d'asparragina dins de seqüències diana composades per Asn-X-Ser/Thr, on X és qualsevol aminoàcid excepte prolina (R. Kornfeld and S. Kornfeld, 1985). No totes les dianes són glicosilades. La detecció d'oligosacàrids en una proteïna es pot realitzar a través d'un assaig de desglicosilació que modificaria el pes molecular de la proteïna, i es podria observar per Western blot com la presència de bandes a dues alçades diferents en comparar la proteïna tractada o no tractada amb l'enzim desglicosilador (en aquest cas PNGasa F).

Per utilitzar aquest abordatge vam identificar la presència de dianes endògenes de glicosilació que es van trobar en la regió C-terminal (després dels dominis transmembrana). Llavors en la regió N-terminal (abans del primer transmembrana) i en la regió que anomenem del "loop" (regió entremig dels dos transmembrana) vam introduir dianes de glicosilació (Asn-Ile-Thr).

Totes les seqüències es van clonar en el vector pIRES i les construccions obtingudes es van anomenar: pIRES-Nterm, pIRES-Loop i pIRES-CPT1C. Aquestes construccions es van transfectar transitòriament en cèl·lules HEK293T, a les 48h es van lisar, es va obtenir la fracció microsomal, es van realitzar els assaigs de desglicosilació amb l'enzim PNGasa F) i es va analitzar el contingut de les fraccions per Western blot (Figura 44).

Només als microsomes transfectats amb la construcció de CPT1C que incorporava una diana de glicosilació a la regió del loop es va poder observar una caiguda de pes molecular de 2,5 kDa en tractar l'extracte amb l'enzim PNGasa F. Aquest resultat recolza el model en què CPT1C tindria la regió del loop orientada cap a la llum del RE i els dominis N- i C-terminals cap al citoplasma.

Aquesta topologia implica que el producte de la reacció catalitzada per CPT1C s'allibera a l'espai citoplasmàtic, des d'on es podria transportar a través de membranes d'altres orgànuls (inclosa la del RE). La reacció catalitzada per CPT1C podria modificar les concentracions del seus substrats i productes en microdominis propers a l'enzim. Les tres funcions en les que podria estar implicada CPT1C (per la seva baixa activitat, la localització a la membrana del reticle i l'orientació del domini catalític cap a la cara citosòlica del RE) serien:

1) CPT1C REDUEIX LA SÍNTESI DE FOSFOLÍPIDS

Una de les principals vies biosintètiques associades a la cara citosòlica del RE és la síntesi de fosfolípids (alguns d'ells contenen palmitat). S'ha descrit que les MAM estan enriquides en enzims de biosíntesi de fosfolípids (Rusiñol et al., 1994; Wang et al., 2000; Goetz and Nabi, 2006). La biosíntesi de fosfolípids comença amb l'esterificació de dos acils-CoA amb un esquelet de glicerolfosfat, i es forma àcid fosfatídic que quedaria ancorat a la membrana a través de les dues cadenes hidrocarbonades. Posteriors reaccions enzimàtiques donarien lloc a l'ampli ventall de fosfolípids que constitueixen les membranes. La composició en fosfolípids de les membranes determina la seva fluïdesa i forma, i és molt important en l'endocitosi de vesícules sinàptiques per al seu reciclatge (Marza and Lesa, 2006; Darios and Davletov, 2006; Ben Gedalya et al., 2009).

Proposem que l'activitat CPT1C a les neurones podria reduir la síntesi de fosfolípids (disminuint la quantitat d'un dels seus substrats, el palmitoil-CoA) (Figura 51). La menor quantitat de fosfolípids que contindrien palmitat alteraria la fluïdesa de la membrana i fins i tot el reclutament de proteïnes implicades en el tràfic de les vesícules sinàptiques, alterant així la transmissió sinàptica.

També s'ha vist que les vesícules sinàptiques són riques en fosfolípids que contenen àcids grassos poliinsaturats (PUFAs) i sembla que tenen un pare en la neurotransmissió i/o en la biogènesi de les vesícules sinàptiques a través d'un mecanisme que encara no està molt ben aclarit (Marza and Lesa, 2006). Així doncs, es podria especular que l'activitat de CPT1C estigués disminuint la incorporació de palmitat a fosfolípids en microdominis, afavorint la incorporació de PUFAs per a la correcta formació de les vesícules sinàptiques. Segons aquesta hipòtesi, l'activitat CPT1C en diferents regions del cervell tindria diferents conseqüències segons la importància d'aquest mecanisme a cada nucli o àrea.

2) CPT1C REDUEIX LA SÍNTESI DE NOVO DE CERAMIDES I ESFINGOLÍPIDS

La síntesi *de novo* de ceramides es realitza al RE i en membranes associades al RE, com la membrana perinuclear i MAMs. La ceramida es considera la molècula central en el metabolisme dels esfingolípids que té lloc en diferents compartiments subcel·lulars. La ceramida també es pot obtenir de la hidròlisi de l'esfingomielina, cerebròsids o a partir de l'esfingosina per l'acció de diferents enzims (Ogretmen i Hannun, 2004; Hannun i Obeid, 2008). A les neurones, la síntesi de novo de ceramides s'ha implicat en el desenvolupament axonal i dendrític de les neurones hipocampals i les cèl·lules de Purkinje (Buccoliero and Futerman, 2003). També s'ha descrit que increments en els nivells de ceramides sensibilitzen les neurones al dany excitotòxic i promouen l'apoptosi, que són dues característiques presents en moltes patologies neurodegeneratives (Haughey et al., 2004; Jana et al., 2009).

Els esfingolípids (com la ceramida, dihidroceramida, ceramida-1-fosfat, esfingosina, esfingosina-1-fosfat, glucosilceramida, liso-esfingomielina) són lípids bioactius que tenen un paper en la regulació del creixement cel·lular, mort cel·lular, senescència, adhesió, migració, inflamació, angiogènesi i tràfic intracel·lular. Recentment s'ha vist que l'esfingosina activa la sinaptobrevina a les vesícules sinàptiques per formar el complex SNARE implicat en la fusió de membranes (Darios et al., 2009), relacionant així els esfingolípids amb noves funcions en la neurotransmissió. A més els esfingolípids tenen un paper important en la regulació de la fluïdesa de les membranes i en l'estructuració de la bicapa lipídica en dominis, com ara els "lipid rafts" (són dominis de la membrana importants en senyalització intracel·lular i tràfic de vesícules (Ogretmen i Hannun, 2004; Lingwood i Simons, 2010). En els cons de creixement de les neurones s'ha relacionat els "lipid rafts" amb el creixement axonal i la direcció del creixement a través de la reorganització de components del citoesquelet (Kamiguchi, 2006).

La síntesi *de novo* de les ceramides comença amb la condensació del palmitat (a partir del palmitoil-CoA) i la serina per formar 3-ceto-dihidroesfingosina per l'acció de la serina palmitoiltransferasa (SPT) que es localitza a la membrana del RE. EN aquest context, l'activitat CPT1C podria estar disminuint la quantitat del substrat palmitoil-CoA disponible per a la síntesi de ceramides, reduint el flux a través d'aquesta via i reduint la producció *de novo* de ceramides (Figura 52). Aquesta hipòtesi ve recolzada per resultats del nostre grup (A. Sierra i N. Casals, resultats no publicats) que demostren que en sobreexpressar CPT1C en cèl·lules HEK293T i PC-12, es redueix la producció *de novo* de ceramides (que no els nivells totals de ceramida) aproximadament en un 20%. Aquests resultats suggereixen que la regulació de la síntesi *de novo* de ceramides es pot regular per la quantitat de palmitat incorporat en aquestes neurones, i aquest podria ser el paper de CPT1C, afectant processos com la neurotransmissió i el desenvolupament axonal o dendrític.

3) CPT1C REDUEIX LA PALMITOILACIÓ DE PROTEÏNES

Resultats del nostre grup obtinguts de l'estudi de ratolins KO per CPT1C suggereixen que aquest nou isoenzim podria tenir un paper en la formació de noves memòries, en l'aprenentatge i en la coordinació motora (P. Carrasco i N. Casals, resultats no publicats). Aquestes alteracions compartirien un mecanisme subjacent en relació amb la neurotransmissió. En aquest context, es podria pensar que una modificació postraduccional com la palmitoilació relacionés aquests esdeveniments. Aquesta modificació consisteix en l'addició d'un palmitat (a partir del palmitoil-CoA) a un residu de cisteïna present a la cèl·lula diana a través de la formació d'un enllaç tioèster. La incorporació de palmitat la realitzen una família d'enzims amb activitat palmitoil-acil transferasa i reben el nom de DHHC (per la presència d'un domini Asp-His-His-Cys en la regió catalítica). Es localitzen a la membrana del RE (entre d'altres

localitzacions com ara el Golgi, vesícules de secreció i la membrana plasmàtica) i molts d'ells s'expressen al sistema nerviós central. La incorporació de lípids a les proteïnes facilita el seu direccionament a les membranes i permet canvis de localització de les proteïnes diana o n'altera la funció. Moltes proteïnes neuronals incorporen aquesta modificació reversiblement (com la sinaptotagmina, sinaptobrevina, SNAP25, PSD95, GluR4 i 6) i s'ha vist que és imoprtant per la regulació de la transmissió sinàptica i el desenvolupament neuronal (El-Husseini and Bredt, 2002; Ohno et al., 2006; Linder and Deschenes, 2007; Fukata and Fukata, 2010).

Així doncs es podria proposar que l'activitat CPT1C regulés la quantitat de substrat (palmitoil-CoA) disponible per a la palmitoilació de proteïnes (Figura 54). A més activitat de CPT1C menor grau de palmitoilació de proteïnes. Això tindria sentit fisiològic sobretot en el cas que la reacció de CPT1C pogués funcionar a diferents velocitats de catàlisi, fet que encara es desconeix, i així es podria parlar d'un nou nivell de regulació en la reacció de palmitoilació. Així doncs, la funció de CPT1C podria afectar la transmissió sinàptica i repercutir en la formació de noves memòries, l'aprenentatge o la coordinació motora.

PROTEÏNES D'UNIÓ A CPT1C

En aquest punt del treball encara no s'havia pogut aclarir la funció fisiològica de CPT1C, i vam voler obtenir informació que ens permetés obrir noves línies de recerca que ens acabessin portant a esbrinar la funció de la proteïna. Una de les aproximacions que ens podia donar informació sobre les vies en les que participa CPT1C era conèixer possibles proteïnes interaccionants. Per fer-ho es va realitzar un assaig de dobles-híbrids en llevats (Y2H, de "yeast two-hybrid") (Fields and Song, 1989).

L'assaig es va realitzar utilitzant CPT1C com a esquer i una genoteca de cDNA de cervell fetal (HFB) com a preses potencials per unir-se a la proteïna esquer.

La regió de CPT1C que es va utilitzar en aquest sistema es correspon amb la regió del centre catalític que sabem que està orientat cap al citoplasma (on podrà interaccionar amb un ampli ventall de proteïnes) i que és el domini més gran de la proteïna. Vam excloure els dominis transmembrana per evitar que la proteïna quedés retinguda en membranes i no es dirigís al nucli on es realitza la interacció en aquest sistema. Tampoc es va incorporar la regió N-terminal ja que segons els nostres resultats aquesta regió patiria un processament. Es va realitzar l'assaig amb la regió descrita de la seqüència humana de CPT1C i la de ratolí, per posar en relleu les interaccions més conservades entre espècies.

Les proteïnes que van mostrar haver interaccionat amb CPT1C es van identificar realitzant PCRs de les colònies, seqüenciant aquests fragments i cercant homologia en les bases de dades de GeneBank (utilitzant BLAST). Així es van identificar les proteïnes

interaccionants de les que es va fer una cerca bibliogràfica per aclarir si la interacció es podria produir en un entorn fisiològic. En comparar els positius obtinguts en els dos assaigs (el que contenia com a esquer la seqüència humana de CPT1C i el que contenia les seqüència de ratolí), no es va trobar cap clon repetit.

- Es van identificar 13 proteïnes interaccionants en el cas de l'assaig de la genoteca humana (HFB) i la seqüència humana de CPT1C. Només una proteïna (DCTN3) es va identificar en dos clons independents, la resta són clons únics:

DCTN3	**TICAM1**	**NCAPH2**
DNAJB6	**CRYL1**	**CXXC1**
PKM2	**MSTO1**	**UBAP2L**
BTBD1	**NDUFB9**	
RNF40	**BCAS2**	

- Es van identificar 18 proteïnes interaccionants en el cas de l'assaig de la genoteca humana (HFB) i la seqüència de ratolí de CPT1C. Només una proteïna (PSMB4) es va identificar en dos clons independents, la resta són clons únics:

PSMB4	**BCAN**	**hnRNP M**
FANCL	**GCA**	**TPP1**
PELI1	**WDR6**	**CTSB**
NPLOC4/NPL4	**BAT2**	**ARID1A**
SNX9	**ZMYM3**	**ANKS3**
DLL3	**hnRNP H3**	**WDR 73**

Tenint en compte que hem utilitzat com a esquer el domini citosòlic de la proteïna, hem descartat les proteïnes interaccionants que es localitzen a la llum d'altres orgànuls (lisosomes, nucli o membrana mitocondrial interna). És per això que les proteïnes NDUFB9, BCAS2, NCAPH2, CXXC1, hnRNP H3, hnRNP M, ARID1A, TPP1, CTSB i BCAN s'han considerat falsos positius.

Les proteïnes que no s'expressen al cervell també s'han descartat (com la GCA).

El laboratori d'Erica Golemis proveeix d'una llista dels falsos positius més habituals en un Y2H (http://www.fccc.edu/research/labs/golemis/InteractionTrapInWork.html). entre els que podem trobar subunitats del proteasoma, proteïnes de xoc tèrmic i proteïnes que contenen dominis de dits de Zinc. Així doncs, també es van descartar PSMB4 i DNAJB6.

De la interacció de CPT1C amb diferents E3 ubiqüitina lligases (FANCL, PELI1, RNF40 i indirectament BTBD1) podríem pensar que CPT1C fos ella mateixa ubiqüitinada. Per testar aquesta hipòtesi s'han realitzat algunes proves que descarten aquesta hipòtesi (Dades suplementàries, Figura S5) ja que no s'ha observat ubiqüitinització de CPT1C. Així doncs, aquestes proteïnes també s'han descartat.

Altres clons positius es corresponen amb proteïnes de funció encara desconeguda i que no aporten informació de les vies en les que pot participar CPT1C, i que no es comenten en aquest escrit.

La resta de clons positius es poden agrupar en quatre grups que presentarien característiques funcionals similars:

1) Degradació de proteïnes

Una de les proteïnes amb les que ha interaccionat CPT1C s'anomena **Npl4**. Aquesta proteïna forma part d'un complex encarregat de treure proteïnes mal plegades del RE cap al citoplasma (retrotranslocació) per a què posteriorment, al citoplasma, siguin ubiqüitinades i degradades pel sistema del proteasoma. Aquest procés es coneix amb el nom de degradació associada al RE (ERAD). S'ha vist que aquest mecanisme no funciona correctament en algunes malalties neurodegeneratives com la malaltia de Huntington (Paschen, 2003; Duennwald i Lindquist, 2008).

Utilitzant la tecnologia del RNA d'interferència, es va interferir el RNA corresponent a Npl4 i es va observar que disminuïa la quantitat Ufd1 (un altre component del complex que es forma junt amb Npl4), també disminuïen algun dels substrats de la resposta davant de proteïnes mal plegades (UPR) i s'induïa un increment del doble de proteïnes ubiqüitinades (Nowis et al., 2006). Resultats preliminars del nostre grup en què es comparaven els nivells de proteïnes ubiqüitinades en ratolins salvatges i en KO per CPT1C (Dades suplementàries, Figura S5), no es va observar cap diferència en els nivells generals d'ubiqüitinització. Caldria confirmar els nivells de Ufd1 i de substrats de UPR en els ratolins salvatges i KO per veure si aquesta via es veu afectada, i per esbrinar si realment Npl4 i CPT1C interaccionen en condicions fisiològiques.

2) Tràfic de membranes i estructura cel·lular

La **Dinactina 3** (DCTN3) és la subunitat més petita de la dinactina (composada per 10 subunitats). La dinactina s'uneix als microtúbuls i a la dineïna citoplasmàtica que es relaciona amb múltiples funcions cel·lulars com són: transport del RE a l'Aparell de Golgi, moviment centrípet de lisosomes i endosomes, formació del fus mitòtic, citocinesi, moviment dels cromosomes, posicionament del nucli i axonogènesi (Grabham et al., 2007). Una mutació concreta en aquesta proteïna s'ha associat a una malaltia de motoneurones que s'hereda de forma autosòmica dominant (Lin et al., 2007). Tot i que semblaria una bona candidata per a una interacció amb CPT1C en un entorn fisiològic (s'han obtingut 2 clons independents en l'assaig Y2H), el fet que la

dinactina 3 representi una subunitat molt petita i inaccessible de tot el complex proteic de la dinactina ens suggereix que aquesta interacció seria més aviat improbable.

La proteïna **sorting nexin 9** (SNX9) s'expressa en terminals presinàptics i coordina l'endocitosi de vesícules sinàptiques (Shin et al., 2007). Disminuint la quantitat de SNX9 endògena amb siRNA en neurones hipocampals en cultiu es va observar un enlentiment en l'endocitosi de vesícules sinàptiques (Shin et al., 2007). Per avaluar la validesa d'aquesta interacció primer caldria verificar si CPT1C s'expressa en els terminals presinàptics i avaluar si en el ratolí KO per CPT1C s'observen alteracions en l'endocitosi de les vesícules sinàptiques.

També s'ha vist interacció de CPT1C amb una proteïna implicada en la morfologia i distribució de les mitocòndries, **Misato** (MSTO1). Com que CPT1C sembla que s'expressi en MAM, no sembla del tot incoherent pensar que es pogués relacionar amb aquestes funcions. El silenciament de Mistao en cèl·lules HeLa s'ha observat que resulta en una fragmentació i desaparició de la xarxa de mitocòndries (Kimura i Okano, 2007). Per tant es podria començar avaluant la morfologia de les mitocòndries en neurones dels ratolins KO per CPT1C.

3) Metabolisme

L'enzim **piruvat quinasa** (PKM2) genera piruvat i ATP a partir del fosfoenolpiruvat. S'ha vist que l'activitat d'aquest enzim estava augmentada en mostres de cervell humà de persones amb alteracions cognitives lleus (Poon et al., 2006; Butterfield and Sultana, 2007; Reed et al., 2008). S'ha suggerit que l'oxidació d'enzims implicats en el metabolisme de la glucosa podrien portar a alteracions en la formació i recuperació de memòries (Butterfield i Sultana, 2007). Els resultats preliminars del nostre grup obtinguts de l'estudi del fenotip dels ratolins KO per CPT1C mostren que aquests ratolins presenten alteracions en la memòria i en la capacitat per aprendre, i per tant suggereixen que caldria aprofundir en la veracitat d'aquesta interacció de CPT1C amb PKM2.

4) Transducció de la senyal

La proteïna **WDR6** pertany a la família de proteïnes que contenen repeticions WD (faciliten la formació de complexes multiproteïcs). WDR6 interacciona amb la serina/treonina quinasa LKB1, que entre d'altres funcions s'ha vist que pot fosforilar la quinasa depenent d'AMP o AMPK (revisat a Jansen et al., 2009). Canvis en l'activitat d'AMPK s'han associat a canvis en l'expressió de neuropèptids orexigènics i anorexigènics que modifiquen el comportament alimenari (Kim et al., 2004).

L'AMPK alhora, pot fosforilar l'enzim acetil-CoA carboxilasa, ACC en les seves dues isoformes (ambdues expessades en neurones hipotalàmiques) inactivant l'enzim. D'aquesta manera es disminuiria el fluxe de substractes cap a la biosíntesi d'àcids grassos i es reduirien els nivells de malonil-CoA que comportarien un increment en la

beta-oxidació (per augment de l'activitat CPT1 a l'hipotàlem, deguda a la baixa concentració del seu inhibidor fisiològic, el malonil-CoA) i en darrer terme a un increment en la ingesta i disminució de la despesa energètica als teixits perifèrics (Hardie, 2007; López et al., 2007).

Així doncs, la interacció de CPT1C amb WDR6 podria mediar el reclutament del complexe multiproteïc CPT1C-WDR6-LKB1-AMPK-ACC en regions properes a les mitocòndries (MAM) permetent la regulació de l'activitat CPT1 mitocondrial segons els nivells de malonil-CoA produïts per ACC. Aquesta hipòtesi situaria CPT1C per sobre del malonil-CoA en la regulació de la ingesta (Figura 56).

FUNCIÓ FISIOLÒGICA DE CPT1C

El fet que aquest nou enzim tingui tant poca activitat CPT1, com ja hem dit, podria suggerir que aquest enzim funcionés com a sensor molecular d'algun metabolit. De fet els darrers resultats sobre els ratolins KO recolzen un model en el què CPT1C tindria un paper com a diana sensora de l'estat energètic de les cèl·lules a l'hipotàlem (Wolfgang et al., 2006; Gao et al., 2009). A

a) Una possibilitat és que CPT1C actuï per sota del malonil-CoA, i per tant els nivells de malonil-CoA (intermediari de la síntesi d'àcids grassos i inhibidor fisiològic de l'activitat CPT1) estarien indicant l'estat energètic de les neurones hipotalàmiques. De fet, els nivells de malonil-CoA fluctuen entre l'estat alimentat (≈0,1 μM) i dejunat (≈1,4 μM), i modulen l'expressió de pèptids orexi/anorexi-gènics (revisat a Wolfagang i Lane, 2006; Lane et al., 2008). Com que s'ha vist que CPT1C uneix el malonil-CoA amb una K_D≈0,3 μM que es troba en el rang de concentracions entre els que fluctua el malonil-CoA fisiològicament, podria ser que el malonil-CoA inhibís l'activitat CPT1C (per sota de la seva ja baixa activitat catalítica) afectant a altres dianes per sota de CPT1C (encara desconegudes) que modularien la ingesta i la despesa energètica (Figura 55). Es podria especular que en funció de l'estat energètic, CPT1C regulés la palmitoilació de proteïnes o la síntesi de ceramides i/o esfingolípids afectant per exemple, la formació de "lipid rafts", que és important per a la neurotransmissió.

b) Una altra possibilitat és que CPT1C actuï per sobre del malonil-CoA. S'ha vist que el tractament de cèl·lules endotelials amb palmitat provoca increments en la síntesi *de novo* de ceramides i resulta en l'activació de la proteïna fosfatasa PP2A. Aquesta fosfatasa pot desfosforilar l'AMPK, que s'inactivaria, i això portaria a una activació d'ACC que augmentaria la concentració de malonil-CoA (Wu et al., 2007).

   Com que observant el model 3-D sembla que CPT1C tindria, potencialment, la capacitat de catalitzar la reacció amb una major activitat específica, proposem un

model en què en situacions de baixa activitat CPT1C a l'hipotàlem es provocaria un augment en la síntesi *de novo* de ceramides (per augment de disponibilitat de palmitoil-CoA, un dels substrats per la síntesi de ceramides). Aquetes ceramides portarien a l'activació de PP2A, s'inactivaria AMPK i s'activaria ACC produint increments en la concentració de malonil-CoA i a una inhibició de l'activitat CPT1 mitocondrial, reduint la taxa de beta-oxidació d'àcids grassos, i finalment portaria a modificar l'expressió dels pèptids hipotalàmics i a disminuir la ingesta (Figura 57). Contràriament, en situacions en les quals s'incrementés l'activitat CPT1C (encara desconegudes, potser per la presència de proteïnes interaccionants) es produiria un increment en la ingesta.

Amb aquest model CPT1C actuaria en un cercle de retroalimentació positiva.

Resumint, en aquest treball es proposa que l'activitat CPT1C seria modulable per proteïnes interactuants o en contexts metabòlics específics.

També proposem que CPT1C afectaria principalment els nivells de palmitoil-CoA en microdominis per regular posteriorment: 1) la síntesi de novo de ceramides, 2) la síntesi de fosfolípids (sobretot afavorint la formació de fosfolípids que continguin PUFA, enfront els que continguin àcids grassos saturats) o bé, 3) la palmitoilació de proteïnes.

Aquests efectes en neurones hipotalàmiques implicarien a CPT1C en la regulació de la ingesta, però en altres àrees del cervell podrien estar afectant la capacitat d'aprenentatge o les habilitats motores.

CONCLUSIONS

1. Les dades aportades pel model 3-D de CPT1C suggereixen que aquest isoenzim és capaç de catalitzar la conversió de palmitoil-CoA en palmitoilcarnitina. Els residus catalítics estan ben conservats i els residus en contacte amb els substractes (palmitoil-CoA i carnitina), són tots equivalents als trobats a CPT1A.

2. L'expressió de la seqüència de CPT1C de rata en *Saccharomyces cerevisiae* no és activa ni quan s'assaja en diferents condicions (períodes de temps més curts, augments de temperatura, augment de la concetració de substractes, assaig de fraccions microsomals i de proteïnes quimèriques com ara CPT1·ACA). Per tant, el sistema d'expressió en llevats no és apropiat per estudiar les propietats cinètiques de l'enzim CPT1C ja que segurament al sistema de llevats li manqui alguna modificació que es podria realitzar en cèl·lules de mamífer.

3. Tant la proteïna CPT1C endògena com la sobreexpressada es localitzen a la membrana del reticle endoplasmàtic de cèl·lules de mamífer (HEK293T, PC12, SH-SY5Y, cultius primaris de fibroblastes i de neurones). També s'han trobat evidències que indiquen que CPT1C també es podria trobar, en menor quantitat, a les membranes associades a les mitocòndries (MAM).

4. La seqüència concreta que composa el domini N-terminal de CPT1C (els primers 150 aminoàcids) fa que la proteïna es dirigeixi al reticle endoplasmàtic.

5. El domini N-terminal de la CPT1C endògena en cervells de ratolins salvatges és processat (almenys fins a la Val^{27}) i no es detecta en lisats de còrtex de cervell de ratolí.

6. Els dominis N- i C-terminals de CPT1C es troben orientats cap a la cara citosòlica de la membrana del reticle endoplasmàtic, mentre que la regió del "loop" estaria orientada cap a la llum del reticle endoplamsàtic.

7. Les dades obtingudes de l'assaig de dobles-híbrids no apunta a una única proteïna interaccionant amb CPT1C. Enlloc d'això s'han obtingut proteïnes molt diverses i implicades en diferents functions: degradació de proteïnes, tràfic de membranes, estrucutra cel·lular, transducció de la senyal i metabolisme.

REFERENCES

REFERENCES

Ainscow, E. K., & Rutter, G. A. (2002). Glucose-stimulated oscillations in free cytosolic ATP concentration imaged in single islet beta-cells: Evidence for a Ca2+-dependent mechanism. *Diabetes, 51 Suppl 1*, S162-70.

Aja, S., Bi, S., Knipp, S. B., McFadden, J. M., Ronnett, G. V., Kuhajda, F. P., et al. (2006). Intracerebroventricular C75 decreases meal frequency and reduces AgRP gene expression in rats. *American Journal of Physiology.Regulatory, Integrative and Comparative Physiology, 291*(1), R148-54. doi:10.1152/ajpregu.00041.2006

Andersson, U., Filipsson, K., Abbott, C. R., Woods, A., Smith, K., Bloom, S. R., et al. (2004). AMP-activated protein kinase plays a role in the control of food intake. *The Journal of Biological Chemistry, 279*(13), 12005-12008. doi:10.1074/jbc.C300557200

Arnold, K., Bordoli, L., Kopp, J., & Schwede, T. (2006). The SWISS-MODEL workspace: A web-based environment for protein structure homology modelling. *Bioinformatics (Oxford, England), 22*(2), 195-201. doi:10.1093/bioinformatics/bti770

Bartel, P., Chien, C. T., Sternglanz, R., & Fields, S. (1993). Elimination of false positives that arise in using the two-hybrid system. *BioTechniques, 14*(6), 920-924.

Bekku, Y., Rauch, U., Ninomiya, Y., & Oohashi, T. (2009). Brevican distinctively assembles extracellular components at the large diameter nodes of ranvier in the CNS. *Journal of Neurochemistry, 108*(5), 1266-1276. doi:10.1111/j.1471-4159.2009.05873.x

Ben Gedalya, T., Loeb, V., Israeli, E., Altschuler, Y., Selkoe, D. J., & Sharon, R. (2009). Alpha-synuclein and polyunsaturated fatty acids promote clathrin-mediated endocytosis and synaptic vesicle recycling. *Traffic (Copenhagen, Denmark), 10*(2), 218-234. doi:10.1111/j.1600-0854.2008.00853.x

Bieber, L. L. (1988). Carnitine. *Annual Review of Biochemistry, 57*, 261-283. doi:10.1146/annurev.bi.57.070188.001401

Bieber, L. L., & Wagner, M. (1996). Effect of pH and acyl-CoA chain length on the conversion of heart mitochondrial CPT-I/CPTo to a high affinity, malonyl-CoA-inhibited state. *Biochimica Et Biophysica Acta, 1290*(3), 261-266.

Bionda, C., Portoukalian, J., Schmitt, D., Rodriguez-Lafrasse, C., & Ardail, D. (2004). Subcellular compartmentalization of ceramide metabolism: MAM (mitochondria-associated membrane) and/or mitochondria? *The Biochemical Journal, 382*(Pt 2), 527-533. doi:10.1042/BJ20031819

Bradford, M. M. (1976). A rapid and sensitive method for the quantitation of microgram quantities of protein utilizing the principle of protein-dye binding. *Analytical Biochemistry, 72*, 248-254.

Britton, C. H., Schultz, R. A., Zhang, B., Esser, V., Foster, D. W., & McGarry, J. D. (1995). Human liver mitochondrial carnitine palmitoyltransferase I: Characterization of its cDNA and chromosomal localization and partial analysis of the gene. *Proceedings of the National Academy of Sciences of the United States of America, 92*(6), 1984-1988.

Broadway, N. M., Pease, R. J., Birdsey, G., Shayeghi, M., Turner, N. A., & David Saggerson, E. (2003). The liver isoform of carnitine palmitoyltransferase 1 is not targeted to the endoplasmic reticulum. *The Biochemical Journal, 370*(Pt 1), 223-231. doi:10.1042/BJ20021269

Broadway, N. M., Pease, R. J., Birdsey, G., Shayeghi, M., Turner, N. A., & David Saggerson, E. (2003). The liver isoform of carnitine palmitoyltransferase 1 is not targeted to the endoplasmic reticulum. *The Biochemical Journal, 370*(Pt 1), 223-231. doi:10.1042/BJ20021269

Buccoliero, R., & Futerman, A. H. (2003). The roles of ceramide and complex sphingolipids in neuronal cell function. *Pharmacological Research : The Official Journal of the Italian Pharmacological Society, 47*(5), 409-419.

Butler, M. P., Hanly, J. A., & Moynagh, P. N. (2007). Kinase-active interleukin-1 receptor-associated kinases promote polyubiquitination and degradation of the pellino family: Direct evidence for PELLINO proteins being ubiquitin-protein isopeptide ligases. *The Journal of Biological Chemistry, 282*(41), 29729-29737. doi:10.1074/jbc.M704558200

Butterfield, D. A., & Sultana, R. (2007). Redox proteomics identification of oxidatively modified brain proteins in alzheimer's disease and mild cognitive impairment: Insights into the progression of this dementing disorder. *Journal of Alzheimer's Disease : JAD, 12*(1), 61-72.

Carling, D. (2004). The AMP-activated protein kinase cascade--a unifying system for energy control. *Trends in Biochemical Sciences, 29*(1), 18-24.

Carlone, D. L., & Skalnik, D. G. (2001). CpG binding protein is crucial for early embryonic development. *Molecular and Cellular Biology, 21*(22), 7601-7606. doi:10.1128/MCB.21.22.7601-7606.2001

Chang, X. B., Hou, Y. X., Jensen, T. J., & Riordan, J. R. (1994). Mapping of cystic fibrosis transmembrane conductance regulator membrane topology by glycosylation site insertion. *The Journal of Biological Chemistry, 269*(28), 18572-18575.

Chien, C. T., Bartel, P. L., Sternglanz, R., & Fields, S. (1991). The two-hybrid system: A method to identify and clone genes for proteins that interact with a protein of interest. *Proceedings of the National Academy of Sciences of the United States of America, 88*(21), 9578-9582.

Chin, L. S., Vavalle, J. P., & Li, L. (2002). Staring, a novel E3 ubiquitin-protein ligase that targets syntaxin 1 for degradation. *The Journal of Biological Chemistry, 277*(38), 35071-35079. doi:10.1074/jbc.M203300200

Choi, K. C., Lee, Y. S., Lim, S., Choi, H. K., Lee, C. H., Lee, E. K., et al. (2006). Smad6 negatively regulates interleukin 1-receptor-toll-like receptor signaling through direct interaction with the adaptor pellino-1. *Nature Immunology, 7*(10), 1057-1065. doi:10.1038/ni1383

Chuang, J. Z., Zhou, H., Zhu, M., Li, S. H., Li, X. J., & Sung, C. H. (2002). Characterization of a brain-enriched chaperone, MRJ, that inhibits huntingtin aggregation and toxicity independently. *The Journal of Biological Chemistry, 277*(22), 19831-19838. doi:10.1074/jbc.M109613200

Cohen, I., Guillerault, F., Girard, J., & Prip-Buus, C. (2001). The N-terminal domain of rat liver carnitine palmitoyltransferase 1 contains an internal mitochondrial import signal and residues essential for folding of its C-terminal catalytic domain. *The Journal of Biological Chemistry, 276*(7), 5403-5411. doi:10.1074/jbc.M009555200

Cohen, I., Kohl, C., McGarry, J. D., Girard, J., & Prip-Buus, C. (1998). The N-terminal domain of rat liver carnitine palmitoyltransferase 1 mediates import into the outer mitochondrial membrane and is essential for activity and malonyl-CoA sensitivity. *The Journal of Biological Chemistry, 273*(45), 29896-29904.

Cota, D., Proulx, K., Smith, K. A., Kozma, S. C., Thomas, G., Woods, S. C., et al. (2006). Hypothalamic mTOR signaling regulates food intake. *Science (New York, N.Y.), 312*(5775), 927-930. doi:10.1126/science.1124147

Dai, Y., Wolfgang, M. J., Cha, S. H., & Lane, M. D. (2007). Localization and effect of ectopic expression of CPT1c in CNS feeding centers. *Biochemical and Biophysical Research Communications, 359*(3), 469-474. doi:10.1016/j.bbrc.2007.05.161

Darios, F., & Davletov, B. (2006). Omega-3 and omega-6 fatty acids stimulate cell membrane expansion by acting on syntaxin 3. *Nature, 440*(7085), 813-817. doi:10.1038/nature04598

Darios, F., Wasser, C., Shakirzyanova, A., Giniatullin, A., Goodman, K., Munoz-Bravo, J. L., et al. (2009). Sphingosine facilitates SNARE complex assembly and activates synaptic vesicle exocytosis. *Neuron, 62*(5), 683-694. doi:10.1016/j.neuron.2009.04.024

de Vries, Y., Arvidson, D. N., Waterham, H. R., Cregg, J. M., & Woldegiorgis, G. (1997). Functional characterization of mitochondrial carnitine palmitoyltransferases I and II expressed in the yeast pichia pastoris. *Biochemistry, 36*(17), 5285-5292. doi:10.1021/bi962875p

Duennwald, M. L., & Lindquist, S. (2008). Impaired ERAD and ER stress are early and specific events in polyglutamine toxicity. *Genes & Development, 22*(23), 3308-3319. doi:10.1101/gad.1673408

Dunn-Meynell, A. A., Routh, V. H., Kang, L., Gaspers, L., & Levin, B. E. (2002). Glucokinase is the likely mediator of glucosensing in both glucose-excited and glucose-inhibited central neurons. *Diabetes, 51*(7), 2056-2065.

el-Husseini, A., & Bredt, D. S. (2002). Protein palmitoylation: A regulator of neuronal development and function. *Nature Reviews.Neuroscience, 3*(10), 791-802. doi:10.1038/nrn940

Esser, V., Britton, C. H., Weis, B. C., Foster, D. W., & McGarry, J. D. (1993). Cloning, sequencing, and expression of a cDNA encoding rat liver carnitine palmitoyltransferase I. direct evidence that a single polypeptide is involved in inhibitor interaction and catalytic function. *The Journal of Biological Chemistry, 268*(8), 5817-5822.

Esser, V., Brown, N. F., Cowan, A. T., Foster, D. W., & McGarry, J. D. (1996). Expression of a cDNA isolated from rat brown adipose tissue and heart identifies the product as the muscle isoform of carnitine palmitoyltransferase I (M-CPT I). M-CPT I is the predominant CPT I isoform expressed in both white (epididymal) and brown adipocytes. *The Journal of Biological Chemistry, 271*(12), 6972-6977.

Ferdinandusse, S., Mulders, J., IJlst, L., Denis, S., Dacremont, G., Waterham, H. R., et al. (1999). Molecular cloning and expression of human carnitine octanoyltransferase: Evidence for its role in the peroxisomal beta-oxidation of branched-chain fatty acids. *Biochemical and Biophysical Research Communications, 263*(1), 213-218. doi:10.1006/bbrc.1999.1340

Fields, S., & Song, O. (1989). A novel genetic system to detect protein-protein interactions. *Nature, 340*(6230), 245-246. doi:10.1038/340245a0

Fraser, F., Corstorphine, C. G., & Zammit, V. A. (1997). Topology of carnitine palmitoyltransferase I in the mitochondrial outer membrane. *The Biochemical Journal, 323 (Pt 3)*(Pt 3), 711-718.

Fukata, Y., & Fukata, M. (2010). Protein palmitoylation in neuronal development and synaptic plasticity. *Nature Reviews.Neuroscience, 11*(3), 161-175. doi:10.1038/nrn2788

Gao, S., Kinzig, K. P., Aja, S., Scott, K. A., Keung, W., Kelly, S., et al. (2007). Leptin activates hypothalamic acetyl-CoA carboxylase to inhibit food intake. *Proceedings of the National Academy of Sciences of the United States of America, 104*(44), 17358-17363. doi:10.1073/pnas.0708385104

Gao, S., & Lane, M. D. (2003). Effect of the anorectic fatty acid synthase inhibitor C75 on neuronal activity in the hypothalamus and brainstem. *Proceedings of the National Academy of Sciences of the United States of America, 100*(10), 5628-5633. doi:10.1073/pnas.1031698100

Gao, X. F., Chen, W., Kong, X. P., Xu, A. M., Wang, Z. G., Sweeney, G., et al. (2009). Enhanced susceptibility of Cpt1c knockout mice to glucose intolerance induced by a high-fat diet involves elevated hepatic gluconeogenesis and decreased skeletal muscle glucose uptake. *Diabetologia, 52*(5), 912-920. doi:10.1007/s00125-009-1284-0

Geffers, I., Serth, K., Chapman, G., Jaekel, R., Schuster-Gossler, K., Cordes, R., et al. (2007). Divergent functions and distinct localization of the notch ligands DLL1 and DLL3 in vivo. *The Journal of Cell Biology, 178*(3), 465-476. doi:10.1083/jcb.200702009

Goetz, J. G., & Nabi, I. R. (2006). Interaction of the smooth endoplasmic reticulum and mitochondria. *Biochemical Society Transactions, 34*(Pt 3), 370-373. doi:10.1042/BST0340370

Guex, N., & Peitsch, M. C. (1997). SWISS-MODEL and the swiss-PdbViewer: An environment for comparative protein modeling. *Electrophoresis, 18*(15), 2714-2723. doi:10.1002/elps.1150181505

Gurtan, A. M., Stuckert, P., & D'Andrea, A. D. (2006). The WD40 repeats of FANCL are required for fanconi anemia core complex assembly. *The Journal of Biological Chemistry, 281*(16), 10896-10905. doi:10.1074/jbc.M511411200

Hannun, Y. A., & Obeid, L. M. (2008). Principles of bioactive lipid signalling: Lessons from sphingolipids. *Nature Reviews.Molecular Cell Biology, 9*(2), 139-150. doi:10.1038/nrm2329

Haughey, N. J., Cutler, R. G., Tamara, A., McArthur, J. C., Vargas, D. L., Pardo, C. A., et al. (2004). Perturbation of sphingolipid metabolism and ceramide production in HIV-dementia. *Annals of Neurology, 55*(2), 257-267. doi:10.1002/ana.10828

He, W., Lam, T. K., Obici, S., & Rossetti, L. (2006). Molecular disruption of hypothalamic nutrient sensing induces obesity. *Nature Neuroscience, 9*(2), 227-233. doi:10.1038/nn1626

Hipfner, D. R., Almquist, K. C., Leslie, E. M., Gerlach, J. H., Grant, C. E., Deeley, R. G., et al. (1997). Membrane topology of the multidrug resistance protein (MRP). A study of glycosylation-site mutants reveals an extracytosolic NH2 terminus. *The Journal of Biological Chemistry, 272*(38), 23623-23630.

Hitchcock, A. L., Auld, K., Gygi, S. P., & Silver, P. A. (2003). A subset of membrane-associated proteins is ubiquitinated in response to mutations in the endoplasmic reticulum degradation machinery. *Proceedings of the National Academy of Sciences of the United States of America, 100*(22), 12735-12740. doi:10.1073/pnas.2135500100

Horvath, T. L., Andrews, Z. B., & Diano, S. (2009). Fuel utilization by hypothalamic neurons: Roles for ROS. *Trends in Endocrinology and Metabolism: TEM, 20*(2), 78-87. doi:10.1016/j.tem.2008.10.003

Horvath, T. L., Andrews, Z. B., & Diano, S. (2009). Fuel utilization by hypothalamic neurons: Roles for ROS. *Trends in Endocrinology and Metabolism: TEM, 20*(2), 78-87. doi:10.1016/j.tem.2008.10.003

Hsiao, Y. S., Jogl, G., Esser, V., & Tong, L. (2006). Crystal structure of rat carnitine palmitoyltransferase II (CPT-II). *Biochemical and Biophysical Research Communications, 346*(3), 974-980. doi:10.1016/j.bbrc.2006.06.006

Hu, Z., Cha, S. H., Chohnan, S., & Lane, M. D. (2003). Hypothalamic malonyl-CoA as a mediator of feeding behaviour. *Proceedings of the National Academy of Sciences of the United States of America, 100*(22), 12624-12629. doi:10.1073/pnas.1834402100

Hu, Z., Dai, Y., Prentki, M., Chohnan, S., & Lane, M. D. (2005). A role for hypothalamic malonyl-CoA in the control of food intake. *The Journal of Biological Chemistry, 280*(48), 39681-39683. doi:10.1074/jbc.C500398200

Ishikura, S., Usami, N., Araki, M., & Hara, A. (2005). Structural and functional characterization of rabbit and human L-gulonate 3-dehydrogenase. *Journal of Biochemistry, 137*(3), 303-314. doi:10.1093/jb/mvi033

Iwabuchi, K., Li, B., Bartel, P., & Fields, S. (1993). Use of the two-hybrid system to identify the domain of p53 involved in oligomerization. *Oncogene, 8*(6), 1693-1696.

James, P., Halladay, J., & Craig, E. A. (1996). Genomic libraries and a host strain designed for highly efficient two-hybrid selection in yeast. *Genetics, 144*(4), 1425-1436.

Jana, A., Hogan, E. L., & Pahan, K. (2009). Ceramide and neurodegeneration: Susceptibility of neurons and oligodendrocytes to cell damage and death. *Journal of the Neurological Sciences, 278*(1-2), 5-15. doi:10.1016/j.jns.2008.12.010

Jansen, M., Ten Klooster, J. P., Offerhaus, G. J., & Clevers, H. (2009). LKB1 and AMPK family signaling: The intimate link between cell polarity and energy metabolism. *Physiological Reviews, 89*(3), 777-798. doi:10.1152/physrev.00026.2008

Jauregui, O., Sierra, A. Y., Carrasco, P., Gratacos, E., Hegardt, F. G., & Casals, N. (2007). A new LC-ESI-MS/MS method to measure long-chain acylcarnitine levels in cultured cells. *Analytica Chimica Acta, 599*(1), 1-6. doi:10.1016/j.aca.2007.07.066

Jogl, G., Hsiao, Y. S., & Tong, L. (2005). Crystal structure of mouse carnitine octanoyltransferase and molecular determinants of substrate selectivity. *The Journal of Biological Chemistry, 280*(1), 738-744. doi:10.1074/jbc.M409894200

Jogl, G., & Tong, L. (2003). Crystal structure of carnitine acetyltransferase and implications for the catalytic mechanism and fatty acid transport. *Cell, 112*(1), 113-122.

Kahn, B. B., Alquier, T., Carling, D., & Hardie, D. G. (2005). AMP-activated protein kinase: Ancient energy gauge provides clues to modern understanding of metabolism. *Cell Metabolism, 1*(1), 15-25. doi:10.1016/j.cmet.2004.12.003

Kamiguchi, H. (2006). The region-specific activities of lipid rafts during axon growth and guidance. *Journal of Neurochemistry, 98*(2), 330-335. doi:10.1111/j.1471-4159.2006.03888.x

Kashfi, K., & Cook, G. A. (1995). Temperature effects on malonyl-CoA inhibition of carnitine palmitoyltransferase I. *Biochimica Et Biophysica Acta, 1257*(2), 133-139.

Kerner, J., & Hoppel, C. (2000). Fatty acid import into mitochondria. *Biochimica Et Biophysica Acta, 1486*(1), 1-17.

Kiefer, F., Arnold, K., Kunzli, M., Bordoli, L., & Schwede, T. (2009). The SWISS-MODEL repository and associated resources. *Nucleic Acids Research, 37*(Database issue), D387-92. doi:10.1093/nar/gkn750

Kim, E. K., Miller, I., Aja, S., Landree, L. E., Pinn, M., McFadden, J., et al. (2004). C75, a fatty acid synthase inhibitor, reduces food intake via hypothalamic AMP-activated protein kinase. *The Journal of Biological Chemistry, 279*(19), 19970-19976. doi:10.1074/jbc.M402165200

Kim, E. K., Miller, I., Landree, L. E., Borisy-Rudin, F. F., Brown, P., Tihan, T., et al. (2002). Expression of FAS within hypothalamic neurons: A model for decreased food intake after C75 treatment. *American Journal of Physiology.Endocrinology and Metabolism, 283*(5), E867-79. doi:10.1152/ajpendo.00178.2002

Kimura, M., & Okano, Y. (2007). Human misato regulates mitochondrial distribution and morphology. *Experimental Cell Research, 313*(7), 1393-1404. doi:10.1016/j.yexcr.2007.02.004

Kimura, M., & Okano, Y. (2007). Human misato regulates mitochondrial distribution and morphology. *Experimental Cell Research, 313*(7), 1393-1404. doi:10.1016/j.yexcr.2007.02.004

Kornfeld, R., & Kornfeld, S. (1985). Assembly of asparagine-linked oligosaccharides. *Annual Review of Biochemistry, 54*, 631-664. doi:10.1146/annurev.bi.54.070185.003215

Krogh, A., Larsson, B., von Heijne, G., & Sonnhammer, E. L. (2001). Predicting transmembrane protein topology with a hidden markov model: Application to complete genomes. *Journal of Molecular Biology, 305*(3), 567-580. doi:10.1006/jmbi.2000.4315

Lai, C., Lin, X., Chandran, J., Shim, H., Yang, W. J., & Cai, H. (2007). The G59S mutation in p150(glued) causes dysfunction of dynactin in mice. *The Journal of Neuroscience : The Official Journal of the Society for Neuroscience, 27*(51), 13982-13990. doi:10.1523/JNEUROSCI.4226-07.2007

Lam, T. K., Schwartz, G. J., & Rossetti, L. (2005). Hypothalamic sensing of fatty acids. *Nature Neuroscience, 8*(5), 579-584. doi:10.1038/nn1456

Lane, M. D., Wolfgang, M., Cha, S. H., & Dai, Y. (2008). Regulation of food intake and energy expenditure by hypothalamic malonyl-CoA. *International Journal of Obesity (2005), 32 Suppl 4*, S49-54. doi:10.1038/ijo.2008.123

Lass, A., McConnell, E., Fleck, K., Palamarchuk, A., & Wojcik, C. (2008). Analysis of Npl4 deletion mutants in mammalian cells unravels new Ufd1-interacting motifs and suggests a regulatory role of Npl4 in ERAD. *Experimental Cell Research, 314*(14), 2715-2723. doi:10.1016/j.yexcr.2008.06.008

Lass, A., McConnell, E., Fleck, K., Palamarchuk, A., & Wojcik, C. (2008). Analysis of Npl4 deletion mutants in mammalian cells unravels new Ufd1-interacting motifs and suggests a regulatory role of Npl4 in ERAD. *Experimental Cell Research, 314*(14), 2715-2723. doi:10.1016/j.yexcr.2008.06.008

Li, B., & Fields, S. (1993). Identification of mutations in p53 that affect its binding to SV40 large T antigen by using the yeast two-hybrid system. *The FASEB Journal : Official Publication of the Federation of American Societies for Experimental Biology, 7*(10), 957-963.

Lin, C. C., Huoh, Y. S., Schmitz, K. R., Jensen, L. E., & Ferguson, K. M. (2008). Pellino proteins contain a cryptic FHA domain that mediates interaction with phosphorylated IRAK1. *Structure (London, England : 1993), 16*(12), 1806-1816. doi:10.1016/j.str.2008.09.011

Linder, M. E., & Deschenes, R. J. (2007). Palmitoylation: Policing protein stability and traffic. *Nature Reviews.Molecular Cell Biology, 8*(1), 74-84. doi:10.1038/nrm2084

Ling, C., Ishiai, M., Ali, A. M., Medhurst, A. L., Neveling, K., Kalb, R., et al. (2007). FAAP100 is essential for activation of the fanconi anemia-associated DNA damage response pathway. *The EMBO Journal, 26*(8), 2104-2114. doi:10.1038/sj.emboj.7601666

Lingwood, D., & Simons, K. (2010). Lipid rafts as a membrane-organizing principle. *Science (New York, N.Y.), 327*(5961), 46-50. doi:10.1126/science.1174621

Loftus, T. M., Jaworsky, D. E., Frehywot, G. L., Townsend, C. A., Ronnett, G. V., Lane, M. D., et al. (2000). Reduced food intake and body weight in mice treated with fatty acid synthase inhibitors. *Science (New York, N.Y.), 288*(5475), 2379-2381.

Lopez, M., Lage, R., Saha, A. K., Perez-Tilve, D., Vazquez, M. J., Varela, L., et al. (2008). Hypothalamic fatty acid metabolism mediates the orexigenic action of ghrelin. *Cell Metabolism, 7*(5), 389-399. doi:10.1016/j.cmet.2008.03.006

Lopez, M., Lelliott, C. J., & Vidal-Puig, A. (2007). Hypothalamic fatty acid metabolism: A housekeeping pathway that regulates food intake. *BioEssays : News and Reviews in Molecular, Cellular and Developmental Biology, 29*(3), 248-261. doi:10.1002/bies.20539

Lopez-Vinas, E., Bentebibel, A., Gurunathan, C., Morillas, M., de Arriaga, D., Serra, D., et al. (2007). Definition by functional and structural analysis of two malonyl-CoA sites in carnitine palmitoyltransferase 1A. *The Journal of Biological Chemistry, 282*(25), 18212-18224. doi:10.1074/jbc.M700885200

Lundmark, R., & Carlsson, S. R. (2009). SNX9 - a prelude to vesicle release. *Journal of Cell Scie nce, 122*(Pt 1), 5-11. doi:10.1242/jcs.037135

Maglott, D., Ostell, J., Pruitt, K. D., & Tatusova, T. (2007). Entrez gene: Gene-centered information at NCBI. *Nucleic Acids Research, 35*(Database issue), D26-31. doi:10.1093/nar/gkl993

Martinez, A., Santiago, J. L., Cenit, M. C., de Las Heras, V., de la Calle, H., Fernandez-Arquero, M., et al. (2008). IFIH1-GCA-KCNH7 locus: Influence on multiple sclerosis risk. *European Journal of Human Genetics : EJHG, 16*(7), 861-864. doi:10.1038/ejhg.2008.16

Marza, E., & Lesa, G. M. (2006). Polyunsaturated fatty acids and neurotransmission in caenorhabditis elegans. *Biochemical Society Transactions, 34*(Pt 1), 77-80. doi:10.1042/BST0340077

McGarry, J. D., & Brown, N. F. (1997). The mitochondrial carnitine palmitoyltransferase system. from concept to molecular analysis. *European Journal of Biochemistry / FEBS, 244*(1), 1-14.

McGarry, J. D., & Foster, D. W. (1980). Regulation of hepatic fatty acid oxidation and ketone body production. *Annual Review of Biochemistry, 49*, 395-420. doi:10.1146/annurev.bi.49.070180.002143

McGarry, J. D., Mills, S. E., Long, C. S., & Foster, D. W. (1983). Observations on the affinity for carnitine, and malonyl-CoA sensitivity, of carnitine palmitoyltransferase I in animal and human tissues. demonstration of the presence of malonyl-CoA in non-hepatic tissues of the rat. *The Biochemical Journal, 214*(1), 21-28.

McGarry, J. D., Woeltje, K. F., Kuwajima, M., & Foster, D. W. (1989). Regulation of ketogenesis and the renaissance of carnitine palmitoyltransferase. *Diabetes/metabolism Reviews, 5*(3), 271-284.

Meetei, A. R., de Winter, J. P., Medhurst, A. L., Wallisch, M., Waisfisz, Q., van de Vrugt, H. J., et al. (2003). A novel ubiquitin ligase is deficient in fanconi anemia. *Nature Genetics, 35*(2), 165-170. doi:10.1038/ng1241

Mills, S. E., Foster, D. W., & McGarry, J. D. (1984). Effects of pH on the interaction of substrates and malonyl-CoA with mitochondrial carnitine palmitoyltransferase I. *The Biochemical Journal, 219*(2), 601-608.

Minokoshi, Y., Alquier, T., Furukawa, N., Kim, Y. B., Lee, A., Xue, B., et al. (2004). AMP-kinase regulates food intake by responding to hormonal and nutrient signals in the hypothalamus. *Nature, 428*(6982), 569-574. doi:10.1038/nature02440

Mitchell, D. A., Marshall, T. K., & Deschenes, R. J. (1993). Vectors for the inducible overexpression of glutathione S-transferase fusion proteins in yeast. *Yeast (Chichester, England), 9*(7), 715-722. doi:10.1002/yea.320090705

Moller, S., Croning, M. D., & Apweiler, R. (2001). Evaluation of methods for the prediction of membrane spanning regions. *Bioinformatics (Oxford, England), 17*(7), 646-653.

Morillas, M., Clotet, J., Rubi, B., Serra, D., Asins, G., Arino, J., et al. (2000). Identification of the two histidine residues responsible for the inhibition by malonyl-CoA in peroxisomal carnitine octanoyltransferase from rat liver. *FEBS Letters, 466*(1), 183-186.

Morillas, M., Gomez-Puertas, P., Roca, R., Serra, D., Asins, G., Valencia, A., et al. (2001). Structural model of the catalytic core of carnitine palmitoyltransferase I and carnitine octanoyltransferase (COT): Mutation of CPT I histidine 473 and alanine 381 and COT alanine 238 impairs the catalytic activity. *The Journal of Biological Chemistry, 276*(48), 45001-45008. doi:10.1074/jbc.M106920200

Morillas, M., Gomez-Puertas, P., Rubi, B., Clotet, J., Arino, J., Valencia, A., et al. (2002). Structural model of a malonyl-CoA-binding site of carnitine octanoyltransferase and carnitine palmitoyltransferase I: Mutational analysis of a malonyl-CoA affinity domain. *The Journal of Biological Chemistry, 277*(13), 11473-11480. doi:10.1074/jbc.M111628200

Morillas, M., Lopez-Vinas, E., Valencia, A., Serra, D., Gomez-Puertas, P., Hegardt, F. G., et al. (2004). Structural model of carnitine palmitoyltransferase I based on the carnitine acetyltransferase crystal. *The Biochemical Journal, 379*(Pt 3), 777-784. doi:10.1042/BJ20031373

Morrison, C. D., Xi, X., White, C. L., Ye, J., & Martin, R. J. (2007). Amino acids inhibit agrp gene expression via an mTOR-dependent mechanism. *American Journal of Physiology.Endocrinology and Metabolism, 293*(1), E165-71. doi:10.1152/ajpendo.00675.2006

Moynagh, P. N. (2009). The pellino family: IRAK E3 ligases with emerging roles in innate immune signalling. *Trends in Immunology, 30*(1), 33-42. doi:10.1016/j.it.2008.10.001

Nowis, D., McConnell, E., & Wojcik, C. (2006). Destabilization of the VCP-Ufd1-Npl4 complex is associated with decreased levels of ERAD substrates. *Experimental Cell Research, 312*(15), 2921-2932. doi:10.1016/j.yexcr.2006.05.013

Obici, S., Feng, Z., Arduini, A., Conti, R., & Rossetti, L. (2003). Inhibition of hypothalamic carnitine palmitoyltransferase-1 decreases food intake and glucose production. *Nature Medicine, 9*(6), 756-761. doi:10.1038/nm873

Obici, S., Zhang, B. B., Karkanias, G., & Rossetti, L. (2002). Hypothalamic insulin signaling is required for inhibition of glucose production. *Nature Medicine, 8*(12), 1376-1382. doi:10.1038/nm798

Ogretmen, B., & Hannun, Y. A. (2004). Biologically active sphingolipids in cancer pathogenesis and treatment. *Nature Reviews.Cancer, 4*(8), 604-616. doi:10.1038/nrc1411

Ohno, Y., Kihara, A., Sano, T., & Igarashi, Y. (2006). Intracellular localization and tissue-specific distribution of human and yeast DHHC cysteine-rich domain-containing proteins. *Biochimica Et Biophysica Acta, 1761*(4), 474-483. doi:10.1016/j.bbalip.2006.03.010

Olender, E. H., & Simon, R. D. (1992). The intracellular targeting and membrane topology of 3-hydroxy-3-methylglutaryl-CoA reductase. *The Journal of Biological Chemistry, 267*(6), 4223-4235.

Ono, T., Losada, A., Hirano, M., Myers, M. P., Neuwald, A. F., & Hirano, T. (2003). Differential contributions of condensin I and condensin II to mitotic chromosome architecture in vertebrate cells. *Cell, 115*(1), 109-121.

Paschen, W. (2003). Shutdown of translation: Lethal or protective? unfolded protein response versus apoptosis. *Journal of Cerebral Blood Flow and Metabolism : Official Journal of the International Society of Cerebral Blood Flow and Metabolism, 23*(7), 773-779. doi:10.1097/01.WCB.0000075009.47474.F9

Pisani, D. F., Coldefy, A. S., Elabd, C., Cabane, C., Salles, J., Le Cunff, M., et al. (2007). Involvement of BTBD1 in mesenchymal differentiation. *Experimental Cell Research, 313*(11), 2417-2426. doi:10.1016/j.yexcr.2007.03.030

Poon, H. F., Shepherd, H. M., Reed, T. T., Calabrese, V., Stella, A. M., Pennisi, G., et al. (2006). Proteomics analysis provides insight into caloric restriction mediated oxidation and expression of brain proteins associated with age-related impaired cellular processes: Mitochondrial dysfunction, glutamate dysregulation and impaired protein synthesis. *Neurobiology of Aging, 27*(7), 1020-1034. doi:10.1016/j.neurobiolaging.2005.05.014

Price, N., van der Leij, F., Jackson, V., Corstorphine, C., Thomson, R., Sorensen, A., et al. (2002). A novel brain-expressed protein related to carnitine palmitoyltransferase I. *Genomics, 80*(4), 433-442.

Prip-Buus, C., Cohen, I., Kohl, C., Esser, V., McGarry, J. D., & Girard, J. (1998). Topological and functional analysis of the rat liver carnitine palmitoyltransferase 1 expressed in saccharomyces cerevisiae. *FEBS Letters, 429*(2), 173-178.

Pye, V. E., Beuron, F., Keetch, C. A., McKeown, C., Robinson, C. V., Meyer, H. H., et al. (2007). Structural insights into the p97-Ufd1-Npl4 complex. *Proceedings of the National Academy of Sciences of the United States of America, 104*(2), 467-472. doi:10.1073/pnas.0603408104

Reed, T., Perluigi, M., Sultana, R., Pierce, W. M., Klein, J. B., Turner, D. M., et al. (2008). Redox proteomic identification of 4-hydroxy-2-nonenal-modified brain proteins in amnestic mild cognitive impairment: Insight into the role of lipid peroxidation in the progression and pathogenesis of alzheimer's disease. *Neurobiology of Disease, 30*(1), 107-120. doi:10.1016/j.nbd.2007.12.007

Rufer, A. C., Thoma, R., & Hennig, M. (2009). Structural insight into function and regulation of carnitine palmitoyltransferase. *Cellular and Molecular Life Sciences : CMLS, 66*(15), 2489-2501. doi:10.1007/s00018-009-0035-1

Rusinol, A. E., Cui, Z., Chen, M. H., & Vance, J. E. (1994). A unique mitochondria-associated membrane fraction from rat liver has a high capacity for lipid synthesis and contains pre-golgi secretory proteins including nascent lipoproteins. *The Journal of Biological Chemistry, 269*(44), 27494-27502.

Saggerson, E. D. (1982). Carnitine acyltransferase activities in rat liver and heart measured with palmitoyl-CoA and octanoyl-CoA. latency, effects of K+, bivalent metal ions and malonyl-CoA. *The Biochemical Journal, 202*(2), 397-405.

Saggerson, E. D. (1982). Carnitine acyltransferase activities in rat liver and heart measured with palmitoyl-CoA and octanoyl-CoA. latency, effects of K+, bivalent metal ions and malonyl-CoA. *The Biochemical Journal, 202*(2), 397-405.

Saggerson, E. D., & Carpenter, C. A. (1982). Malonyl CoA inhibition of carnitine acyltransferase activities: Effects of thiol-group reagents. *FEBS Letters, 137*(1), 124-128.

Saggerson, E. D., & Carpenter, C. A. (1982). Malonyl CoA inhibition of carnitine acyltransferase activities: Effects of thiol-group reagents. *FEBS Letters, 137*(1), 124-128.

Saggerson, E. D., & Carpenter, C. A. (1982). Malonyl CoA inhibition of carnitine acyltransferase activities: Effects of thiol-group reagents. *FEBS Letters, 137*(1), 124-128.

Saggerson, E. D., & Carpenter, C. A. (1986). Carnitine palmitoyltransferase in liver and five extrahepatic tissues in the rat. inhibition by DL-2-bromopalmitoyl-CoA and effect of hypothyroidism. *The Biochemical Journal, 236*(1), 137-141.

Saiki, R. K., Gelfand, D. H., Stoffel, S., Scharf, S. J., Higuchi, R., Horn, G. T., et al. (1988). Primer-directed enzymatic amplification of DNA with a thermostable DNA polymerase. *Science (New York, N.Y.), 239*(4839), 487-491.

Schinkel, A. H., Kemp, S., Dolle, M., Rudenko, G., & Wagenaar, E. (1993). N-glycosylation and deletion mutants of the human MDR1 P-glycoprotein. *The Journal of Biological Chemistry, 268*(10), 7474-7481.

Schwede, T., Kopp, J., Guex, N., & Peitsch, M. C. (2003). SWISS-MODEL: An automated protein homology-modeling server. *Nucleic Acids Research, 31*(13), 3381-3385.

Shin, N., Lee, S., Ahn, N., Kim, S. A., Ahn, S. G., YongPark, Z., et al. (2007). Sorting nexin 9 interacts with dynamin 1 and N-WASP and coordinates synaptic vesicle endocytosis. *The Journal of Biological Chemistry, 282*(39), 28939-28950. doi:10.1074/jbc.M700283200

Shin, N., Lee, S., Ahn, N., Kim, S. A., Ahn, S. G., YongPark, Z., et al. (2007). Sorting nexin 9 interacts with dynamin 1 and N-WASP and coordinates synaptic vesicle endocytosis. *The Journal of Biological Chemistry, 282*(39), 28939-28950. doi:10.1074/jbc.M700283200

Sierra, A. Y., Gratacos, E., Carrasco, P., Clotet, J., Urena, J., Serra, D., et al. (2008). CPT1c is localized in endoplasmic reticulum of neurons and has carnitine palmitoyltransferase activity. *The Journal of Biological Chemistry, 283*(11), 6878-6885. doi:10.1074/jbc.M707965200

Sonnhammer, E. L., & Hollich, V. (2005). Scoredist: A simple and robust protein sequence distance estimator. *BMC Bioinformatics, 6*, 108. doi:10.1186/1471-2105-6-108

Sonnhammer, E. L., von Heijne, G., & Krogh, A. (1998). A hidden markov model for predicting transmembrane helices in protein sequences. *Proceedings / ...International Conference on Intelligent Systems for Molecular Biology ; ISMB.International Conference on Intelligent Systems for Molecular Biology, 6*, 175-182.

Sorensen, A., Travers, M. T., Vernon, R. G., Price, N. T., & Barber, M. C. (2002). Localization of messenger RNAs encoding enzymes associated with malonyl-CoA metabolism in mouse brain. *Brain Research.Gene Expression Patterns, 1*(3-4), 167-173.

Tusnady, G. E., & Simon, I. (1998). Principles governing amino acid composition of integral membrane proteins: Application to topology prediction. *Journal of Molecular Biology, 283*(2), 489-506. doi:10.1006/jmbi.1998.2107

Tusnady, G. E., & Simon, I. (2001). The HMMTOP transmembrane topology prediction server. *Bioinformatics (Oxford, England), 17*(9), 849-850.

Wang, H. J., Guay, G., Pogan, L., Sauve, R., & Nabi, I. R. (2000). Calcium regulates the association between mitochondria and a smooth subdomain of the endoplasmic reticulum. *The Journal of Cell Biology, 150*(6), 1489-1498.

Wolfgang, M. J., Cha, S. H., Sidhaye, A., Chohnan, S., Cline, G., Shulman, G. I., et al. (2007). Regulation of hypothalamic malonyl-CoA by central glucose and leptin. *Proceedings of the National Academy of Sciences of the United States of America, 104*(49), 19285-19290. doi:10.1073/pnas.0709778104

Wolfgang, M. J., Kurama, T., Dai, Y., Suwa, A., Asaumi, M., Matsumoto, S., et al. (2006). The brain-specific carnitine palmitoyltransferase-1c regulates energy homeostasis. *Proceedings of the National Academy of Sciences of the United States of America, 103*(19), 7282-7287. doi:10.1073/pnas.0602205103

Wolfgang, M. J., & Lane, M. D. (2006). The role of hypothalamic malonyl-CoA in energy homeostasis. *The Journal of Biological Chemistry, 281*(49), 37265-37269. doi:10.1074/jbc.R600016200

Wu, D., Govindasamy, L., Lian, W., Gu, Y., Kukar, T., Agbandje-McKenna, M., et al. (2003). Structure of human carnitine acetyltransferase. molecular basis for fatty acyl transfer. *The Journal of Biological Chemistry, 278*(15), 13159-13165. doi:10.1074/jbc.M212356200

Wu, Y., Song, P., Xu, J., Zhang, M., & Zou, M. H. (2007). Activation of protein phosphatase 2A by palmitate inhibits AMP-activated protein kinase. *The Journal of Biological Chemistry, 282*(13), 9777-9788. doi:10.1074/jbc.M608310200

Xie, X., Wang, Z., & Chen, Y. (2007). Association of LKB1 with a WD-repeat protein WDR6 is implicated in cell growth arrest and p27(Kip1) induction. *Molecular and Cellular Biochemistry, 301*(1-2), 115-122. doi:10.1007/s11010-006-9402-5

Yamazaki, N., Shinohara, Y., Shima, A., & Terada, H. (1995). High expression of a novel carnitine palmitoyltransferase I like protein in rat brown adipose tissue and heart: Isolation and characterization of its cDNA clone. *FEBS Letters, 363*(1-2), 41-45.

Ye, Q., & Worman, H. J. (1995). Protein-protein interactions between human nuclear lamins expressed in yeast. *Experimental Cell Research, 219*(1), 292-298. doi:10.1006/excr.1995.1230

Ye, Y., Meyer, H. H., & Rapoport, T. A. (2003). Function of the p97-Ufd1-Npl4 complex in retrotranslocation from the ER to the cytosol: Dual recognition of nonubiquitinated polypeptide segments and polyubiquitin chains. *The Journal of Cell Biology, 162*(1), 71-84. doi:10.1083/jcb.200302169

Ye, Y., Meyer, H. H., & Rapoport, T. A. (2003). Function of the p97-Ufd1-Npl4 complex in retrotranslocation from the ER to the cytosol: Dual recognition of nonubiquitinated polypeptide segments and polyubiquitin chains. *The Journal of Cell Biology, 162*(1), 71-84. doi:10.1083/jcb.200302169

Zammit, V. A. (1999). The malonyl-CoA-long-chain acyl-CoA axis in the maintenance of mammalian cell function. *The Biochemical Journal, 343 Pt 3*, 505-515.

Zammit, V. A. (2008). Carnitine palmitoyltransferase 1: Central to cell function. *IUBMB Life, 60*(5), 347-354. doi:10.1002/iub.78

Zhu, H., Shi, J., de Vries, Y., Arvidson, D. N., Cregg, J. M., & Woldegiorgis, G. (1997). Functional studies of yeast-expressed human heart muscle carnitine palmitoyltransferase I. *Archives of Biochemistry and Biophysics, 347*(1), 53-61. doi:10.1006/abbi.1997.0314

PUBLICATIONS

A NEW LC-ESI-MS/MS METHOD TO MEASURE LONG-CHAIN ACYLCARNITINE LEVELS IN CULTURED CELLS.

Jauregui, O., Sierra, A. Y., Carrasco, P., Gratacos, E., Hegardt, F. G., & Casals, N. (2007).

Analytica Chimica Acta, 599(1), 1-6.

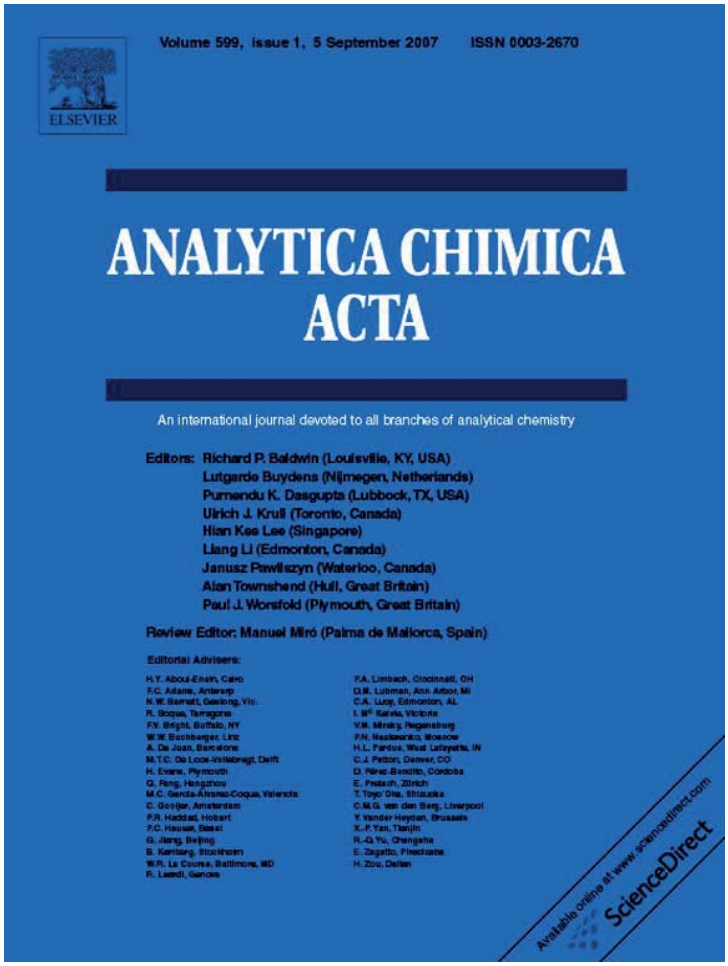

Available online at www.sciencedirect.com
ScienceDirect
Analytica Chimica Acta 599 (2007) 1–6
ANALYTICA CHIMICA ACTA
www.elsevier.com/locate/aca

Review

A new LC–ESI-MS/MS method to measure long-chain acylcarnitine levels in cultured cells

Olga Jáuregui [a], Adriana Y. Sierra [b], Patricia Carrasco [b], Esther Gratacós [b], Fausto G. Hegardt [c], Núria Casals [b,*]

[a] *Scientific & Technical Services, University of Barcelona, Spain*
[b] *Molecular and Cellular Unit, School of Health Sciences, International University of Catalonia, Spain*
[c] *Department of Biochemistry and Molecular Biology, University of Barcelona, School of Pharmacy, Spain*

Received 12 June 2007; received in revised form 27 July 2007; accepted 30 July 2007
Available online 3 August 2007

Abstract

The quantitative evaluation of long-chain acylcarnitines in lipid extracts from cultured cells or tissues is a prerequisite to study carnitine palmitoyltransferase (CPT) activity. There is thus a need for the accurate measurement of the concentration of long-chain acylcarnitines at the lowest concentration present in lipid extracts. Here we report a fast and reliable quantitative method based on the use of weak acid extraction and liquid chromatography–electrospray ionization tandem mass spectrometry (LC–ESI-MS/MS) to quantify acylcarnitines through hydrophilic interaction chromatography. The method was validated using isotopic dilution and the results allow the analysis of a large number of samples at low concentration levels (down to 0.35 nmol L^{-1} for palmitoylcarnitine) with good inter- and intra-day precision. The method was used for the quantitative study of changes in concentration of palmitoylcarnitine and other acylcarnitines in PC-12 cells over-expressing *CPT1a* gene. It was also used to measure CPT1 activity in mitochondria isolated from transfected cells, giving similar results to the more common radiometric method, but with higher sensitivity.

Keywords: Acylcarnitines; Carnitine palmitoyltransferase activity; Liquid chromatography–electrospray ionization tandem mass spectrometry; Hydrophilic interaction chromatography

Contents

* Corresponding author at: Facultat de Ciències de la Salut, Universitat Internacional de Catalunya, C/Josep Trueta s/n. E-08190 Sant Cugat del Valles, Barcelona, Spain.
E-mail address: ncasals@csc.uic.es (N. Casals).

0003-2670/$ – see front matter © 2007 Elsevier B.V. All rights reserved.
doi:10.1016/j.aca.2007.07.066

1. Introduction

Long-chain fatty acids enter the mitochondrial matrix, where they undergo beta-oxidation and the generated reduction equivalents were transferred to the mitochondrial respiratory chain to form ATP. The activated forms of fatty acids, acyl-CoAs, are transported across the mitochondrial membrane to the matrix by the CPT1/CACT/CPT2 system. Carnitine palmitoyl transferase 1 (CPT1) is localized in the outer mitochondrial membrane and facilitates the *trans*-esterification of activated long-chain acyl-CoAs and carnitine to give acylcarnitines. This is subsequently transported across mitochondrial inner membrane by the carnitine acylcarnitine transporter (CACT), and then reconverted to (the corresponding) CoA-esters by carnitine palmitoyl transferase 2 (CPT2) in the mitochondrial matrix [1]. The analysis of long-chain acylcarntines in lipid cell extracts provides a powerful selective tool with which to study the activity and function of the CPT1/CACT/CPT2 system in cells.

Various approaches have been proposed for the analysis of acylcarnitines in biological samples. Among these, HPLC-based methods with UV absorbance or fluorescence detection need derivatization steps. Thus, the classic procedure used in many newbornscreening centers is based on the formation of butyl ester derivatives and direct MS/MS analysis [2–6]. Pentafluorophenacyl esters of acylcarnitines separated by ion-exchange/reversed-phase HPLC [7] and 2-(2,3-naphthalimino)ethyl trifluoromethanesulfonate esters separated by HPLC with fluorescence detection [8] are other approaches for the analysis of acylcarnitines in biological samples. A further method is the use of ion-pairing reagents in the LC mobile phase such as heptafluorobutyric acid (HFBA) [9] in order to allow acylcarnitines to be retained in reversed-phase LC columns. In this case, good separation of the acylcarnitines was obtained, and detection limits of 1 nmol L^{-1} were achieved in MS/MS analysis. Nevertheless, the use of ion-pairing reagents such as HFBA is not recommended because putative contamination of the LC–MS system prevents the analysis in negative-ion mode. Ion exchange solid phase extraction, derivatization and GC-MS have also been applied [10].

Stevens et al. [11] analyzed acylcarnitines in human plasma by isotope-dilution tandem mass spectrometry, and an innovative procedure for the analysis of plasma acylcarnitines using on-line SPE-LC–ESI-MS/MS has recently been presented. The procedure operates without derivatization and uses a mobile phase containing ammonium acetate at pH 7.6 and methanol, and a valve-switching system. Protein precipitation with acetonitrile, centrifugation and extraction/cleaning via the on-line SPE system has also been applied [12,13].

Among the various MS and MS/MS approaches, that most frequently used is direct sample injection, and the precursor-ion scan of *m/z* 85 (the major fragment produced by collision-induced dissociation of all butylated acylcarnitines) produces a profile of all acylcarnitines present in the sample [3–6,13,14]. Given that endogenous materials in biological samples can cause ion suppression, thus introducing error in the results, liquid chromatography is frequently coupled to mass spectrometry in small molecule-metabolism laboratories. This is primarily due to the high sensitivity and selectivity of this combined technique and its ability to separate, detect, and identify metabolites in the presence of endogenous materials.

Here we describe an easy and sensitive method to analyze the changes in long-chain acylcarnitine levels in cells as a consequence of transient over-expression of *CPT1a* (the gene that encodes the liver CPT1 enzyme). A new LC procedure allows acylcarnitines to be separated in 12 min with an ammonium formate/acetonitrile mobile phase at low concentrations, without the need for derivatization, and obviating ion-pairing reagents in the mobile phase. The method also takes advantage of a simple extraction procedure.

2. Experimental methods

2.1. Materials

Standards palmitoylcarnitine, myristoylcarnitine and arachidonoylcarnitine were from Sigma–Aldrich. Palmitoylcarnitine-d_3 (Cambridge Isotope Laboratories, USA) was used as internal standard. Acetonitrile HPLC-grade (Sigma–Aldrich, St. Louis, MO, USA), ammonium formate (Panreac, Montcada i Reixac, Spain) and ultrapure water (MilliQ) from Millipore System (Bedford, USA) were used in HPLC analysis.

2.2. Culture and transfection of PC-12 cells

Clonal neural PC-12 cells were grown at 37 °C in the presence of 5% CO_2 in DMEM with high glucose containing 2 mM glutamine, 5% foetal calf serum, 10% horse serum, penicillin (100 units mL^{-1}) and streptomycin (100 μg mL^{-1}).

Cells cultured in 10 cm plates were transfected with 20 μg of plasmid DNA (purified with the Qiagen Maxi Prep Kit, Quiagen, UK) using Lipofectamine Plus reagent (Roche Applied Science, USA) according to the manufacturer's protocol. Cells were collected 48 h after transfection. Transfection efficiency as assessed by FACS analysis was about 50%.

2.3. Plasmid contructions

The coding region of rat CPT1a gene was cloned in vector pIRES2-EGFP (Clontech, BD Biosciences, Europe), to give pIRES2-EGFP-CPT1a, which permits both CPT1a and EGFP (green fluorescent protein) to be translated from a single bicistronic mRNA. Cells were transfected with empty vector pIRES2-EGFP (control cells) or with pIRES2-EGFP-CPT1a (CPT1 over-expressing cells).

2.4. Cell lipid extraction

Cells were washed in cold PBS buffer and gently collected with a pipette. They were then centrifuged at 700 × *g* max for 5 min at 4 °C and washed in PBS. Aliquots of 20 μL were taken for Bradford protein assay. After that, 200 μL of 0.2 M NaCl was added to the pellet and the mixture was immediately frozen in liquid N_2. To separate aqueous and lipid phases, 750 μL of Folch reagent (chloroform:methanol, 2:1) and 50 μL of 0.1 M KOH were added and, after vigorous mixing using a Vortex mixer, the phases were separated by 15 min centrifugation at 2000 × *g* at 4 °C. The top aqueous phase was removed and the lipid phase was washed in 200 μL of methanol/water/chloroform (48:47:3). After vortex-mixing, it was again centrifuged at 700 × *g* for 5 min at 4 °C and the lower phase (lipid extract) was dried.

2.5. Mitochondria isolation

Cells were recovered by centrifugation at 1200 × *g* for 5 min at 4 °C, washed in 1.5 mL PBS, and re-suspended in 2 mL of lysis buffer (250 mM sucrose, 10 mM Tris pH 7.4, 1 mM EDTA, supplemented with 1 mM PMSF, 0.5 mM benzamidine, 10 ng mL^{-1} leupeptin and 100 ng mL^{-1} pepstatin). Cells were disrupted by Douncer homogenization (30 pulses with loose pestle and 30 pulses with tight pestle). Homogenates were centrifuged at 2000 × *g* max for 3 min at 4 °C to remove cell debris. This crude extracted was further centrifuged at 10,000 × *g* for 30 min at 4 °C to give the mitochondrial pellet. The supernatant was discarded and pellet was immediately used for the carnitine palmitoyltransferase activity assay.

2.6. CPT1 activity

The substrates were palmitoyl-CoA and carnitine. In the radiometric assay L-(methyl-3H) carnitine (Amersham Bioscience, USA) was used. Enzyme activity was assayed for 4 min at 30 °C in a total volume of 200 μL. The protein sample, 40 μL (20–40 μg), was pre-incubated for 1 min, and 160 μL of the reaction mixture was then added. The final concentrations were 105 mM Tris–HCl (pH 7.2), 2 mM KCN, 15 mM KCl, 4 mM $MgCl_2$, 4 mM ATP, 250 μM reduced glutathione, 50 μM palmitoyl-CoA, 400 μM carnitine or L-(methyl-3H) carnitine (0.3 μCi), and 0.1% defatted bovine albumin. Reactions were arrested by the addition of 200 μL HCl 1.2N. The internal standard pamitoylcarnitine-d_3 was added at that moment. Acylcarnitine products formed in the assay reaction were extracted with water-saturated *n*-butanol and analyzed by HPLC–MS/MS or by a Coulter counter (radiometric method). Values were given as means of three independent experiments performed. All protein concentrations were determined using the Bradford protein assay (Bio-Rad, USA) with bovine serum albumin as standard.

2.7. LC–MS/MS conditions

The HPLC system used was a Perkin-Elmer Series 200 (Norwalk, CT, USA) quaternary pump equipped with an autosampler. For the analysis of the extracts, an Atlantis HILIC Silica (Waters, Milford, USA) column (150 mm × 2.1 mm, 3.0 μm) was used. Isocratic separation was done with 200 mmol L^{-1} ammonium formate pH 3, acetonitrile and water at the proportions 5:86:9 (v/v) and a constant flow-rate of 200 μL min^{-1}. To reduce the residual matrix effect reaching the mass spectrometer, a divert valve (Valco, Houston, USA) drained off the LC eluent. MS and MS/MS experiments were performed on an API 3000 triple quadrupole mass spectrometer (PE Sciex, Concord, Ont., Canada). All the analyses were performed using the Turbo Ionspray source in positive ion mode with the following settings: capillary voltage +4500 V, nebulizer gas (N_2) 10 a.u., curtain gas (N_2) 12 a.u., collision gas (N_2) 4 a.u. The drying gas (N_2) was heated to 400 °C and introduced at a flow-rate of 5000 cm^3 min^{-1}.

All the MS and MS/MS parameters were optimized by infusion experiments: individual standard solutions of acylcarnitines (1 ng μL^{-1}) were infused into the mass spectrometer at a constant flow-rate of 5 μL min^{-1} using a Model 11 syringe pump (Harvard Apparatus, Holliston, MA, USA). Full scan data acquisition was performed by scanning from *m/z* 50 to 500 in a profile mode and using a cycle time of 2 s with a step size of 0.1 u and a pause between each scan of 2 ms. In product ion-scan experiments MS/MS product ions were produced by collision-activated dissociation (CAD) of selected precursor ions in the collision cell of the triple quadrupole mass spectrometer, and mass was analyzed using the second analyzer of the instrument. However, in precursor ion-scan experiments, Q1 gives information on all the possible precursors of the selected ion in Q3 of the triple quadrupole. Additional experimental conditions for MS/MS included collision energy (depending on the compound), CAD gas (N_2) at 6 (arbitrary) units, and scan range, as necessary for the precursor selected. Precursor ion scan experiments were performed by scanning Q1 between 150 and 700 u. In all the experiments both quadrupoles Q1 and Q3 operated at unit resolution.

MRM (multiple reaction monitoring) acquisition was done monitoring one transition for each compound (see Table 1) with a dwell time of 700 ms. The MRM mode was required because many compounds could present the same nominal molecular mass, and the combination of the parent mass and unique fragment ions was used to selectively monitor acylcarnitines. Internal standard palmitoylcarnitine-d_3 (4 μL of a solution of 20 μg mL^{-1}) was added to samples before extraction to give a final concentration of 0.2 μg mL^{-1}. The same concentration was present in the standards used for quantification. A graph plotting area of palmitoylcarnitine/palmitoylcarnitine-d_3 ratios against concentration of palmitoylcarnitine/palmitoylcarnitine-d_3 ratios

Table 1
MS/MS data for the compounds studied

Compound	Full scan (*m/z*)	Product ion scan	MRM transition	DP	CE
Myristoylcarnitine	372.3	313.3, 211.1, 85.2	372.3/85.2	40	30
Arachidonoylcarnitine	456.4	397.4, 85.2	456.4/85.2	40	40
Palmitoylcarnitine	400.4	341.4, 239.5, 144.3, 85.2	400.4/85.2[a]	40	35
			400.4/341.4[b]		
Palmitoylcarnitine-d_3	403.4	341.1, 239.5, 85.2	403.4/85.2	40	35

[a] MRM transition used for quantification purposes.
[b] MRM transition used for confirmation purposes.

was used for quantification. The MRM transitions used for this purpose were 400.4/85.2 for palmitoylcarnitine and 403.4/85.2 for palmitoylcarnitine-d_3.

3. Results and discussion

3.1. LC separation

The HILIC column uses hydrophilic interaction chromatography to retain and separate polar compounds. It was used successfully to separate acylcarnitines, thus avoiding ion-pairing reagents, with good resolution, reproducible retention times and good peak shapes. Fig. 1A shows the chromatogram for a standard solution containing all the standards of acylcarnitines at individual concentrations of 200 ng mL^{-1}. Fig. 1B shows the chromatogram for a lipid cell extract. Elution occurred in the order of increasing hydrophilicity. This approach has the advantage of using an MS-friendly mobile phase (acetonitrile/water/ammonium formate) with a high content of organic modifier (86%), which improves ESI signal. In addition, since polar compounds eluted later than the hydrophobic compounds, ion

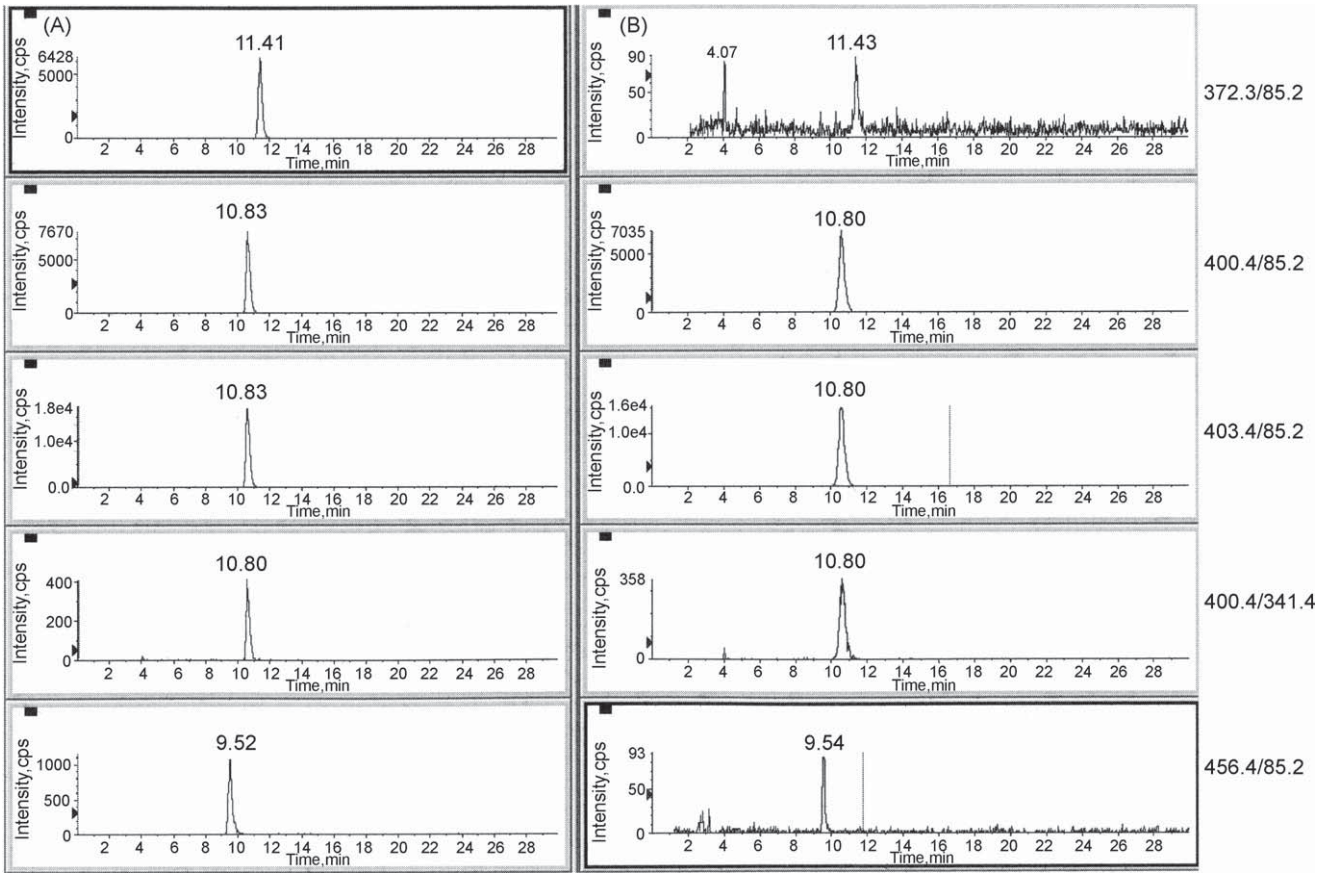

Fig. 1. Trace chromatogram of acylcarnitines using the LC–ESI-MS/MS conditions (MRM mode) described in the text: *x*-axis = time (min); *y*-axis = intensity (cps). Peaks: 456.4/85.2 arachidonoylcarnitine, 400.4/85.2 palmitoylcarnitine (identification and quantification), 400.4/341.4 palmitoylcarnitine (confirmation), 403.4/85.2 palmitoylcarnitine-d_3 (internal standard), 372.3/85.2 miristoylcarnitine. (A) Standard solution, 200 ng mL^{-1} for each compound. (B) Lipid extract from CPT1a over-expressing cells.

suppression at the beginning of the chromatograms was minimized.

3.2. Mass spectrometry

Analyses were carried out in positive-ion mode since sensitivity was higher than in negative-ion mode. Moreover, only in this mode there was a common *m/z* 85 product ion for all acylcarnitines. In positive mode, the spectrum for acylcarnitines gave the positively charged molecule $[M+H]^+$ in full scan mode. The carboxylic group of acylcarnitines is protonated under acidic conditions, resulting in the production of positively charged quaternary amines. Product ion-scan spectra were studied for each compound and similar behaviour was observed: loss of the $N(CH_3)_3$-fragment gave the $[M-59]^+$ ion. In the same way, all compounds showed the loss of 102 u. Finally, *m/z* 144 and *m/z* 85 were common fragment ions for all the acylcarnitines studied. Collision energy was optimized for each transition in infusion experiments. Optimum values are presented in Table 1. Fragmentation involves the loss of the fatty acid and trimethylamine, resulting in the generation of a stable fragment ion with *m/z* 85.

The chromatogram of blank sample was examined and no interference was found.

Isotope dilution mass spectrometry is the technique of choice for most clinical analyses, since it does not depend on sample recovery, and it also generates results with high precision. Although MS/MS can be considered a selective technique, this selectivity may be overestimated owing to the complexity of biological samples. This technique can produce false-positive results, especially when low resolution MS detection is used. In order to minimize this risk, appropriate confirmation was performed in low-resolution instruments (e.g. triple quadrupole instruments) by acquiring two transitions and measuring the ratio between them. In our case three transitions were monitored for the determination of palmitoylcarnitine in a lipid environment: 400.4/85.2 for quantitation purposes, 400.4/341.4 for confirmation purposes and 403.4/85.2 for the labelled internal standard. The ratio between the two transitions for palmitoylcarnitine was also calculated for each sample in order to avoid false positives. All the samples gave an ion ratio that was within the ion ratio for the standards, ±20%. It should be pointed out that the ion ratio criterion was only applicable for concentrations above 0.6 ng mL^{-1} owing to the lower intensity of the 400.4/341.4 as compared to the 400.4/85 transition.

3.3. Performance characteristics

Linearity. Calibration curves were prepared in the LC mobile phase and injected into the LC–ESI-MS/MS system. The peak areas were plotted against the corresponding concentration to obtain the calibration curve. The method was linear over the range from 2 to 2000 ng mL^{-1}. The residuals analysis for this concentration range was (mean (S.D.)): 96.8% (±8.8) using $1/x^2$ weighting [15]. As mentioned above, the internal standard approach using labelled compounds is the most valid method for quantitation purposes in LC–MS. In our case, palmitoylcarnitine-d_3 was used. Five calibration curves were plotted on five separate days in order to establish the robustness of the method. Low relative standard deviation (2.95%) was obtained in the measured slope of the calibration curves on 5 different days.

Sensitivity. The limit of detection (LoD) and the limit of quantification (LoQ) were calculated by repeated injections of diluted standard solutions. The LoD was estimated as the concentration of palmitoylcarnitine that generated a peak with a signal-to-noise ratio of 3. LoQ was calculated at a signal-to-noise ratio of 10. The LoD and LoQ were 0.14 ng mL^{-1} (0.35 nmol L^{-1}) and 0.48 ng mL^{-1} (1.2 nmol L^{-1}). respectively (in standard solutions), similar to the limits of 1 nmol L^{-1}, as published by other authors [9].

Precision. To assess the precision, 10 repetitive injections of three standard solutions of 10, 100 and 800 ng mL^{-1} were done in one day (intra-day precision) and on three different days (inter-day precision). The results expressed as coefficient of variation (%) are satisfactory in terms of concentration for run-to-run (9.1, 10.1 and 4.5% for 10, 100 and 800 ng mL^{-1}, respectively) and for day-to-day precision (12.1, 11.3 and 6.2% for 10, 100 and 800 ng mL^{-1}, respectively). The precision in terms of retention time also showed acceptable values (0.24% and 2.74% for run-to-run and for day-to-day precision, respectively).

3.4. Quantification of palmitoyl carnitine in lipid fraction of cell extracts

To determine whether this method could be used to study long-chain acylcarnitine levels in cell extracts, we altered the proportions of CPT1/CACT/CPT2 in PC-12 cultured cells by over-expressing CPT1a gene, and we measured the alteration of acylcarnitine profiles in lipid cell extracts. Samples were first analyzed in full-scan mode and then in precursor ion-scan mode of *m/z* 85. Cells over-expressing CPT1a were expected to have increased levels of palmitoylcarnitine in the lipid fraction. Major differences between control and CPT1a over-expressing cells were found in chromatographic peak areas corresponding to palmitoylcarnitine levels (Fig. 2). There was also a strong

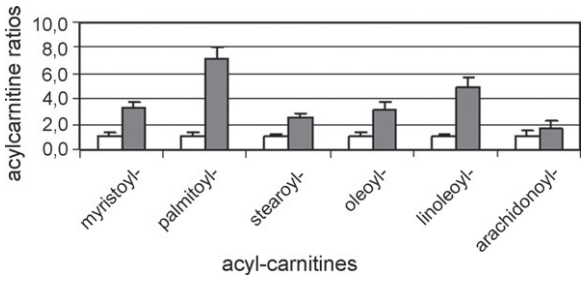

Fig. 2. Levels of different acylcarnitines in PC12 cells over-expressing CPT1a. Control PC-12 cells were transfected with empty pIres vector (white columns) and CPT1a over-expressing cells were transfected by pIres-CPT1a plasmid (grey columns). Forty eight hours after transfection, lipid cell extracts were obtained and acylcarnitines were determined by LC–ESI-MS/MS in precursor ion scan mode of *m/z* 85. Palmitoylcarnitine ratios = area below the chromatographic peak respect to control cells. These values represent the mean of three independent experiments.

Table 2
CPT1 activity (nmol mg^{-1} min^{-1}) in mitochondria of PC-12 cells

PC-12 cells	HPLC–MS/MS method	Radiometric method
Control cells	2.91 ± 0.43	3.12 ± 0.56
CPT1a over-expressing cells	7.13 ± 0.51	8.03 ± 0.41

Mitochondria were isolated from PC-12 cells 48 h after transfection. CPT1 activity was assayed in 40 μg of mitochondria using both methods: the HPLC–MS/MS method and the radiometric assay. Three separate experiments were performed. Control cells are PC-12 cells transfected with the empty expression vector.

increase in other acylcarnitines that may have been produced by CPT1a enzyme, like stearoylcarnitine and oleoylcarnitine. Levels of palmitoylcarnitine were also measured using MRM mode, with palmitoylcarnitine-d_3 as internal standard. About 1.59 and 8.84 ng mL^{-1} ($n = 3$) of palmitoylcarnitine were present in lipid extracts of control and CPT1a over-expressing cells. There was a 5–6-fold increase in palmitoylcarnitine levels as a consequence of the increase of CPT1 activity. The LC–ESI-MS/MS method described allows the simple measurement of differences in acylcarnitine levels in cells, with great accuracy.

3.5. CPT1 activity in isolated mitochondria of cells

CPT1 activity in cell extracts has traditionally been measured by a radiometric assay [16], using palmitoyl-CoA and L-(methyl-3H) carnitine as substrates. Recently, van Vlies et al. [17] described an improved enzyme assay for CPT1 activity in fibroblasts using tandem mass spectrometry, but propylation of the sample was required. We decided to use our HPLC–MS/MS method to measure CPT1 activity in mitochondria isolated from PC-12 cells. About 40 μg of mitochondria was incubated with palmitoyl-CoA and carnitine for 4 min, and levels of palmitoyl-carnitine were determined in MRM mode, with palmitoylcarnitine-d_3 as internal standard (Table 2). CPT1 activity in PC-12 cells measured by the HPLC–MS/MS method gave similar values to those returned by the radiometric assay.

The LC–ESI-MS/MS technique was more sensitive than the radiometric method. The limit of sensitivity of the LC–ESI-MS/MS method described here was 0.48 ng mL^{-1}, which corresponds to a CPT1 activity of 0.001 nmol (min mg)$^{-1}$ in our assay conditions (40 μg of protein, 4 min of assay time. To establish the limit of sensitivity of the radiometric assay we calculated the standard deviation of ten blank points (the assay mix solution without cell sample), in cpm values. The standard deviation of the blank was 27 cpm, with a coefficient of variation of 2%. The limit of sensitivity (a signal-to-noise ratio of 3) was 81 cpm, which corresponds to a CPT1 activity of 0.401 nmol mg^{-1} min^{-1}, about 400 times less sensitive than the LC–ESI-MS/MS described herein.

The method presented here constitutes an optimal procedure not only to measure acylcarnitine levels in cells, but also to measure CPT1 activity that is below the detection limit of the radiometric assay.

4. Conclusions

The use of quantitative LC–ESI-MS/MS has been shown to be highly sensitive and specific for the analysis of long-chain acylcarnitines in metabolic studies. The use of the HILIC column affords the ability to analyse acylcarnitines without prior derivatization. Analysis of underivatized acylcarnitines simplifies sample preparation and offers the added advantage of removing any potential errors caused by the derivatization procedure itself. Using three identification points (retention time and when possible, two MRM transitions), LoQ values of 1.2 nmol L^{-1} were obtained. In addition, a high confidence level was attained through the isotope ratio of two ions monitored within 20% of the theoretical isotopic ratio, even in complex samples such as lipid cell extracts. LC–ESI-MS/MS can also be used to measure CPT1 activity in cells with much higher sensitivity than the radiometric method.

Acknowledgments

The editorial help of Robin Rycroft is gratefully acknowledged. This study was supported by grants SAF2004-06843-C03 and SAF2007-61926 from the *Ministerio de Educación y Ciencia*, Spain, by CIBER Institute of Fisiopatologia, Obesidad y Nutrición (CB06/03), Instituto de Salud Carlos III, Spain, by the *Ajut de Suport als Grups de Recerca de Catalunya* (2005SGR-00733), and by grant from *Fundació La Marató de TV3* (2007), Catalunya. AYS and PC are recipients of fellowships from Universitat Internacional de Catalunya.

References

[1] J.D. McGarry, N.F. Brown, Eur. J. Biochem. 244 (1997) 1–14.
[2] C.T. Cavedon, P. Bourdoux, K. Mertens, H.V. Van Thi, N. Herremans, C. de Laet, P. Goyens, Clin. Chem. 51 (2005) 745–752.
[3] A. Liu, M. Pasquali, J. Chromatogr. B: Analyt. Technol. Biomed. Life Sci. 827 (2005) 193–198.
[4] D.H. Chace, S.L. Hillman, J.L. Van Hove, E.W. Naylor, Clin. Chem. 43 (1997) 2106–2113.
[5] P. Mueller, A. Schulze, I. Schindler, T. Ethofer, P. Buehrdel, U. Ceglarek, Clin. Chim. Acta 327 (2003) 47–57.
[6] Y. Hasegawa, M. Iga, M. Kimura, Y. Shigematsu, S. Yamaguchi, J. Chromatogr. B: Analyt. Technol. Biomed. Life Sci. 823 (2005) 13–17.
[7] P.E. Minkler, S.T. Ingalls, C.L. Hoppel, Anal. Chem. 77 (2005) 1448–1457.
[8] P.E. Minkler, J. Kerner, K.N. North, C.L. Hoppel, Clin. Chim. Acta 352 (2005) 81–92.
[9] S.H. Cho, J. Lee, W.Y. Lee, B.C. Chung, Rapid Commun. Mass Spectrom. 20 (2006) 1741–1746.
[10] J.F. Van Bocxlaer, A.P. De Leenheer, Clin. Chem. 39 (1993) 1911–1917.
[11] R.D. Stevens, S.L. Hillman, S. Worthy, D. Sanders, D.S. Millington, Clin. Chem. 46 (2000) 727–729.
[12] A.K. Ghoshal, T. Guo, N. Soukhova, S.J. Soldin, Clin. Chim. Acta 358 (2005) 104–112.
[13] A.K. Ghoshal, J. Balay, S.J. Soldin, Clin. Chim. Acta 365 (2006) 352–353.
[14] D.H. Chace, J.C. DiPerna, B.L. Mitchell, B. Sgroi, L.F. Hofman, E.W. Naylor, Clin. Chem. 47 (2001) 1166–1182.
[15] M.M. Kiser, J.W. Dolan, LC–GC Eur. 17 (2004) 138–143.
[16] M. Morillas, P. Gomez-Puertas, A. Bentebibel, E. Selles, N. Casals, A. Valencia, F.G. Hegardt, G. Asins, D. Serra, J. Biol. Chem. 278 (2003) 9058–9063.
[17] N. van Vlies, J.P. Ruiter, M. Doolaard, R.J. Wanders, F.M. Vaz, Mol. Genet. Metab. 90 (2007) 24–29.

CPT1C IS LOCALIZED IN ENDOPLASMIC RETICULUM OF NEURONS AND HAS CARNITINE PALMITOYLTRANSFERASE ACTIVITY.

Sierra, A. Y., Gratacòs, E., Carrasco, P., Clotet, J., Ureña, J., Serra, D., et al. (2008).

The Journal of Biological Chemistry, 283(11), 6878-6885.

ADDITIONS AND CORRECTIONS

This paper is available online at www.jbc.org

THE JOURNAL OF BIOLOGICAL CHEMISTRY VOL. 283, NO. 18, p. 12680, May 2, 2008

VOLUME 283 (2008) PAGES 7733–7744

Amyloidogenic processing but not amyloid precursor protein (APP) intracellular C-terminal domain production requires a precisely oriented APP dimer assembled by transmembrane G*XXX*G motifs.

Pascal Kienlen-Campard, Bernadette Tasiaux, Joanne Van Hees, Mingli Li, Sandra Huysseune, Takeshi Sato, Jeffrey Z. Fei, Saburo Aimoto, Pierre J. Courtoy, Steven O. Smith, Stefan N. Constantinescu, and Jean-Noël Octave

On Page 7743, the "Acknowledgments" should read as follows. "We thank T. C. Südhof for the generous gift of APPGal4 constructs, L. Mercken for help with sαAPP and sβAPP quantification, N. Sergeant and A. Delacourte for antibodies directed against the APP C terminus, and F. N'Kuli for excellent technical assistance. The mass spectrometric analysis of immunoprecipitated Aβ samples shown in Supplemental Fig. 1 was performed at the Freie University Berlin in the Mass Spectrometry Core Facility of the Institute for Chemistry and Biochemistry (Prof. Gerd Multhaup) by Lisa Münter and Chris Weise."

VOLUME 283 (2008) PAGES 6878–6885

CPT1c is localized in endoplasmic reticulum of neurons and has carnitine palmitoyltransferase activity.

Adriana Y. Sierra, Esther Gratacós, Patricia Carrasco, Josep Clotet, Jesús Ureña, Dolors Serra, Guillermina Asins, Fausto G. Hegardt, and Núria Casals

On Page 6878, right column, line 8 from the bottom, the following sentence should be added after "contact sites between ER and mitochondria (5)": Price *et al.* (6) demonstrated that when rat CPT1c was expressed heterologously in *Pichia pastoris*, it was targeted exclusively to the microsomes. In addition, these authors found CPT1c in the endoplasmic reticular and mitochondrial fractions of homogenized rat brain, although they indicated that the mutual contamination of the two cell membrane fractions was very substantial.

THE JOURNAL OF BIOLOGICAL CHEMISTRY VOL. 283, NO. 11, pp. 6878–6885, March 14, 2008

CPT1c Is Localized in Endoplasmic Reticulum of Neurons and Has Carnitine Palmitoyltransferase Activity*

Received for publication, September 24, 2007, and in revised form, December 13, 2007 Published, JBC Papers in Press, January 11, 2008, DOI 10.1074/jbc.M707965200

Adriana Y. Sierra[‡1,2], **Esther Gratacós**[‡1], **Patricia Carrasco**[‡2], **Josep Clotet**[‡], **Jesús Ureña**[§], **Dolors Serra**[¶‖], **Guillermina Asins**[¶‖], **Fausto G. Hegardt**[¶‖], **and Núria Casals**[‡‖3]

From the [‡]*Molecular and Cellular Unit, School of Health Sciences, Universitat Internacional de Catalunya, Josep Trueta s/n, Sant Cugat del Vallés, Barcelona 08195, the* [§]*Department of Cell Biology, Faculty of Biology, University of Barcelona, Diagonal 645, and Institute de Recerca Biomédica de Barcelona, Josep Samitier 1–5, 08028 Barcelona, the* [¶]*Department of Biochemistry and Molecular Biology, University of Barcelona, School of Pharmacy, 08028 Barcelona, and the* [‖]*Centro de Investigación Biomédica en Red (CIBER) Institute of Fisiopatología de la Obesidad y Nutrición (CB06/03), Instituto de Salud Carlos III, 28029 Madrid, Spain*

CPT1c is a carnitine palmitoyltransferase 1 (CPT1) isoform that is expressed only in the brain. The enzyme has recently been localized in neuron mitochondria. Although it has high sequence identity with the other two CPT1 isoenzymes (a and b), no CPT activity has been detected to date. Our results indicate that CPT1c is expressed in neurons but not in astrocytes of mouse brain sections. Overexpression of CPT1c fused to the green fluorescent protein in cultured cells demonstrates that CPT1c is localized in the endoplasmic reticulum rather than mitochondria and that the N-terminal region of CPT1c is responsible for endoplasmic reticulum protein localization. Western blot experiments with cell fractions from adult mouse brain corroborate these results. In addition, overexpression studies demonstrate that CPT1c does not participate in mitochondrial fatty acid oxidation, as would be expected from its subcellular localization. To identify the substrate of CPT1c enzyme, rat cDNA was overexpressed in neuronal PC-12 cells, and the levels of acylcarnitines were measured by high-performance liquid chromatography-mass spectrometry. Palmitoylcarnitine was the only acylcarnitine to increase in transfected cells, which indicates that palmitoyl-CoA is the enzyme substrate and that CPT1c has CPT1 activity. Microsomal fractions of PC-12 and HEK293T cells overexpressing CPT1c protein showed a significant increase in CPT1 activity of 0.57 and 0.13 nmol·mg^{-1}·min^{-1}, respectively, which is ~50% higher than endogenous CPT1 activity. Kinetic studies demonstrate that CPT1c has similar affinity to CPT1a for both substrates but 20–300 times lower catalytic efficiency.

Carnitine palmitoyltransferase 1 (CPT1)[4] catalyzes the conversion of long chain fatty acyl-CoAs into acylcarnitines, the first step in the transport of long chain fatty acids from the cytoplasm to the mitochondrial matrix, where they undergo β-oxidation. This reaction is not only central to the control of fatty acid oxidation, but it also determines the availability of long chain acyl-CoA for other processes, notably the synthesis of complex lipids.

There are three different CPT1 isozymes: CPT1a (also called L-CPT1) encoded by *CPT1a*, CPT1b (also called M-CPT1) encoded by *CPT1b*, and the recently described CPT1c (also called CPT1-C) encoded by *CPT1c*. *CPT1a* and *CPT1b* have been extensively studied since they were cloned for the first time, in 1993 and 1995, respectively (1, 2). CPT1a is the most ubiquitous expressed isoform and is found not only in liver but also in pancreas, kidney, brain, blood, and embryonic tissues. CPT1b is expressed only in brown adipose tissue, muscle, and heart. Both isozymes present significantly different kinetic and regulatory properties: CPT1a displays higher affinity for its substrate carnitine and a lower affinity for the physiological inhibitor malonyl-CoA than the muscle isoform (3). In addition, the amino acid residues that are critical for catalytic activity or malonyl-CoA sensitivity have been identified for both enzymes, and three-dimensional structures have been predicted based on the carnitine acetyl transferase, carnitine octanoyl transferase, and carnitine palmitoyltransferase II crystals (4). CPT1a and CPT1b are localized in the outer mitochondrial membrane with the N and C termini facing to the cytosolic side. Western blotting and activity characterization suggested that CPT1a is also localized in microsomes, but expression studies with EGFP fused to the C terminus of CPT1a showed that CPT1a is targeted only to mitochondria and that previous detection of CPT1a in microsomes was probably derived from membrane contact sites between ER and mitochondria (5). CPT1a and CPT1b have a critical role in the heart, liver, and pancreatic β-cells and are potential targets for the treatment of metabolic disorders, including diabetes and coronary heart disease.

Less is known about CPT1c. Although the protein sequence is highly similar to that of the other two isozymes, CPT1c expressed in yeast or HEK293T cells displays no catalytic activity with common acyl-CoA esters as substrates (6, 7). One

* This work was supported in part by the Ministerio de Educación y Ciencia, Spain (Grants SAF2004-06843-C03 and SAF2007-61926), by Ajut de Suport als Grups de Recerca de Catalunya (Grant 2005SGR-00733), and by the Fundació La Marató de TV3 (2007), Catalunya. The costs of publication of this article were defrayed in part by the payment of page charges. This article must therefore be hereby marked "*advertisement*" in accordance with 18 U.S.C. Section 1734 solely to indicate this fact.

[1] Both authors contributed equally to this work.

[2] Recipients of fellowships from the Universitat Internacional de Catalunya.

[3] To whom correspondence should be addressed. Tel.: 93-50-42005; Fax: 93-50-42001; E-mail: ncasals@csc.uic.es.

[4] The abbreviations used are: CPT1, carnitine palmitoyltransferase 1; EGFP, enhanced green fluorescent protein; ER, endoplasmic reticulum; PBS, phosphate-buffered saline; BSA, bovine serum albumin; HPLC, high-performance liquid chromatography; LC, liquid chromatography; ESI, electrospray ionization; MS/MS, tandem mass spectrometry.

explanation is that palmitoyl-CoA is not a substrate for CPT1c and that another brain-specific acyl-CoA might be its natural substrate. Expression studies indicate that CPT1c is localized exclusively in the central nervous system, with homogeneous distribution in all areas (hippocampus, cortex, hypothalamus, and others). The pattern resembles that of FAS, acetyl-CoA carboxylase-α (enzymes related to biosynthesis) rather than CPT1a or ACC-β (enzymes related to oxidation) (6, 8). The capacity of CPT1c to bind malonyl-CoA has been demonstrated, and it has been suggested that CPT1c regulates malonyl-CoA availability in the brain cell.

It has recently been reported that knock-out mice for CPT1c ingest less food and have a lower body weight when fed a standard diet. When these animals are fed high fat chow, body weight increases more than control animals, and they become resistant to insulin, suggesting that CPT1c is involved in energy homeostasis and control of body weight (7). Moreover, ectopic overexpression of CPT1c by stereotactic hypothalamic injection of a CPT1c adenoviral vector protects mice from adverse weight gain caused by high fat diet (9).

Herein we report that CPT1c is localized in neurons but not in astrocytes of adult brain. We also demonstrate that CPT1c is localized in the ER of the cells and not in mitochondria, and that CPT1c shows carnitine palmitoyltransferase activity.

EXPERIMENTAL PROCEDURES

Culture of PC-12, SHSY5Y, Fibroblasts, and HEK293T Cells

The human neuroblastoma cell line, SHSY5Y, the human embryonic kidney-derived cell line, HEK293T, and human fibroblasts cells were grown at 37 °C in the presence of 5% CO_2 in Dulbecco's modified Eagle's medium with high glucose containing 2 mM glutamine, 10% fetal calf serum, penicillin (100 units/ml), and streptomycin (100 μg/ml). Medium for PC-12 cells was Dulbecco's modified Eagle's medium with high glucose containing 2 mM glutamine, sodium pyruvate, 5% fetal calf serum, 10% horse serum, penicillin (100 units/ml), and streptomycin (100 μg/ml).

Cells cultured in 24-wells plates were transfected with 0.8 μg of plasmid (purified with the Qiagen Maxi Prep Kit) using Lipofectamine Plus reagent (Invitrogen) according to the manufacturer's protocol. Transfection efficiency was ~30–50%.

Plasmid Constructions

For pCPT1c-EGFP and pCPT1a-EGFP, rat CPT1c cDNA was obtained by reverse transcription-PCR performed with 2 μg of total rat brain RNA. The 2700-bp fragment amplified was cloned in pBluescript and sequenced. pEGFP-N3 vector (from Clontech, BD Biosciences) was used to clone the coding region of *CPT1c* or *CPT1a*, to create pCPT1c-EGFP and pCPT1a-EGFP, respectively. pCPT1c-EGFP and pCPT1a-EGFP plasmids encode CPT1c and CPT1a proteins fused to the N-terminal region of EGFP, respectively.

Chimera Constructions

pCPT1ac-EGFP—460 bp of the 5′ coding sequence of rat *CPT1a* gene was PCR-amplified with primers that created an HindIII site and an HpaI site at the ends of the amplified fragment. This PCR product was cloned into a pCPT1c-EGFP plasmid previously digested by HindIII and HpaI (which deleted the 460 bp of the 5′ terminus of *CPT1c* coding sequence). The resulting plasmid encodes a fused protein constituted by the N terminus and the two transmembrane domains of CPT1a, the catalytic domain of CPT1c, and EGFP.

pCPTca-EGFP—A segment of the first 462 bp of rat *CPT1c* gene was PCR-amplified with two primers that created a HindIII site a PpuMI site at the ends of the amplified fragment. This PCR product was digested and cloned into a pCPT1a-EGFP plasmid, previously digested by HindIII and PpuMI (which deleted the 460 bp of the 5′ terminus of *CPT1c* coding sequence). The resulting vector contained the N terminus, the two transmembrane domains of CPT1c, and the catalytic domain of CPT1a fused to EGFP.

pIRES-CPT1a and pIRES-CPT1c—The coding regions of rat *CPT1a* and *CPT1c* were cloned in vector pIRES2-EGFP (Clontech, BD Biosciences), which permits both the gene of interest and the EGFP gene to be translated from a single bicistronic mRNA.

Co-localization Studies in Brain Sections

For co-localization studies we performed combined *in situ* hybridization/immunocytochemistry or double immunofluorescence, using standard protocols.

For combined *in situ* hybridization, coronal sections (30 μm) from adult mouse forebrains were used. Processed sections were hybridized overnight at 56 °C, with *cpt1c* Riboprobes (full rat cDNA) labeled with digoxigenin-d-UTP (Roche Applied Science) at a concentration of 500 ng/ml. After stringent washing, sections were incubated at 4 °C overnight with an anti-DIG antibody (1/2000) conjugated to alkaline phosphatase (Roche Applied Science) and developed with 5-bromo-4-chloro-3-indolyl phosphate/nitro blue tetrazolium substrate (Invitrogen). Tissue sections were mounted on gelatinized slides with Mowiol. Those sections that were hybridized with control sense Riboprobes did not give any hybridization signal.

After *in situ* hybridization, some slices were collected and processed by immunofluorescence. The primary antibody was mouse anti-NeuN (1:75, Chemicon). The secondary antibody was biotinylated (Vector Laboratories, Inc., Burlingame, CA). The streptavidin-horseradish peroxidase complex was from Amersham Biosciences. Sections were developed with 0.03% diaminobenzidine and 0.003% hydrogen peroxide, mounted onto slides, and dehydrated, and coverslips were added with synthetic resin.

In double immunofluorescence experiments, sections obtained as indicated above were incubated with primary antibodies against glial fibrillary acidic protein (1/500, Chemicon MAB360) and CPT1c (1/100) overnight at 4 °C in the same blocking solution. The sections were washed three times in PBS (0.1 M) and incubated for 2 h with secondary antibodies coupled to fluorochromes Alexa 488 (for green fluorescence) and Alexa 568 (for red fluorescence) at a dilution of 1/500. Sections were mounted with Mowiol and observed using a confocal Leica TCS SP2 microscope (Leica Lasertechnik GmbH, Mannheim, Germany). Images were saved in TIFF format and analyzed using Adobe Photoshop 3.0.

Co-localization Studies in Culture Cells

Cultured cells were grown on lysine-treated coverslips in 24-well plates. Co-localization studies were performed 48 h after transfection with plasmids containing *CPT1c* or *CPT1a* fused to the 5′-end of EGFP. To visualize the ER, cells were washed twice in PBS (10 mM), fixed with 3% paraformaldehyde in 100 mM phosphate buffer and 60 mM sucrose for 15 min at room temperature, and then washed twice in PBS. Cells were permeabilized with 1% (w/v) of Triton X-100 in PBS and 20 mM glycine for 10 min at room temperature and then washed twice in PBS. Nonspecific binding of antibody was blocked by incubation with 1% (w/v) BSA in PBS with glycine 20 mM at room temperature for 30 min. Cells were then incubated with mouse anti-calnexin polyclonal antibody (BD Biosciences, 1:50 in 1% (w/v) BSA/PBS/20 mM glycine/0.2% Triton X-100) for 1 h at 37 °C. After washing twice in PBS/20 mM glycine, cells were incubated with goat anti-mouse Alexafluor 546 (Molecular Probes, 1:500 in 1% (w/v) BSA/PBS/20 mM glycine/0.2% Triton X-100) for 1 h at 37 °C, and then washed twice in PBS. Coverslips were mounted on glass slides with Mowiol. Mitochondria were visualized by incubating cells with 500 nM MitoTracker Orange CM-H2TMRos (Molecular Probes) in complete medium for 30 min, followed by 30 min in complete medium without MitoTracker, after which they were fixed as mentioned above.

Fluorescent staining patterns were visualized by using a fluorescence microscope (Leica). The captured images were processed using Adobe Photoshop 5.0.

RNA Extraction and Real-time PCR Conditions

RNA was extracted from cells by the TRIzol method (Invitrogen) and quantified spectrophotometrically. 2 μg of total RNA was incubated with DNase and reverse transcribed by Superscript III (Invitrogen) following the manufacturer's conditions. 2 μl of reaction was used in the real-time PCR amplification with TaqMan and primers designed by Applied Biosystems, following the manufacturer's conditions. An 18 S expression assay was used to normalize the samples.

Lipid Extraction

Cells were washed in cold PBS buffer and gently collected with a pipette. They were then centrifuged at 700 × *g* for 5 min at 4 °C and washed in PBS. 20 μl of samples was taken for Bradford protein assay. After that, 200 μl of 0.2 M NaCl was added to the pellet, and the mixture was immediately frozen in liquid N_2. To separate aqueous and lipid phases, 750 μl of Folch reagent (chloroform:methanol, 2:1) and 50 μl of 0.1 M KOH were added, and, after vigorous vortex mixing, the phases were separated by 15-min centrifugation at 2000 × *g* at 4 °C. The top aqueous phase was removed, and the lipid phase was washed in 200 μl of methanol/water/chloroform (48:47:3). After vortex mixing, centrifugation was performed at 700 × *g* for 5 min at 4 °C, and the lower phase (lipid extract) was dried.

Quantification of Acylcarnitines by HPLC

Acylcarnitines were analyzed via an LC-ESI-MS/MS System (API 3000 PE Sciex) in positive ionization mode as described in a previous study (10). Quantification was done through multiple reaction monitoring experiments using the isotope dilution method with deuterated palmitoylcarnitine as internal standard (200 ng·ml^{-1}). 10 μl of sample was injected in the LC-ESI-MS/MS system. Multiple reaction monitoring transitions were as follows: 400.4/85.2 for quantification of palmitoylcarnitine, 4001.4/341.4 for confirmation of palmitoylcarnitine, and 403.4/85.2 for quantification of d_2-palmitoylcarnitine. The method was linear over the range from 2 to 2000 ng·ml^{-1}. The limit of detection and the limit of quantification were 0.14 ng·ml^{-1} (0.35 nmol·liter^{-1}) and 0.48 ng·ml^{-1} (1.2 nmol·liter^{-1}), respectively (in standard solutions).

Microsome Purification

Cells were recovered by centrifugation at 1200 × *g* for 5 min at 4 °C, washed in 1.5 ml of PBS, and re-suspended in 2 ml of lysis buffer (250 mM sucrose, 10 mM Tris, pH 7.4, 1 mM EDTA, supplemented with 1 mM phenylmethylsulfonyl fluoride, 0.5 mM benzamidine, 10 ng/ml leupeptin, and 100 ng/ml pepstatin). Cells were disrupted by Dounce homogenization (30 pulses with loose pestle and 30 pulses with tight pestle). Homogenates were centrifuged at 2,000 × *g* for 3 min at 4 °C to remove cell debris. This crude extracted was further centrifuged at 10,000 × *g* for 30 min at 4 °C to remove the mitochondrial fraction. Supernatant was centrifuged at 10,000 × *g* for 1 h at 4 °C to sediment the microsomal fraction. Pellets were immediately used in the carnitine palmitoyltransferase activity assay.

CPT1 Activity

Radiometric Method—Carnitine acyltransferase activity was determined by the radiometric method as previously described (11). The substrates were palmitoyl-CoA and L-[*methyl*-^{3}H]carnitine. Enzyme activity was assayed for 4 min at 30 °C in a total volume of 200 μl. The protein sample, 40 μl (20 μg), was preincubated for 1 min, and then 160 μl of the reaction mixture was added. The final concentrations were 105 mM Tris-HCl (pH 7.2), 2 mM KCN, 15 mM KCl, 4 mM $MgCl_2$, 4 mM ATP, 250 μM reduced glutathione, 50 μM palmitoyl-CoA, 400 μM L-[*methyl*-^{3}H]carnitine (0.3 μCi), and 0.1% defatted bovine albumin. Reactions were stopped by the addition of 200 μl of HCl 1.2 N, and the product acyl-L-[*methyl*-^{3}H]carnitine was extracted with water-saturated *n*-butanol. Values were estimated by analyzing the data from three experiments performed in triplicate. All protein concentrations were determined using the Bio-Rad protein assay with bovine albumin as standard.

Chromatographic Method—The same procedure used previously (11) was followed except that all carnitine used was cold (not radioactive). In addition, acylcarnitines extracted with water-saturated *n*-butanol were analyzed by an LC-ESI-MS/MS system, as described above.

Western Blot Experiments

A polyclonal rabbit antibody against the last 15 residues (796–810) of mouse CPT1c was developed following the indications in a previous study (7), by Sigma-Genosys. The specificity of the antibody was determined by enzyme-linked immunosorbent assay and Western blot experiments. For CPT1a detection, a polyclonal antibody against amino acids 317–430

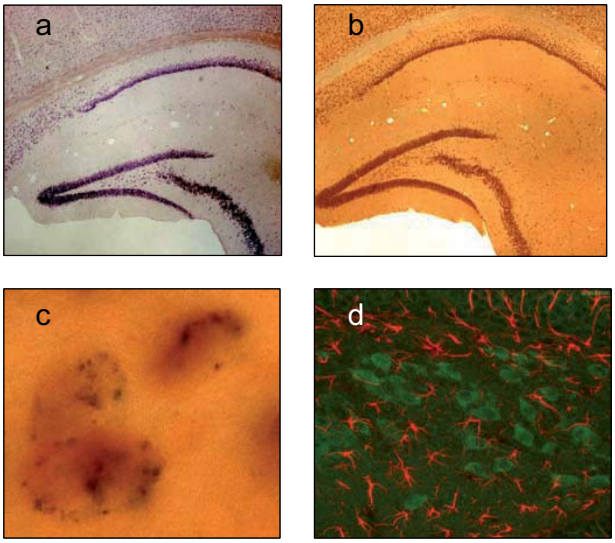

FIGURE 1. **Co-localization studies of CPT1c mRNA with NeuN and glial fibrillary acidic protein proteins in brain sections.** Brain sections were processed using *in situ* hybridization with *CPT1c* antisense Riboprobe (*a*) or immunocytochemistry with NeuN primary antibodies and biotinylated secondary antibodies (*b*) or both methods (*c*). Mouse adult brain sections were processed by double immunocytochemistry with CPT1c antibodies (*green* stain) and glial fibrillary acidic protein (molecular marker of astrocytes, *red* stain) (*d*).

of rat-CPT1a (12) was used. Generally, 60 μg of protein extracts was subjected to SDS-PAGE. A 1:2000 dilution of anti-CPT1c was used as primary antibody. The secondary antibody was used at 1:5000 dilution. The blots were developed with the ECL Western blotting system from Amersham Biosciences.

Palmitate Oxidation

Palmitate oxidation to CO_2 and acid-soluble products were measured in PC-12 cells 48 h after transfection. On the day of the assay, cells were washed in Krebs-Ringer bicarbonate/Hepes buffer (KRBH)/0.1% BSA, preincubated at 37 °C for 30 min in KRBH/1% BSA, and washed again. Cells were incubated for 2 h at 37 °C with fresh KRBH containing 2.5 mM glucose, 0.8 mM carnitine, 0.25 mM palmitate, and 1 μCi/ml [1-^{14}C]palmitate bound to 1% BSA. Oxidation measurements were performed as previously described (13).

RESULTS

CPT1c Cell Type Localization

To identify the types of brain cell in which *CPT1c* is expressed, co-localization studies with NeuN (a nuclear neuronal marker), or glial fibrillary acidic protein (an astrocyte marker), antibodies were performed in adult mouse brain sections. Fig. 1 shows co-labeling of *CPT1c* mRNA, as revealed by *in situ* hybridization studies, with NeuN. This pattern confirms that *CPT1c* is expressed mainly in neurons. In addition, no co-localization was detected between CPT1c and glial fibrillary acidic protein (double immunohistochemistry) (Fig. 1*d*), indicating that CPT1c is not present in brain astrocytes.

CPT1c Subcellular Localization

CPT1c Is Localized in ER of Cultured Cells—To study the intracellular localization of CPT1c, fibroblasts were transiently transfected with pCPT1a-EGFP or pCPT1c-EGFP, which

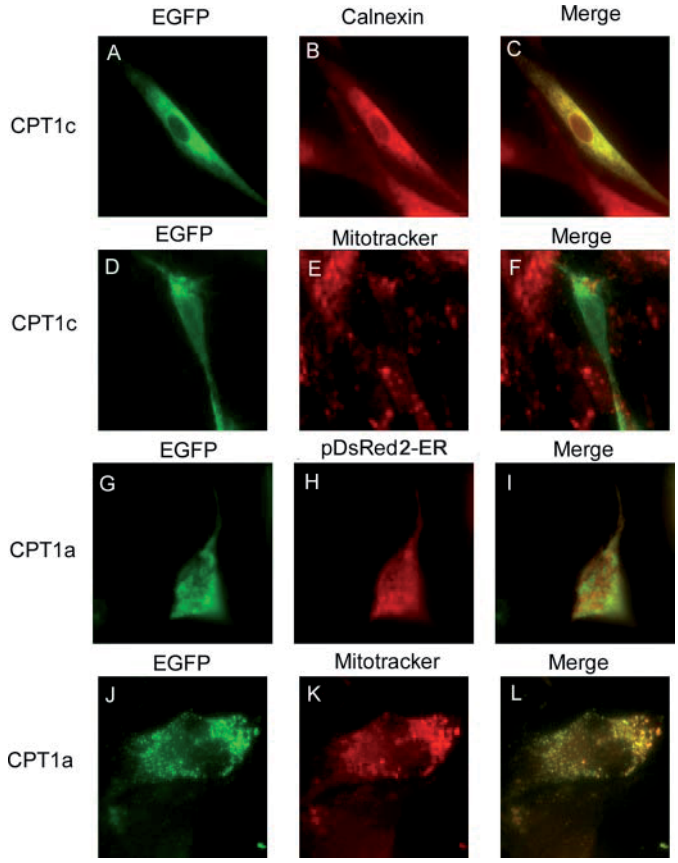

FIGURE 2. **Co-localization studies of CPT1c in mitochondria and ER.** Fibroblasts were transfected with pCPT1c-EGFP (*A–F*) or pCPT1a-EGFP (*G–L*) and incubated with anti-calnexin as primary antibody (*B*) or stained by MitoTracker (*E* and *K*) or co-transfected with pDsRed2-ER (*H*). Images were taken by confocal microscopy with a filter to see *green* emission, *red* emission, or the *merged image* (*C*, *F*, *I*, and *L*).

encode CPT1a or CPT1c proteins, respectively, fused at their C-terminal end to EGFP. 48–52 h after transfection, the fluorescence pattern shown by CPT1a-EGFP (which was expressed in a punctuate manner) was different from that of CPT1c-EGFP (which was expressed in a reticular manner). Co-localization studies were performed with MitoTracker, a potential-sensitive dye that accumulates in mitochondria, and with anti-calnexin, an ER integral protein. In some experiments cells were co-transfected with pDsRed2-ER (Clontech, Takara BioEurope, SAS), a subcellular localization vector that stains the ER red. Fig. 2 clearly shows that CPT1c is localized in the ER membrane, but not in mitochondria. In contrast, CPT1a is localized in mitochondria, as previously described in other cells (5). The slight co-localization of CPT1a with the product of pDsRed2-ER may be due to the contacts between the ER membrane and the mitochondrial outer membrane, labeled as mitochondrial-associated membranes. To assess whether either isoform is localized in peroxisomes, other organelles implicated in fatty acid oxidation, co-localization studies were performed with anti-PMP70, a peroxisomal membrane protein. No major co-localization was observed between PMP70 and CPT1c or CPT1a. The slight co-localization of CPT1c with PM70 may be due to a residual localization of this protein in peroxisomes (Fig. 3). The same experiments were performed with SH-SY5Y cells, PC-12 cells, and HEK293T cells with same results.

CPT1c Is Localized in Microsomal Fraction of Adult Mouse Brain—To eliminate the possibility that overexpression experiments in cultured cells could modify the subcellular localization of CPT1c, we performed Western blot experiments with different cellular fractions of some adult mouse tissues. CPT1c was only present in brain tissue and absent in any other tissues analyzed (Fig. 4). In addition, CPT1c was localized in the microsomal fraction of brain (Fig. 4). Only some levels of CPT1c protein were present in brain mitochondria, probably by residual contamination from microsomes. The same membranes, once de-hybridized, were used with CPT1a antibodies, as a positive control for mitochondria. CPT1a was present at high levels in mitochondria from liver and kidney, and some residual levels were found in the microsomal fraction of all tissues examined.

The N-terminal Region of the Protein Is Responsible for CPT1c-specific Subcellular Localization—We aimed to test whether the N-terminal end of CPT1c was responsible for the ER localization. We made new chimeric plasmid constructions in which 460 bp of the 5′ end of *CPT1a* gene (which encodes the two trans-membrane domains) and the mitochondrial import signal described by the Prip-Buus group (14) was replaced by the 5′ end of *CPT1c*, and *vice versa* (see *scheme* in Fig. 5). The recombinant plasmids were called pCPT1ca-EGFP and pCPT1ac-EGFP, respectively. SY-SHSY cells transiently transfected with those constructions showed that CPT1ca-EGFP was localized in ER, and that CPT1ac-EGFP was localized in mitochondria, indicating that exchange of N-terminal ends between the two CPT1 isoforms swapped the intracellular localization of recombinant chimeric proteins (Fig. 5). These results demonstrate that the N-terminal end of CPT1c lacks the mitochondrial import signal present in CPT1a and contains a putative microsomal targeting signal responsible for ER localization.

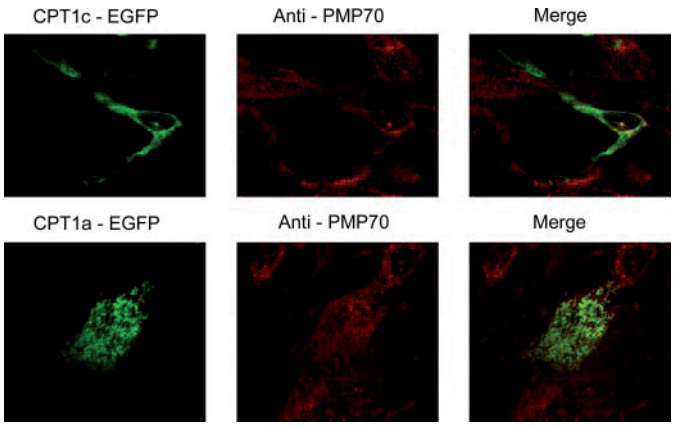

FIGURE 3. **Co-localization studies of CPT1c in perixosomes.** HEK293T cells transfected by pCPT1c-EGFP or pCPT1a-EGFP were incubated with anti-PMP70 as primary antibody. Images were taken by confocal microscopy with a filter to see *green* emission, *red* emission, or the *merged image*.

CPT1c Does Not Participate in Fatty Acid Oxidation—To examine whether CPT1c participates in mitochondrial fatty acid oxidation, we measured increases in CO_2 in PC-12 cells overexpressing CPT1c. As expected by its subcellular localization, CPT1c did not increase fatty acid oxidation, whereas CPT1a did (Table 1).

CPT1c Substrate Identification

To identify the substrate of CPT1c, we overexpressed the enzyme in PC-12 cells and attempted to identify any increased acylcarnitine species present in the lipid cell extract, 48 h after transient transfection. PC-12 cells were easily transfected with Lipofectamine (Invitrogen) or Metafecten (Biontex, Germany) with transfection efficiencies of ~40–70% of total PC-12 cells, as measured by the fluorescence in a cell-counter FACS Scan. PC-12 cells were transfected with pIRES-CPT1c, pIRES-CPT1a, or empty pIRES. Western blot experiments showed a 5- to 10-fold increase in CPT1c and CPT1a levels in transfected cells. The lipid fraction of transfected cells was extracted, and the levels of acylcarnitines were measured. To quantify acylcarnitines, we used a new HPLC-MS/MS method where no derivatization or ionic-pair chromatography is needed (10). Precursor ion scan of *m/z* 85 experiment allows the identification of all acylcarnitines present in the sample. Areas below chromatographic peaks (chromatograms acquired in multiple reaction monitoring mode) were measured for all acylcarnitines detected. Fig. 6 shows relative areas from chromatographic peaks present in overexpressing cells compared with control (cells transfected with empty expression vector). Cells transfected with pIRES-CPT1c showed an increase of >2-fold in palmitoylcarnitine levels (Fig. 6). No other acylcarnitine was significantly increased. Cells transfected with pIRES-CPT1a (positive control) showed a 5-fold increase in palmitoylcarnitine levels and a 2- to 3-fold increase in other long chain acylcarnitines. The Wilcoxon statistic test (a non-parametric test for two paired samples) between CPT1c-transfected cells and control cells indicated that only palmitoylcarnitine levels increased significantly in CPT1c-transfected cells. These results indicate that CPT1c has carnitine palmitoyltransferase activity and that palmitoyl-CoA is a substrate for the CPT1c isoenzyme.

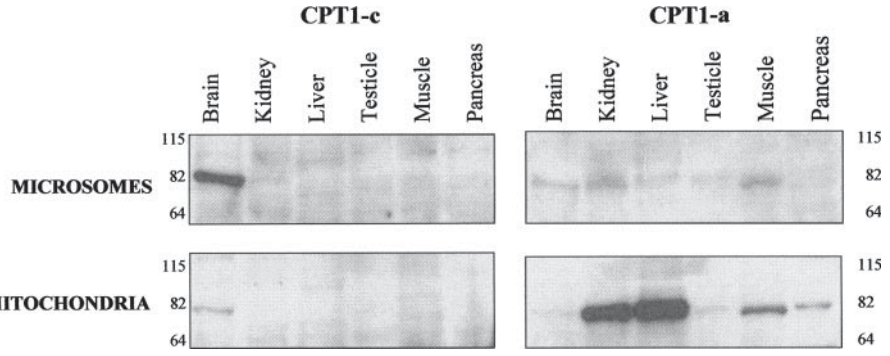

FIGURE 4. **Western blot of CPT1c in mitochondrial and ER cell fractions from different tissues of adult mouse.** 60 μg of protein cell fraction was run in each line. The same membranes were incubated with anti-CPT1c and anti-CPT1a antibodies.

CPT1c Activity

Once palmitoyl-CoA had been identified as a CPT1c substrate, we compared CPT1 activity in isolated microsomal fractions of PC-12 and

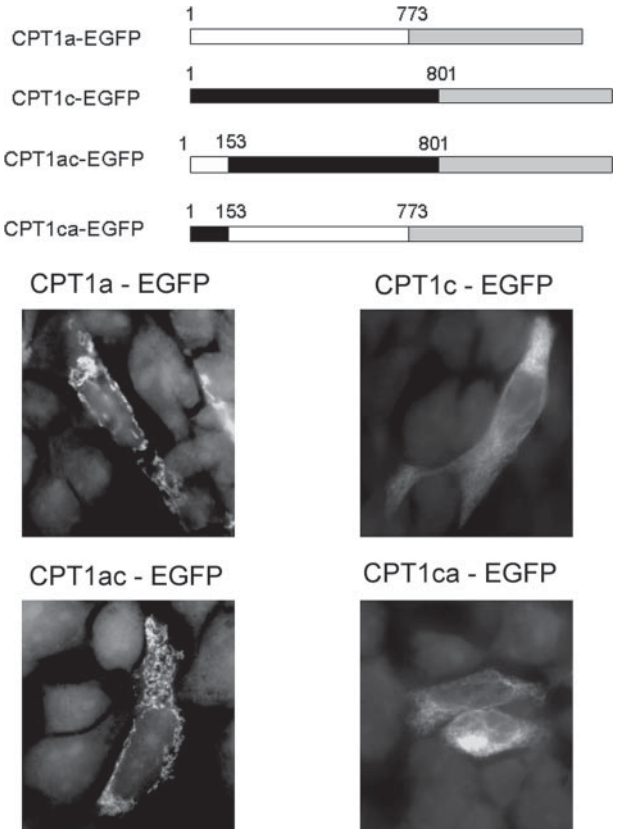

FIGURE 5. **Subcellular localization of fused proteins CPT1a-EGFP, CPT1c-EGFP, CPT1ca-EGFP, and CPT1ac-EGFP in cultured cells.** *Top*, schematic representation of fusion proteins. *CPT1a* coding region is represented in *white*, *CPT1c* coding region in *black*, and *EGFP* coding region in *gray*. *Bottom*, SH-SY5Y human neuroblastoma cells were transfected with recombinant plasmids. 48 h after transfection, cells were visualized in a fluorescence microscope using a 100× objective. CPT1a-EGFP and CPT1ac-EGPF have mitochondrial localization (punctuate pattern). CPT1c-EGFP and CPT1ca-EGFP present a ER localization (reticular pattern).

TABLE 1

Palmitate oxidation in PC-12 cells overexpressing CPT1c

48 h after transfection of cultured cells with pIRES-CPT1c, pIRES-CPT1a, or empty pIRES, cells were incubated for 2 h with [1-^{14}C]palmitate. Palmitate oxidation to CO_2 was determined. Data are presented as the mean ± S.E. of three independent experiments. Data for CPT1a are significantly different from control cells ($p < 0.05$).

	$[^{14}C]CO_2$ production
	nmol/mg/h
Empty pIRES	6.1 ± 0.9
pIRES-CPT1c	5.7 ± 0.7
pIRES-CPT1a	9.2 ± 2.1

HEK293T cells transfected with pIRES-CPT1c with the activity in fractions transfected with empty pIRES vector. CPT1c was overexpressed >10-fold, and the protein was found mainly in the microsomal fraction (Fig. 7*A*). Western blot membrane was reprobed with mouse anti-CPT1a antibodies to determine the residual CPT1a protein present in the microsomal fraction of PC-12 cells (Fig. 7*B*), which is responsible for the endogenous activity in microsomes of control cells. The same antibodies could not be used in HEK293T cells, because they do not recognize the human CPT1a protein. Palmitoylcarnitine formed in the CPT1 assay was measured by the same HPLC-MS/MS method used to identify the substrate (10). Microsomes from CPT1c-transfected cells showed a 50% increase in CPT1 activity compared with control cells (endogenous activity) (Table 2). K_m and V_{max} values for both substrates were calculated (Fig. 8 and Table 3). K_m values were similar to those of CPT1a (25), whereas V_{max} values were 66 times lower than those of CPT1a (25). For example, CPT1c catalytic efficiencies for palmitoyl-CoA and carnitine were 320 and 25 times lower, respectively, than those of CPT1a. CPT1 sensitivity to malonyl-CoA was not measured in cultured transfected cells, because CPT1c activity was too low and the microsomal fraction always retained residual CPT1a activity that masked any inhibitory effect of malonyl-CoA.

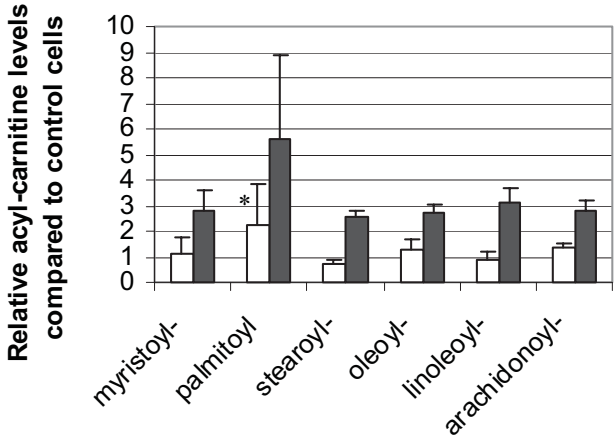

FIGURE 6. **Relative levels of different acyl-carnitines in PC12 cells.** PC-12 cells were transfected with empty pIRES vector (control cells), or pIRES-CPT1c (*white columns*), or pIRES-CPT1a (*black columns*). 48 h after transfection lipid extracts were obtained, and acylcarnitines were determined by HPLC-mass spectrum chromatography. The *y*-axis represents the area below the chromatographic peak compared with control cells. These values represent the mean of three independent experiments except for palmitoylcarnitine, which represents the mean of six independent experiments. *, $p < 0.05$ *versus* control cells. The amounts of palmitoylcarnitine, myristoylcarnitine, and arachidonoylcarnitine in control cells were 0.5 ± 0.2, 0.2 ± 0.1, and 0.02 ± 0.01 nmol/mg, respectively. For oleoylcarnitine and linoleoylcarnitine, only the chromatographic peak was measured.

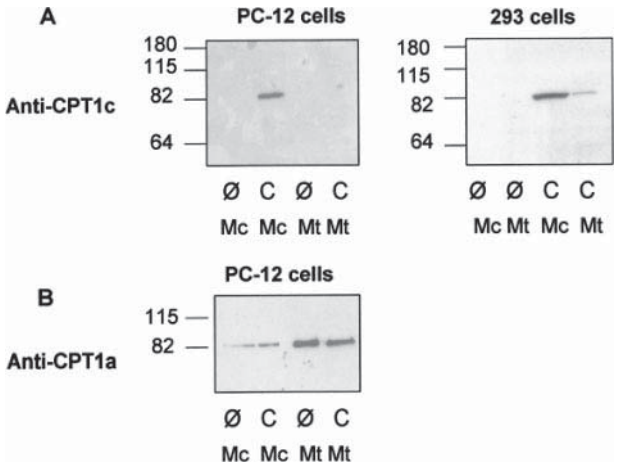

FIGURE 7. **Western blot of transfected PC-12 and HEK293T cells.** Cells were transfected with pIRES-CPT1c (*C*), or empty pIRES (Ø). 40 μg of microsomes (*mc*) or mitochondria (*mt*) were run in each lane of SDS-acrylamide gel. *A*, anti-ratCPT1c antibody; *B*, anti-rat-CPT1a antibody.

DISCUSSION

The presence of a third CPT1 isoform, CPT1c, in the mammalian brain is intriguing. It might show specific expression

TABLE 2

Carnitine palmitoyl transferase activity in PC-12 and HEK293T cells

Cells were transfected with pIRES-CPT1c or empty vector pIRES (control cells). 48 h after transfection, cells were collected and 40 mg of microsomal fraction was assayed for CPT1 activity. The palmitoylcarnitine formed in the assay was determined by HPLC-mass chromatography. Activity is presented as the mean ± S.E. Wilcoxon test for non-parametric paired samples was used. n = number of experiments. Absolute and percent increases in CPT1c activity are compared to control cells.

Cells	Plasmid transfection	n	Activity	p	Absolute increase	Percent increase
			nmol palmitoylcarnitine/mg/min			%
PC12	Control	7	1.37 ± 0.81	<0.05		
	CPT1c	7	1.94 ± 0.96	<0.05	0.57	41.6
293	Control	9	0.22 ± 0.11	<0.05		
	CPT1c	9	0.35 ± 0.18	<0.05	0.13	59

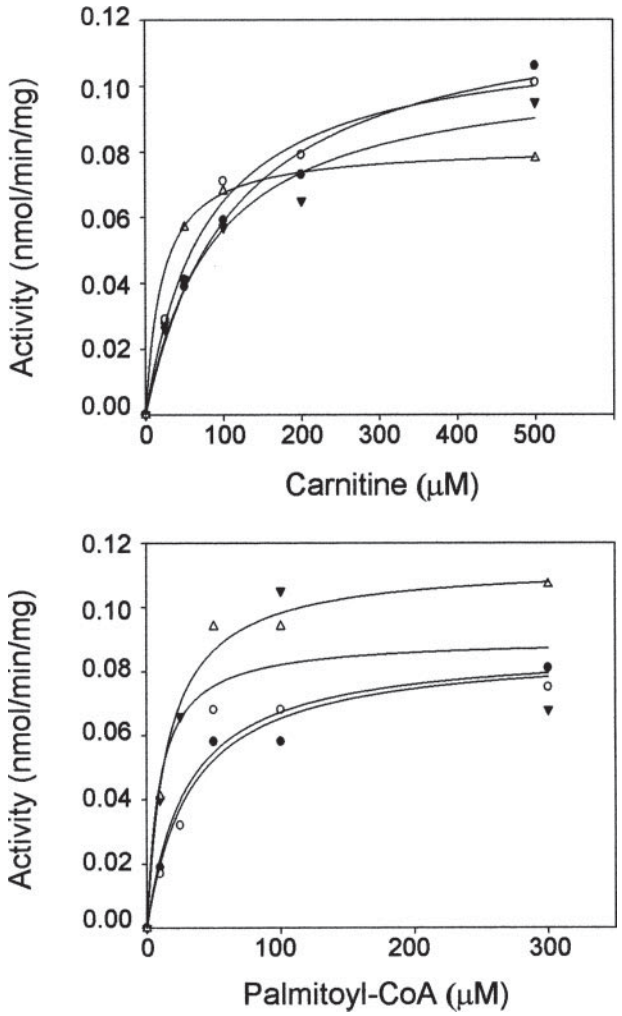

FIGURE 8. **Kinetic analysis of CPT1c overexpressed in PC-12 cells.** 20 μg of microsomes was incubated at increasing concentrations of carnitine (*upper*) and palmitoyl-CoA (*lower*), and CPT1 activity was measured.

patterns, cellular localization, or biochemical properties that would make it different enough from the other two isoforms to explain its occurrence. The data we report here on the peculiarities of CPT1c may provide clues to its cellular function.

CPT1c is expressed only in the mammalian brain. The other CPT1 isoforms are expressed in other tissues and are present in other organisms like birds, fishes, reptiles, amphibians, or insects. This suggests that CPT1c has a specific function in more evolved brains. Price *et al.* (6) showed that CPT1c is expressed in all regions of brain, in a similar pattern to that shown by neurons. Dai *et al.*, have recently demonstrated that CPT1c is localized to neurons of the central nervous system (9). Our results confirm these findings and demonstrate that CPT1c is not expressed in astrocytes, suggesting that CPT1c function is specific to neurons.

TABLE 3

Kinetic parameters of CPT1c overexpressed in PC-12 cells

Microsomes of PC-12 cells overexpressing CPT1c were assayed for activity with different palmitoyl-CoA and carnitine concentrations to calculate K_m and V_{max} values for both substrates. The results are the mean ± S.D. of three experiments. CPT1a kinetic parameters were obtained from a previous study (25).

Parameter	Isoform	
	CPT1c	CPT1a
K_m palmitoyl-CoA (mM)	25.35 ± 7.77	4.9 ± 0.3
V_{max} palmitoyl-CoA (nmol/min/mg)	0.095 ± 0.012	6.3 ± 0.4
Catalytic efficiency palmitoyl-CoA (V_{max}/K_m)	0.004	1.28
K_m carnitine (mM)	58.53 ± 21.31	127.0 ± 4.5
V_{max} carnitine (nmol/min/mg)	0.090 ± 0.010	6.6 ± 0.8
Catalytic efficiency carnitine (V_{max}/K_m)	0.002	0.05

The notion that CPT1c is localized in mitochondria stems from an observation of CPT1c protein in mitochondrial fraction of cells (6) and from co-localization studies with MitoTracker in GT1–7 hypothalamic cells (9). In the first study (6), CPT1c was also found in the microsomal fraction, as revealed by Western blot experiments, although the authors attributed this to contamination problems in cellular fractioning process. In the second study (9) the authors conclude that CPT1c co-localizes with MitoTracker, although the images did not show perfect matching and co-localization studies were not performed with any ER marker. In contrast, subcellular localization studies performed by our group in cultured cells and also in adult brain clearly demonstrate that CPT1c is localized in the ER, not in mitochondria. These results indicate that CPT1c has a different metabolic function than CPT1a or CPT1b, which is other than facilitating the import of long chain fatty acid into mitochondria or peroxisomes to undergo β-oxidation, as demonstrated in palmitate oxidation experiments. Localization of CPT1c in the ER implicates it in a biosynthetic rather than a catabolic pathway.

Intracellular localization experiments with chimeric proteins indicate that the N-terminal region of CPT1c, which includes the two transmembrane domains, is responsible for ER-specific localization. These results complement previous studies in CPT1a protein (14). Prip-Buus and colleagues demonstrate that a region just downstream of the second transmembrane domain (residues 123–147) is important for mitochondrial transport of CPT1a. Amino acid sequence comparison between CPT1a and CPT1c demonstrates that the putative mitochondrial transport sequence is partially altered in CPT1c, with fewer positively charged amino acids (one charged residue *versus* four). In addition, the second transmembrane domain is longer in CPT1c than in the other two isoforms, which may enable it to sort proteins to the ER rather than to mitochondrial outer membrane (15).

Previous studies (6, 7) had shown that CPT1c had no enzyme activity in yeast or HEK293T cells with palmitoyl-CoA or other acyl-CoA molecules as substrate. This indicated that the CPT1c

substrate could be a rare acyl-CoA specific to the brain. We thus attempted to measure variations in all acylcarnitine levels in neural cells overexpressing CPT1c. We found that palmitoylcarnitine was the only product that was increased, indicating that palmitoyl-CoA is the preferred acyl-CoA substrate for CPT1c. Activity measurements in microsomal fractions from PC-12 and HKE293T cells confirmed that CPT1c has carnitine palmitoyltransferase activity. The failure of other authors (6, 7) to detect CPT1c activity has two possible explanations: 1) they used mitochondrial fractions instead of microsomal and 2) they used a radiometric assay instead of a chromatographic method. The HPLC-MS/MS method produces reliable and accurate measurements of palmitoylcarnitine concentrations in biological samples with a sensitivity limit of 0.48 ng/ml, which corresponds to a specific activity of 0.0045 nmol·mg^{-1}·min^{-1} in our CPT1 assay conditions (10). The limit of sensitivity of the radiometric assay, calculated as the standard deviation of ten blank points with a signal-to-noise ratio of 3, corresponds to specific activity of 0.4 nmol·mg^{-1}·min^{-1}. This indicates that the chromatographic method is 100 times more sensitive than the radiometric, as described elsewhere (10). Recently, other authors have also measured CPT1 activity by a tandem mass spectrometry method because of its accuracy and sensitivity (16).

CPT1c has 100 times lower specific activity than CPT1a and CPT1b. One explanation is that CPT1c participates in a biosynthetic pathway, facilitating the constant transport of palmitate across the ER membrane, rather than in a highly active catabolic pathway such as fatty acid oxidation. Another explanation is that CPT1c acts as a metabolic sensor. CPT1c may have low activity in standard or optimal conditions (assay conditions), but its activity increases in certain situations (stress, presence of signal molecules, and others).

Lane and co-workers (7) conclude that hypothalamic CPT1c has a role in energy homeostasis and the control of food ingestion. In addition to this localized function, the wide distribution of the protein in the brain suggests a more general, ubiquitous function, perhaps related with the equilibrium between acyl-CoA pools in the cytosol and the ER lumen. Although it is not known whether CPT2 is present in ER of neurons, we hypothesize that CPT1c facilitates the entry of palmitoyl-CoA to the ER lumen. It is been reported that palmitoyl-CoA cannot cross the ER membrane, although palmitoylcarnitine can (17–20). CPT1a or CPT1b, probably localized in mitochondria-endoplasmic reticulum connections (mitochondrial-associated membrane) (21) may facilitate the entry of palmitoyl-CoA to the reticulum. In the brain, however, fatty acids are not usually oxidized, and levels of CPT1a or CPT1b are low or nonexistent. Thus the occurrence of a specific CPT1c localized in the ER membrane may ensure the entry of palmitoyl-CoA to the lumen of ER. Another possibility is that CPT1c modulates the palmitoyl-CoA pool associated with the ER, thus regulating the synthesis of ceramide and sphingolipids, which are important for signal transduction, modification of neuronal membranes, and brain plasticity (22–24).

Acknowledgments—The editorial help of Robin Rycroft is gratefully acknowledged. We also thank Prof. M. D. Lane for the gift of anti-CPT1c antibodies for use in the initial experiments.

REFERENCES

1. Esser, V., Britton, C. H., Weis, B. C., Foster, D. W., and McGarry, J. D. (1993) *J. Biol. Chem.* **268,** 5817–5822
2. Yamazaki, N., Shinohara, Y., Shima, A., and Terada, H. (1995) *FEBS Lett.* **363,** 41–45
3. McGarry, J. D., and Brown, N. F. (1997) *Eur. J. Biochem.* **244,** 1–14
4. Lopez-Vinas, E., Bentebibel, A., Gurunathan, C., Morillas, M., de Arriaga, D., Serra, D., Asins, G., Hegardt, F. G., and Gomez-Puertas, P. (2007) *J. Biol. Chem.* **282,** 18212–18224
5. Broadway, N. M., Pease, R. J., Birdsey, G., Shayeghi, M., Turner, N. A., and David Saggerson, E. (2003) *Biochem. J.* **370,** 223–231
6. Price, N., van der Leij, F., Jackson, V., Corstorphine, C., Thomson, R., Sorensen, A., and Zammit, V. (2002) *Genomics* **80,** 433–442
7. Wolfgang, M. J., Kurama, T., Dai, Y., Suwa, A., Asaumi, M., Matsumoto, S., Cha, S. H., Shimokawa, T., and Lane, M. D. (2006) *Proc. Natl. Acad. Sci. U. S. A.* **103,** 7282–7287
8. Sorensen, A., Travers, M. T., Vernon, R. G., Price, N. T., and Barber, M. C. (2002) *Brain Res. Gene Expr. Patterns* **1,** 167–173
9. Dai, Y., Wolfgang, M. J., Cha, S. H., and Lane, M. D. (2007) *Biochem. Biophys. Res. Commun.* **359,** 469–474
10. Jáuregui, O., Sierra, A. Y., Carrasco, P., Gratacós, E., Hegardt, F. G., and Casals, N. (2007) *Anal. Chim. Acta* **599,** 1–6
11. Morillas, M., Gomez-Puertas, P., Roca, R., Serra, D., Asins, G., Valencia, A., and Hegardt, F. G. (2001) *J. Biol. Chem.* **276,** 45001–45008
12. Prip-Buus, C., Cohen, I., Kohl, C., Esser, V., McGarry, J. D., and Girard, J. (1998) *FEBS Lett.* **429,** 173–178
13. Herrero, L., Rubi, B., Sebastian, D., Serra, D., Asins, G., Maechler, P., Prentki, M., and Hegardt, F. G. (2005) *Diabetes* **54,** 462–471
14. Cohen, I., Guillerault, F., Girard, J., and Prip-Buus, C. (2001) *J. Biol. Chem.* **276,** 5403–5411
15. Horie, C., Suzuki, H., Sakaguchi, M., and Mihara, K. (2002) *Mol. Biol. Cell* **13,** 1615–1625
16. van Vlies, N., Ruiter, J. P., Doolaard, M., Wanders, R. J., and Vaz, F. M. (2007) *Mol. Genet. Metab.* **90,** 24–29
17. Washington, L., Cook, G. A., and Mansbach, C. M., 2nd. (2003) *J. Lipid Res.* **44,** 1395–1403
18. Abo-Hashema, K. A., Cake, M. H., Power, G. W., and Clarke, D. (1999) *J. Biol. Chem.* **274,** 35577–35582
19. Gooding, J. M., Shayeghi, M., and Saggerson, E. D. (2004) *Eur. J. Biochem.* **271,** 954–961
20. Arduini, A., Denisova, N., Virmani, A., Avrova, N., Federici, G., and Arrigoni-Martelli, E. (1994) *J. Neurochem.* **62,** 1530–1538
21. Rusinol, A. E., Cui, Z., Chen, M. H., and Vance, J. E. (1994) *J. Biol. Chem.* **269,** 27494–27502
22. Buccoliero, R., and Futerman, A. H. (2003) *Pharmacol. Res.* **47,** 409–419
23. Ohanian, J., and Ohanian, V. (2001) *Cell Mol. Life Sci.* **58,** 2053–2068
24. van Echten-Deckert, G., and Herget, T. (2006) *Biochim. Biophys. Acta* **1758,** 1978–1994
25. Morillas, M., Gómez-Puertas, P., Bentebibel, A., Sellés, E., Casals, N., Valencia, A., Hegardt, F. G., Asins, G., and Serra, D. (2003) *J. Biol. Chem.* **278,** 9058–9063